NASA CONTRACTOR REPORT

NASA CR-2786

NASA CR-2786

HEAT TRANSFER TO A FULL-COVERAGE FILM-COOLED SURFACE WITH 30° SLANT-HOLE INJECTION

M. E. Crawford, W. M. Kays, and R. J. Moffat

Prepared by
STANFORD UNIVERSITY
Stanford, Calif. 94305
for Lewis Research Center

NATIONAL AERONAUTICS AND SPACE ADMINISTRATION • WASHINGTON, D. C. • DECEMBER 1976

1. Report No. NASA CR-2786	2. Government Accession No.	3. Rec.,
4. Title and Subtitle HEAT TRANSFER TO A FULL-COVERAGE FILM-COOLED SURFACE WITH 30° SLANT-HOLE INJECTION		5. Report Date December 1976
		6. Performing Organization Code
7. Author(s) M. E. Crawford, W. M. Kays, and R. J. Moffat		8. Performing Organization Report No. HMT-25
		10. Work Unit No.
9. Performing Organization Name and Address Stanford University Stanford, California 94305		11. Contract or Grant No. NAS3-14336
		13. Type of Report and Period Covered Contractor Report
12. Sponsoring Agency Name and Address National Aeronautics and Space Administration Washington, D.C. 20546		14. Sponsoring Agency Code
15. Supplementary Notes Final Report. Project Manager, Raymond S. Colladay, Fluid System Components Division, NASA Lewis Research Center, Cleveland, Ohio		

16. Abstract

Heat transfer behavior was studied in a turbulent boundary layer with full-coverage film cooling through an array of discrete holes and with injection 30° to the wall surface in the downstream direction. Stanton numbers were measured for a staggered hole pattern with pitch-to-diameter ratios of 5 and 10, an injection mass flux ratio range of 0.1 to 1.3, and a range of Reynolds number Re_x of 1.5×10^5 to 5×10^6. Air was used as the working fluid, and the mainstream velocity varied from 9.8 to 34.2 m/sec (32 to 112 ft/sec). The data were taken for secondary injection temperatures equal to the wall temperature and also equal to the mainstream temperature. The data may be used to obtain Stanton number as a continuous function of the injectant temperature by use of linear superposition theory. The heat transfer coefficient is defined on the basis of a mainstream-to-wall temperature difference. This definition permits direct comparison of performance between film cooling and transpiration cooling. A differential prediction method was developed to predict the film cooling data base. The method utilizes a two-dimensional boundary layer program with routines to model the injection process and turbulence augmentation. The program marches in the streamwise direction, and when a row of holes is encountered, it stops and injects fluid into the boundary layer. The turbulence level is modeled by algebraically augmenting the mixing length, with the augmentation keyed to a penetration distance for the injected fluid. Most of the five-hole diameter data were successfully predicted.

17. Key Words (Suggested by Author(s)) Boundary layer Film cooling Heat transfer Turbulence	18. Distribution Statement Unclassified - unlimited STAR category 34

19. Security Classif. (of this report)	20. Security Classif. (of this page)	21. No. of Pages	22. Price*
Unclassified	Unclassified	245	$8.00

*For sale by the National Technical Information Service, Springfield, Virginia 22161

Table of Contents

List of Figures

Figure		Page

Figure Page

List of Tables

Nomenclature

A	heat transfer area, including hole area (see Figure 1.2)
A_h	hole cross-sectional area (see Figure 1.2)
A_{tot}	test section plate surface area
A^+	van Driest damping coefficient, mixing-length model
B_h	blowing parameter, $F/St(\theta = 1)$
c	specific heat, mainstream fluid
C	damping constant, equation for A^+_{eff}
CL1, CL2	constants for adjustment of $(\ell/\delta)_{max,a,eff}$
C_D	drag coefficient, injection model
c_f	skin friction coefficient, $\tau_o = c_f/2\ \rho_\infty U_\infty^2$
D	hole diameter of injection tube van Driest damping function, mixing-length model
DELMR	mass shed ratio, injection model
$\dot{E}_{supplied}$ power	electrical power supplied to plate
EMIS	emissivity of plate to determine $\dot{q}_{rad}$
F	blowing fraction, $(\dot{m}_{jet}/A)/(\rho_\infty U_\infty)$ drag force, injection model
g_c	proportionality constant, Newton's Second Law
h	heat transfer coefficient, $\dot{q}''_o/(T_o-T_\infty)$, with wall mass flux (transpiration or film cooling)
h^*	heat transfer coefficient, $\dot{q}''_o/(T_o-T_{aw})$, with film cooling
h_o	heat transfer coefficient, without wall mass flux
H	velocity profile shape factor, δ_1/δ_2

I	static enthalpy
I^*	stagnation enthalpy, $I + U^2/(2g_c J)$
J	conversion constant, mechanical to thermal energy
k	thermal conductivity
K	conductance between plate and cavity to determine $\dot{q}_{cond}$
KFL	conductance to determine $\dot{q}_{flow}$
KCONV	conductance-area product to determine T_2
ℓ	mixing-length
$(\ell/\delta)_{max,a}$	maximum mixing-length constant, turbulence-augmentation model
$\dot{m}$	mass flow rate in stream tube, injection model
M	blowing parameter, $(\rho_2 U_2)/(\rho_\infty U_\infty)$
P	hole spacing, or pitch (see Figure 1.2) pressure
Pr	Prandtl number, $\mu c/k$
Pr_t	turbulent Prandtl number
PD	penetration distance, injection model
$\dot{q}''_o$	wall heat flux, $\dot{q}_{conv}/A_{tot}$
$\dot{q}_{cond}$	heat transferred from plate to cavity and adjacent plates to determine $\dot{q}_{losses}$
$\dot{q}_{conv}$	heat transferred from plate by convection to define Stanton number
$\dot{q}_{flow}$	heat transferred from plate to secondary air flow
$\dot{q}_{losses}$	heat transferred from plate other than by convection, $\dot{q}_{cond} + \dot{q}_{flow} + \dot{q}_{rad}$
$\dot{q}_{rad}$	heat transferred from plate by radiation
r	recovery factor, $Pr^{0.33}$

$Re_{D,\infty}$	hole-diameter Reynolds number, DU_∞/ν
Re_x	x-Reynolds number, $(x-x_{vo})U_\infty/\nu$
Re_{δ_2}	momentum thickness Reynolds number, $\delta_2 U_\infty/\nu$
Re_{Δ_2}	enthalpy thickness Reynolds number, $\Delta_2 U_\infty/\nu$
S	conductance between adjacent plates to determine $\dot{q}_{cond}$
St	Stanton number, $h/(\rho_\infty c U_\infty)$, see equation (2.1)
St_o	Stanton number at $M = 0$
SAFR	injectant flow rate through one tube
T	temperature
T_g	temperature of secondary air delivered to test section
T^+	non-dimensional temperature, $(T-T_\infty)\sqrt{c_f/2}/\{(T_o-T_\infty)St\}$
$T_{\infty,r}$	mainstream recovery temperature, $T_\infty + \{rU_\infty^2\}/\{2g_c Jc\}$
U	velocity component, x-direction
U_τ	friction velocity, $\sqrt{g_c \tau_o/\rho_o}$, determined by Clauser plot method
U^+	non-dimensional velocity, U/U_τ
V	velocity component, y-direction
x	distance along surface, measured from nozzle exit
x_{vo}	distance, nozzle exit to virtual origin of turbulent boundary layer
x^+	non-dimensional distance, xU_τ/ν
y	distance normal to surface
y^+	non-dimensional distance, yU_τ/ν
α	hole axis angle, measured from surface
$\delta(\ )$	uncertainty in ( )
δ	boundary layer thickness where $U/U_\infty = 0.99$

$\delta\dot{m}$	mass shed into stream tube, injection model
δ_1	displacement thickness, $\int_0^\infty (1 - \frac{\rho U}{\rho_\infty U_\infty})dy$
δ_2	momentum thickness, $\int_0^\infty \frac{\rho U}{\rho_\infty U_\infty}(1 - \frac{U}{U_\infty})dy$
Δ_2	enthalpy thickness, $\int_0^\infty \frac{\rho U}{\rho_\infty U_\infty}(\frac{T - T_\infty}{T_o - T_\infty})dy$
ε_m	eddy diffusivity for momentum
η	adiabatic wall effectiveness, $(T_{aw}-T_\infty)/(T_2-T_\infty)$
θ	temperature parameter, $(T_2-T_\infty)/(T_o-T_\infty)$
κ	von Karman constant, 2-d mixing-length
κ_o	constant, turbulence-augmentation model
λ	outer length scale constant, 2-d mixing-length
μ	dynamic viscosity
ν	kinematic viscosity
ρ	density
σ	Stefan-Boltzmann constant
τ	shear stress
τ^+	non-dimensional shear stress, τ/τ_o
ϕ	function in $\theta = 1$ data correlation, $\{St(\theta = 1)/St_o\}/\{\ell n(1 + B_h)/B_h\}$
ψ	stream tube, injection model

Subscripts

a	augmented value, turbulence-augmentation model

aw	adiabatic wall value in presence of film cooling
eff	effective value
jet 2	injectant value
new	immediately downstream of injection location, injection model
o	wall value (except with h_o or St_o)
old	immediately upstream of injection location, injection model
t	turbulent value
2-d	two-dimensional value, turbulence-augmentation model
∞	mainstream value

Chapter 1

INTRODUCTION

1.1 Background for the Problem

High-temperature gases passing over a surface may result in a large heat flux to the surface. Film cooling the exposed surface is one means of reducing heat flux, and thus surface temperature. With this method, coolant is injected through the surface and into the boundary layer over the surface. Providing the coolant is distributed properly, it will act as an effective heat sink and protect the surface from the hot mainstream gases.

A primary use for film cooling is to protect the blades of the high-pressure turbine component of a gas turbine engine from hot combustion gases. Conventional film cooling may be accomplished by coolant injection through one or more rows of slots or discrete holes in the surface or through a porous strip in the surface. With these methods the region of greatest blade protection is the local region downstream of the injection sites, which are generally at the blade leading and trailing edges.

As turbine inlet gas temperature is increased in an effort to improve engine thermodynamic efficiency, it will become important to cool the high-pressure turbine blades over their entire exterior, as opposed to locally film cooling the leading and trailing edges. This may be accomplished either by transpiration cooling through a porous blade surface or by full-coverage film cooling through an array of small discrete holes that covers the entire blade surface (Esgar 1971). In principle, either method will allow the use of a mainstream gas temperature well in excess of that which will melt a metallic surface. At the present time, though, transpiration cooling appears the least feasible of the two cooling schemes, because of difficulties with the structural integrity of the porous "skin" which forms the surface, and because of susceptibility to pore clogging. Discrete hole, full-coverage cooling looks promising. The work described herein is an experimental and analytical study of heat transfer to the turbulent boundary layer over a full-coverage film-cooled surface.

1.2 Full-Coverage Film Cooling

The concept of full-coverage film cooling is illustrated in Figure 1.1, showing a blade and blade cavity. The holes on the blade surface form a staggered array; the injectant leaves the surface at an acute angle. In the film-cooling process, coolant is delivered into the interior of the blade thru an insert which forces the coolant to impinge on the inner surface of the blade. The coolant then exits through the holes and into the boundary layer over the surface at velocity U_2 and temperature T_2. The mainstream velocity is U_∞, the mainstream gas temperature is T_∞, and T_o is the blade temperature.

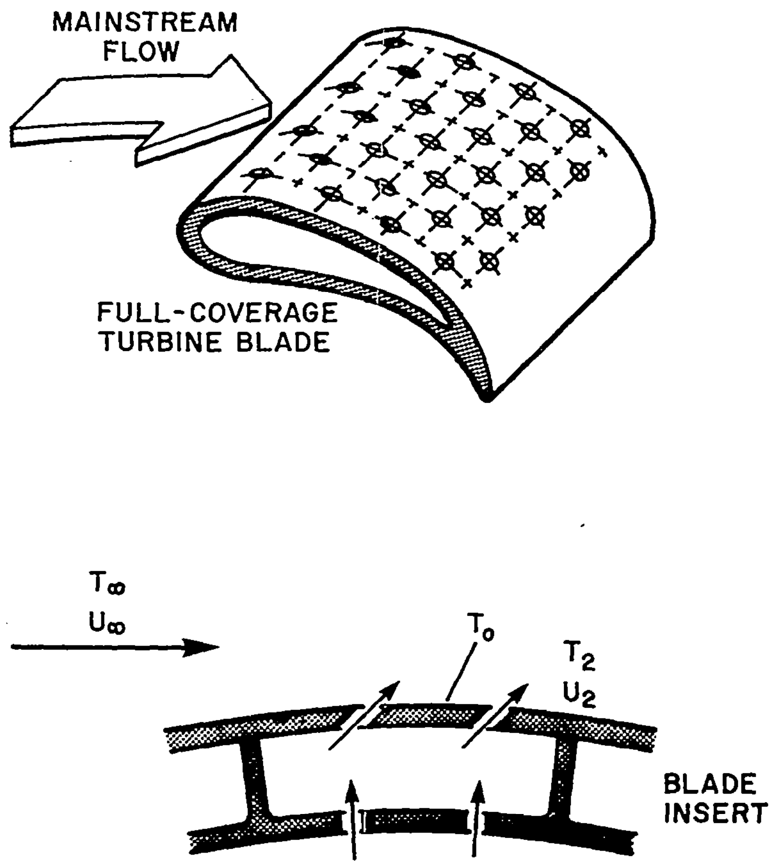

Figure 1.1 Full-coverage film-cooled turbine blade and blade cavity

Heat transfer between a surface and the fluid flowing over the surface in the presence of film cooling is affected by the hydrodynamic and thermal characteristics of the injectant and mainstream flow, the surface thermal boundary condition, and the coolant hole pattern and injection angle. One important hydrodynamic characteristic is a blowing ratio, the ratio of the injectant-to-mainstream mass flux. This can be described in two ways: averaged over the area of one hole,

$$M = \frac{\rho_2 U_2}{\rho_\infty U_\infty} \tag{1.1}$$

or averaged over the area associated with one hole (Figure 1.2)

$$F = \frac{\dot{m}_{jet}/A}{\rho_\infty U_\infty} = M \frac{\pi D^2}{4P^2} \tag{1.2}$$

The thermal characteristics of the injectant and mainstream flow can be linked to the surface thermal boundary condition,

$$\theta = \frac{T_2 - T_\infty}{T_o - T_\infty} \tag{1.3}$$

Other useful parameters include: the ratio of boundary layer enthalpy thickness-to-hole diameter, Δ_2/D ; the ratio of boundary layer momentum thickness-to-hole diameter, δ_2/D ; and the ratio of the viscous length scale to the hole diameter, $(\nu/U_\infty)/D$. The cooling configuration is described by the ratio of the hole spacing to the hole diameter, P/D , and by the hole axis angle, α .

A study of the fluid mechanics and heat transfer of a film-cooled surface has been in progress at Stanford for the past several years. The study, which includes the work reported herein, has been carried out using flat full-coverage film-cooled surfaces. The study has been conducted using geometrical and Reynolds number similarity to actual film-cooled turbine blades, but not Mach number or Eckert number similarity. Surface curvature, rotation, high mainstream turbulence, and pressure gradient effects are not considered.

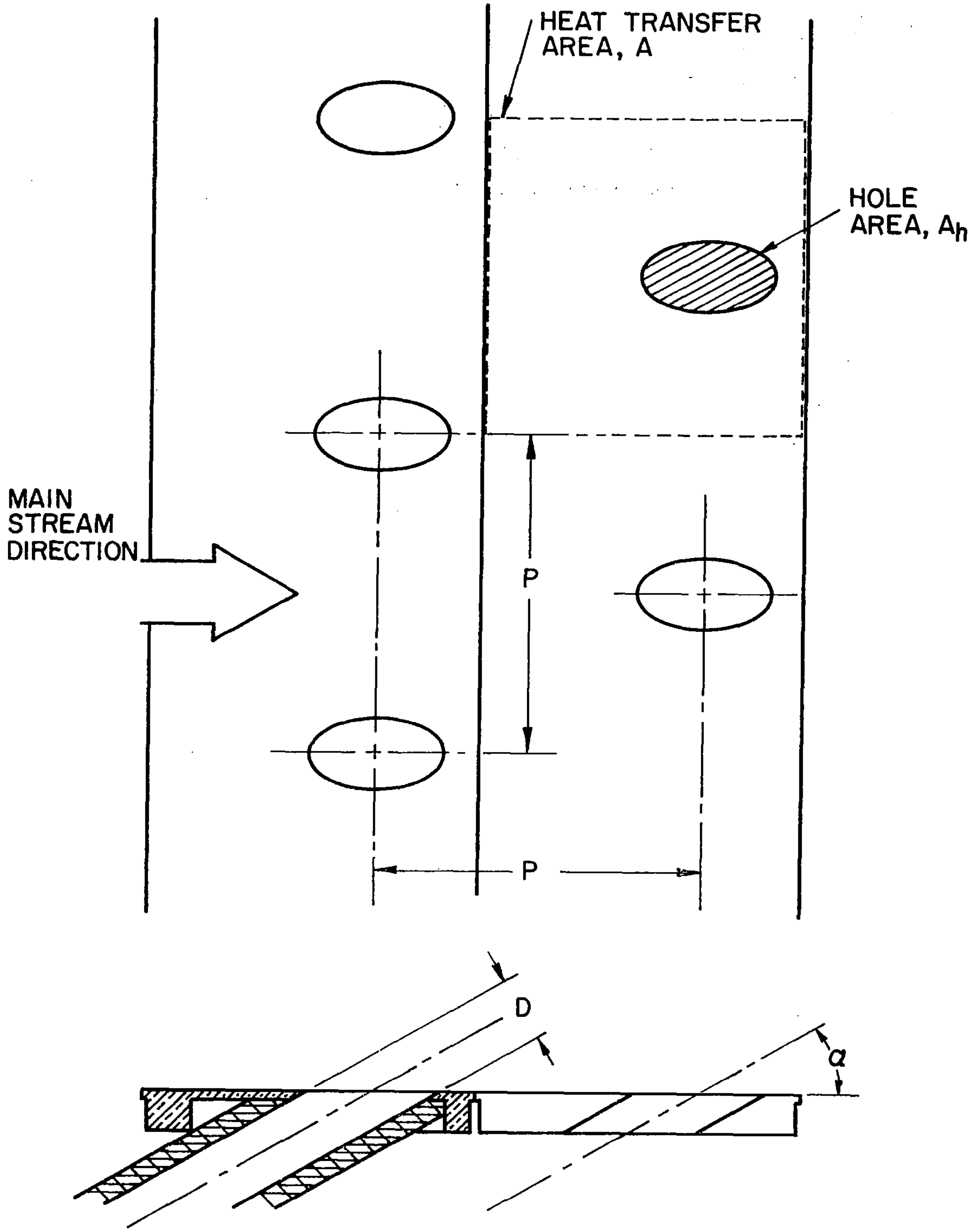

Figure 1.2 Hole-pattern and heat transfer area for slant-hole injection test surface

1.3 Heat Transfer with Film Cooling

The convective rate equation used to describe surface heat flux in boundary-layer flows with wall mass flux is

$$\dot{q}_o'' = h(T_o - T_\infty) \tag{1.4}$$

where h is a heat-transfer coefficient and T_o and T_∞ are wall and mainstream temperatures, respectively (mainstream recovery temperature, $T_{\infty,r}$, for high-velocity flows). For film cooling, the convention accepted in the past was to alter the above equation by replacing T_∞ with T_{aw}, the temperature the wall would assume in the presence of film cooling but with zero heat flux, and by replacing h with h_o, the heat transfer coefficient without wall mass flux (film cooling)

$$\dot{q}_o'' = h_o(T_o - T_{aw}) \tag{1.5}$$

In using equation (1.5) it is assumed that h_o, the heat transfer coefficient in the absence of film cooling, is also appropriate for use with film cooling. Based on this assumption, most experimental investigations to date (Goldstein 1971) have concentrated upon obtaining T_{aw} for various injection geometries and blowing ratios and correlating it in terms of a film-effectiveness parameter,

$$\eta = \frac{T_{aw} - T_\infty}{T_2 - T_\infty} \tag{1.6}$$

However, as pointed out by Metzger and Fletcher (1971) and others, the heat-transfer coefficient in the region immediately downstream of injection can be significantly different from h_o. Thus an experimental heat transfer coefficient, h^*, is required to replace h_o in equation (1.5) to predict surface heat flux.

A new approach to film cooling has been developed at Stanford, based on equation 1.4 instead of equation 1.5 (Choe, Kays, and Moffat 1976). This was evolved from consideration of transpiration cooling.

The similarities between full coverage film cooling and transpiration cooling suggested this approach; the differences proved easy to handle.

There are two important regions on a film-cooled surface, the full-coverage region and the downstream recovery region. The major concern here is in the full-coverage region, i.e., the area around the holes. Geometrically, transpiration cooling differs from full-coverage film cooling in that with the latter the holes are usually large relative to the boundary layer thickness and consequently the injectant temperature is often different from the surface temperature. From a fluid mechanics standpoint, full-coverage film cooling jets penetrate the sublayer of the turbulent boundary layer, while with transpiration cooling the injectant stays within the sublayer. From a heat transfer standpoint, with full-coverage film cooling the surface heat flux decreases to a minimum as the blowing rate increases. With a further increase in the blowing rate heat flux may begin to increase, whereas with transpiration cooling the heat flux continuously decreases. Despite these differences it is suggested that full-coverage film cooling be treated using the variables found useful in transpiration cooling since, physically, transpiration is a limiting case of discrete-hole, full-coverage film cooling as hole diameter and spacing is decreased relative to boundary layer thickness.

To approach full-coverage film cooling from the viewpoint of transpiration cooling, the concepts of h^* and T_{aw}, developed for the recovery region downstream of a slot or row of holes are abandoned, and the heat transfer convective rate equation (1.4) used with transpiration cooling is employed. In this equation the heat flux is the local average over the surface area associated with each hole (shown in Figure 1.2).

Equation (1.4) defines the heat transfer coefficient which, for the work reported herein, can be functionally described in terms of a Stanton number, dependent upon several parameters.

$$\frac{h}{\rho_\infty U_\infty c} = St = f\left[M, \theta, \frac{\delta_2}{D}, \frac{\Delta_2}{D}, \frac{\nu/U_\infty}{D}, Pr, \frac{P}{D}, \alpha, \cdots\right] \qquad (1.7)$$

As mentioned above, full-coverage film cooling differs from transpiration cooling in that the injectant can leave the surface with a temperature T_2, different from the surface temperature T_o. The heat transfer problem involves three temperature potentials as reflected by the θ parameter. With the new approach to film cooling, using equation (1.4) to define h, the dependence of the Stanton number upon injection temperature, or θ, is easily described.

To obtain Stanton number as a function of θ, experiments using two injectant temperatures are required, with all other parameters fixed, to provide two fundamental data sets. Then, appealing to the linearity of the constant-property thermal energy equation, superposition is applied to determine h or St as a continuous function of θ,

$$St(\theta) = St(\theta=0) - \theta \times [St(\theta=0) - St(\theta=1)] \qquad (1.8)$$

The θ parameter and superposition were first defined for use with film cooling by Metzger, Carper, and Swank (1968) in conjunction with transient film cooling heat transfer measurements.

1.4 Literature Review

A general review of film cooling can be found in Goldstein (1971), and a review of discrete hole film cooling is given by Choe et al. (1976). Work done at Stanford on transpiration cooling is reviewed by Kays and Moffat (1975). Contained in this section will be a review of experimental and analytical works associated with full-coverage film cooling.

1.4.1 Experimental Works

LeBrocq, Launder, and Pridden (1971) studied the effects of hole-pattern arrangement, injection angle, coolant-mainstream density ratio, and blowing ratio on η. Their tests were primarily conducted on plates with a pitch-diameter ratio of 8. The hole patterns were in-line and staggered, with normal injection (hole axis perpendicular to the surface), and staggered with 45° downstream-angled injection. Results of their investigation include: the staggered hole pattern is more effective because the jets penetrate less into the boundary layer;

there exists a blowing ratio for which η is a maximum, and for higher blowing ratios, η decreases; angled injection is more effective than normal injection.

Launder and York (1973) studied the effects of mainstream acceleration and turbulence level on η using the staggered, 45° slant-hole test section described in the previous paragraph. Bascially it was a study of laminar film-cooling jets issuing into a turbulent mainstream, and their results hinged on this fact. They found that in the presence of an accelerated mainstream the effectiveness increases due to delayed transition of the laminar jets. When the mainstream turbulence level is increased, in the accelerated region, the values of η go down 10 percent. For high mainstream turbulence without acceleration the effectiveness values remain unchanged.

Metzger, Takeuchi, and Kuenstler (1973) studied both effectiveness and heat transfer on a full-coverage surface with normal holes spaced 4.8 diameters apart and arranged in both in-line and staggered patterns. They appear to be the first investigators to report measurements of local heat transfer coefficients, h^*, within a discrete-hole array. Their investigation concludes that a staggered pattern yields a higher η than does an in-line pattern, and that h^* can be 20 to 25 percent higher than h_o (without film cooling).

Mayle and Camarata (1975) examined the effects of hole spacing and blowing ratio on heat transfer and film effectiveness for a staggered hole array with compound-angle injection. The holes were angled 30° to the plate surface and 45° to the mainstream with P/D values of 8, 10, and 14. Their results include: higher effectivenesses are obtained with P/D values of 10 and 8 than with 14, regardless of coolant-flow ratio; there is a blowing ratio that yields a maximum η; the heat transfer coefficient, h^*, is significantly higher than h_o and becomes almost constant (independent of the number of rows of holes) for all M at $P/D = 8$, but only for high blowing ratios with a $P/D = 10$; and past the last row of holes, h^* rapidly returns to h_o.

Choe, Kays, and Moffat (1976) studied the effects on heat transfer of hole spacing, blowing ratio, mainstream velocity, and initial conditions upstream of the discrete-hole array. They used normal injection with a staggered array and hole spacings of 5 and 10 diameters. Stanton number data were taken for two values of injectant temperature, corresponding to θ equal to 0 and 1, and linear superposition was applied to obtain Stanton number as a continuous function of injectant temperature. The data were correlated using the same parameters used with transpiration investigations. Their results include: for a constant mass flow F, a P/D of 10 produces a much-diminished cooling effect when compared with a P/D of 5; in the initial region (first few rows of holes) there is not much cooling and, in fact, St/St_o can be greater than unity; changes of mainstream velocity and upstream initial conditions have little if any effect on St/St_o; in the downstream recovery region, the ratio St/St_o rapidly returns to unity.

1.4.2 Analytical Works

Methods presently available to predict wall temperature, film effectiveness, and heat transfer coefficient can be categorized into three types: superposition of single-jet effectiveness data, boundary layer finite-difference methods, and energy integral equation analysis.

Superposition of film-effectiveness data for individual jets to predict η is described by Goldstein et al. (1969) and Eriksen, Eckert, and Goldstein (1971). With the method, the injection is modeled as a point heat source located above the wall, and a reduced form of the energy equation is solved and normalized to give η as a function of both spanwise and streamwise distance. Mayle and Camarata (1975) developed an improved superposition method to predict their full-coverage data. Their final prediction equation contained two parameters that are functions of M and P/D.

Prediction of wall temperature and effectiveness downstream of two- and three-dimensional film-cooling slots has been investigated by Pai and Whitelaw (1971), and Patankar, Rastogi, and Whitelaw (1973), respectively. For two-dimensional slots, the boundary layer differential equations were solved, using a mixing-length hypothesis to model the eddy viscosity. The mixing-length was augmented algebraically to reflect the large increase in turbulent mixing associated with the injection process.

For three-dimensional slots, the Navier-Stokes equations were reduced to elliptic in the cross-plane and parabolic in the direction of flow and solved numerically. Again a mixing-length hypothesis was used, with an algebraic augmentation to account for increased turbulent mixing.

A finite-difference method for predicting flow over a full-coverage film-cooled surface is reported by Herring (1975). He started with the Navier-Stokes equations and stagnation enthalpy equation and spanwise-averaged them using a decomposition that reflects the periodic nature of the flow in the lateral direction. Boundary layer assumptions were then invoked to render them parabolic. The nonlinear convective terms arising from the spanwise-averaging process were obtained from a simultaneous solution to a set of ordinary differential equations describing a jet in crossflow. Augmentation of the turbulent shear stress due to jet-boundary layer interaction was considered. He reports velocity profile predictions but no heat transfer.

Choe et al. (1976) developed both integral and differential analyses to predict their data. For the integral analysis, they developed an energy integral equation and successfully correlated their data for use in the equation, in conjunction with linear superposition. They also developed a finite-difference method for predicting heat transfer with full-coverage film cooling, solving equations of similar form to those given by Herring (1975). However, Choe et al. (1976) arrived at the equations using <u>local</u> averaging, and used different models for the injection process, the nonlinear terms, and the augmented turbulent mixing. With local averaging, the area for averaging moves continuously over the area associated with one hole (similar to that shown in Figure 1.2). With this concept they were able to model the injection process as transpiration rather than discrete injection. The nonlinear terms were modeled by decomposing them into two parts, and interpreting one part to be a contribution to increased turbulent mixing and the second part as a momentum or energy source. The augmented turbulent mixing was modeled using an algebraic equation. Choe et al. (1976) successfully predicted most of their Stanton number data for low to moderate blowing ratios and P/D values of 5 and 10 . Two constants were used in the modeling process.

To date, the only fully three-dimensional, finite-difference prediction method is given by Bergeles, Gosman, and Launder (1975). They developed a procedure for predicting the laminar hydrodynamic and thermal field over a full-coverage film-cooled surface. Their numerical scheme is a partially parabolic type, with similarities to that described by Patankar et al. (1973), but with one very important exception: the pressure field is held in a three-dimensional array to account for local mainstream-direction pressure gradients, especially in the vicinity of the injection location. The solution procedure is thus an iterative type, requiring a fairly lengthy computation time.

1.5 Objectives for the Present Research

The present study had three main objectives relating to heat transfer with full-coverage film cooling.

The first objective was to provide a broad experimental data base for use in developing integral or differential methods to predict surface heat flux on a full-coverage film-cooled surface. The data base was to contain spanwise-averaged heat transfer coefficients within the discrete-hole array, and local coefficients in the downstream recovery region past the final row of holes. Upstream initial velocity and temperature profiles were to accompany the data. The data were to be taken using two test surfaces (i.e., two different hole spacings) with systematic variation of the blowing ratio, various upstream initial conditions, and with two values of injectant temperature at each blowing ratio.

The second objective was to provide velocity and temperature profiles of the boundary layer over the discrete-hole array. The velocity profiles when spanwise-averaged would permit computation of a mixing-length profile for use in developing a mixing-length model for differential prediction of the data. The temperature profiles when spanwise-averaged would be used to compute enthalpy thicknesses for comparison with those obtained from integration of the energy integral equation.

The third objective was to carry out both an integral and a differential analysis of the data. The integral analysis was to consist of correlating the data for use in an integral energy equation prediction method. The differential analysis was to develop a finite-difference prediction method which could reproduce the experimental data base.

Chapter 2

EXPERIMENTAL FACILITY AND METHODOLOGY

2.1 Discrete Hole Rig

The heat transfer facility, hereafter referred to as the Discrete Hole Rig, was designed and built specifically for the purpose of studying full-coverage film cooling over a flat surface. The facility is documented in Choe, Kays, and Moffat (1976) and in the doctoral thesis of Choe (1975).

The Discrete Hole Rig is a closed-loop wind tunnel which delivers air at ambient pressure and constant temperature. The test section and its preplate and afterplate can be heated as much as 20°C above the mainstream air temperature. A secondary loop of the wind tunnel delivers the blowing air, heated or cooled, to the test section. Figure 2.1 shows a flow schematic of the systems that comprise the Discrete Hole Rig. A photograph is shown in Figure 2.2 .

2.1.1 Primary Air Supply System

The main loop is driven by a fan which delivers air to an oblique header which turns the flow into a heat exchanger. The flow passes through the exchanger, a screen pack, and a contraction nozzle before entering the tunnel test section. Flow leaves the test section via a plenum box which serves to supply both the secondary blower and primary fan. The test duct is 20.3 cm high by 50.8 cm wide by 3.05 m in the flow direction. The flow entering the duct has a velocity profile that is flat to within about 0.15 percent, and a longitudinal turbulence intensity of about 0.5 percent. The tunnel velocity is controlled by changing pulleys and belts on the fan and drive, and it can be varied in steps from 9 m/s to 35 m/s .

The tunnel floor consists of an upstream preplate, a test section, and a downstream afterplate. The sidewalls and topwall are plexiglass. The topwall is flexible and is adjusted to produce the desired static pressure distribution in the flow direction. For the experiments described herein a zero pressure gradient, i.e., constant velocity, boundary condition was used. To obtain this condition the top wall was set to produce a uniform static pressure for each data run, with permissible deviation of no more than 0.25 mm of water-pressure difference from the beginning of the test section to the downstream edge of the afterplate.

2.1.2 Secondary Air Supply System

The secondary loop is driven by a blower which delivers air through a flexible duct to an oblique header which turns the flow into a secondary heat exchanger to control the blowing air temperature. The flow passes through the exchanger, a bank of finned heaters, a screen pack, and into a plenum box which contains an 11-pipe manifold, with each pipe containing a valve for flow rate control.

The 11-pipe manifold splits the secondary flow into 11 channels, one for each row of holes, and delivers it via delivery tubes to the distribution manifolds. Valves in each leg of the 11-pipe manifold regulate the flow channel by channel. Hot-wire flowmeters installed in the delivery tubes measure the secondary air flow rate for each channel. Each distribution manifold contains trim-adjust valves for assuring uniform flow rate, within 1.5 percent, to each of the 8 or 9 tubes that supply a row of holes in the test section. Secondary air flow rate can be varied through pulleys and belts on the blower and drive, in conjunction with the 11 main valves, to yield a range of blowing ratios from 0 to 1.5 over the range of mainstream velocities given in the preceding section.

2.1.3 Test Plate Electrical Power System

The test-plate electrical power system delivers heater power to each of 12 plates that comprise the discrete-hole test section. Power is supplied from a 120-volt AC, 1ϕ source that is passed through two voltage stabilizers and delivered to 12 step-down variable transformers. The power is then delivered to each plate. A switching circuit allows a wattmeter to be inserted for plate power measurements.

2.1.4 Preplate/Afterplate Heating System

The preplate and afterplate heating system is a closed-loop hot-water system which operates with continuous water flow. Recirculated water passes through two water heaters in series and is delivered to an inlet manifold where it passes through rectangular tubes within the plates. From the exit manifold the water is returned to the recirculation pump. Water temperature is held constant using a set-point proportional controller connected to one of the heaters. The rectangular tubes are coupled to the feeder manifolds with individual tubes. This feature allows the preplate to be disconnected from the manifolds for tests with an unheated starting length.

2.1.5 Heat Exchanger Cooling Water System

The heat exchanger cooling system is a semi-closed loop system which continuously circulates water from an insulated holding tank. Flow rate is maintained high enough to ensure uniform temperature of the mainstream air being cooled. The secondary air heat exchanger is also plumbed into the system. Temperature control of the cooling water is achieved by dumping a portion of the recirculated water and replenishing with make-up water from a cold-water supply main.

2.2 The Test Surface

The floor of the tunnel duct constitutes the test surface, and it is formed by three sections: a preplate, a test section, and an afterplate. The preplate and afterplate are isolated from the test section with balsa wood, and the three surfaces are leveled to form a continuous, smooth surface.

2.2.1 Discrete Hole Test Section

The test section is composed of a frame and 12 plates. The frame consists of aluminum side rails with phenolic cross ribs. It is 4 cm wider than the tunnel floor span, and 61 cm long in the flow direction. Copper plates, 0.6 cm deep by 46 cm wide by 5 cm long in the flow direction, form the test surface, with the first plate blank and the 11 downstream plates containing alternating rows of 9 holes and 8 holes. The blank plate serves as a guard heater for the first blowing plate. Each of the 94 holes is connected to an individually adjusted flow tube. The holes are each 1.03 cm diameter and are spaced on 5-diameter centers to form a staggered hole array. Figure 2.3 is a photograph of the array.

The plates are heated by resistance wires installed in slots machined into the back side of each plate. There are two resistance wires for each plate, made of size 28 AWG Chromel wire, and bussed across one end with copper wire to give an overall resistance of about 8 ohms. The wire leads are connected to the test-plate electrical power system. Four iron-constantan thermocouples, made of size 30 AWG duplex wire, are installed into each plate from the back side, with each thermocouple located midway between two adjacent holes.

The plates are supported on phenolic cross ribs. The ribs have steps machined into them to support the plates and contain clearance holes for the delivery tubes, which leave the plate at a 30° angle. The side rails contain water passages for heating, to minimize conduction heat loss from the plates. Bottom plates with tube clearance holes close the frame cavity. Heating water tubes on the bottom plates, parallel to the cross ribs, serve to regulate the cavity temperature. Figure 2.4 shows a cross-sectional view of the discrete hole test section, and Figure 2.5 shows a photograph of a close-up of the test surface.

Delivery tubes for the slant-hole test section are glued into recesses cut into the back side of each plate, as shown in the photograph in Figure 2.6 . The tubes, made of linen phenolic, extend back at a 30° angle to the plate surface for a distance of 35 cm and are then turned in the downward direction by elbows. One tube in each plate contains an iron-constantan thermocouple located upstream of the point where the tube enters the frame cavity. The cavity is loosely packed with insulating material to minimize heat loss from the back sides of the plates.

2.2.2 Preplate and Afterplate

The preplate and afterplate test surfaces are identical in design. Each plate is formed by 48 rectangular copper tubes and insulated on the back side. Each tube, 2.6 cm long in the flow direction, is covered by 3 thin sheets of bakelite and a thin copper sheet. The tubes are isolated from each other with thin spacers across the tube span. An iron-constantan thermocouple is imbedded in the back side of the copper sheet. Hot water can be passed through 24 tubes in each plate for surface temperature control. The heating section of each plate butts against the test section.

Surface heat flux for each water-heated tube can be measured with a heat flux meter installed in the middle bakelite laminate and below the thermocouple location. Each meter is 5 cm wide by 0.4 mm thick and wound with multiple silver-constantan thermocouples to measure temperature difference across its thickness.

2.3 Rig Instrumentation and Measurement

Measurements of the various physical quantities necessary to compute Stanton numbers or velocity and temperature profiles are described in this section. In addition, uncertainties in their measurements are given, obtained following Kline and McClintock (1953).

2.3.1 Temperature

All surface temperatures, secondary air temperatures, and the mainstream temperature were measured with iron-constantan thermocouples. Samples of the wire were calibrated against a precision quartz thermometer, and the resulting calibration curves were incorporated into the data-reduction program.

All thermocouple wires were brought to constant temperature zone boxes at the measurement console and attached to selector switches. To avoid sharp temperature gradients along the wires, most of the wires were sheathed in plastic tubing from point of origin to the zone boxes.

The thermocouples were installed in the test section plates and side rails, following Moffat (1968), to ensure adequate immersion depth. The four thermocouples in each plate were initially used to ensure the plate was operating at near-isothermal conditions, and then were connected in parallel to provide an average surface temperature. The use of thick copper plates plus the heating of the side rails to near plate temperature gave an isothermal boundary condition.

The temperature of the mainstream air was measured with a thermocouple whose junction was normal to the flow. The indicated temperature was corrected for velocity error following Moffat (1962), and then to recovery gas temperature using a recovery factor equal to the air Prandtl number raised to the one-third power. The recovery temperature was most important in formulating the Stanton number for the $U_\infty = 35$ m/s data, where the kinetic temperature is about 5 percent of the plate-to-mainstream temperature driving potential.

Uncertainty in a thermocouple measurement was 0.14°C.

2.3.2 Pressure

Tunnel static pressure and mainstream dynamic pressure were measured with inclined manometers. Static pressure was measured from taps located in one of the tunnel sidewalls. The mainstream dynamic pressure was measured with a Kiel probe. Uncertainty in these pressure measurements was 0.25 mm water. This uncertainty also applies to the zero pressure gradient tunnel condition (recall that this condition was established by requiring a static pressure difference of no more than 0.25 mm of water between the upstream edge of the test section and the downstream edge of the afterplate).

2.3.3 Test Plate Power

Power delivered to each of the discrete-hole test plates was measured by inserting a precision AC wattmeter into the plate power circuit. Because the insertion changes the circuit impedance, a circuit analysis was carried out to account for insertion loss. The analysis is similar to the one described in Choe (1975). The insertion-loss analysis, along with the wattmeter calibration, is incorporated into the data-reduction program. Uncertainty in plate power measurement was 0.3 watts.

2.3.4 Afterplate Heat Flux

Heat transfer from each afterplate cell was measured by a heat flux meter. Each meter was calibrated by Choe (1975) to account for heat loss through the meter to adjacent plates and to the plate surface, and the calibrations are incorporated into the data-reduction program. Uncertainty in a heat flux meter measurement was 2 percent of calculated heat flux.

2.3.5 Secondary Air Flow Rate

The hot-wire flowmeters used to measure secondary air flow rate and their calibrations are described by Choe (1975). Each flowmeter consists of a constant-current heating element and a thermocouple circuit, with the circuit measuring the temperature difference between the upstream air and the heating element. The flowmeters are installed at the downstream end of 2 m delivery tubes and calibrated in place. Flowmeter calculations in the data-reduction program consider corrections due to air property changes and zero shift. Uncertainty in secondary air flow rate for a row of holes was about 3 percent of calculated flow rate.

2.3.6 Velocity and Temperature Profiles

Velocity profiles were obtained by traversing the boundary layer with a round, 0.5 mm outside diameter pitot probe. The resulting dynamic pressure was measured with a pressure transducer, calibrated with a resulting uncertainty of about 0.05 mm of water over the pressure range of interest. Uncertainty in velocity was about 1.5 percent of calculated velocity.

Temperature profiles were acquired by traversing the boundary layer with an 0.08 mm diameter chromel-constantan thermocouple probe. The probe was calibrated using a precision quartz thermometer to give an uncertainty in temperature of 0.08°C.

2.4 Formulation of the Heat Transfer Data

Experimental heat transfer data from the discrete-hole test section are presented in terms of a Stanton number, defined as

$$St = \frac{\dot{q}_{conv}}{A_{tot}\rho_\infty U_\infty c\ (T_o - T_{\infty,r})} \qquad (2.1)$$

In the above definition, A_{tot} is the total surface area for one plate, including the holes; ρ_∞, c, and U_∞ are density, specific heat, and velocity for the mainstream air; T_o and $T_{\infty,r}$ are the plate temperature and mainstream recovery temperature (see 2.3.1 for a discussion of $T_{\infty,r}$).

The $\dot{q}_{conv}$ term represents heat transferred from the test plate to the boundary layer by forced convection. To evaluate this term (based on total measured power) requires construction of a model for the heat transfer behavior of the experimental system. The model consists of an energy balance on the plate, summarized by:

$$\dot{q}_{conv} = \dot{E}_{\substack{supplied\\power}} - \dot{q}_{losses} \tag{2.2}$$

The heat losses in the above equation are decomposed into

$$\dot{q}_{losses} = \dot{q}_{rad} + \dot{q}_{cond} + \dot{q}_{flow} \tag{2.3}$$

where $\dot{q}_{rad}$ is thermal radiation from the plate top, $\dot{q}_{cond}$ is heat conduction between adjacent plates (or end plates and preplate and after-plate) and between the plate and frame, and $\dot{q}_{flow}$ is heat transferred by convection from the plate to the secondary air as it passes through the plate.

Experimental heat transfer data from the cells that form the after-plate are also presented in terms of a Stanton number, with equation (2.1) modified by replacing $\dot{q}_{conv}/A_{tot}$ with the heat flux meter signal, appropriately converted. To obtain the heat flux, equation (2.2) was used, with the terms considered to be on a per unit area basis. Equation (2.3) was also used, with the loss modes considered on a per unit area basis and $\dot{q}_{flow}$ neglected.

In the following sub-sections, heat loss components and the secondary air exit temperature will be described, along with energy balance closure tests to validate the use of equations (2.2) and (2.3). In addition, uncertainty in the Stanton number is discussed. Values of the constants used in the following section are contained in the Stanton Number Data Reduction Program in Appendix III.

2.4.1 Radiation Loss

Radiation from the plate top surface is modeled using

$$\dot{q}_{rad} = \mathrm{EMIS} \cdot A_{tot}\, \sigma\, (T_o^4 - T_\infty^4) \tag{2.4}$$

This model assumes that the radiation shape factor is 1.0, i.e., the plate sees only the plexiglass tunnel walls at T_∞, and that the air radiation absorption is negligible. There will be no radiation loss from the back side of the plate because the cavity is packed with insulation.

2.4.2 Conduction Loss

Heat transfer by conduction is modeled as

$$\dot{q}_{cond} = K_i \cdot (T_{o,i} - T_{cav,i}) + S_i \cdot (T_{o,i} - T_{o,i+1}) + S_{i-1} \cdot (T_{o,i} - T_{o,i-1}) \tag{2.5}$$

where the subscripts denote the plate under consideration and its adjacent plates, and K and S are conductances. For the afterplate, the lateral conductances were measured by Choe (1975).

The S conductances between the preplate and the first test section plate, and between the last test section plate and the afterplate, were established by experiments of the type described by Choe (1975). A calibration unit containing three heaters in an insulated shell was placed over the area where the test section joins the preplate (or afterplate), with one element over the test section plate and the other elements over the two adjacent cells. The heaters were operated in three modes: the first with the same power to all heaters; the second with one of the guard heaters off; the third with both guard heaters off. An energy balance for the cell adjacent to the test section plate (under the middle heater) permitted the values for S between the cell and the plate to be obtained.

The S conductances between adjacent plates within the test section were calculated based on the geometries and materials involved. Heat transfer results are not very sensitive to these values since all plates were operated at the same temperature in any case, within a fraction of a degree.

The K conductances between the test section plates and the frame were established by experiments of the type described by Choe (1975). The sidewalls and topwall were removed and a 9-cm thick styrofoam block was placed on top of the discrete hole test section. The plates were then heated to a uniform temperature and the frame and cavity cooled by the cold water supply, resulting in a temperature difference of about 15°C. Plate and cavity temperatures and plate power were measured and a resulting K conductance was calculated. In the calculations, heat loss through the styrofoam was considered to be 11 percent of the power provided (obtained from analytical considerations).

Definition of the effective cavity temperature was based on analysis of the frame and cavity temperature distribution. The frame was instrumented with two thermocouples each in the front and rear rails of the frame, three thermocouples along each of the two aluminum side rails, and one thermocouple in each of the four aluminum bottom plates. From this resulting temperature field, coupled with analysis, it was determined that, because the cavity was composed of low thermal-conductivity materials, base-plate temperatures had a negligible influence on the plate conduction losses. Therefore the arithmetic average of the siderail temperatures were used along with linear interpolation to obtain cavity temperatures. In fact, since the siderails and bottom plates were heated to near plate temperature to minimize conduction losses, a precise formulation of the cavity temperatures was not required.

Uncertainty in an experimentally obtained conductance was about 15 percent of its indicated value.

2.4.3 Secondary Air Exit Temperature

The secondary air exit temperature was different from the inlet temperature due to heat transfer between the air and the test section. The exit temperature is modeled by considering the system as a heat exchanger, given by

$$\frac{T_2 - T_g}{\overline{T} - T_g} = 1 - \exp\left(-\frac{KCONV}{SAFR}\right) \tag{2.6}$$

where T_g is the secondary air inlet temperature, T_2 is the exit temperature, and $\overline{T}$ is the arithmetic average of the plate and cavity temperatures (defined similarly to that in the previous section but with linear interpolation of one-third contributions from the left and right side rails and base plate temperatures). The secondary air flow rate through the tube is SAFR, and the conductance-heat transfer area product is KCONV. Both analysis and experiments were conducted to determine KCONV as a function of secondary air flow rate.

In the analysis the heat exchanger problem was defined in terms of heat transfer between the air and the tube in the cavity region, and between the air and the tube/copper lip as it passes through the plate. The analysis was performed and the predicted total conductance-area product, KCONV, and the partial conductance-area product, KFL (for the tube/lip region) were graphed on log-log paper as a function of flow rate. Experiments were then conducted to determine KCONV (and KFL, to be discussed in the next section). The sidewalls and topwall were removed for the experiments, and a 9 cm-thick styrofoam block, fabricated to cover three adjacent copper plates, was installed. Holes in the block allowed secondary air to pass through the block. For these experiments, all test section plates and the frame side rails were heated, while cooled secondary air was passed through the tubes. Power supplied to the middle of the three covered plates was measured. In addition, for one tube supplying secondary air to the middle plate, the air temperature entering the test section and leaving the styrofoam block was measured.

The experimental KCONV values were determined from equation (2.6). These data were plotted on the analysis graph and found to be a nearly constant percentage below the theoretical values, and thus the theoretical KCONV curve was shifted downward to pass through the experimental points. The theoretical KFL curve was also shifted downward by the same percentage. Experimental uncertainty in KCONV was about 25 percent of indicated value.

2.4.4 Convection Between Plate and Secondary Air

Heat transferred by convection between the plate and secondary air as it passes through the plate is modeled as

$$\dot{q}_{flow} = KFL \cdot (T_o - T_2) \tag{2.7}$$

where T_o is the plate temperature, T_2 is the secondary air exit temperature, and KFL is a conductance.

The experimental KFL values were determined from equation (2.7), using the experimental procedure described in the preceding section. In the calculation, $\dot{q}_{flow}$ was the plate power minus the power at no-flow conditions (obtained from the zero intercept of a plate power versus flow rate graph). The exit temperature was used in the definition for convenience. In principle, the secondary air temperature changes slightly while passing through the plate area, but this is insignificant because the temperature driving potential is either nominally zero, or 10-20°C.

The experimental KFL values, divided by the number of holes in the row, were plotted on the graph containing the theoretical KFL (discussed in the previous section), and they agreed within 10 to 15 percent. Experimental uncertainty in KFL was about 25 percent of indicated value.

2.4.5 Energy Balance Closure

The Stanton number is determined by measuring plate power input, corrected for wattmeter calibration and insertion losses, and subtracting the heat losses. The energy loss modes were modeled and incorporated into the data-reduction program shown in Appendix III. Energy balance closure tests were conducted to assess the validity of the models used to calculate the energy loss modes for the test section. In these tests the tunnel was operated without mainstream cooling, and the plate power was adjusted to bring each plate up to the mainstream temperature. Cold water was used to cool the frame of the test section, resulting in a plate-to-frame temperature potential of about 10°C. Tests were conducted for $M = 0$, $M = 0.41$, and $M = 0.59$. For the blowing runs, the secondary air temperature was within 0.6°C of the plate temperature. The thermal boundary conditions for these tests were designed primarily to check the conduction loss constants. Similar tests with $\theta = 0$ were not possible due to the configuration of the heat exchanger cooling system.

The closure tests showed how much energy imbalance existed for a given set of conditions and evaluated the accuracy of the energy measurement system. In principle, when equation (2.2) is evaluated for these conditions, it should sum to zero. The results of these tests, shown in

Table 2.1, indicate closure to within ± 0.24 watts (typical power supplied to each plate during a Stanton number run was 12 to 20 watts). The energy imbalance can be converted to a Stanton number uncertainty,

$$\delta St = \frac{\delta \dot{E}}{A_{tot}\rho_\infty U_\infty c\ (T_o - T_{\infty,r})} \tag{2.8}$$

To evaluate this equation, typical operating values of 13°C for $(T_o - T_{\infty,r})$ and 16.8 m/s for U_∞ were used, along with properties for air. This converts to a Stanton number uncertainty, δSt, of $\pm 4 \times 10^{-4}$.

Table 2.1

Energy balance closure tests

Plate	M = 0		M = 0.41		M = 0.59	
	$\delta\dot{E}$ (watts)	δSt	$\delta\dot{E}$ (watts)	δSt	$\delta\dot{E}$ (watts)	δSt
1	-.24	-.424E-04	.01	.255E-05	-.05	-.979E-05
2	.09	.157E-04	-.05	-.927E-05	.10	.188E-04
3	.01	.239E-05	-.08	-.148E-04	.08	.148E-04
4	.12	.218E-04	-.05	-.921E-05	.08	.140E-04
5	.06	.104E-04	-.09	-.164E-04	.06	.103E-04
6	-.11	-.208E-04	-.08	-.152E-04	.11	.206E-04
7	-.01	-.195E-05	.03	.620E-05	.07	.126E-04
8	-.10	-.172E-04	0.	0.	-.02	-.328E-05
9	-.15	-.277E-04	-.07	-.127E-04	.14	.261E-04
10	-.19	-.333E-04	-.12	-.228E-04	.15	.276E-04
11	-.20	-.360E-04	-.05	-.960E-05	.21	.386E-04
12	-	-	-.07	-.136E-04	.22	.389E-04

Using the procedure of Kline and McClintock (1953) for propagation of uncertainties through equation (2.2) and (2.3) to evaluate Stanton number, uncertainty bands on the data are predicted to be $\pm$ 2.5% for $\theta = 1$ and $\pm$ 5% for $\theta = 0$. The uncertainty analysis is in agreement with the energy balance closure tests for $\theta \simeq 1$. The larger uncertainty band for $\theta = 0$ reflects uncertainty in the plate-secondary air loss constants.

2.5 Rig Qualification

Once the energy balances were established, it was possible to run baseline checks for the hydrodynamic and heat transfer performance. Earlier qualification tests of this apparatus were reported by Choe et al. (1976).

2.5.1 Hydrodynamics

The hydrodynamic qualification consisted of determining that the tunnel flow was two-dimensional and that the approaching boundary layer velocity profiles were typically turbulent.

Two-dimensionality of the tunnel was examined by measuring the boundary layer momentum thickness at five locations across the span over the midpoint of the test section guard plate. The thicknesses were found to be uniform within 2 percent for the case of no injection at a uniform tunnel velocity of 16.8 m/s. For the low momentum thickness Reynolds number runs, the flow was accelerated over the preplate and recovered to zero pressure gradient over the test section and afterplate. For these conditions, the momentum thickness uniformity was within 10 percent. Figure 2.7 shows the topwall configurations and boundary layer trip locations for these two types of runs.

Velocity profile qualification consisted of examining the experimental profiles, checking for accepted behavior in the logarithmic and wake regions, and comparing with accepted correlations. In addition, profile shape factors were measured. These comparisons are shown on the profile graphs that accompany the Stanton number runs for $M = 0$ (given in the next chapter). They are plotted in "wall coordinates", U^+ versus y^+. The skin friction coefficient, used to form U^+ and y^+, was found by fitting the velocity data to a logarithmic law-of-the-wall in the range of 75 to 125 for y^+ (Clauser plot). Velocity profiles for the low momentum thickness Reynolds number cases are not plotted in wall coordinates because the flow was still transitional, as evidenced by the high shape factors.

For each Stanton number run, a velocity profile was taken over the guard plate midpoint to obtain the initial momentum thickness Reynolds number. From this information the turbulent boundary layer virtual origin was computed, using a relation between momentum thickness and distance, x . This relation, given in Kays (1966), is derived by integrating the momentum integral equation with a power-law velocity profile assumption.

Experimental momentum thicknesses on the guard plate were found to increase as M increased, due to the downstream flow blockage effects from the secondary air injection. This resulted in a slight decrease in the virtual origin with increasing M . To facilitate comparison of the data at the same x location, the virtual origin from the $M = 0$ velocity profile was used to compute x-Reynolds numbers for a given data set.

2.5.2 Heat Transfer

The heat transfer qualification consisted of comparing the unblown Stanton number data (the $M = 0$ run for a given data set) with accepted correlations for two-dimensional equilibrium flow over a smooth plate with constant wall temperature (see, for instance, Kays 1966). Additional comparisons were made between the unblown Stanton number data and predicted results using a boundary layer computer program.

The comparison of data with accepted correlations is shown on the graphs in the next chapter and discussed there as well. The comparisons are, perhaps, most meaningful for the data that are plotted in enthalpy thickness Reynolds number coordinates. The enthalpy thickness for those graphs are computed from the energy integral equation for constant properties and constant wall temperatures, as derived by Choe et al. (1976).

$$\frac{dRe_{\Delta_2}}{dRe_x} = St + F \times \theta \tag{2.9}$$

where $Re_{\Delta_2} = \frac{U_\infty \Delta_2}{\nu}$ and $d(Re_x) = \frac{U_\infty}{\nu} dx$. The interval of integration for the above equation, to determine $Re_{\Delta_2}(x)$, is from the midpoint of the upstream plate to the midpoint of the next downstream plate, to define the enthalpy thickness Reynolds number at that downstream location.

The unblown Stanton number data were nominally 5-7 percent above the baseline correlations in the blowing region for the P/D = 5 case. For the case of P/D = 10 , alternate holes and alternate rows in the test section were plugged, thus producing a much smoother surface with every other row completely smooth. The Stanton number deviation was nominally 3 percent for the P/D = 10 unblown case for the plates containing holes, with almost no Stanton number deviation on those plates that were completely plugged.

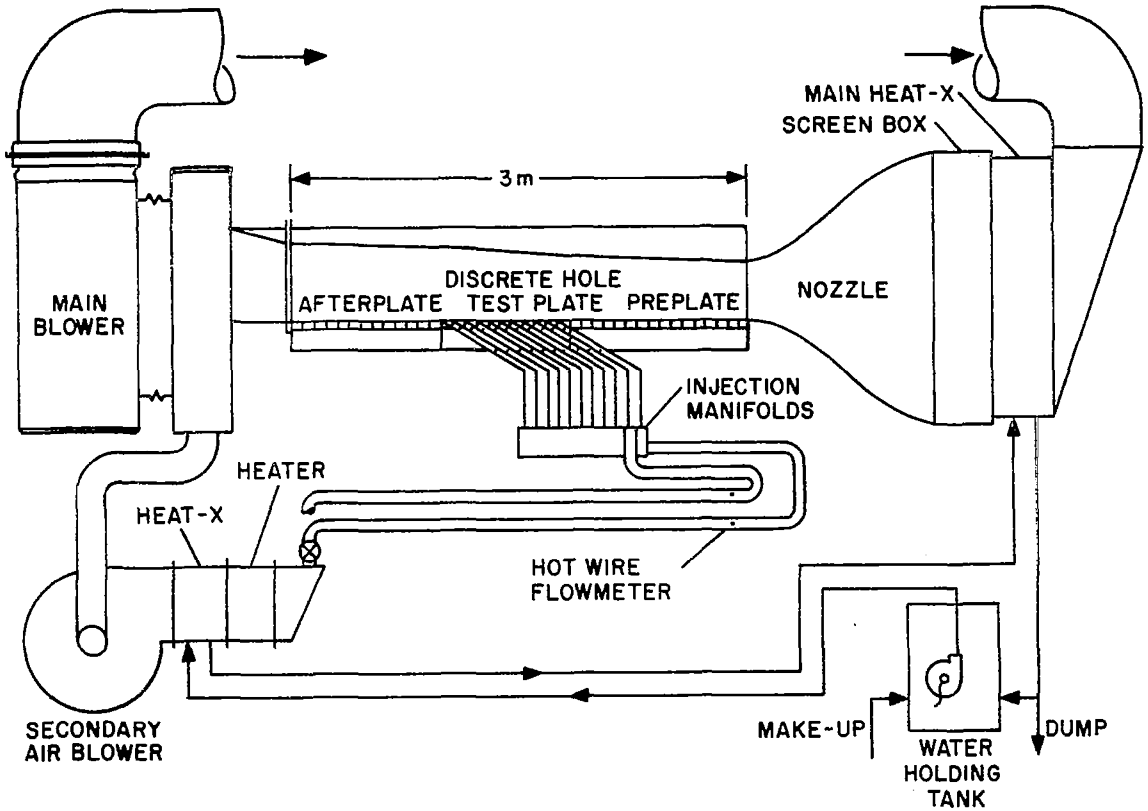

Figure 2.1 Flow schematic of wind tunnel facility, the Discrete Hole Rig

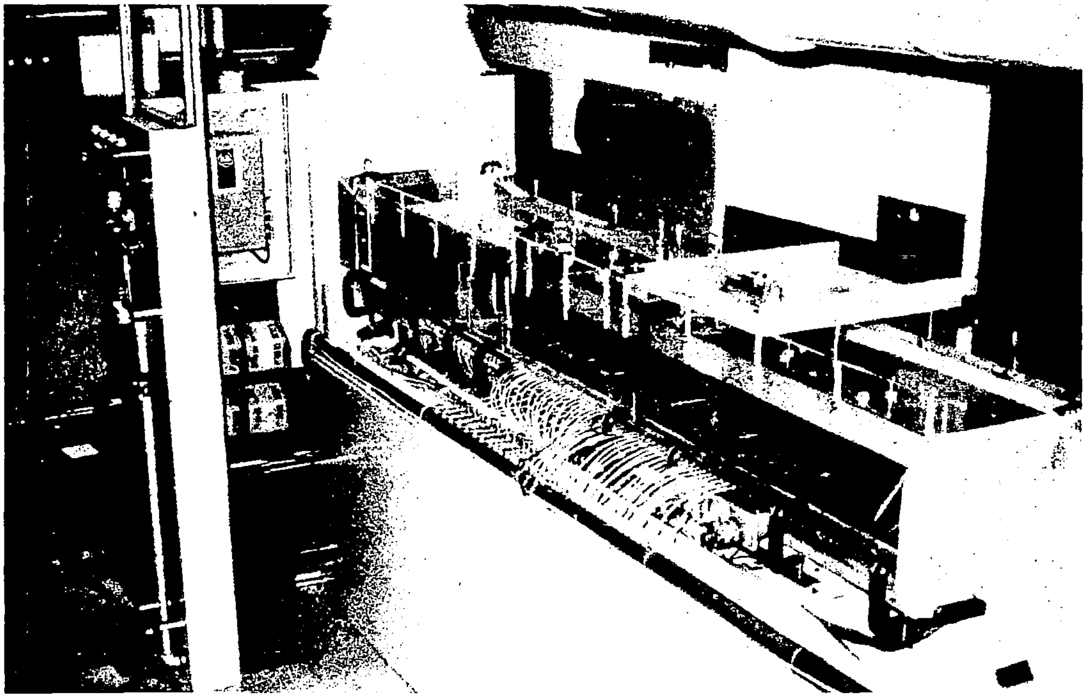

Figure 2.2 Photograph of Discrete Hole Rig

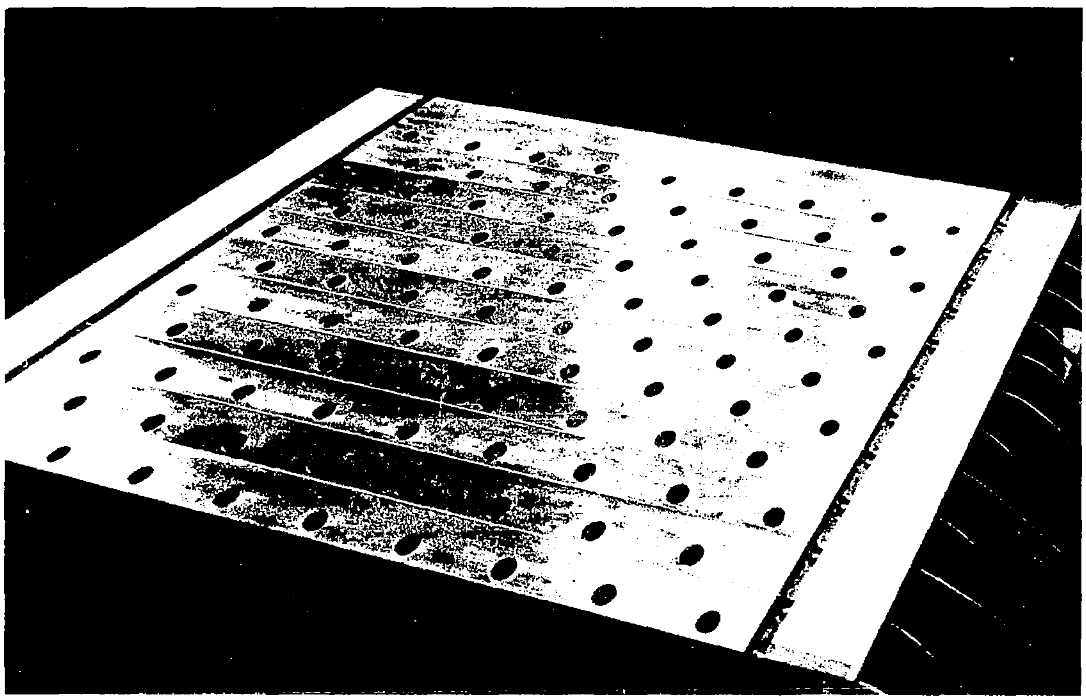

Figure 2.3 Photograph of slant-hole injection test surface, showing staggered hole array

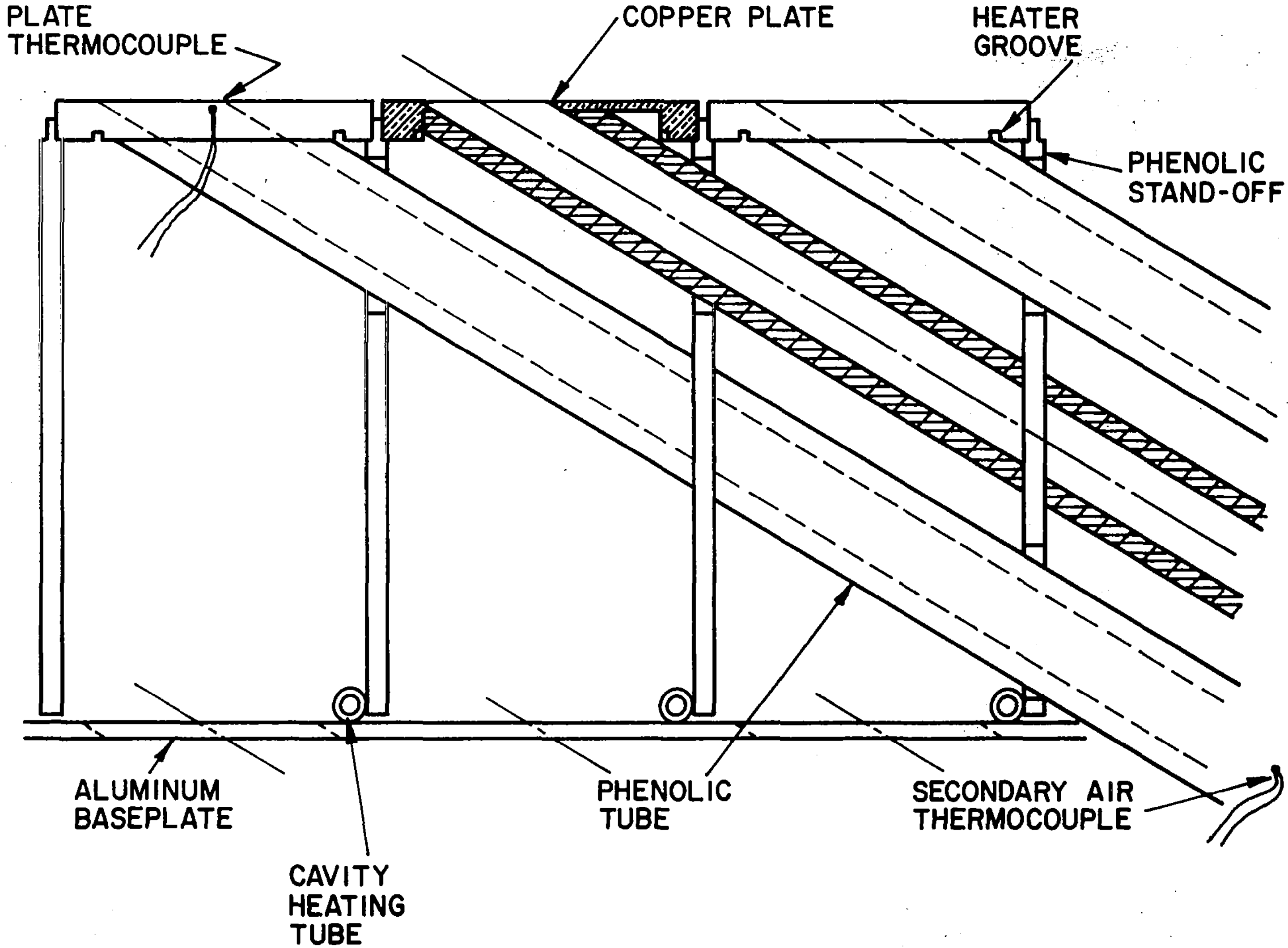

Figure 2.4 Cross-sectional drawing of the discrete hole test section

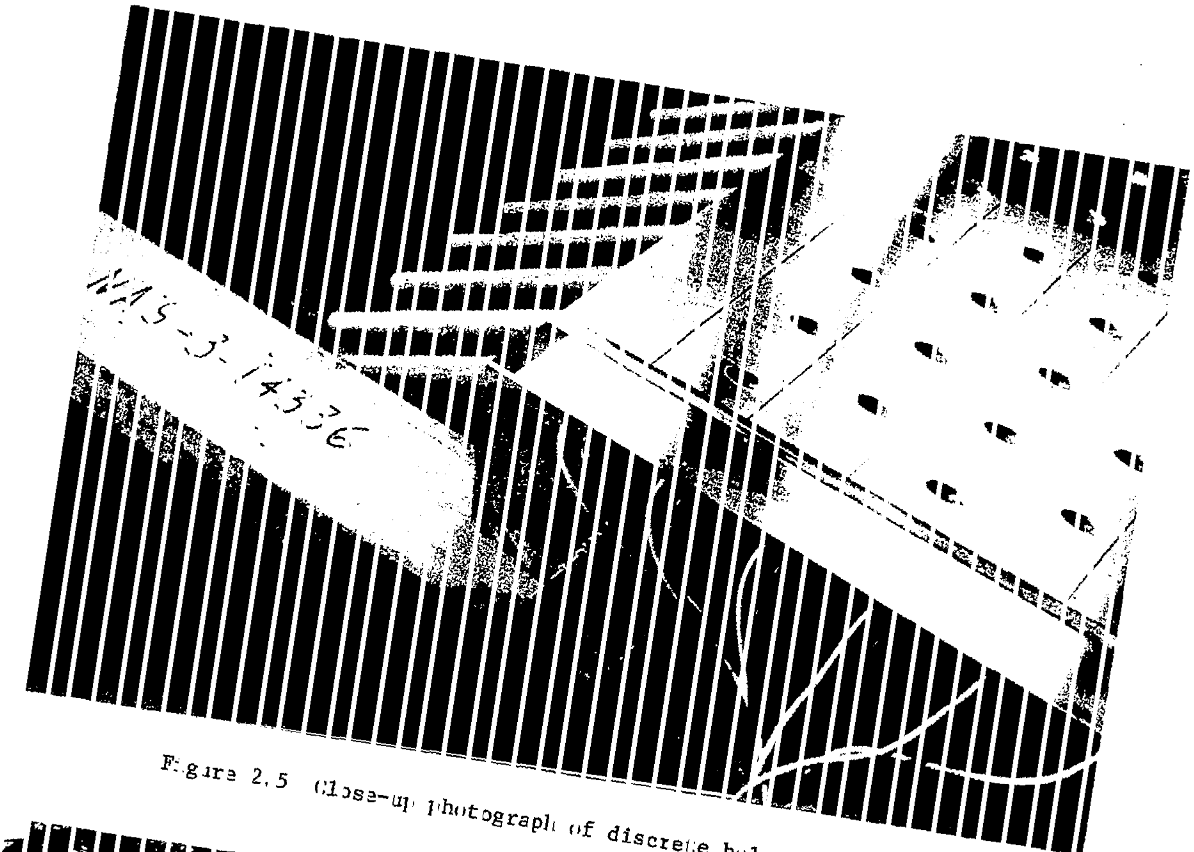

Figure 2.5 Close-up photograph of discrete hole test surface

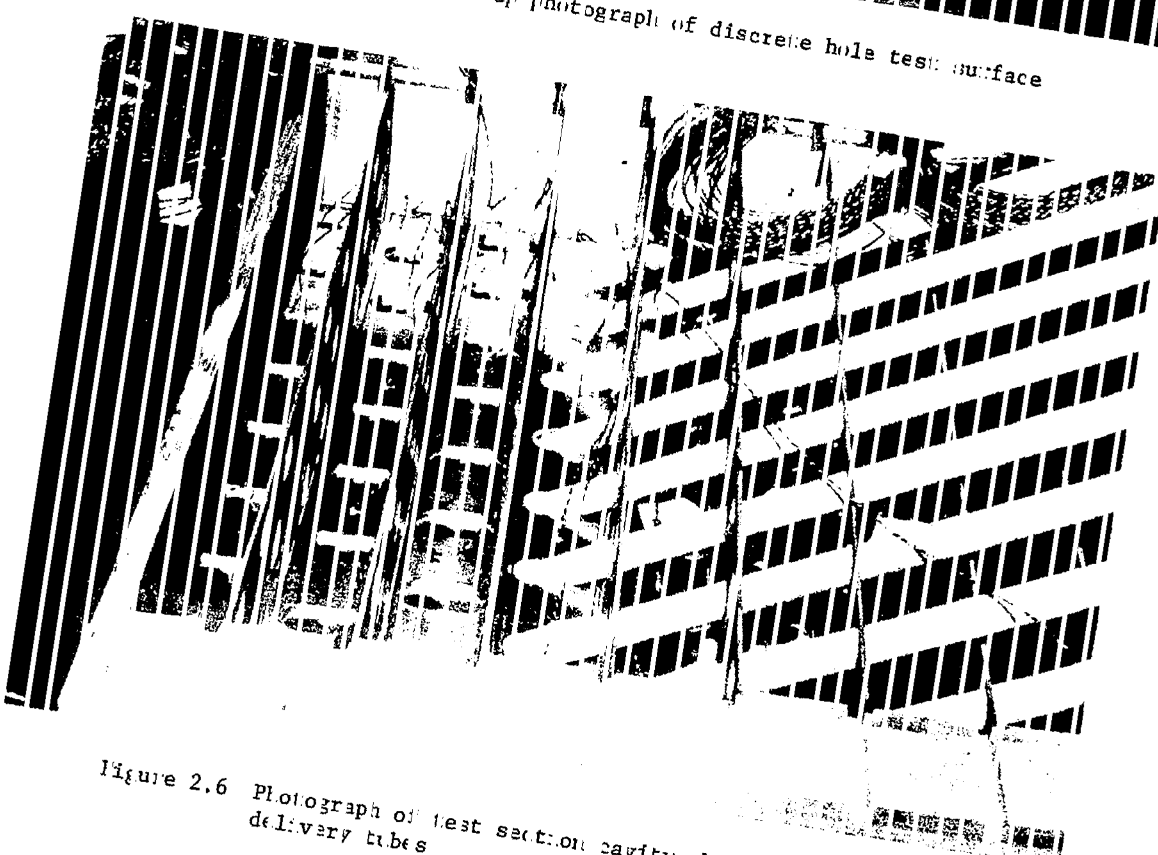

Figure 2.6 Photograph of test section cavity showing secondary air delivery tubes

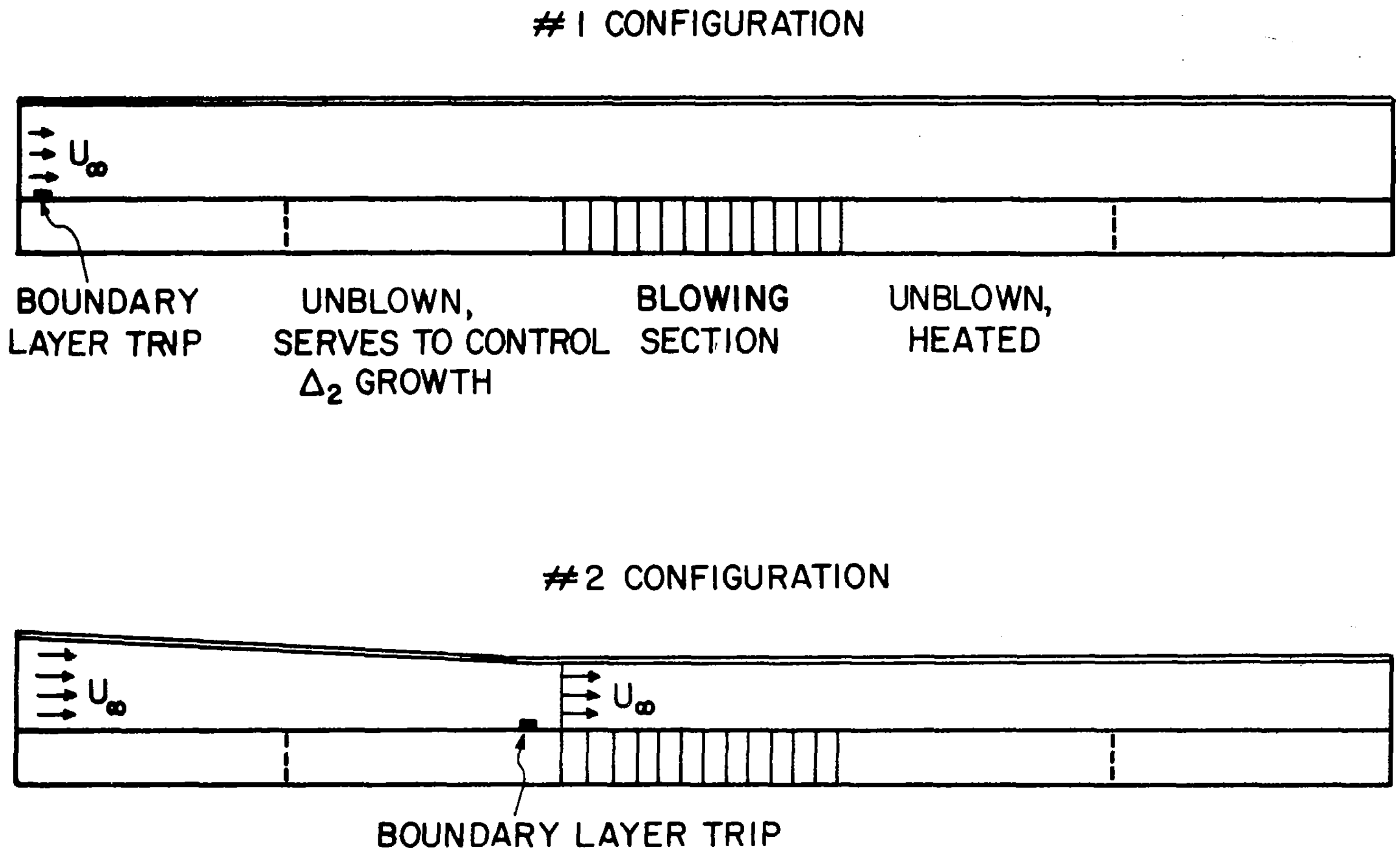

Figure 2.7 Configurations for tunnel topwall and boundary layer trip: #1 is for thick initial boundary layer; #2 is for thin initial boundary layer

Chapter 3

EXPERIMENTAL DATA

3.1 Types of Data

The primary emphasis of the experimental program was the acquisition of Stanton number data for a wide range of initial conditions and blowing ratios, and two injectant temperatures at each blowing ratio. The data were acquired for full-coverage surfaces with two different hole spacings, and for the recovery region downstream of the full-coverage surface. Mean velocity and temperature profiles of the boundary layer upstream of the blowing region were obtained to accompany the Stanton number runs. Table 3.1 summarizes the data.

A secondary emphasis of the experimental program was the acquisition of a series of mean velocity and temperature profiles within the blowing region, behind a hole in the ninth blowing row. The profiles were taken for one set of initial conditions and for one blowing ratio and two injectant temperatures at that set of conditions.

3.2 Description of the Stanton Number Data

The primary investigation was a study of the effects of the blowing ratio on Stanton number for a hole spacing-to-hole diameter ratio of 5. The tests were carried out with a mainstream velocity of about 16.8 m/s and an initial momentum thickness Reynolds number of about 2700 (in all data reported, initial conditions are those of the boundary layer over the midpoint of the upstream guard plate). In these tests an unheated thermal starting length was used to give a well-defined initial thermal condition (recall only the downstream half of the preplate could be heated).

To determine the effects on Stanton number of a thick thermal boundary layer at the upstream edge of the blowing region, data at a single value of M were taken for the hydrodynamic condition described above and with the preplate heated. The initial enthalpy thickness Reynolds number for the test with heating was about 1800. The effects of

Table 3.1

Summary of slant-hole injection data
(note, Re_{δ_2} and Re_{Δ_2} are upstream initial conditions at guard plate midpoint)

30° SLANT-HOLE INJECTION										
	Unheated Preplate						Partly Heated Preplate		Heated Preplate	
U_∞(m/s)	9.8		16.8		34.2		16.8		11.8	
Re_{δ_2}	1900		2700		4700		2700		515	
Re_{Δ_2}	70		100		160		1800		490	
P/D	5	10	5	10	5	10	5	10	5	10
M = 0	X		X	X	X		X		X	X
M = 0.2			X							
M = 0.4	X		X	X	X		X		X	X
M = 0.6			X							
M = 0.75			X	X					X	X
M = 0.95			X							
M = 1.30			X							

hole spacing on Stanton number were examined (for the hydrodynamic condition mentioned above)by reconfiguring the hole array to P/D = 10 using plugs. For these tests an unheated starting length initial condition was used, and tests were conducted at two blowing ratios.

The effects on Stanton number of changing the initial hydrodynamic boundary layer were examined in two ways: (1) Tests were conducted with a single blowing ratio, P/D = 5 , and upstream initial conditions of $Re_{\delta_2} \simeq 1900$ and 4700 and an unheated starting length. Initial boundary layer thickness-to-hole diameter ratios for these tests varied from 2.4 down to 1.9, and the tests were primarily considered to be an examination of the effects of changing the mainstream velocity, or hole diameter Reynolds number, $Re_{D,\infty}$. (2) Tests were conducted with two values of blowing ratio M , for $P/D = 5$ and 10 , and upstream initial conditions of $Re_{\delta_2} \simeq Re_{\Delta_2} \simeq 500$. The initial boundary layer thickness was about 0.5 hole diameters, and the tests were designed to examine the effects of a very thin upstream boundary layer.

At each blowing ratio, data runs were taken with two injectant temperatures: $0.0 \leq \theta \leq 0.1$, corresponding to a mainstream-temperature fluid and $0.9 \leq \theta \leq 1.1$, corresponding to surface-temperature fluid. The linear superposition equation (1.8) was then applied to the two data runs (for a given M) to adjust the data to Stanton numbers at $\theta = 0$, 1 . To adjust the recovery region data, the average value of θ for blowing rows 10 and 11 were used. The validity of the superposition principle was checked by acquiring data at $M = 0.3$ and $\theta \simeq 0$, 1 and 1.26 and comparing Stanton number predicted by superposition at $\theta \simeq 1.26$ with the experimental data at $\theta = 1.26$. The results are shown in Table 3.2 .

The data shown in the graphs are the superposition-adjusted data at $\theta = 0$, 1 . A tabular form of all the unadjusted Stanton number data, along with their adjusted values (which are plotted) are given in Appendix I.

The Stanton number data have been plotted versus x-Reynolds number and enthalpy thickness Reynolds number. The x-Reynolds number is a convenient nondimensional x coordinate that shows Stanton number as a function of M and θ for the same x location on the test surface. Enthalpy thickness Reynolds number reflects the energy content of the boundary layer and is perhaps most meaningful for the $\theta = 1$ data plots. Determination of the virtual origin for Re_x , and the enthalpy thickness for Re_{Δ_2} , is discussed in Sections 2.5.1 and 2.5.2 .

On the Stanton number graphs, the first 12 points are for the test section plates. An arrow denotes the twelfth data point. The remaining points are for every other recovery region plate. As indicated in Section 2.5.2, the reference lines shown on the x-Reynolds

Table 3.2

Comparison of experimental Stanton numbers with Stanton numbers predicted by applying superposition to experimental data at $\theta \simeq 0,1$

Plate	St($\theta \simeq$ 1.26) experimental	St(θ = 1.26) theoretical	Error %
2	.00250	.00249	- 0.4
3	.00178	.00180	+ 1.1
4	.00147	.00148	+ 0.6
5	.00136	.00139	+ 2.2
6	.00129	.00124	- 3.9
7	.00118	.00118	0
8	.00113	.00114	+ 0.9
9	.00104	.00102	- 1.9
10	.00102	.00097	- 5.0
11	.00095	.00093	- 2.1
12	.00093	.00093	0
15	.00114	.00106	- 7.0
18	.00118	.00116	- 1.7
21	.00118	.00116	- 1.7
24	.00120	.00118	- 1.7
27	.00126	.00124	- 1.6
30	.00133	.00128	- 3.8
33	.00132	.00131	- 0.8

number and enthalpy thickness Reynolds number graphs are accepted correlations for two-dimensional equilibrium flow over a smooth plate with constant wall temperature and hydrodynamic and thermal boundary layers beginning at the same point.

3.3 Stanton Number Data

The experimental Stanton number data have been segregated into four sections for discussion. Certain data trends are common to all the data; these will be discussed in detail only in Section 3.3.1. More complete analysis of the data will be found in Chapter 4.

3.3.1 Thick Initial Boundary Layer with Heated Starting Length

The first data set to be discussed is for $M = 0$ and for $M = 0.4$. The trends exemplify the general behavior common to all of the full-coverage Stanton number data sets which follow. Also, the $M = 0.4$ blowing ratio for this data set will be common to all the data sets which follow. Initial conditions of the boundary layer for this set were $Re_{\delta_2} \simeq 2700$ and $Re_{\Delta_2} \simeq 1800$.

M = 0. The first data obtained in each data set were with $M = 0$ to establish a baseline. Figure 3.1 shows the initial velocity profile over the midpoint of the guard plate for this run, and Figure 3.2 shows the initial temperature profile. Information concerning the profiles is given in the profile graphs. The velocity profile is seen to be a typical turbulent boundary layer profile, with a boundary layer thickness of about two hole diameters. The Stanton number data are plotted versus Re_x in Figure 3.3, and versus Re_{Δ_2} in Figure 3.4. In the latter figure, the data are seen to rise 8 to 10 percent above the generally accepted St_o curve, hereafter called the equilibrium line. This is attributed to a roughness effect of the open holes on the boundary layer. In the recovery region the Stanton number drops to within two percent of the equilibrium line within a few boundary layer thicknesses. The roughness effect will be seen more clearly in conjunction with the $P/D = 10$ data in Section 3.3.4.

$\theta = 1$ $(T_2 = T_o)$. In Figure 3.3 (Re_x) the Stanton number is seen to drop 10 percent below St_o for the first blowing plate and 30 percent below St_o for the second plate. This 10 and 30 percent drop is common to all $P/D = 5$ data and low M, and it is discussed in Appendix IV. The Stanton number continues to monotonically decrease throughout the blowing region. In the recovery region Stanton number shows a gradual rise. The data are replotted in Figure 3.4 (Re_{Δ_2}). There is a wide spacing between data points because the injectant greatly increases the enthalpy content of the boundary layer. By the end of the blowing section $Re_{\Delta_2} \simeq 10{,}000$, and the momentum boundary layer thickness was 6 to 7 cm.

The boundary layer is highly non-equilibrium at the end of the blowing section, and over the 60 cm recovery region test plate (about 10 boundary layer thicknesses) the Stanton number does not recover to the equilibrium line. The retarded recovery is related to the excess enthalpy content of the thermal profile associated with a momentum boundary layer that does not have the turbulent transport necessary to diffuse the profile. This is discussed in more detail in Chapter 4.

The monotonic decrease in Stanton number in the blowing region is also typical of transpiration cooling. The two cooling schemes can be compared for any M by computing an equivalent blowing fraction, F, using equation (1.2). Transpiration Stanton numbers as a function of F can be found in Kays and Moffat (1975). For all low M data the $St(\theta = 1)$ data for discrete hole injection are much higher than the equivalent transpiration Stanton numbers. Blowing at $M = 0.4$ with $P/D = 5$ converts to $F = 0.012$, which would "blow off" a transpiration boundary layer, producing zero heat flux.

<u>$\theta = 0$ $(T_2 = T_\infty)$.</u> In Figure 3.3 (Re_x) the Stanton number rises for the first few blowing rows and then drops down slightly and levels out to an almost asymptotic value, independent of the number of rows of holes. The asymptotic behavior is exhibited by all of the slant-hole data for $M \geq 0.4$ at $P/D = 5$, and for $M = 0.8$ at $P/D = 10$. For the recovery region, once the intense mixing from the jet-mainstream interaction is removed, the Stanton number rapidly drops below the St_o data over a distance of about five boundary layer thicknesses, and then returns towards the St_o data. The drop is in response to a much-thickened boundary layer without increased turbulent mixing. The data are replotted in Figure 3.4 (Re_{Δ_2}). The closely spaced data reflect the fact that the mainstream-temperature injectant does not increase the enthalpy content of the boundary layer (see equation 2.9). In the recovery region, the boundary layer rapidly adjusts to no-blowing conditions. A similar fast adjustment is seen in transpiration cooling data (Kays and Moffat 1975). By the end of the recovery region the boundary layer has almost returned to the equilibrium line.

Asymptotic behavior for the $\theta = 0$ thermal condition was also observed by Mayle and Camarata (1975) for compound-angle injection with $P/D = 8$ and 10 and moderate M. They write, in explanation:

> "This indicates that the flow field near the surface is streamwise periodic and dominated by the jets. Thus, it appears that as the hole spacing is decreased or the coolant flow increased, a transition is gradually made in which the usual streamwise growth of the thermal boundary layer yields to a periodic growth governed by the jets."

This assessment seems plausible. However, as will be discussed in Chapter 4, it is believed that the phenomenon of a nearly constant Stanton number also implies a nearly constant turbulent transport or eddy viscosity/conductivity with respect to the streamwise direction, independent of boundary layer growth. Appendix V contains a discussion of a possible similar type of asymptotic behavior for the $\theta = 1$ data, along with a discussion of possible jet coalescence, which might contribute to it.

3.3.2 Thick Initial Boundary Layer with Unheated Starting Length

The second data set to be discussed is the most comprehensive set in that it formed the basis for the study of the effects of blowing ratio and hole spacing on Stanton number. This data set includes P/D of 5 and 10 with the initial $Re_{\delta_2} \approx 2700$ and an unheated starting length.

$M = 0.$ The initial velocity profiles for the unblown Stanton number runs are shown in Figure 3.5 . The St_o data are plotted versus Re_x and Re_{Δ_2} in Figures 3.6 through 3.10 . In the Re_{Δ_2} plots the data approach the equilibrium line and pass slightly above it near the downstream edge of the test section. The approach from below is indicative of an unheated starting length, and the pass over the line, coupled with the drop in the recovery region, again suggests the roughness effect on Stanton number due to the discrete holes. The roughness effect is diminished, though, for the wider hole spacing.

$\theta = 1$ $(T_2 = T_o)$. In Figure 3.6 (Re_x) Stanton number data are plotted for $P/D = 5$ and with M varying from 0 to ~ 1.2 in increments of ~ 0.2 . In the blowing region $M = 0.18$ yields the lowest Stanton number over the first three plates, with $M = 0.37$ producing the lowest value over the rest of the blowing region. Note the $\sim$ 10 percent and $\sim$ 30 percent drop in St for the first two blowing rows. Values of M greater than 0.37 cause the Stanton number to rise above the minimum values, with $M = 1.21$ causing the Stanton number to pass above the $M = 0$ curve over most of the blowing region. This increase in Stanton number with increase in blowing is attributed to the jets penetrating farther into the boundary layer to provide less protection and to increase the turbulent mixing. In the downstream recovery region the Stanton number data appear to rise immediately for $M = 0.18$ and to remain unchanged for $M = 0.37$. For all larger M the Stanton number continues to decrease throughout the recovery region. The recovery region flow length is about 63 cm. Thus, for a δ of 5 to 7 cm at the start of this region, the recovery flow length for the data is about 9 to 12 δ. These data are replotted in Figure 3.7 (Re_{Δ_2}). The $M = 0.18$ and 0.37 data lie below the two-dimensional equilibrium line in a manner characteristic of transpiration-cooled surfaces. Data for $M = 0.52$ lie near the equilibrium line, with all larger values of M lying above the equilibrium line. In the recovery region the data for $M \leq 0.4$ appear to be returning to the equilibrium line. For higher blowing, the data trend is uncertain.

The $P/D = 10$ data are shown plotted versus Re_x in Figure 3.9. The $M = 0.36$ data produce a minimum Stanton number in the blown region with the $M = 0.75$ data lying above the low blowing ratio data. Stanton number variation in the blowing region is due to alternate rows of holes being plugged. The data from Figure 3.9 are replotted in Figure 3.10 (Re_{Δ_2}). In the recovery region, the Stanton number for $M = 0.36$ and $\theta = 1$ is seen to return to the equilibrium line. However, the recovery region data for $M = 0.75$ and $\theta = 1$ appear not to be returning to the line. This is attributed to a problem with the heat flux sensor response to a three-dimensional flow in the recovery region. For $P/D = 10$ and high M, the flow should be much more three-dimensional than its counterpart at $P/D = 5$, primarily due to increased jet penetration because of the "individuality" of the jets for the wider spacing. Because the flow width for "averaging" of the heat flux with afterplate is 5 cm and the discrete holes are spaced about 10 cm apart, any three-dimensional effects will greatly affect the sensor. A similar anomaly was seen by Choe et al. (1976) for the data set obtained with natural transition over the blowing region, indicating the heat flux sensors were not responding to give a spanwise-averaged heat transfer coefficient, when compared to the test section plate values.

Visual comparison of the $P/D = 10$ data with the $P/D = 5$ data reveals that the major effect of increased hole spacing is to reduce the effect of blowing i.e. to reduce the Stanton number departure from St_o. Stanton number is the nondimensional heat transfer coefficient, averaged over the area associated with one hole. This area increases by a factor of four for the increased hole spacing, and thus there is much less coverage for each jet. There are two bases for comparison of heat transfer performance of the two P/D surface configurations. The first basis is at the same blowing ratio, M, and the second basis is at the same blowing fraction, F. At a specified F, the same mass flow of coolant will be injected for the two P/D surfaces to provide protection. The data for $P/D = 5$, 10 will be compared on an F basis in Chapter 4.

<u>$\theta = 0$ $(T_2 = T_\infty)$.</u> In Figure 3.6 (Re_x) Stanton number data are plotted for $P/D = 5$. In the blowing region the $M = 0.2$ and 0.4 data have a pattern that is different from the higher blowing ratio data. The $M = 0.20$ curve follows the $M = 0$ curve over the first eight blowing rows and then gradually diverges. The $M = 0.40$ curve follows the $M = 0$ curve over the first four blowing plates before diverging. For all higher values of M the data depart abruptly from St_o after the second data point. In the downstream blowing region the curves exhibit an asymptotic behavior, indicating that a local equilibrium has been established between the surface and the fluid in the near-wall region. In the recovery region the data for $M = 0.2$ and 0.4 immediately dip below the $M = 0$ curve. For $M \geq 0.58$ the Stanton number data decrease much more slowly in the recovery region, and for $M \geq 0.93$ the data lie above the $M = 0$ curve over the entire recovery region. The data are replotted versus Re_{Δ_2} in Figure 3.8. Most of the data lie above the

two-dimensional equilibrium line in the blowing region. For $M \leq 0.4$ the data dip below the reference line in the initial recovery region, and then appear to return toward it. Trends in the data are uncertain for higher blowing ratios, but they appear to be returning toward the equilibrium line.

In the initial blowing region for high blowing ratios, the Stanton number is seen to rise and then drop back towards its eventual asymptote. A similar Stanton number rise is seen in the initial blowing rows for the $\theta = 1$ data. This behavior may be due to less jet penetration, coupled with increased turbulent mixing in the near-wall region. Flow visualization photographs by Colladay and Russell (1975) support the less penetration idea, and the computer predictions in Chapter 4 support the increased mixing idea. Physically, there should be higher upstream boundary layer momentum in the near-wall region to turn the jets. As the boundary layer flows over the rows of holes, though, a larger boundary layer momentum deficit is created, and the jets are able to penetrate farther into the boundary layer before being turned into the downstream direction.

The $P/D = 10$ data are shown plotted versus Re_x in Figure 3.9 and versus Re_{Δ_2} in Figure 3.10. The data for the high blowing ratio do not appear to reach an asymptote, whereas the data at the same M and $P/D = 5$ do reach an asymptote. This is partly attributed to the unheated starting length initial condition. The same type of tests were conducted at P/D of 5 and 10 with a heated starting length, discussed in the following section.

3.3.3 Thick Initial Boundary Layer with Change in Mainstream Velocity

The third data set to be discussed is part of the study of the effects on Stanton number of changes in the upstream hydrodynamic boundary layer. For this data set, obtained on the $P/D = 5$ surface, blowing ratios of $M = 0$ and $M = 0.4$ were used, and initial conditions were $Re_{\delta_2} \simeq 1900$ and 4700 and an unheated starting length.

$M = 0$. Initial velocity profiles for the $Re_{\delta_2} \simeq 1900$ data and $Re_{\delta_2} \simeq 4700$ data are shown in Figures 3.11 and 3.14, respectively.

Parameters for these boundary layers are compared with the $Re_{\delta_2} \simeq 2700$ profile parameters (discussed in Sections 3.3.1 and 3.3.2), as shown below

Re_{Δ_2}(inl.)	Re_{δ_2}(inl.)	U_∞ (m/s)	$Re_{D,\infty}$	$\delta_{.99}/D$	δ_2/D
70	1900	9.8	6500	2.4	.30
100, 1800	2700	16.8	11200	2.0	.23
160	4700	34.2	22400	1.9	.21

In the above table, $Re_{D,\infty}$ is a hole-diameter Reynolds number, $Re_{D,\infty} = U_\infty D/\nu$ (see Section 4.2 for a discussion of this Reynolds number). The three boundary layers have about the same thickness ratios, while the mainstream velocity is significantly different for the three runs.

$\underline{\theta = 1 \quad (T_2 = T_o)}$. The initial $Re_{\delta_2} \simeq 1900$ data are plotted in Figure 3.12 (Re_x) and 3.13 (Re_{Δ_2}) . The initial $Re_{\delta_2} \simeq 4700$ data are plotted in Figure 3.15 (Re_x) and 3.16 (Re_{Δ_2}) . All of the data drop below the St_o data in the blowing region and indicate a slight rise in the recovery region. The trend is identical to the initial $Re_{\delta_2} \simeq 2700$ data of Section 3.3.1 .

$\underline{\theta = 0 \quad (T_2 = T_\infty)}$. The initial $Re_{\delta_2} \simeq 1900$ data are plotted in Figure 3.12 (Re_x) and 3.13 (Re_{Δ_2}) . The Stanton number is seen to depart from the St_o data after the first blowing row, and in the recovery region it dips significantly below the St_o data before returning. The initial $Re_{\delta_2} \simeq 4700$ data are plotted in Figure 3.15 (Re_x) and 3.16 (Re_{Δ_2}) . The data are seen to follow the St_o data for about five blowing rows before departing, and in the recovery region the Stanton number returns to the equilibrium line without dipping below it.

The response of the Stanton number to $\theta = 0$ injectant and $M = 0.4$ is entirely different for each of the four initial conditions discussed to this point. In all cases the Stanton number data for $\theta = 0$ appear not to reflect the presence of the mainstream-temperature injectant (at least for low M) until the thermal boundary layer grows beyond the penetration distance of the injectant. For the initial condition of an unheated starting length and for the first few rows of holes, the thermal boundary layer was extremely thin when compared to the diameter of the jet. For this initial condition, $St(\theta = 0) \simeq St_o$ until the thermal boundary layer thickens. For the heated starting length data of Section 3.3.1, $St(\theta = 0) >> St_o$ beginning with the second blowing plate, reflecting the already existing thermal layer. The various data at $M = 0.4$ will be compared in Chapter 4.

3.3.4 Thin Initial Boundary Layer with Heated Starting Length

The last data set to be discussed is the second part of the study of the effects of the upstream hydrodynamics. This data set was obtained on the $P/D = 5$ and 10 surfaces, and the initial conditions were $Re_{\delta_2} \simeq Re_{\Delta_2} \simeq 500$.

M = 0. Figure 3.17 shows two initial velocity profiles, taken for the St_o data runs, and Figure 3.18 shows corresponding temperature profiles. The profiles exhibit outer region similarity, but the inner region differences, plus the shape factor information for the velocity profiles, indicate the flow is still probably transitional on the guard plate (the virtual origin is about 19 cm upstream). The St_o data in Figures 3.19 through 3.22 indicate, however, that by time the second plate is reached, the flow is completely turbulent and the boundary layer is an equilibrium layer (see Section 2.5.1 for a discussion of how the thin boundary layer was obtained). The initial boundary layer thickness is about one-half of one hole diameter, while the mainstream velocity is midway between that for the $Re_{\delta_2} \simeq 1900$ and 2700 boundary layers.

The St_o data for $P/D = 5$ are seen to be about 8 to 10 percent above the equilibrium line in the test plate region, and for $P/D = 10$, the St_o data lie on the equilibrium line. Presumably the difference is due to the effect of hole roughness on the boundary layer; with this wide hole spacing, 71 percent of the holes were plugged, thus yielding an effectively smoother surface. Note that the alternate data points in the blowing region (where all the holes in the blowing row are plugged) deviate even less. The St_o data in the recovery region are seen to lie slightly below the equilibrium lines, in either Re_x or

Re_{Δ_2} coordinates, partly because no variable property correction has been applied to the data. This correction, for an experimental ΔT of about 15°C is about 2 percent (see Kays 1966).

$\underline{\theta = 1 \ (T_2 = T_o)}$. The data for $P/D = 5$ are plotted in Figure 3.19 (Re_x) and 3.20 (Re_{Δ_2}). The data trend is the same as that exhibited by the $Re_{\delta_2} \simeq 2700$ data in Figure 3.3 or 3.6. The $M = 0.4$ data provide the lowest values of Stanton number, with higher blowing ratios causing an increase in Stanton number over the blowing region. In the recovery region, the $M = 0.4$ data level out, while Stanton number for the higher blowing ratio drops, indicative of a much-thickened thermal boundary layer. The $P/D = 10$ data are plotted in Figure 3.21 (Re_x) and 3.22 (Re_{Δ_2}). The major effect of the increased hole spacing is, again, a much diminished departure of the Stanton number from St_o.

$\underline{\theta = 0 \ (T_2 = T_\infty)}$. The data for $P/D = 5$ are plotted in Figure 3.19 (Re_x). The data trend follows that of Figure 3.3 for a heated starting length condition in that it reaches an asymptote, independent of the number of blowing rows. In the recovery region, the Stanton number appears to be slower in returning to the equilibrium line when compared to the high Reynolds number data of Figure 3.3. The data are replotted in Figure 3.20 (Re_{Δ_2}). The slow return to equilibrium can be more easily seen in this graph. This apparent slow return may be due to the thin momentum boundary layer and its effect on the turbulent mixing. During the course of prediction of the $M = 0.4$ data (see Chapter 4), the same two "model constants" satisfactorily predicted the initial $Re_{\delta_2} \simeq 1900$, 2700, and 4700 data, with either heated or unheated starting length, but the mixing length model constant was low for the initial $Re_{\delta_2} \simeq 500$ data. This result, coupled with the slow return of St to equilibrium downstream of the blowing region, may be an indication of a different turbulent structure for a boundary layer whose thickness is on the order of the diameter of the jets.

The $P/D = 10$ data are plotted in Figure 3.21 (Re_x) and 3.22 (Re_{Δ_2}). Visual comparison with the $P/D = 5$ data of Figures 3.19 and 3.20 reveals again (see Section 3.3.2 for a parallel study and discussion at high Re_{δ_2}) that the major effect of increased hole spacing is to reduce the overall level of the Stanton number departure from St_o . The data for $P/D = 5$ and 10 will be compared on a blowing fraction basis in Chapter 4.

3.4 Spanwise Velocity and Temperature Profiles

The boundary layer over the film-cooled surface was probed to obtain profiles for use in developing a mixing-length turbulence model, and for confirmation of computed $Re_{\Delta_2}(x)$ from equation 2.9 . The profile data were obtained for initial and boundary conditions of the data set described in Section 3.3.1 ($Re_{\delta_2} \simeq 2700$, $Re_{\Delta_2} \simeq 1800$, $M = 0.4$, and $\theta = 0, 1$) . The profile data are tabulated in Appendix II.

Figure 3.23 shows 11 velocity profiles acquired downstream of an injection hole in the ninth blowing row, along with a sketch of the locations where they were acquired. The profiles were taken with isothermal conditions to eliminate variable property effects. Profiles 1 and 11, 2 and 10, 3 and 9, etc., would be identical if the flow were perfectly symmetrical. Note that locations 1, 6, and 11 are symmetry line locations for the discrete hole array. Comparison of profiles 1 and 11 show the flow is indeed symmetrical at these locations, but at the intermediate locations, a slight lack of symmetry is found. Uncertainty in the experimentally-acquired profiles is 5-10 percent in the near-wall region because of uncertainty in the static pressure field around the jets (especially for profiles 5 through 7).

Profiles 1 and 11, taken five hole diameters downstream of an injection site, show the presence of the upstream jet. It is attached to the wall with a peak velocity of about $0.5\ U_\infty$, whereas the fluid was injected with a velocity of $0.4\ U_\infty$. This increased velocity is in response to conservation of the jet axial and transverse momentum as the jet is turned into the downstream direction by the boundary layer flow (Campbell and Schetz 1973 give a very comprehensive and excellent treatment of the equations governing a jet in cross flow). Profile 6 shows the jet lifted from the surface due to the 30 degree injection angle.

The velocity profiles from Figure 3.23 have been spanwise-averaged using a Simpson's rule type of quadrature, and the averaged velocity profile is plotted in Figure 3.24. Shown also in the figure is a one-sixth power velocity profile. Comparison of the two profiles shows the large momentum deficit created by the discrete hole injection process. From the spanwise-averaged velocity profile a shear stress profile was obtained and is plotted in Figure 3.25. From the spanwise-averaged velocity profile and shear stress profile, a mixing-length distribution was computed and it is plotted in Figure 3.26. The mixing-length profile will be used in Chapter 4 to deduce the general form of an augmented mixing-length expression. Details of the computing equations for the shear stress profile and mixing-length profile are given in Appendix VI.

Temperature profiles for $\theta = 1.00$ (injectant temperature equal to wall temperature) are shown in Figure 3.27. The presence of the jet can be seen in profile 6. Profiles 1 and 11 show a large enthalpy excess over a three-hole-diameter region above the surface. A similar set of profiles were taken for $\theta = 0.16$ (injectant temperature about equal to mainstream temperature), and they are shown in Figure 3.28. Again profile 6 shows the presence of the mainstream-temperature fluid. In profiles 1 and 11 the presence of the "sink-type" injectant is not detected. The temperature profiles for $\theta = 1$ and $\theta = 0.16$ have been spanwise-averaged, and they are plotted in Figures 3.29 and 3.30 respectively.

Table 3.3 summarizes the momentum and enthalpy thickness Reynolds numbers for the velocity and temperature profiles of Figures 3.23, 3.27, and 3.28 (from tabulations in Appendix II). Also shown in the table are: (1) $\Sigma Re/11$, the arithmetic-averaged Reynolds numbers for the 11 profiles; (2) the Re values for the spanwise-averaged velocity and temperature profiles of Figures 3.24, 3.29, and 3.30; and (3) the Re_{Δ_2} values computed by integration of the data in Figure 3.3 using the energy integral equation (2.9). The quantities referred to in (1) and (2) are almost identical. The comparison between (2) and (3) shows that the calculated Re_{Δ_2} (using experimental Stanton numbers) agree with the spanwise-averaged Re_{Δ_2} to within five percent.

Table 3.3

Momentum and enthalpy thickness Reynolds numbers for the velocity and temperature profiles in Figures 3.23 through 3.30

Profile	Re_{δ_2}	$Re_{\Delta_2}(\theta = 1.00)$	$Re_{\Delta_2}(\theta = 0.16)$
1	6833	10,259	3898
2	6759	8,861	3924
3	6181	8,137	3920
4	5769	8,341	3991
5	6654	9,920	3910
6	6814	9,642	3409
7	7734	10,138	4001
8	7051	9,070	4296
9	6381	8,617	4181
10	6720	9,158	4158
11	7255	9,490	4079
$\Sigma Re/11$	6741	9,240	3979
Spanwise-averaged profile	6792	9,200	3978
Data reduction program (midpoint plate 11)	----	8,734	4052

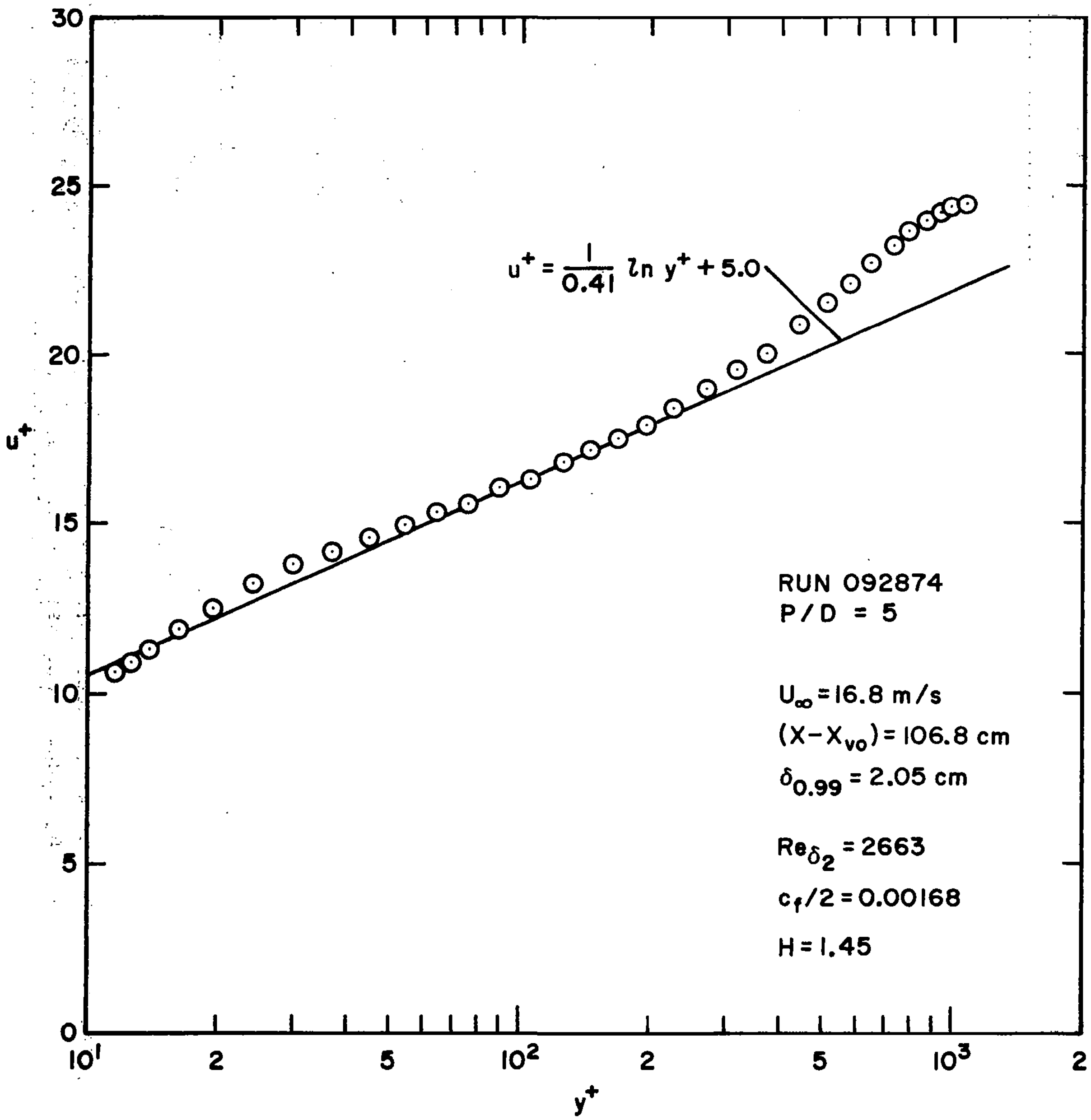

Figure 3.1 Upstream velocity profile for initially high Re_{δ_2}, heated starting length runs (see Section 3.3.1)

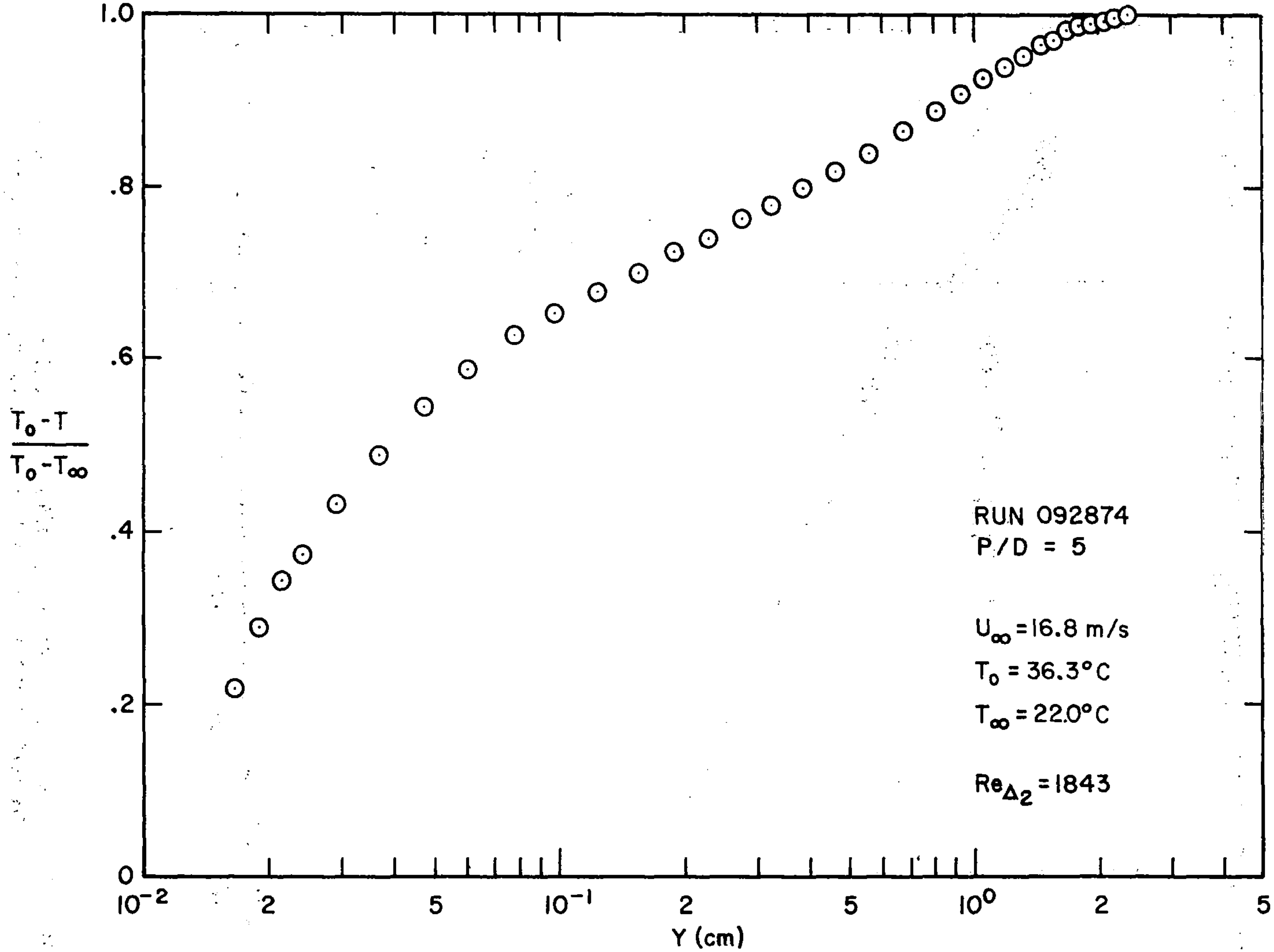

Figure 3.2 Upstream temperature profile for initially high Re_{δ_2}, heated starting length runs (see Section 3.3.1)

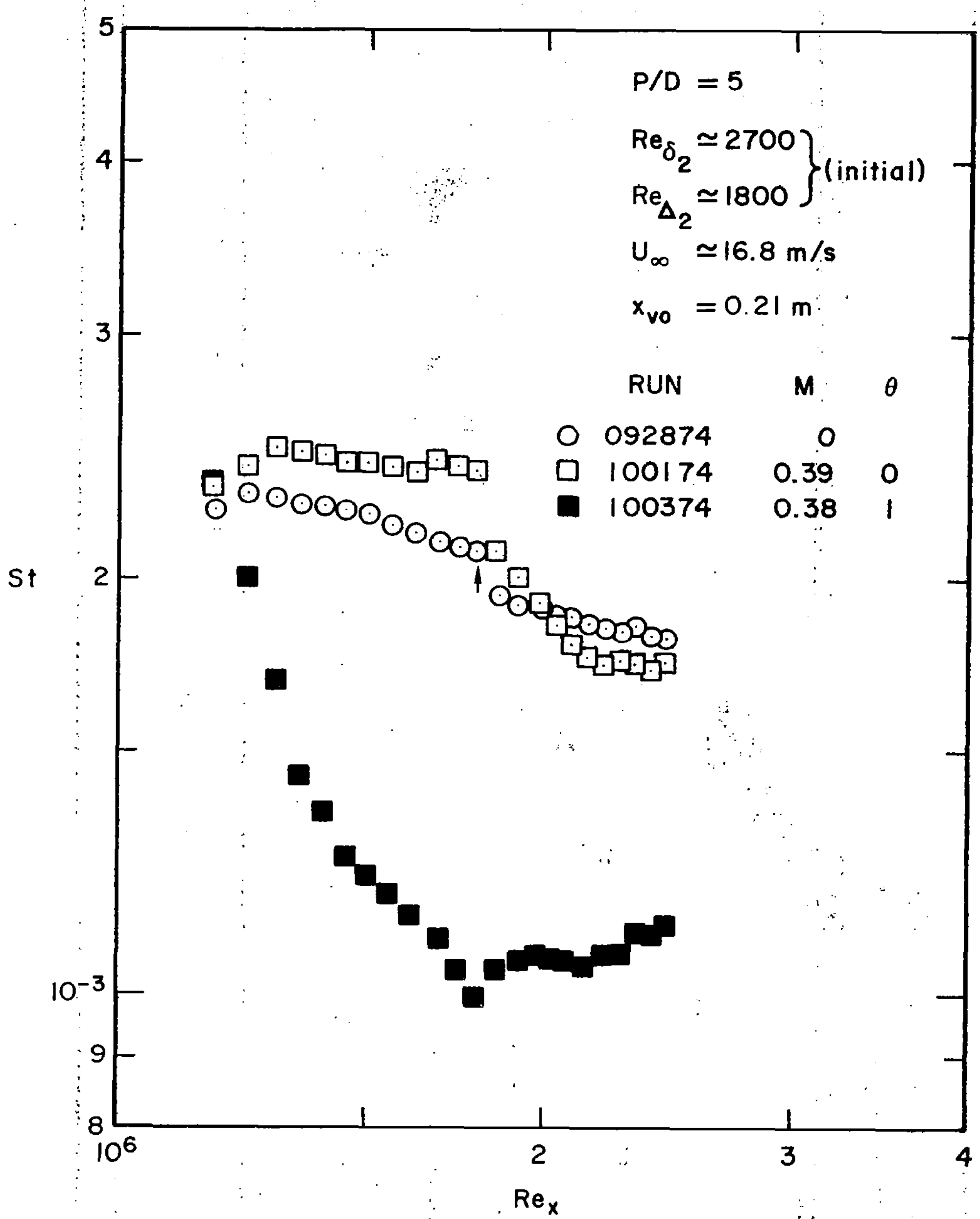

Figure 3.3 Stanton number data versus non-dimensional distance along surface for initial conditions in Figures 3.1 and 3.2, to study effects of heated starting length

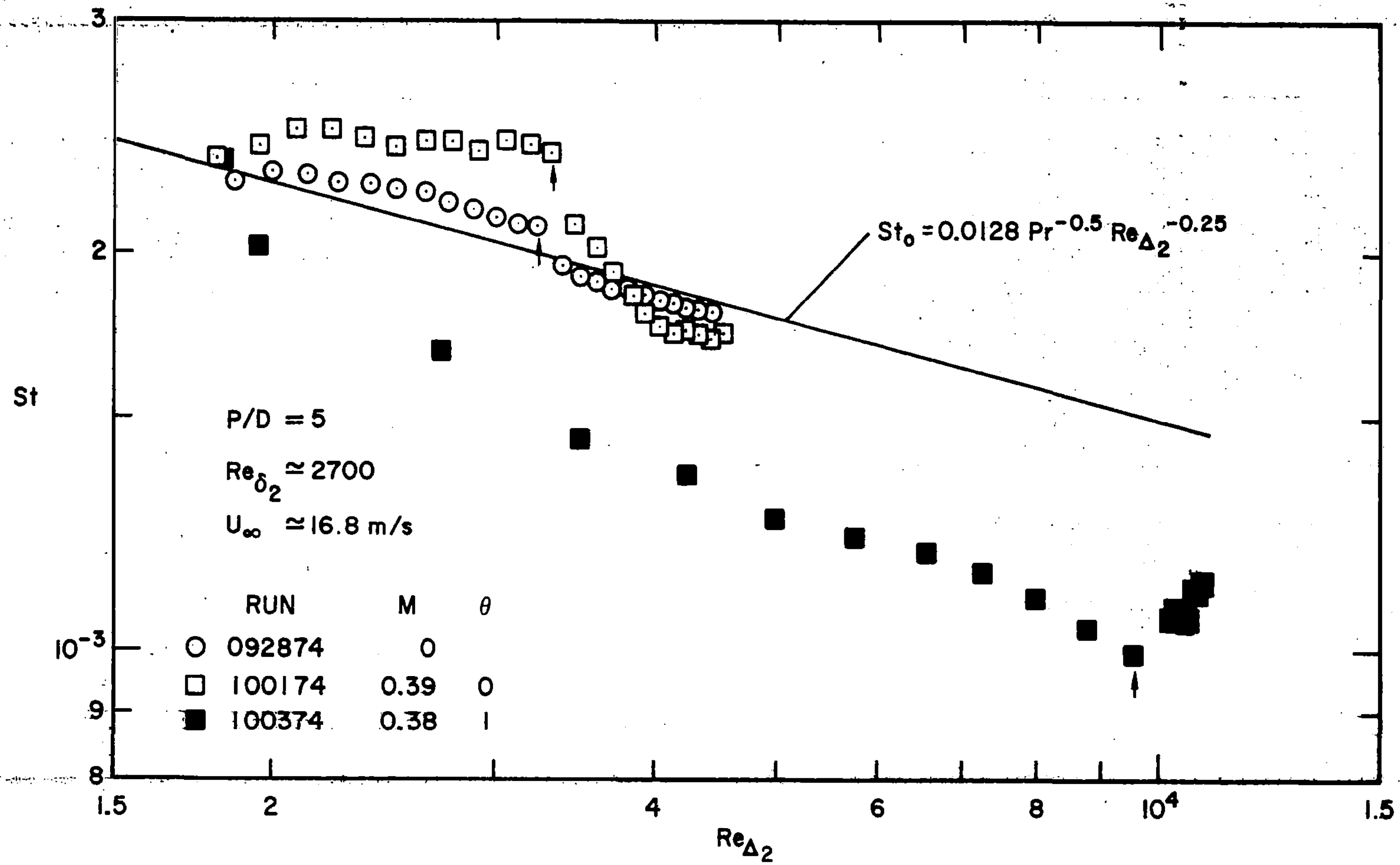

Figure 3.4 Data from Figure 3.3, replotted versus enthalpy thickness Reynolds number

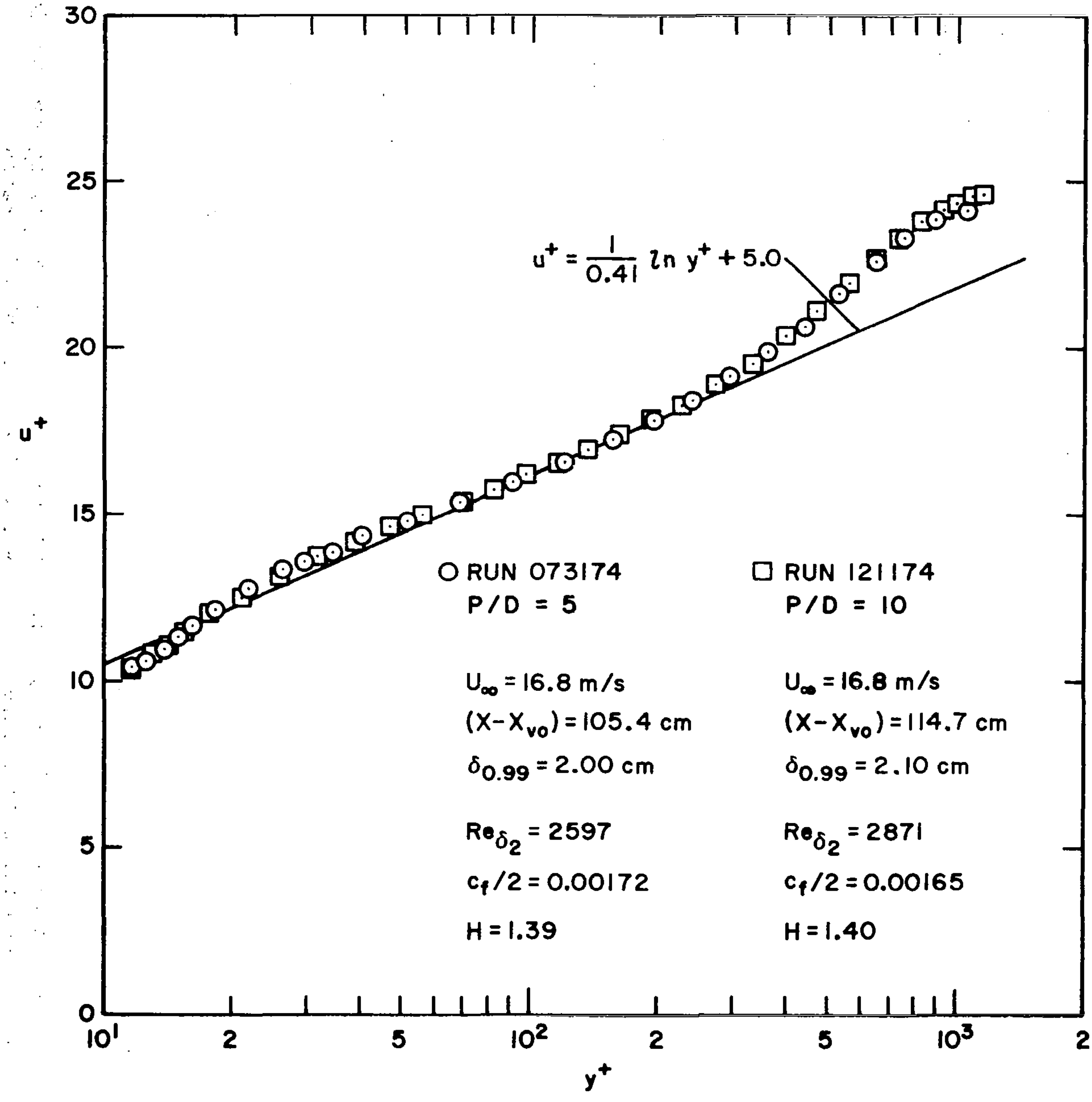

Figure 3.5 Upstream velocity profiles (P/D = 5, 10) for initially high Re_{δ_2} , unheated starting length runs (see Section 3.3.2)

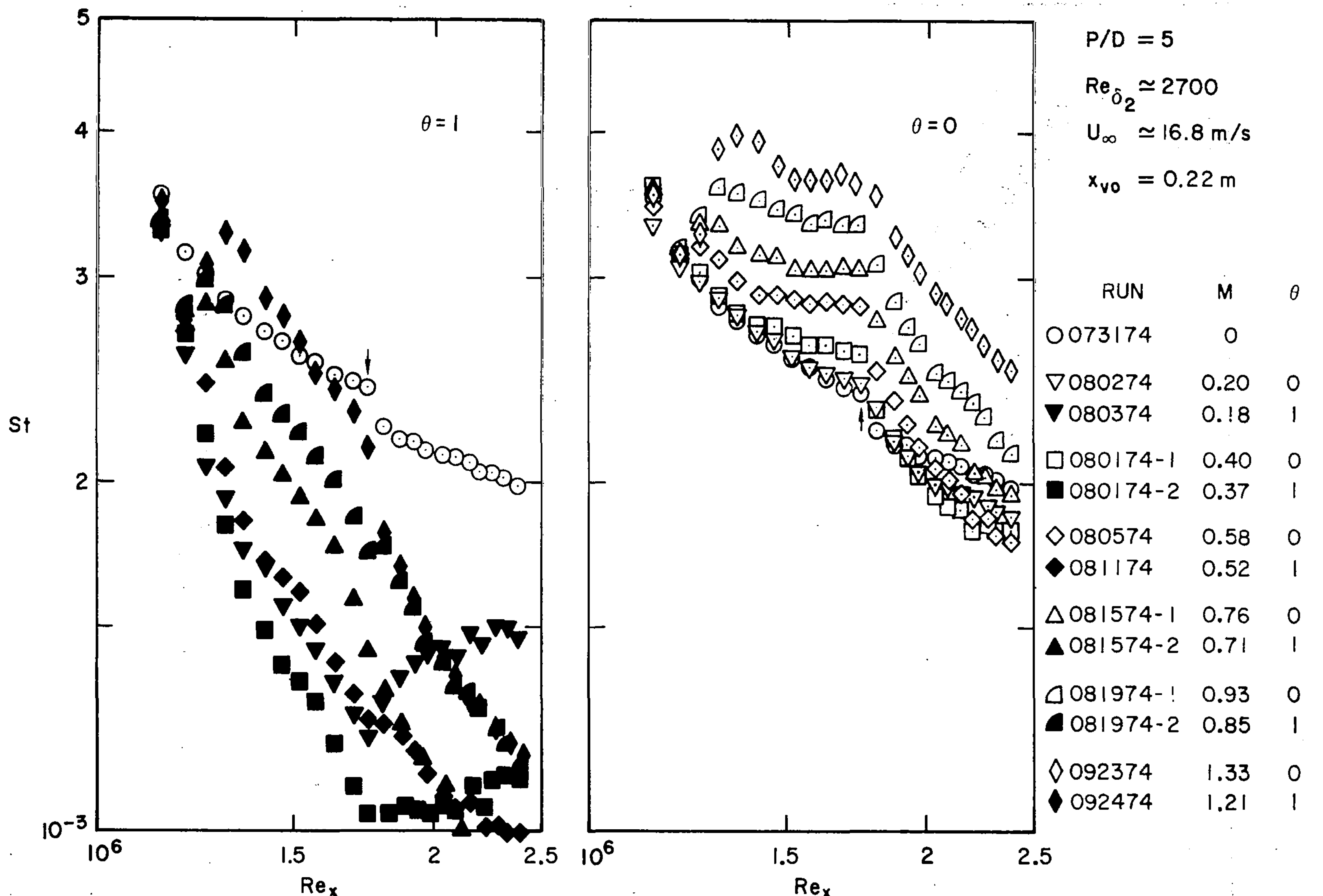

Figure 3.6 Stanton number data (P/D = 5) versus non-dimensional distance along surface for initial conditions in Figure 3.5, to study effects of blowing ratio

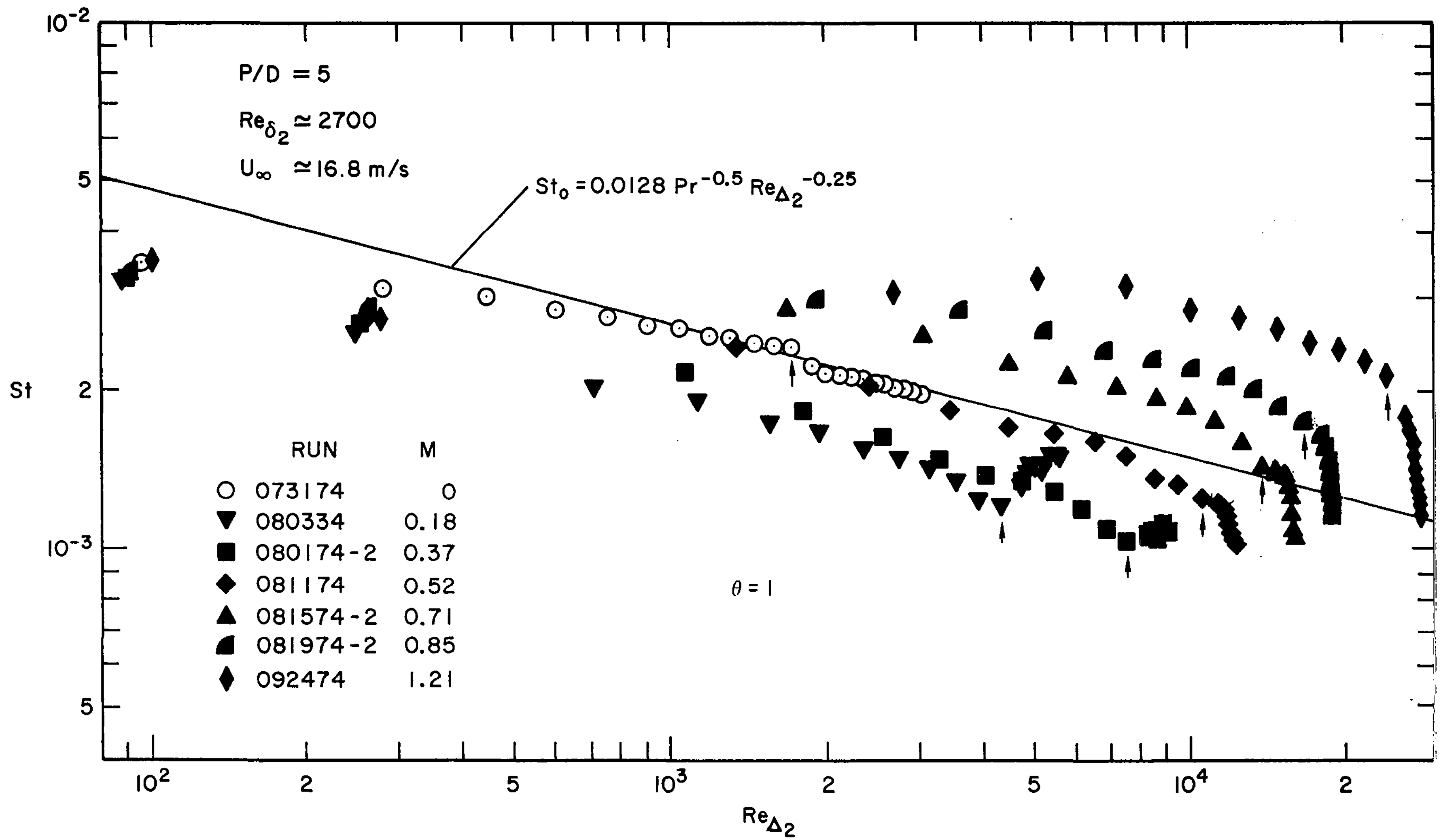

Figure 3.7 $\theta = 1$ data from Figure 3.6, replotted versus enthalpy thickness Reynolds number

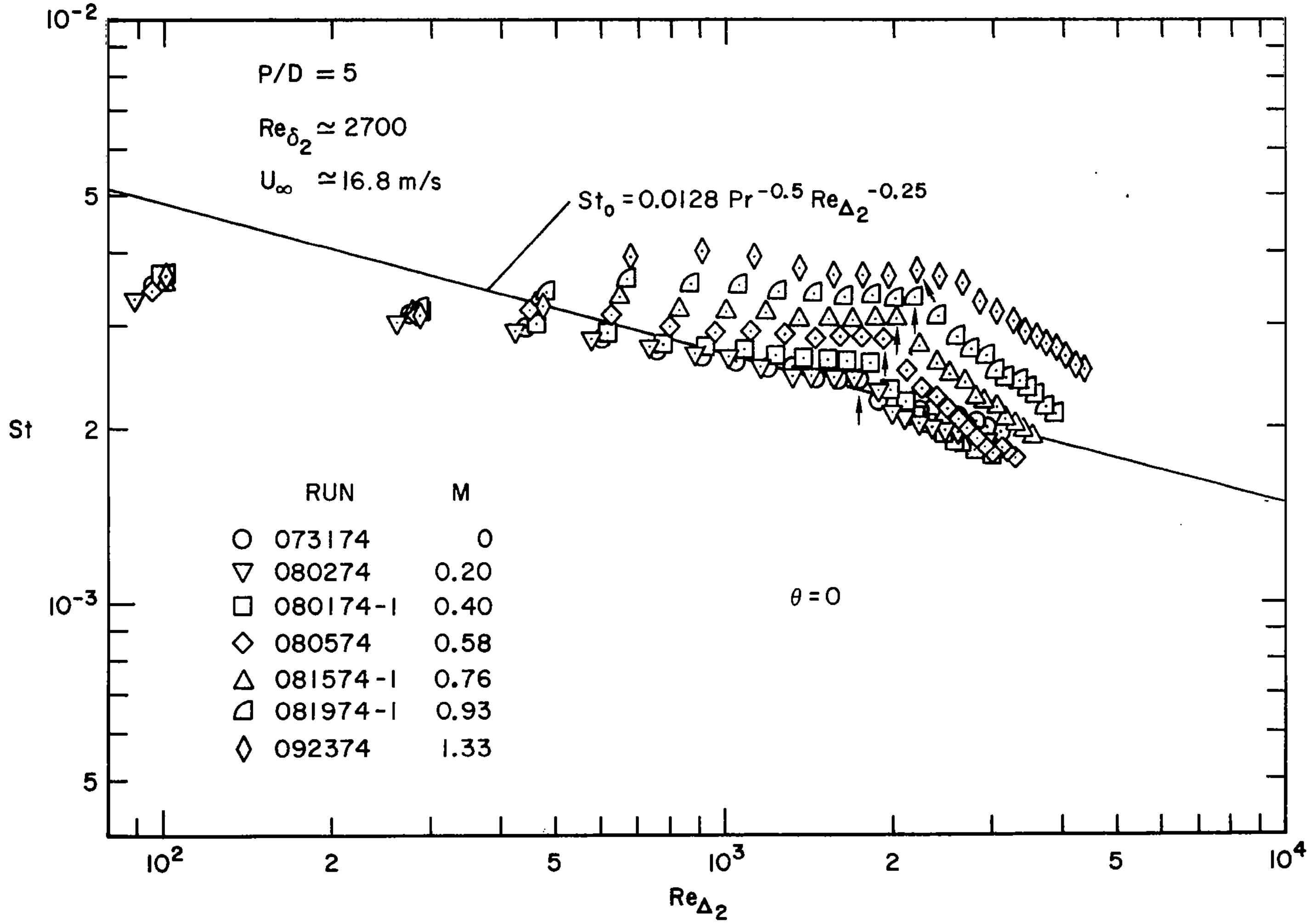

Figure 3.8 θ = 0 data from Figure 3.6, replotted versus enthalpy thickness Reynolds number

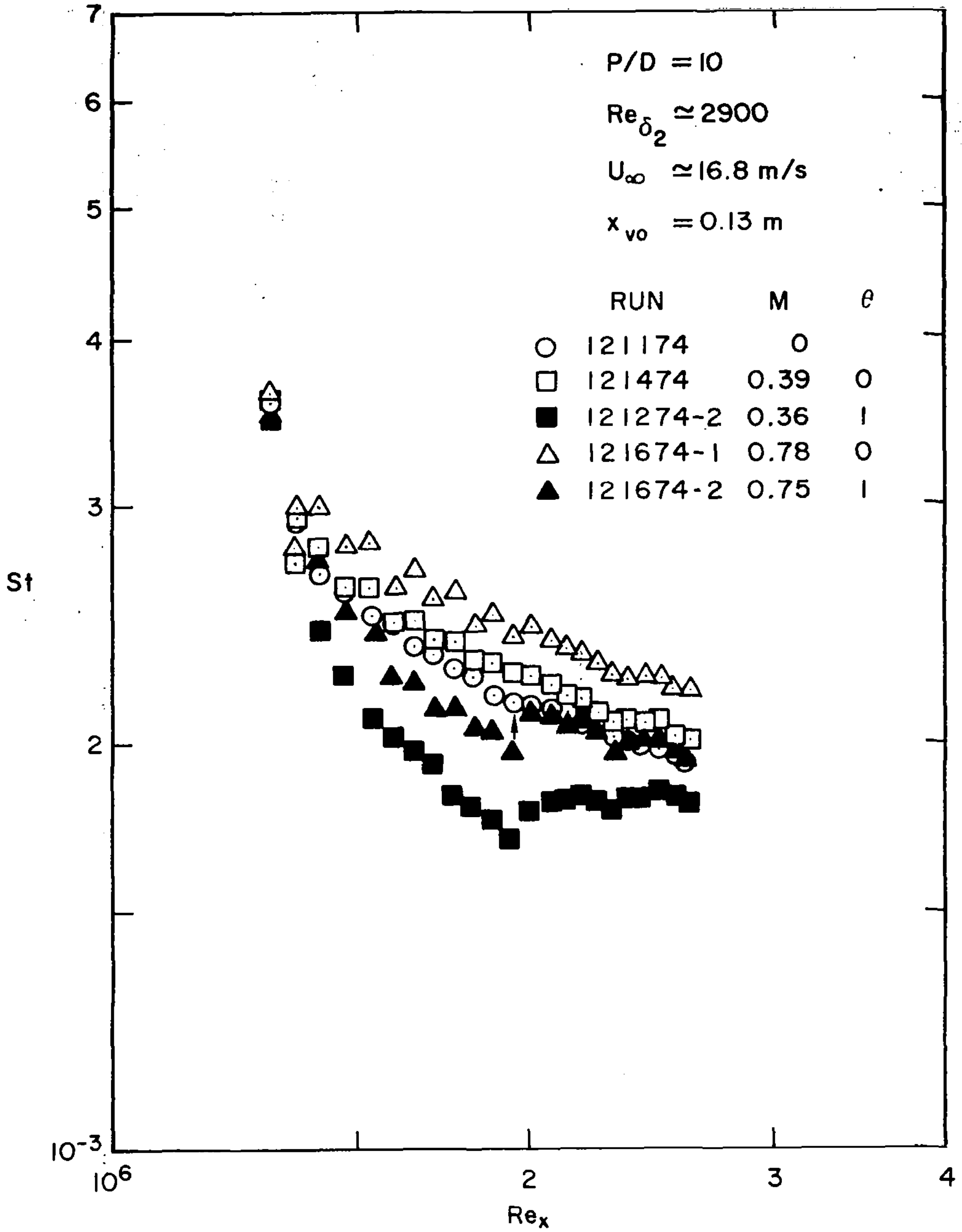

Figure 3.9 Stanton number data (P/D = 10) versus non-dimensional distance along surface for initial conditions in Figure 3.5, to study effects of change in hole spacing

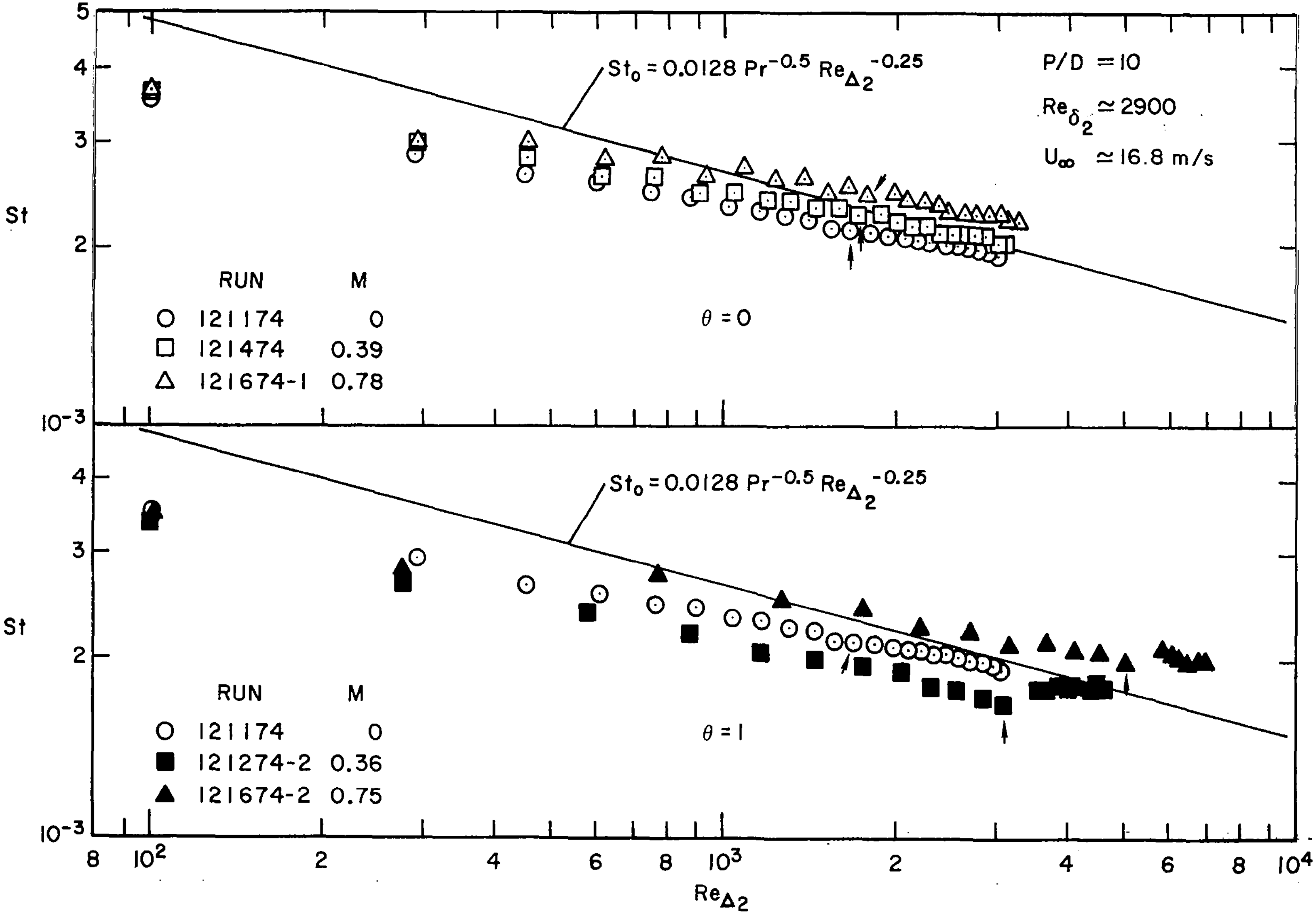

Figure 3.10 Data from Figure 3.9, replotted versus enthalpy thickness Reynolds number

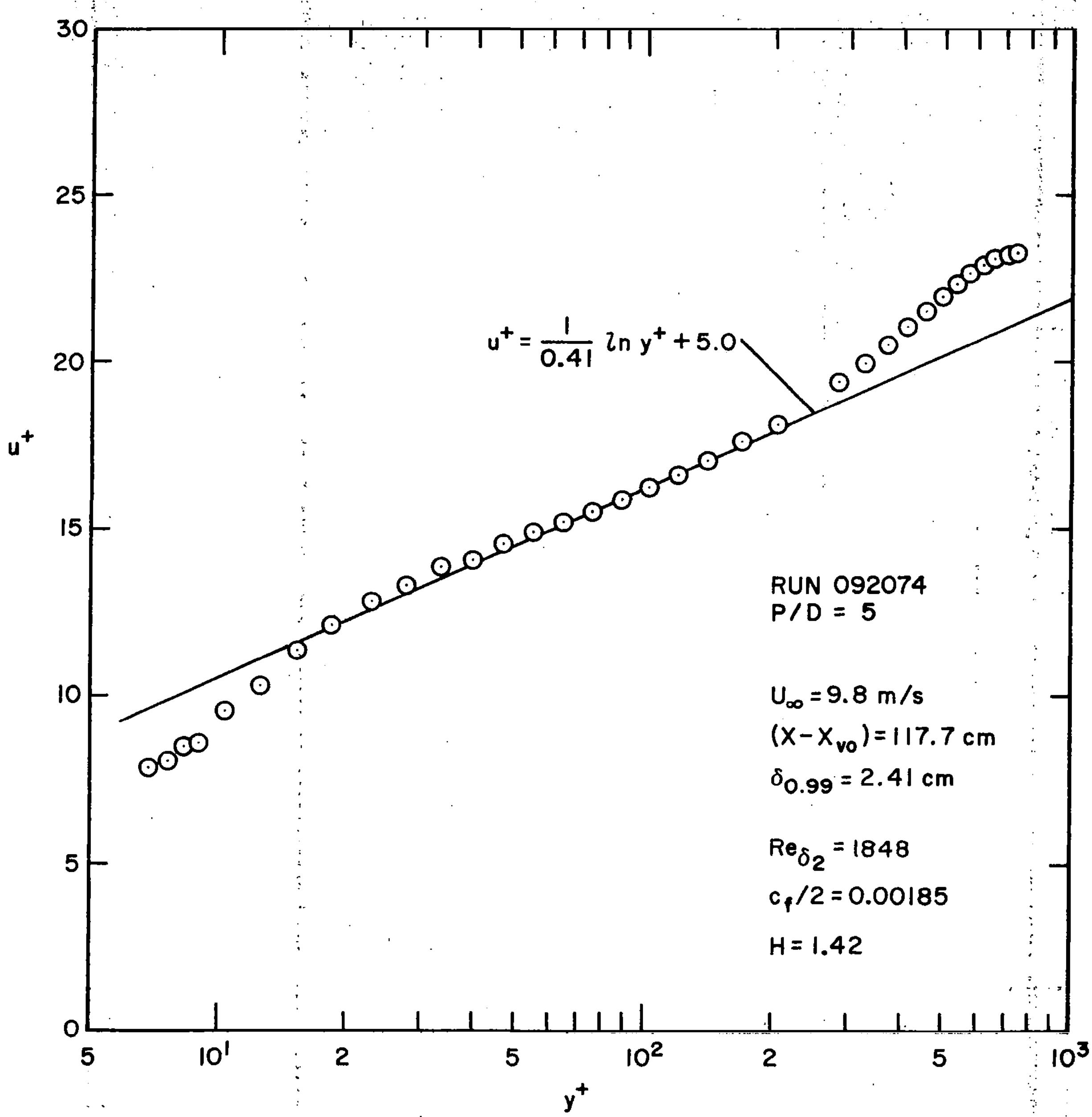

Figure 3.11 Upstream velocity profile for initially high Re_{δ_2}, unheated starting length runs (see Section 3.3.3)

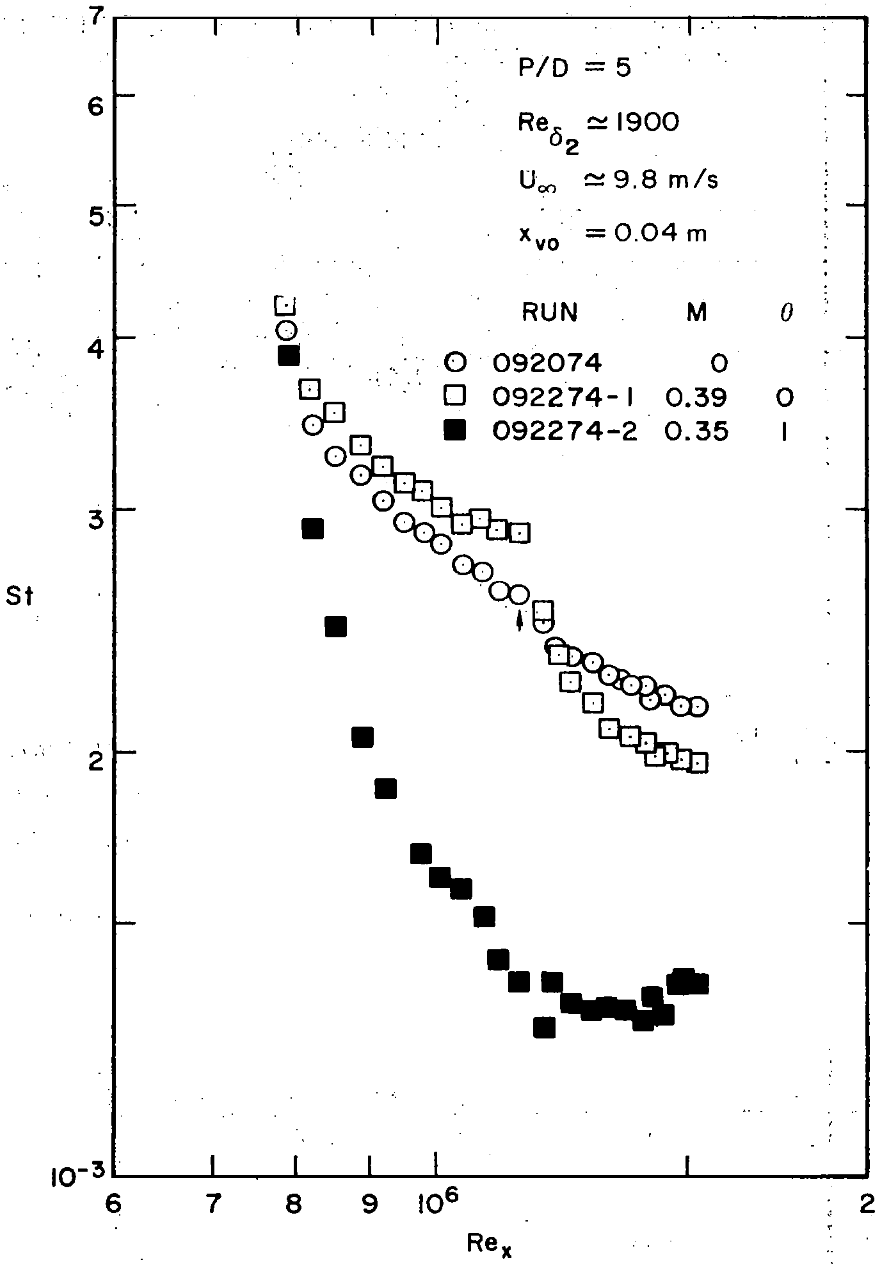

Figure 3.12 Stanton number data versus non-dimensional distance along surface for initial conditions in Figure 3.11, to study effects of change in U_∞

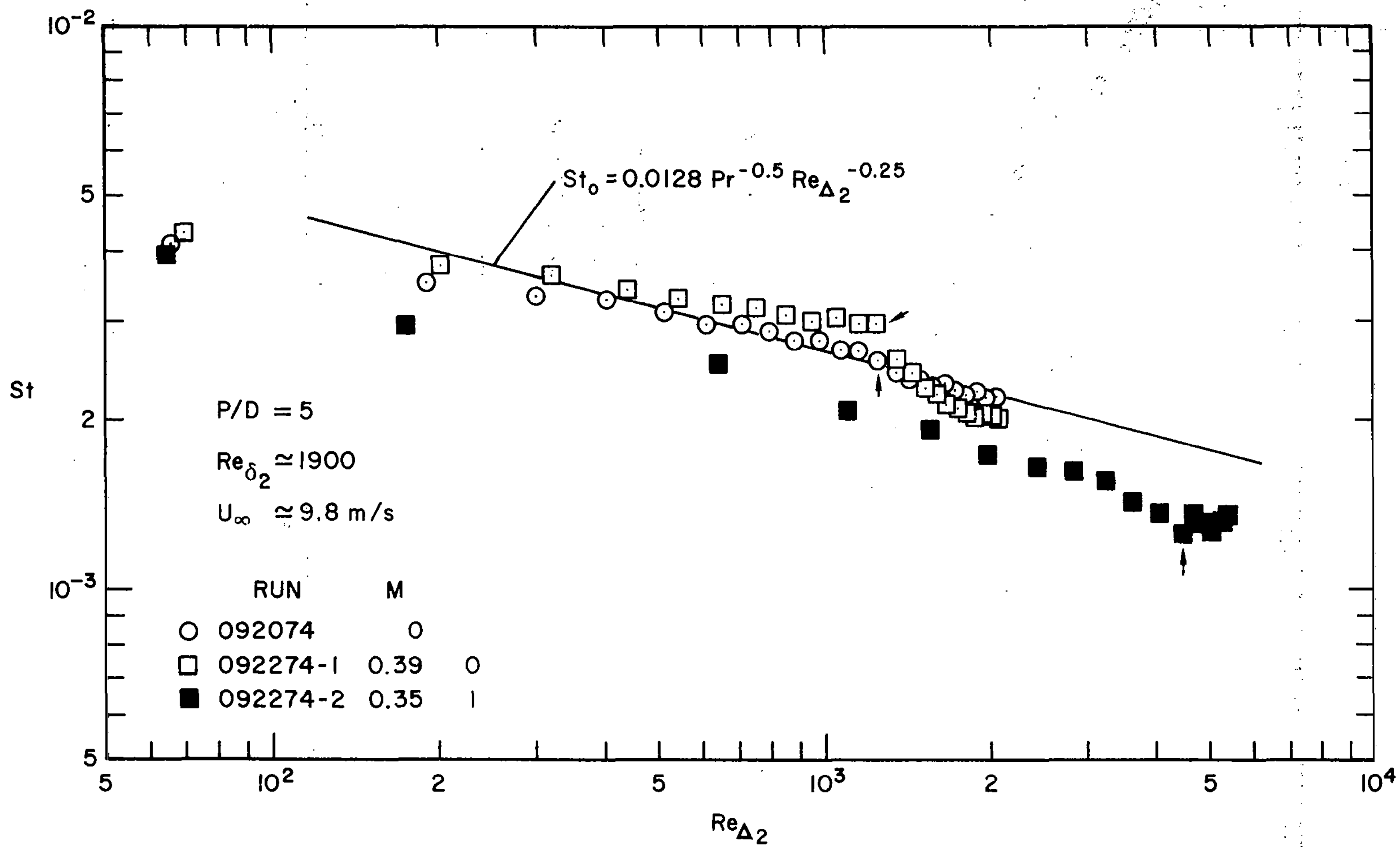

Figure 3.13 Data from Figure 3.12, replotted versus enthalpy thickness Reynolds number

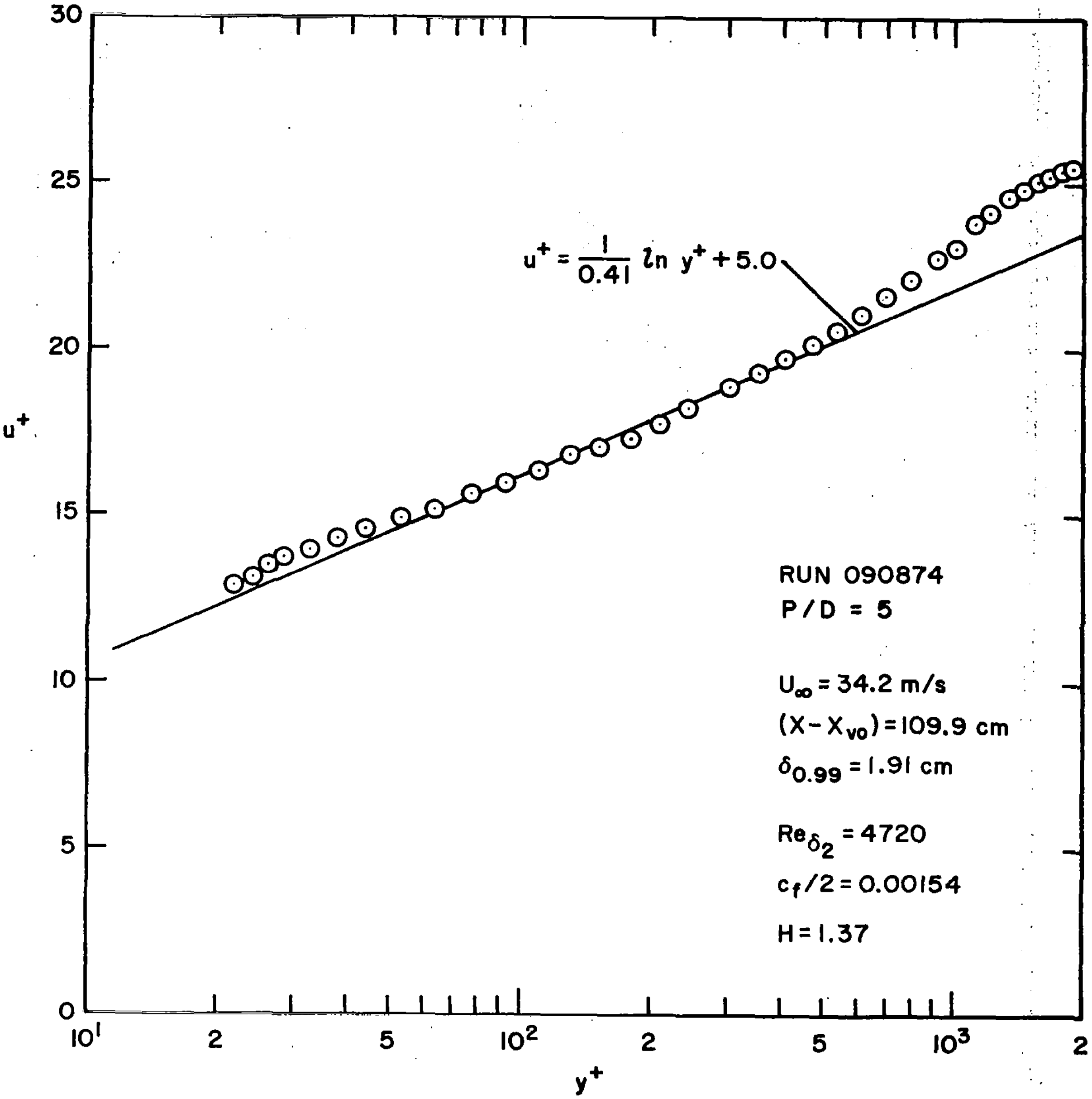

Figure 3.14 Upstream velocity profile for initially high Re_{δ_2}, unheated starting length runs (see Section 3.3.3)

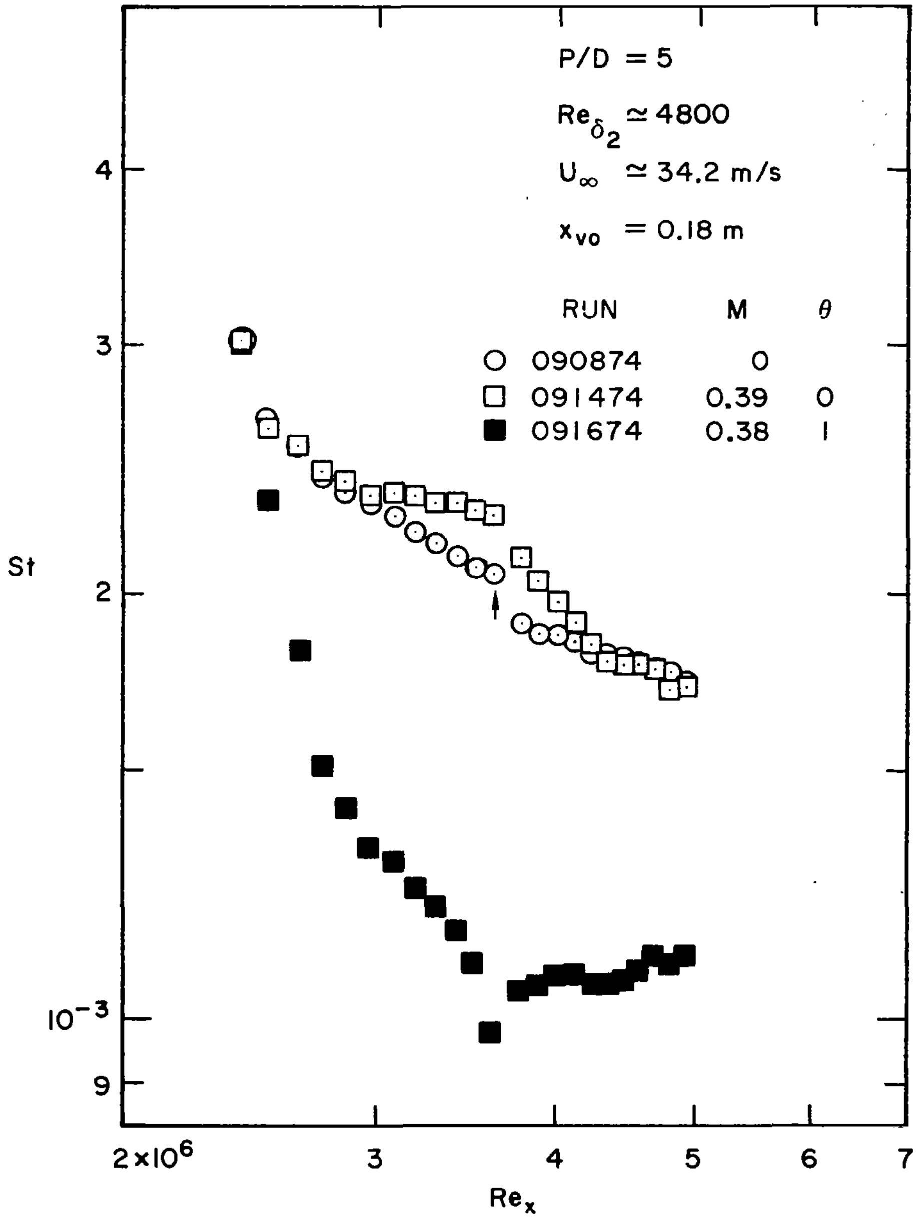

Figure 3.15 Stanton number data versus non-dimensional distance along surface for initial conditions in Figure 3.14, to study effects of change in U_∞

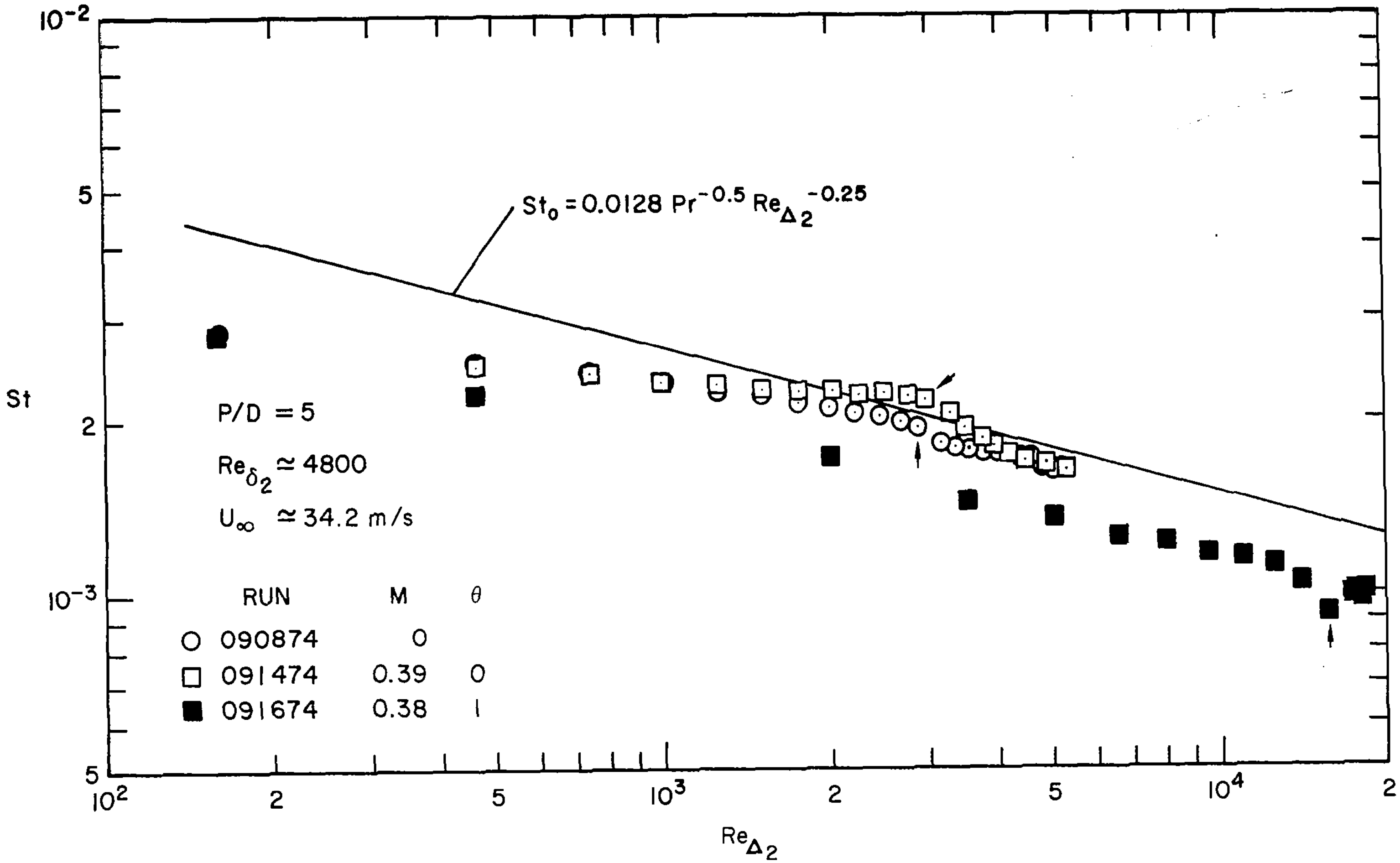

Figure 3.16 Data for Figure 3.15, replotted versus enthalpy thickness Reynolds number

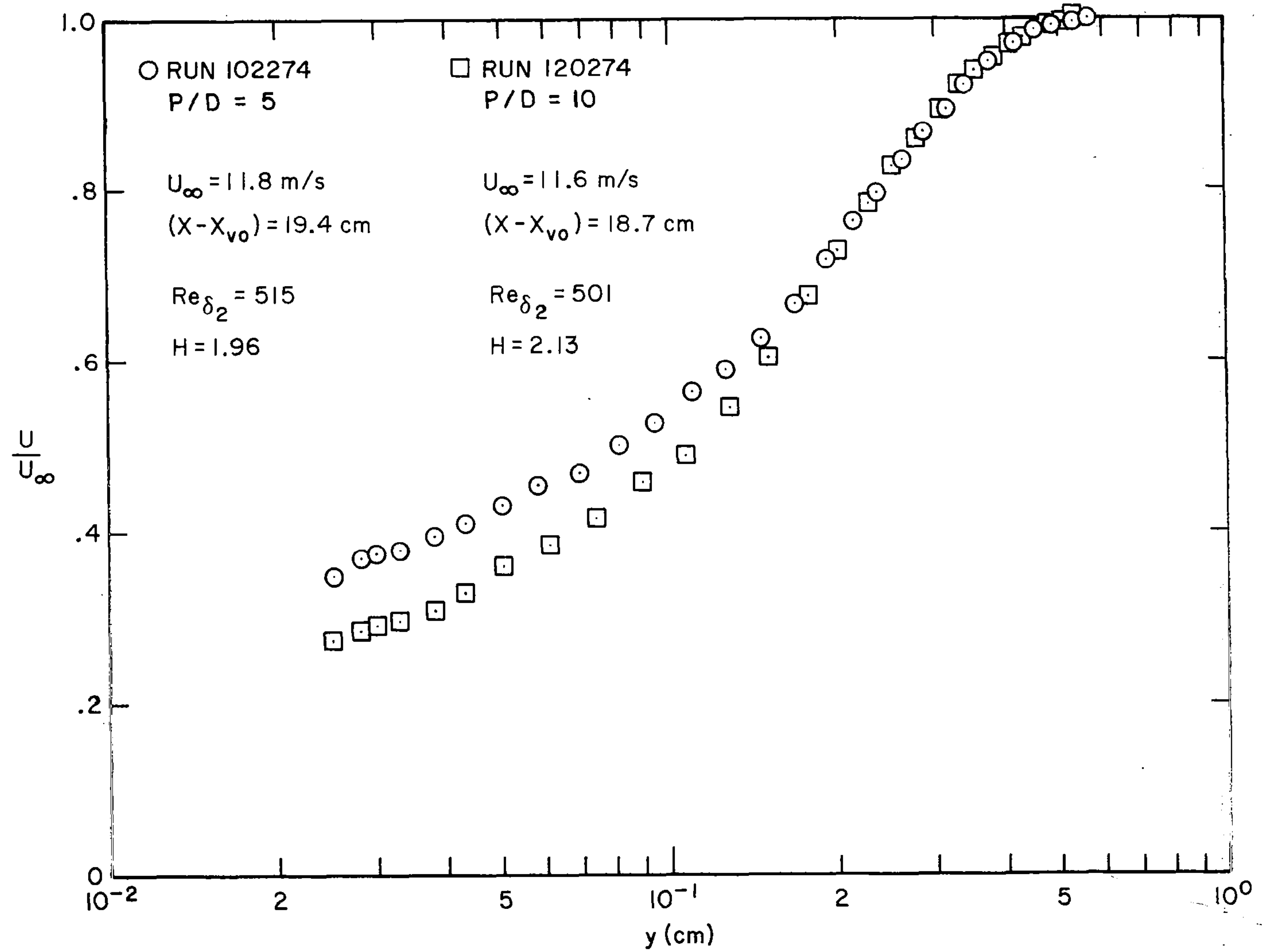

Figure 3.17 Upstream velocity profiles (P/D = 5, 10) for initially low Re_{δ_2}, heated starting length runs (see Section 3.3.4)

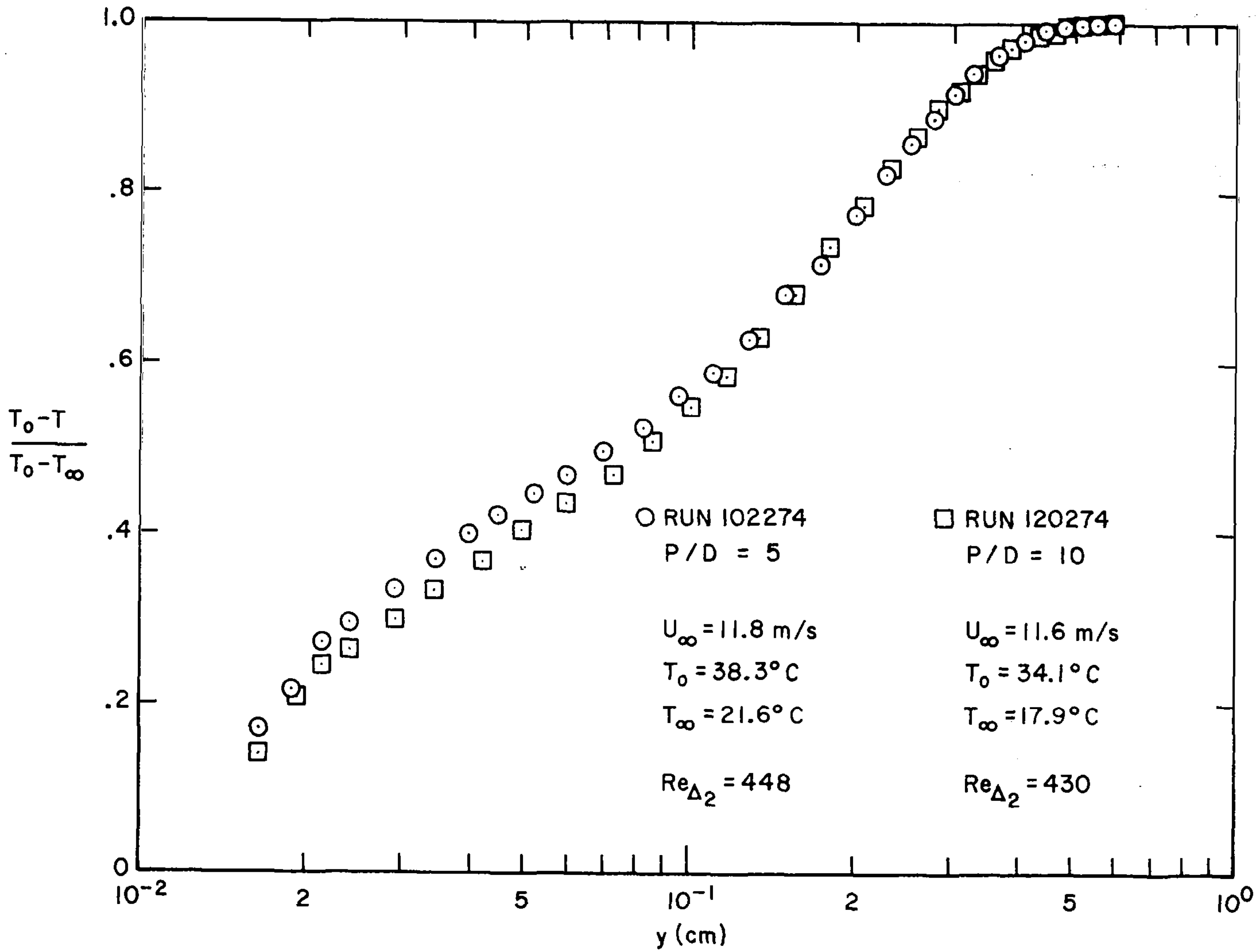

Figure 3.18 Upstream temperature profiles (P/D = 5, 10) for initially low Re_{δ_2}, heated starting length runs (see Section 3.3.4)

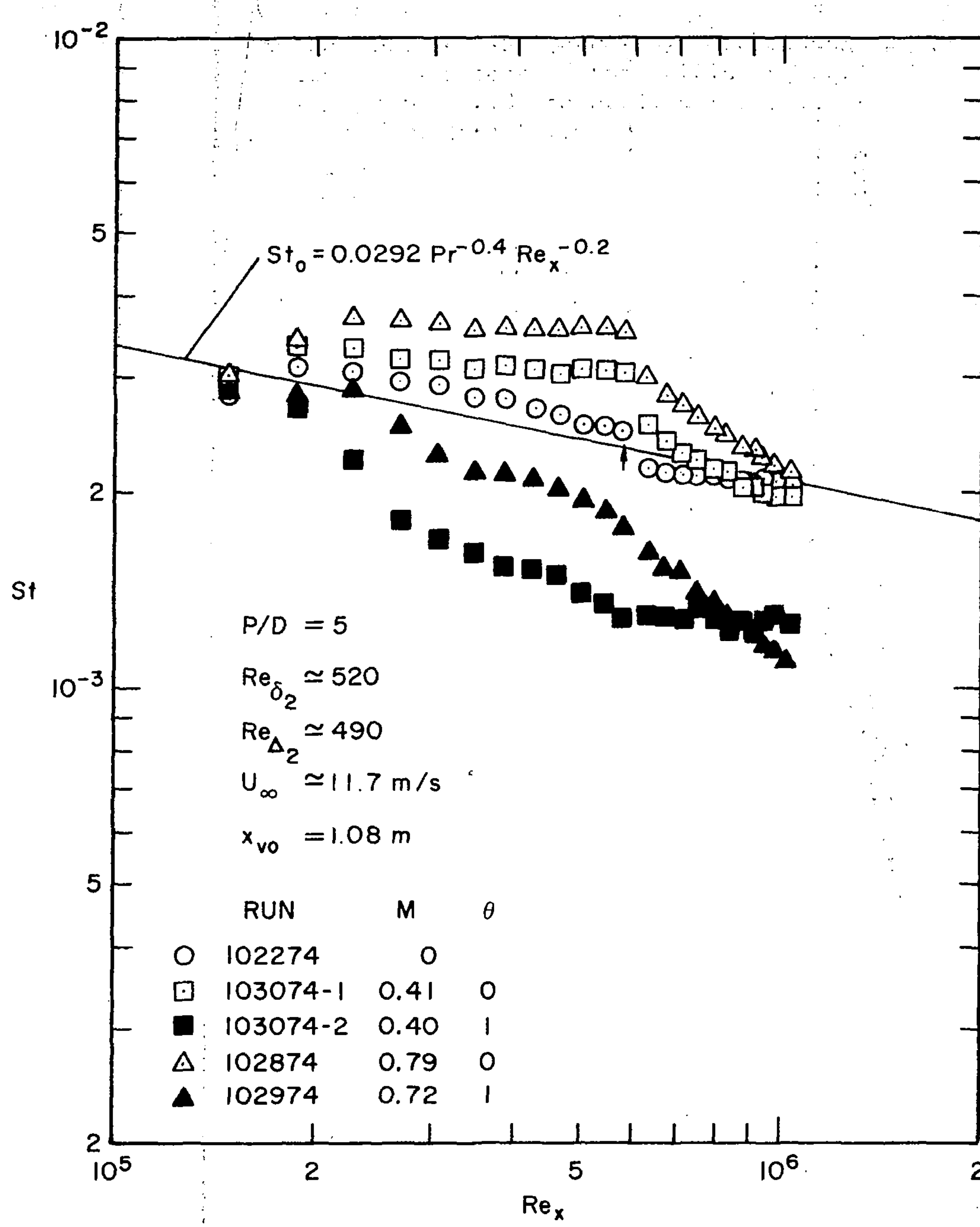

Figure 3.19 Stanton number data (P/D = 5) versus non-dimensional distance along surface for initial conditions in Figures 3.17 and 3.18, to study effects of thin initial momentum boundary layer

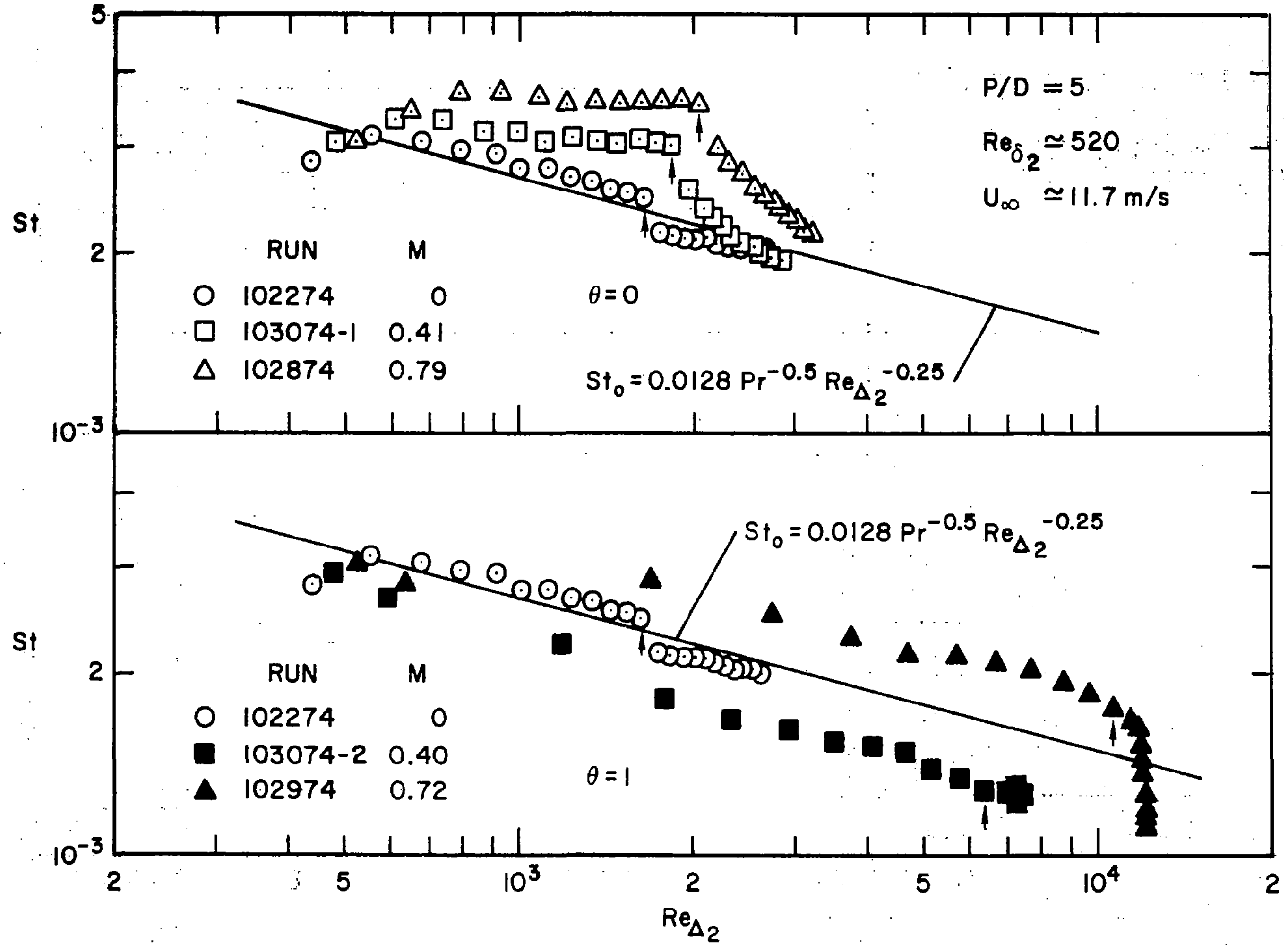

Figure 3.20 Data from Figure 3.19, replotted versus enthalpy thickness Reynolds number

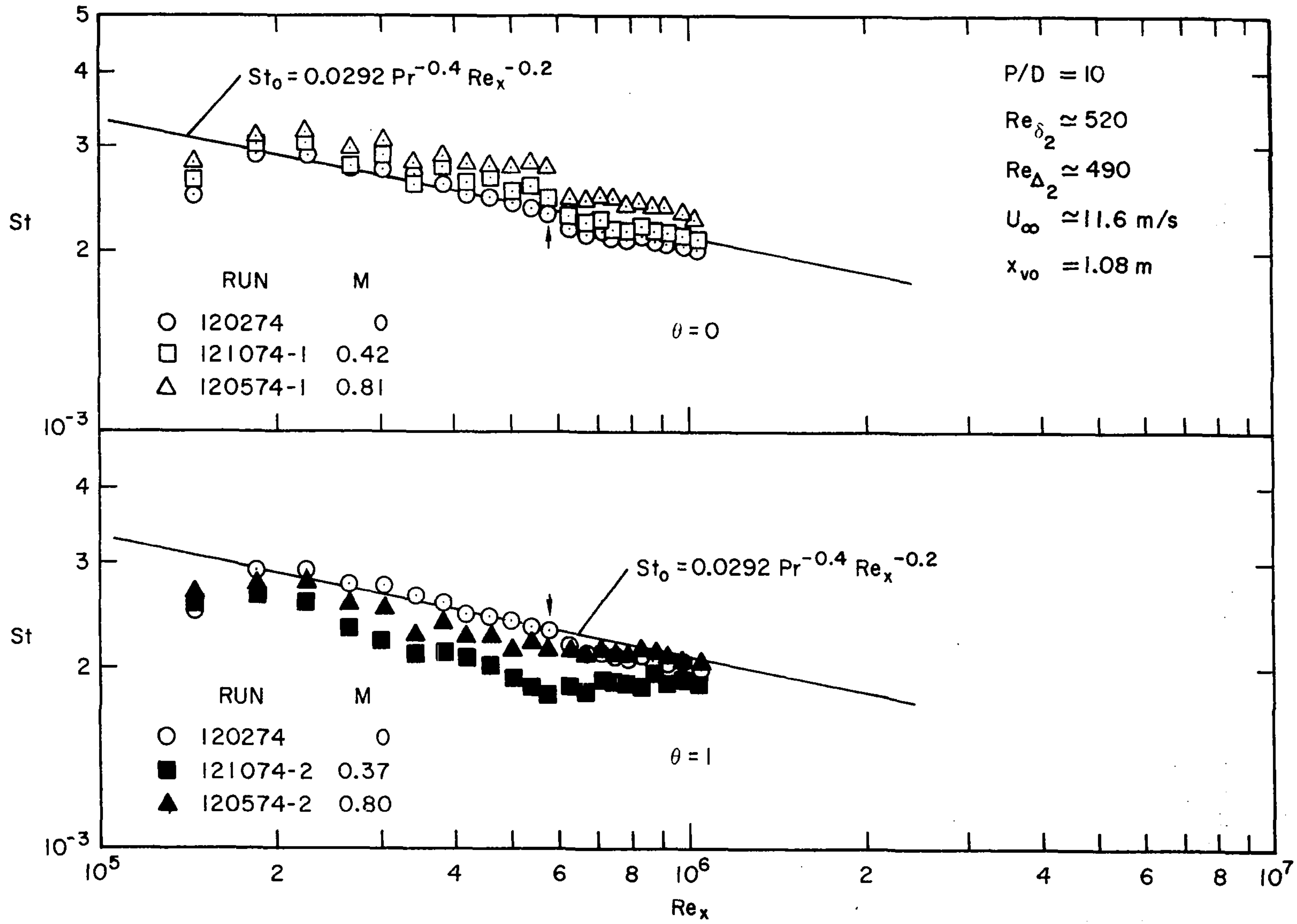

Figure 3.21 Stanton number data (P/D = 10) versus non-dimensional distance along surface for initial conditions in Figures 3.17 and 3.18, to study effects of change in hole spacing

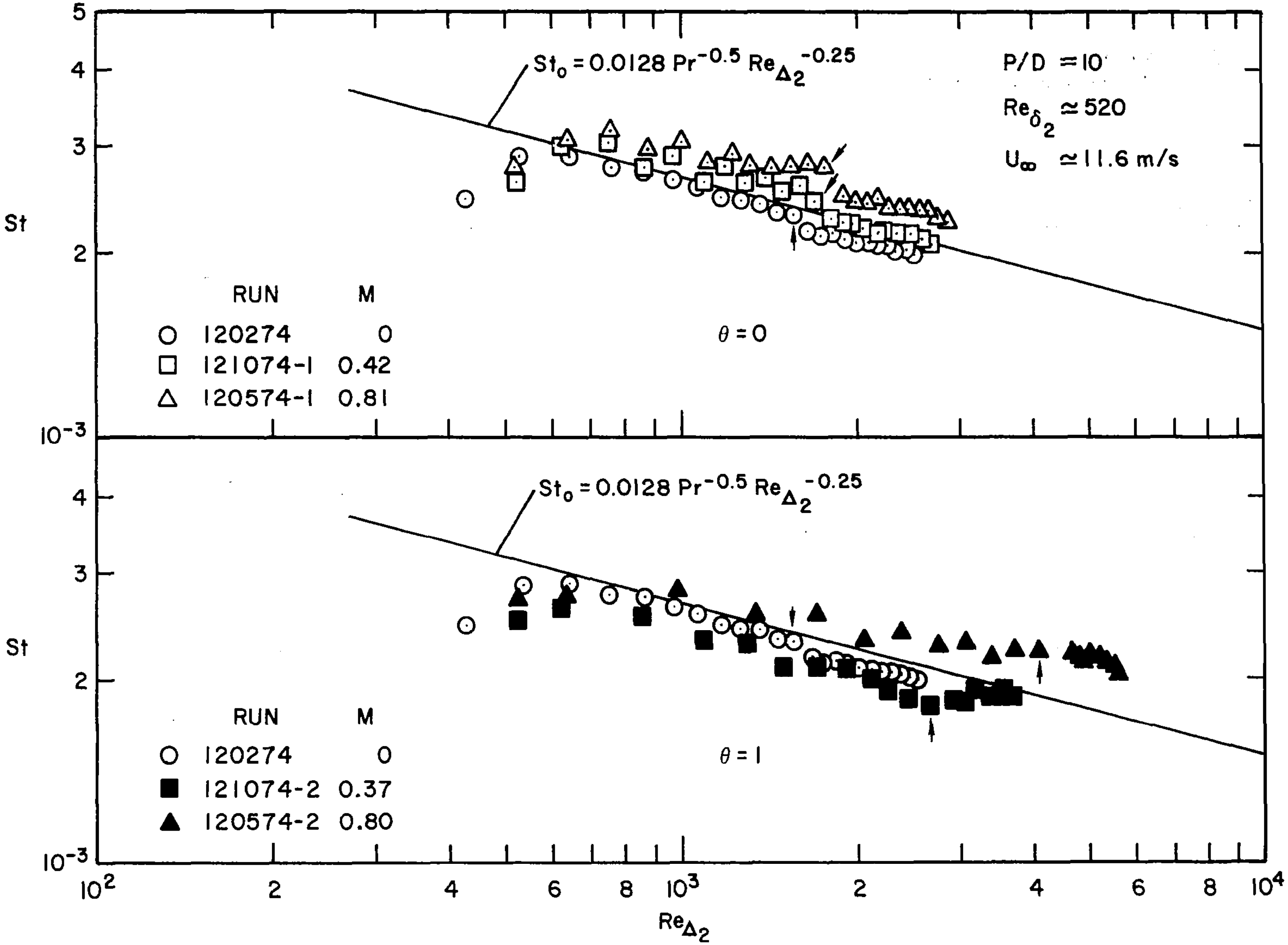

Figure 3.22 Data from Figure 3.21, replotted versus enthalpy thickness Reynolds number

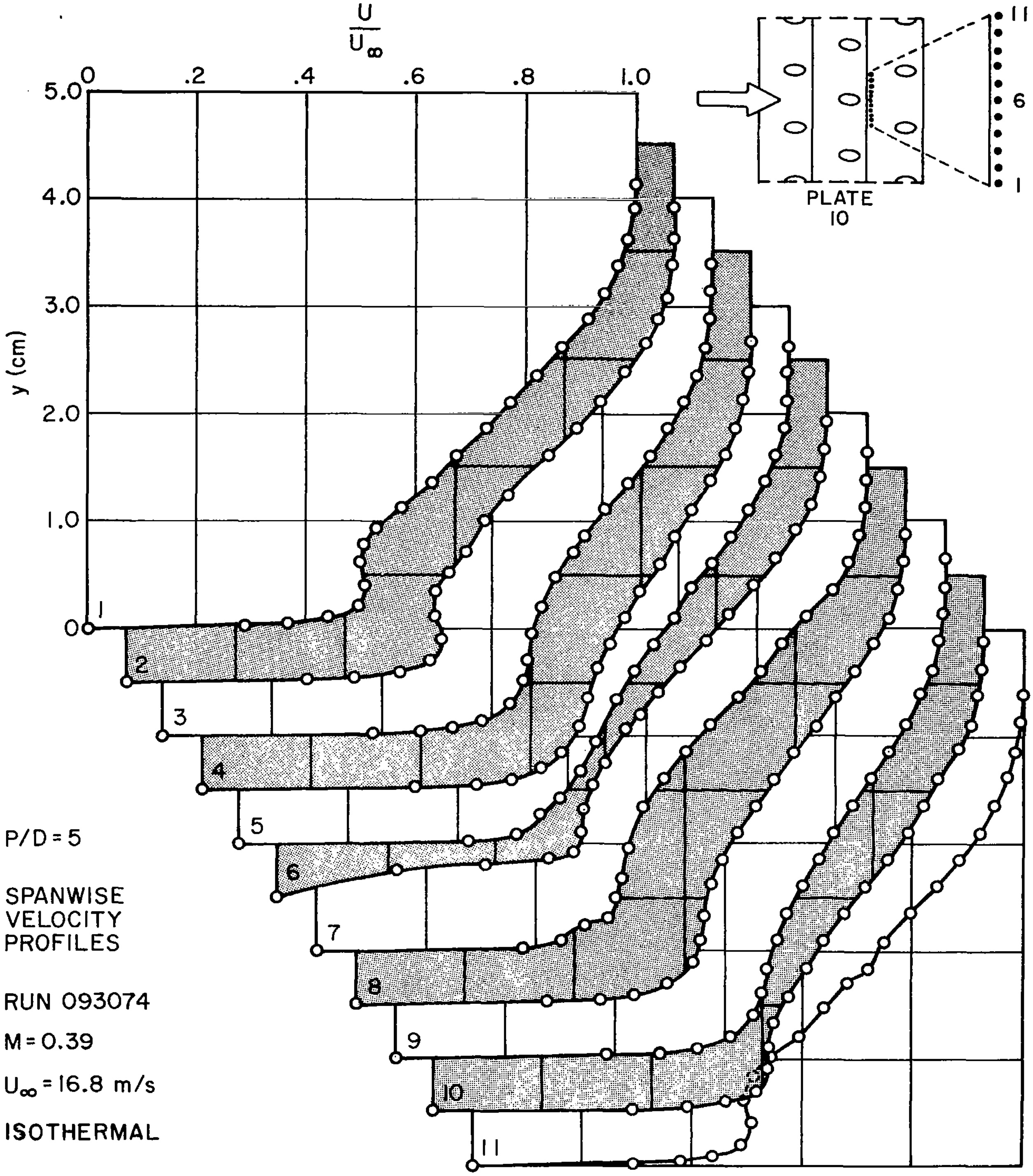

Figure 3.23 Velocity profiles downstream of ninth blowing row (see Figure 3.1 for boundary layer initial conditions)

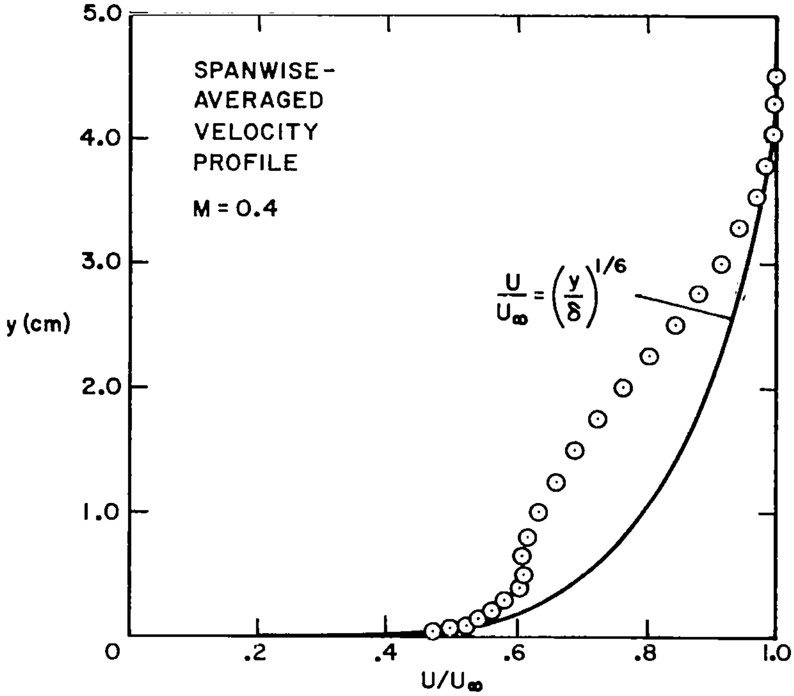

Figure 3.24 Velocity profile obtained by spanwise-averaging the profiles in Figure 3.23

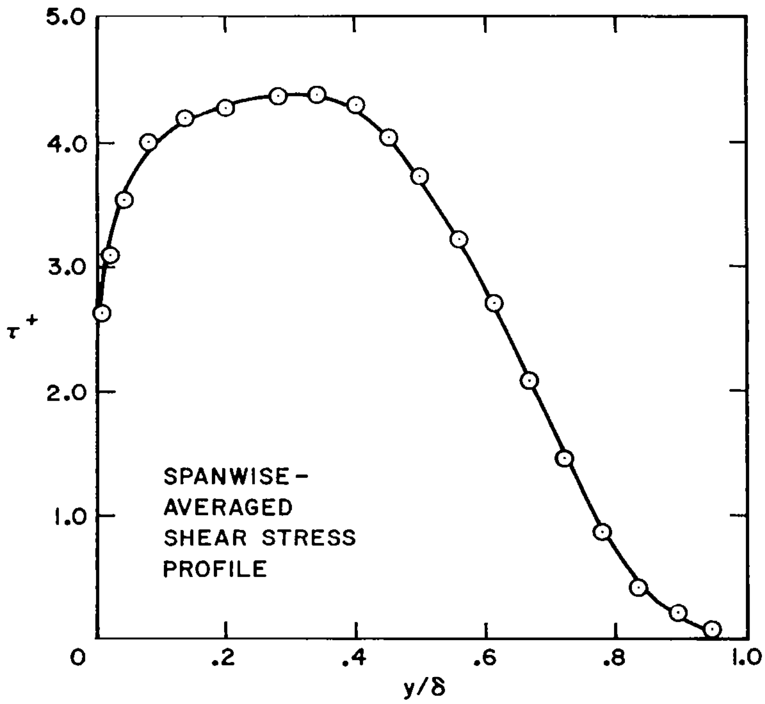

Figure 3.25 Shear stress profile obtained using the spanwise-averaged velocity profile

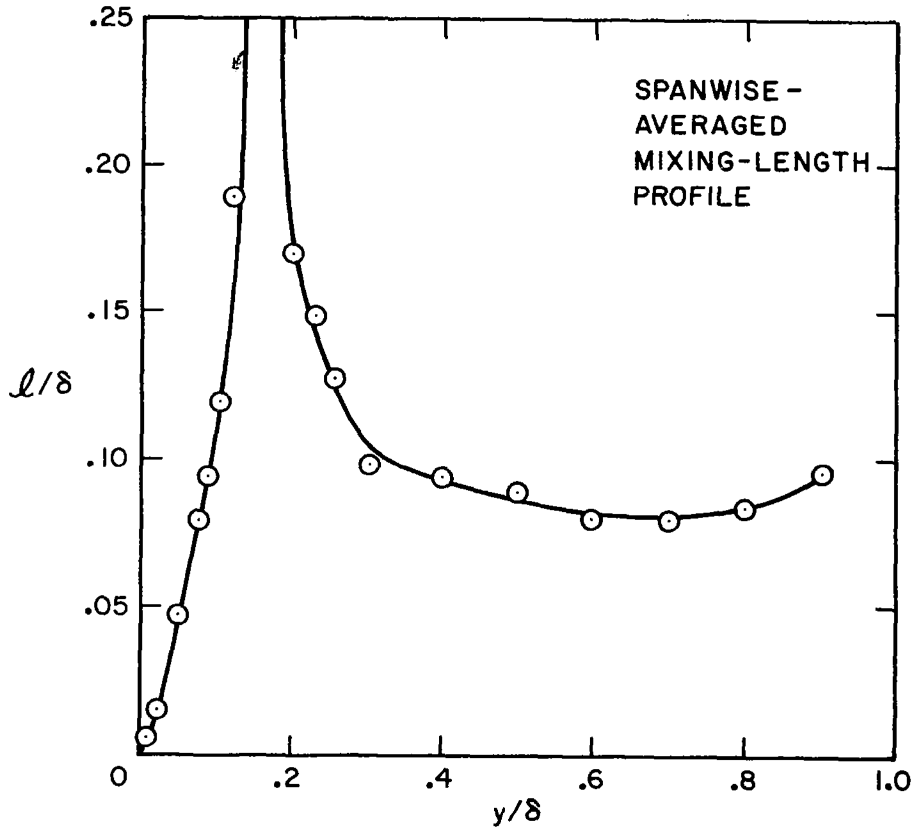

Figure 3.26 Mixing-length profile obtained using the shear stress profile and the spanwise-averaged velocity profile

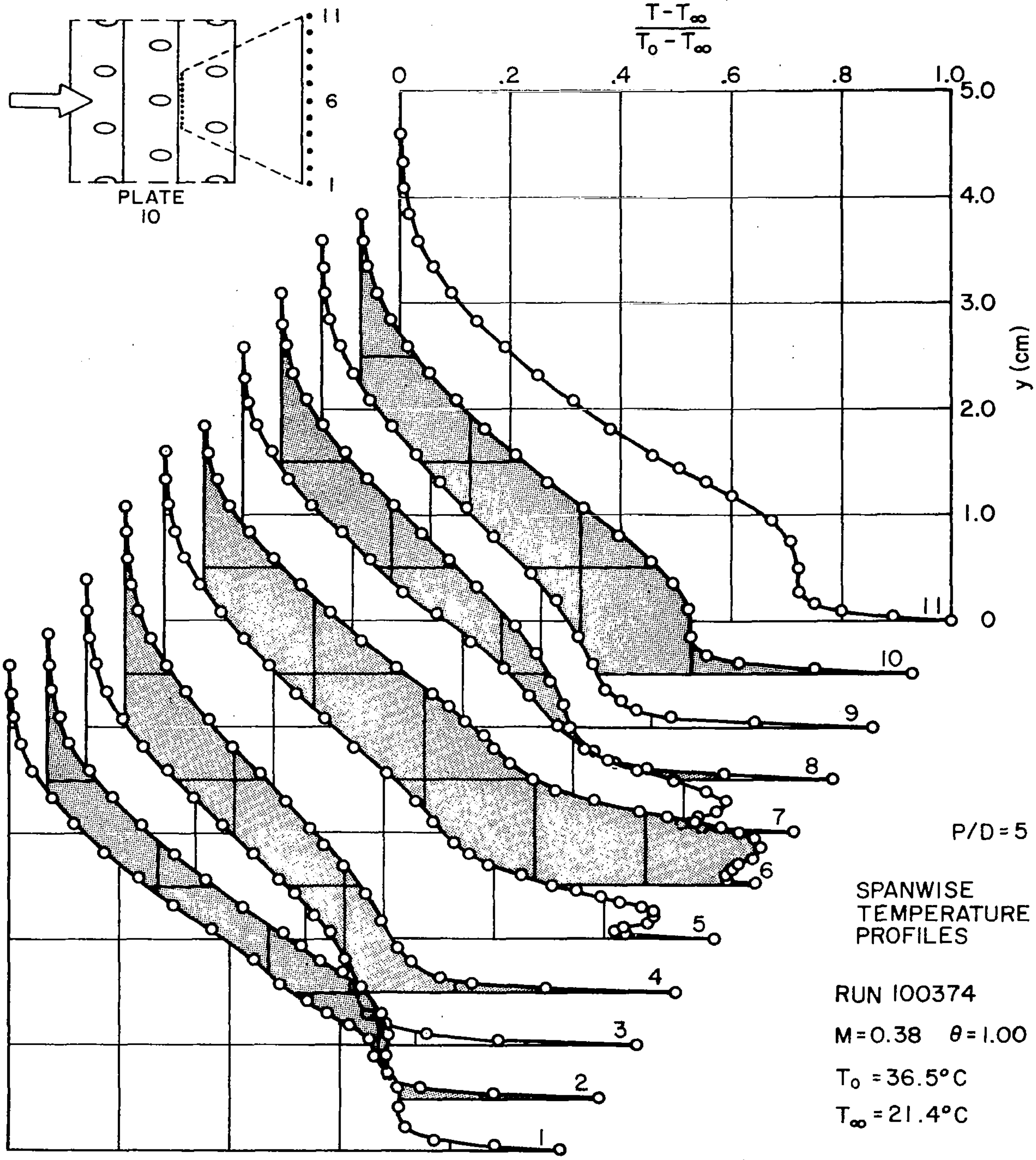

Figure 3.27 Temperature profiles downstream of ninth blowing row, θ = 1.00 (see Figures 3.1 and 3.2 for boundary layer initial conditions)

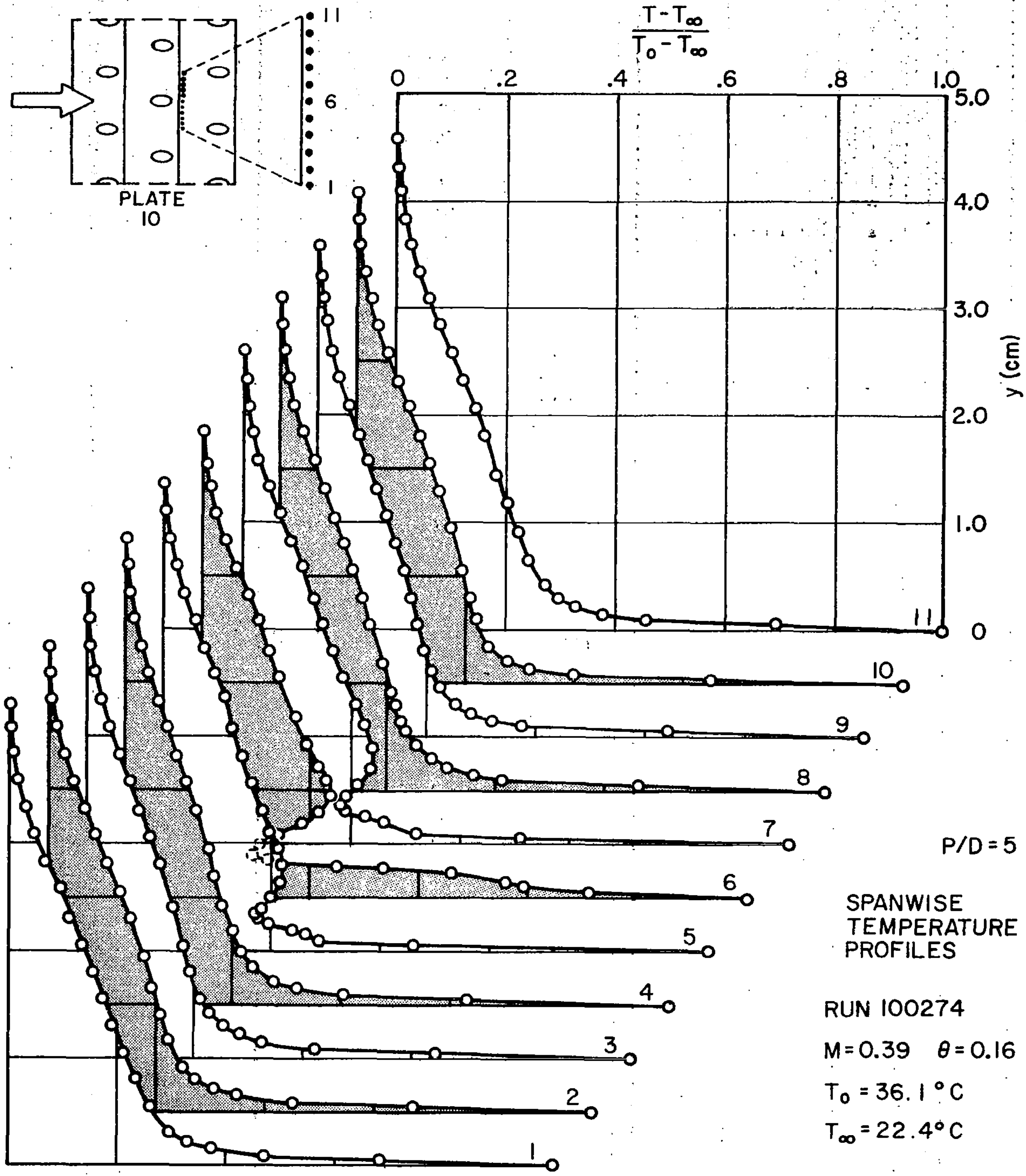

Figure 3.28 Temperature profiles downstream of ninth blowing row, θ = 0.16 (see Figures 3.1 and 3.2 for boundary layer initial conditions)

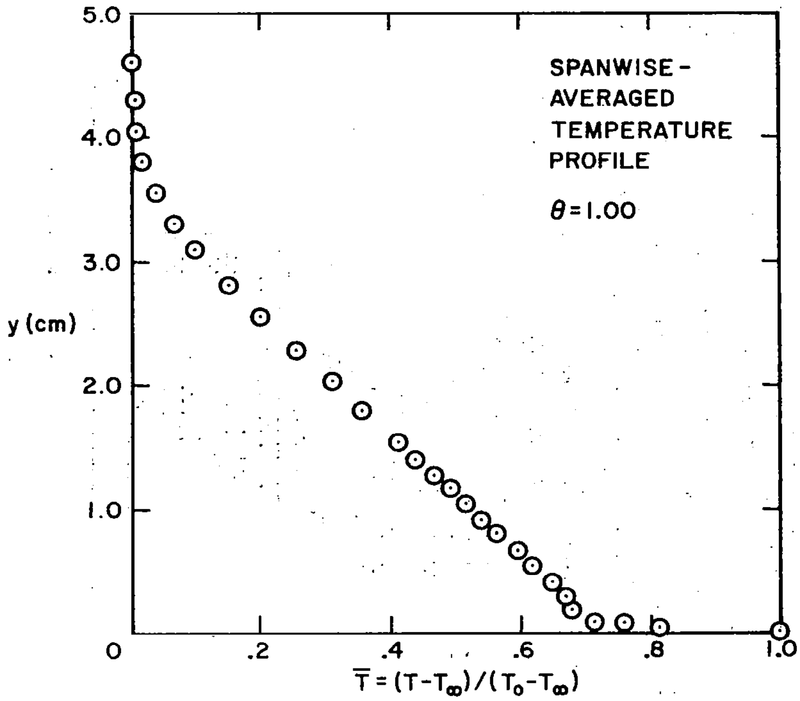

Figure 3.29 Temperature profile obtained by spanwise-averaging the profiles in Figure 3.27, $\theta = 1.00$

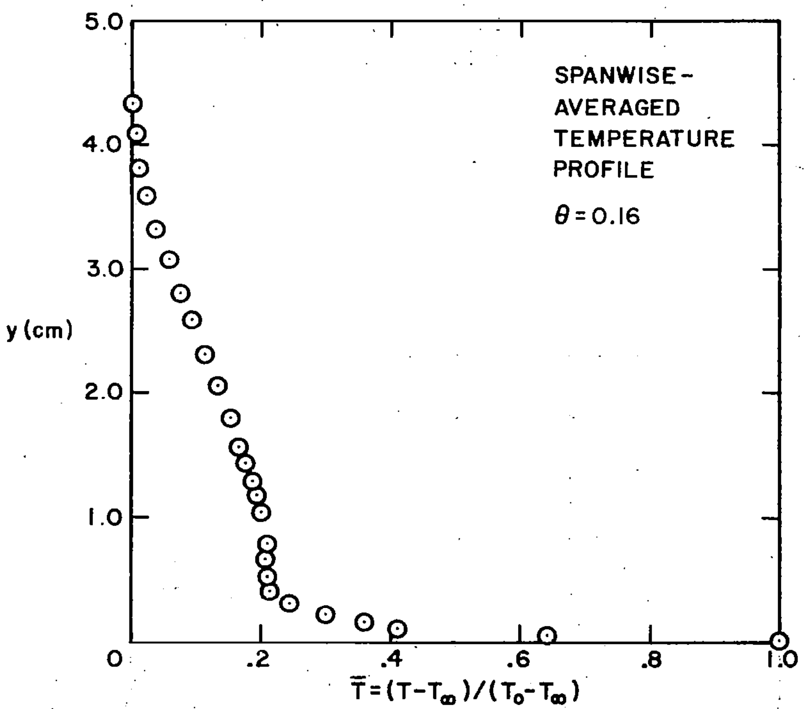

Figure 3.30 Temperature profile obtained by spanwise-averaging the profiles in Figure 3.28, $\theta = 0.16$

Chapter 4

ANALYSIS OF THE DATA

4.1 Effects of Full-Coverage Film Cooling on Stanton Number

The heat transfer data have been presented in some detail in the previous chapter. The purpose of this section of Chapter 4 is to summarize the effects of injectant temperature and blowing ratio, upstream initial conditions, and hole spacing on Stanton number.

4.1.1 Injectant Temperature and Blowing Ratio

One of the important factors in heat transfer with full-coverage film cooling is the injectant temperature level, T_2 , compared with the surface and mainstream temperatures. Because of the linearity of the governing energy equation for small temperature differences, the heat transfer is a linear function of T_2 . Thus, the acquisition of Stanton number data for two injectant temperatures (all other parameters fixed) provided sufficient information to define the Stanton number as a continuous function of T_2 . For the steady state heat transfer tests described herein, the injectant temperatures were $T_2 = T_o$ $(\theta = 0)$ and $T_2 = T_\infty$ $(\theta = 1)$. For gas turbine applications $T_2 < T_o < T_\infty$, resulting in a θ parameter slightly larger than unity (Colladay 1972). Therefore the $\theta = 1$ data trends described in Chapter 3 should be indicative of the Stanton number behavior on a full-coverage turbine blade.

While Stanton number is a simple function of θ , it is a very complex function of blowing ratio. Figure 4.1 shows Stanton numbers from plate 11, Figure 3.6, plotted versus blowing ratio. The data exhibit a nonlinear dependence of St on M for $P/D = 5$. Also shown in Figure 4.1 are predicted Stanton numbers for a typical θ operating condition to demonstrate the superposition principle. The predicted Stanton number decreases to a minimum at $M \simeq 0.4$ and then rises as M increases. This minimum in St for a typical θ operating condition is clearly seen in the $\theta = 1$ data. This minimum appears to be independent of upstream initial conditions. For example the data in Section 3.3.4 (thin initial boundary layer) shows $M \simeq 0.4$ produces a lower $St(\theta = 1)$ than does the $M \simeq 0.8$ data, for both $P/D = 5$ and 10 .

The drop in Stanton number for low M and $\theta = 1$ is similar to that found in transpiration cooling, but not as pronounced. With both cooling schemes the heat transfer is reduced due to addition of wall temperature fluid which significantly alters the temperature profile in the near-wall region. However, the cooling effect is diminished with full-coverage cooling because of increased turbulent transport. The spanwise velocity profiles indicate the full-coverage jets affect the transport over a range from the wall to at least two hole diameters above the wall, whereas with transpiration only the sublayer is affected. Thus, for an equivalent wall mass flux of coolant (equal F), the Stanton number with film cooling will be higher.

The change in Stanton number with M for $M > 0.4$ suggests the film cooling jets are delivering the coolant further out into the boundary layer. This increased penetration distance has a two-pronged effect. By depositing the coolant farther away from the surface, the coolant must be convected or diffused back into the near-wall region in order to reduce the wall heat transfer. During this process the coolant entrains boundary layer fluid, and in particular, near-mainstream temperature fluid, and equilibration with the entrained fluid severely reduces the effectiveness of the coolant. The second major effect of increased penetration is increased turbulence production. The resulting increased turbulent transport in the outer layer may enhance the coolant diffusion back to the surface, but it also enhances the jet entrainment process which "dilutes" the coolant.

In the recovery region the Stanton number response for $\theta = 1$ has three distinct patterns. For low blowing ratio ($M < 0.4$) the boundary layer immediately begins to recover in a manner similar to the region downstream of a transpiration section. For $M = 0.4$ the recovery region heat transfer becomes a constant, at least for the recovery region of these experiments (about 60 hole diameters). For $M > 0.4$ the Stanton number continues to decrease throughout the recovery region.

The recovery region response suggests that it may be possible to use an interrupted hole array pattern for turbine blade cooling. If the thermal boundary layer can be "pumped up" with coolant from several rows of holes, then downstream of those rows the Stanton number will be delayed in rising. (This conclusion is based on $P/D = 5$ data only, and for a very low mainstream turbulence level).

Presumably what happens in the recovery region is that the thermal boundary layer is spatially "frozen" because there no longer exists a mechanism for fast diffusion of the "pumped up" temperature profile (see Figure 3.24 for a typical $\theta = 1$ temperature profile). The profile restoration must come from turbulent mixing, but its predominant source will be wall-generated turbulence. In effect, a new momentum boundary layer begins in the recovery region, and until it engulfs the major part of the existing thermal boundary layer, the Stanton number will be depressed.

4.1.2 Upstream Initial Conditions

The initial conditions of the turbulent boundary layer were systematically varied to obtain data for developing integral correlations and for testing differential prediction models. Figure 4.2 shows all the data for $M = 0.4$ and $P/D = 5$, replotted as $St(\theta)/St_o$ versus the downstream distance, x, where St_o is Stanton number for $M = 0$ and the same upstream initial conditions as $St(\theta)$.

In Figure 4.2 the Stanton number ratios for $\theta = 1$ drop below unity in a fairly tight band for both the blowing and recovery region (note there is no apparent explanation of why the $Re_{\delta_2} \simeq 2700$ unheated starting length data should be low, when corresponding data at $Re_{\delta_2} \simeq 1900$ and 4700 are within the band). This tight grouping for $\theta = 1$ suggests there is, at most, a slight effect of U_∞ on Stanton number. For example, the $Re_{\delta_2} \simeq 1900$ and 520 data, both with about the same U_∞ but much different initial boundary layer thicknesses, have slightly higher Stanton number ratios than data with higher mainstream velocities. This velocity dependence is introduced into the data correlation in Section 4.2 in terms of a hole-diameter Reynolds number, $Re_{D,\infty} = DU_\infty/\nu$.

Also shown in Figure 4.2 are Stanton number ratios for $\theta = 0$. The low and high Re_{δ_2} data with heated starting length rise in the initial blowing region whereas the high Re_{δ_2} data without a heated starting length do not. This is a thermal boundary layer effect. Injecting $\theta = 0$ fluid does not directly contribute to the growth of Re_{Δ_2} , so until the thermal boundary layer grows beyond the penetration height of the jets, the Stanton number is only marginally different from St_o .

4.1.3 Hole Spacing

Stanton numbers were obtained for $P/D = 5$ and 10 and visual comparison of these data in Chapter 3 revealed a much diminished effect for the same M with the wider hole spacing. The comparison is more meaningful when the data are compared at equal F , which implies equal mass flux of coolant injected over a given surface area. This comparison will be made in the next section.

4.2 Correlation of the Stanton Number Data

One method of evaluating film-cooling performance is to evaluate surface heat flux with and without film cooling, $\dot{q}''(\theta)/\dot{q}''_o$, at the same location on the surface. Because both heat fluxes are defined using the same convective rate equation, the film-cooling performance can be simplified to evaluation of $h(\theta)/h_o$ or $St(\theta)/St_o$. The $St(\theta)$ information can be obtained by applying superposition to correlations of the fundamental Stanton number data sets at $\theta = 0$ and $\theta = 1$.

The data for $\theta = 1$ were correlated based on a Couette flow analysis developed by Choe et al. (1976),

$$\left.\frac{St(\theta = 1)}{St_o}\right|_{Re_x} = \frac{\ln(1 + B_h)}{B_h} \cdot \phi \tag{4.1}$$

where B_h is the blowing parameter, defined as $B_h = F/St(\theta = 1)$, and ϕ is a function that is unity for transpiration cooling, and greater than unity for full-coverage film cooling. Thus, ϕ is a measure of departure from the ideal case of transpiration cooling.

Figure 4.3 shows all data for $\theta = 1$ plotted as ϕ versus $F \cdot Re_{D,\infty}^{0.2}$. The solid line for $P/D = 5$ and the dashed line for $P/D = 10$ are best-fit lines for the data. Both lines change slope at an F corresponding to $M \approx 0.4$. As discussed in Chapter 3, this blowing ratio appears to be the highest value for which the cooling jets remain attached to the surface (at least for the $P/D = 5$ data).

The mainstream velocity effect mentioned in Section 4.1.2 is reflected in the $F \cdot Re_{D,\infty}^{0.2}$ product. The 0.2 power indicates a small effect on Stanton number ratio for changes in U_∞. It is presumed that $Re_{D,\infty}$ is the correct correlating parameter; no tests were conducted with changes in hole diameter to verify it. However, the trend in the functional dependence for $Re_{D,\infty}$ is in the right direction, i.e., as D becomes smaller, ϕ becomes smaller for the same F, and in the limit as it approaches zero, ϕ approaches unity, which is transpiration cooling.

The effect of changing the pitch-to-diameter ratio is also seen in Figure 4.3. For a given blowing fraction, the ϕ value increases, indicating even less effective surface protection, i.e., higher heat transfer coefficients. This is not surprising, since, to have equal F (mass flux of coolant), as P/D increases, M must also increase, resulting in greater jet penetration and increased turbulent mixing.

Correlations of the $\theta = 1.0$ data for $P/D = 5$ and $M \geq 0.4$ are as follows:

$$\left.\frac{St}{St_o}\right|_{Re_x} = \left[0.5 + 23.2\ F \cdot Re_{D,\infty}^{0.2}\right] \frac{\ln(1 + B_h)}{B_h} \tag{4.2}$$

or, in Re_{Δ_2} coordinates (following Whitten, Kays, and Moffat 1967)

$$\left.\frac{St}{St_o}\right|_{Re_{\Delta_2}} = \left[0.5 + 23.2\ F \cdot Re_{D,\infty}^{0.2}\right]^{1.25} \cdot \left[\frac{\ln(1 + B_h)}{B_h}\right]^{1.25} \cdot (1 + B_h)^{0.25} \tag{4.3}$$

The values for St_o in equation (4.2) or (4.3) are the typical smooth flat plate values, as recommended by Kays (1966), for example. The data summary sheets in Appendix I give values for ϕ and the equation used to generate St_o values.

For $\theta = 0$, the Stanton number data could be correlated as a function of $Re_{D,\infty}$ for those data which reached an asymptotic state, independent of the number of rows of holes upstream. Correlation of the data was particularly troublesome because of insufficient asymptote data. Stanton numbers for $M < 0.4$ at $P/D = 5$ failed to reach an asymptote because of the unheated starting length initial condition. Stanton numbers for $P/D = 10$ did not reach an asymptote because of insufficient test surface length; i.e., only six rows of holes were available when the test section was reconfigured.

For $M \geq 0.4$ and initial $Re_{\delta_2} \simeq 500$ ($Re_{D,\infty} = 7900$), the correlating equation for $P/D = 5$ data is

$$St(\theta = 0) = 0.0132\ F^{0.35} \tag{4.4}$$

For $Re_{\delta_2} \simeq 2700$ ($Re_{D,\infty} = 11,200$) and $P/D = 5$ the correlating equation is

$$St(\theta = 0) = 0.0112\ F^{0.35} \tag{4.5}$$

4.3 Development of a Prediction Model

The overall goal of the full-coverage film-cooling research at Stanford is to develop a prediction method to aid in design of full-coverage turbine blades. Three types of methods were considered: (1) integral analysis, (2) two-dimensional differential analysis, and (3) three-dimensional differential analysis. A differential type of analysis was chosen primarily because of its provision for a greater flexibility in turbulence modeling.

In choosing between using a two-dimensional differential analysis (coupled with simple empirical models for the film-cooling process) and a three-dimensional analysis (perhaps the only "true" analysis), the following were considered: the computation scheme had to have a relatively short execution time to make it attractive as a "design tool", and the scheme had to have a relatively small computer core requirement. Based on these criteria, a two-dimensional scheme was pursued.

The differential method that was developed consisted of the two-dimensional boundary layer program, STAN5, with added routines to model the injection process and turbulence augmentation. Flow over the full-coverage surface was considered to be describable by boundary layer equations (see Herring 1975 or Choe et al. 1976 for a discussion of the applicability of these equations). The program solves these equations, marching in the streamwise direction. Fluid is injected into the boundary layer by stopping the program when a row of holes is encountered and dividing the injected fluid among the stream tubes between the wall and some "jet penetration point". The jet-boundary layer interaction is modeled by augmenting the Prandtl mixing-length. Two "constants" are required, in addition to the accepted constants for predicting boundary layer flow over a flat, slightly rough plate.

The boundary layer equations being solved are those described in the STAN5 documentation report (Crawford and Kays 1975) for flow over a flat surface

$$\frac{\partial}{\partial x}(\rho U) + \frac{\partial}{\partial y}(\rho V) = 0 \tag{4.6}$$

$$\rho U\frac{\partial U}{\partial x} + \rho V\frac{\partial U}{\partial y} = -g_c \frac{dP}{dx} + \frac{\partial}{\partial y}\left(\mu_{eff} \frac{\partial U}{\partial y}\right) \tag{4.7}$$

$$\rho U\frac{\partial I^*}{\partial x} + \rho V\frac{\partial I^*}{\partial y} = \frac{\partial}{\partial y}\left[\mu_{eff} \frac{\partial I^*}{\partial y} + \frac{\mu_{eff}}{g_c J}\left(1 - \frac{1}{Pr_{eff}}\right) \frac{\partial}{\partial y}\left(\frac{U^2}{2}\right)\right] \tag{4.8}$$

where $I^* = I + U^2/2g_cJ$. The effective viscosity and effective Prandtl number are defined in terms of an eddy viscosity and turbulent Prandtl number,

$$\mu_{eff} = (\mu + \mu_t) = \rho(\nu + \varepsilon_M) \tag{4.9}$$

$$Pr_{eff} = \frac{\mu_{eff}}{\left(\frac{k}{c}\right) + \left(\frac{k}{c}\right)_t} = \frac{1 + \frac{\varepsilon_M}{\nu}}{\frac{1}{Pr} + \frac{\varepsilon_M}{\nu} \cdot \frac{1}{Pr_t}} \tag{4.10}$$

where μ_t is the turbulent viscosity, k_t is the turbulent conductivity, and c is the specific heat.

The eddy diffusivity for momentum is modeled by the Prandtl mixing-length

$$\varepsilon_M = \ell^2 \left|\frac{\partial U}{\partial y}\right| \tag{4.11}$$

The mixing-length distribution will be described in Section 4.3.2.

The turbulent Prandtl number, Pr_t, is presumed to follow the flat plate variation described in Crawford and Kays (1975). The Pr_t distribution is for air; it is 1.72 at the wall and drops to 0.86 in the outer region.

Boundary conditions for the "two-dimensional" flow equations are

$$U(x,0) = 0 \tag{4.12a}$$

$$V(x,0) = 0 \tag{4.12b}$$

$$\lim_{y\to\infty} U(x,y) = U_\infty \text{ (constant)} \tag{4.12c}$$

and

$$I^*(x,0) = I_o^* \text{ (constant)} \tag{4.12d}$$

$$\lim_{y\to\infty} I^*(x,y) = I_\infty^* \text{ (constant)} \tag{4.12e}$$

4.3.1 Injection Model

In constructing a model for the film-cooling injection process, consideration was made of the physical process occurring when the jets enter the boundary layer. For low M the jets do not penetrate; they are immediately "knocked over" by drag forces on the emerging jets (primarily pressure forces from the retarded boundary layer flow upstream of the jets). For higher M the jets emerge from the surface and are turned into the downstream direction by pressure and shear forces which overcome the jets' resistance to direction change. As each emerging jet moves through the boundary layer, the shear layer at the injectant-boundary layer interface promotes entrainment of boundary layer fluid into the jet. This spreads the jet and slows it; eventually the injectant becomes diffused into the existing boundary layer fluid.

The injection process and the entrainment-diffusion process are modeled together. As a jet passes through the stream tubes that comprise the boundary layer, drag forces arising due to the jet/cross-stream interaction are presumed to "tear off" some of the injectant. The injectant that is shed into a given stream tube is then accelerated by the drag forces. This process is depicted below. Shedding continues into successive stream tubes until the amount shed equals the mass flow of the injectant. The distance where shedding is complete is called the penetration distance.

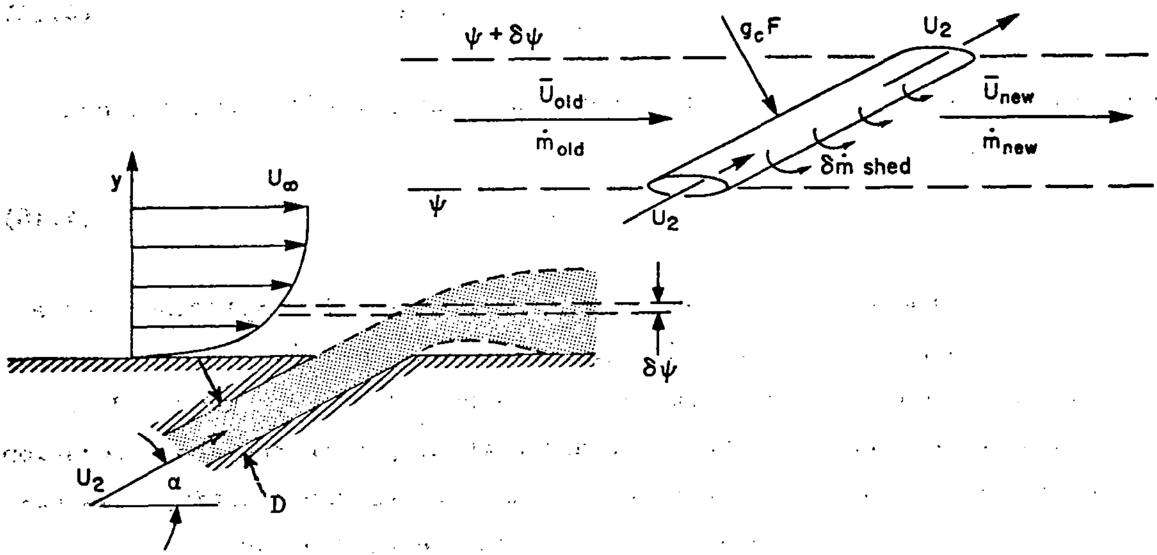

Equations that describe the model are obtained from one-dimensional mass, momentum, and thermal energy balances on the element of injectant bounded between two stream surfaces. For flow between these surfaces,

$$\dot{m}_{new} = \dot{m}_{old} + \delta\dot{m} \tag{4.13}$$

where $\dot{m}_{old}$ is the flow rate upstream and $\delta\dot{m}$ is the injectant that is shed (on a rate basis). From a momentum balance consideration,

$$(\dot{m}_{old} + \delta\dot{m})\overline{U}_{new} = \dot{m}_{old}\overline{U}_{old} + \delta\dot{m}U_2\cos\alpha \qquad (4.14)$$

where $\overline{U}_{old}$ is the mass-averaged velocity of the upstream fluid and U_2 is the velocity of the injectant. The U_2 velocity is assumed not to vary with y. This is the simplest way to preserve overall momentum within the boundary layer (i.e., $\Sigma\delta\dot{m}U_2 = \dot{m}_{jet}U_2$, where $U_2 = M\rho_\infty U_\infty/\rho_2$

The drag forces that "tear-off" the injectant are assumed to accelerate $\delta\dot{m}$ from its initial velocity up to the new stream-tube velocity,

$$g_c F = \delta\dot{m}(\overline{U}_{new} - U_2\cos\alpha) \qquad (4.15)$$

The drag forces can be defined in terms of a drag coefficient for convenience,

$$g_c F = C_D \frac{1}{2}\rho A_j (\overline{U}_{old} \sin\alpha)^2 \qquad (4.16)$$

where A_j is the cross-sectional area of the jet, $(D \cdot \delta y)/\sin\alpha$ for a stream tube that is δy in width (proportional to $\delta\psi$).

By introducing the definition $\dot{m}_{old} = \rho\overline{U}_{old}(\delta y \cdot P)$, where P is the distance between adjacent jets, and combining with the above equations, the ratio of the mass shed from the coolant jet to the existing mass between the stream tubes (on a rate basis) can be written as

$$\frac{\delta\dot{m}}{\dot{m}_{old}} = \frac{1}{\dfrac{2(P/D)}{C_D \sin\alpha}\left(1 - \dfrac{U_2\cos\alpha}{\overline{U}_{old}}\right) - 1} \qquad (4.17)$$

A mass-averaged velocity ratio can be formed by rearranging equation (4.14):

$$\frac{\overline{U}_{new}}{\overline{U}_{old}} = \frac{1}{\left(1 + \dfrac{\delta m}{\dot{m}_{old}}\right)}\left[1 + \left(\frac{\delta\dot{m}}{\dot{m}_{old}}\right)\frac{U_2\cos\alpha}{\overline{U}_{old}}\right] \qquad (4.18)$$

From energy balance considerations,

$$\bar{I}^*_{new}(\dot{m}_{old} + \delta\dot{m}) = \dot{m}_{old}\bar{I}^*_{old} + \delta\dot{m}I^*_{jet} \qquad (4.19)$$

where $\bar{I}^*_{old}$ is the mass-averaged stagnation enthalpy of the upstream fluid and I^*_{jet} is that of the injectant (assumed not to vary with y to satisfy overall energy conservation). A mass-averaged enthalpy ratio can be formed by rearranging equation (4.19):

$$\frac{\bar{I}^*_{new}}{\bar{I}^*_{old}} = \frac{1 + \left(\frac{\delta\dot{m}}{\dot{m}_{old}}\right)\frac{I^*_{jet}}{\bar{I}^*_{old}}}{\left(1 + \frac{\delta\dot{m}}{\dot{m}_{old}}\right)} \qquad (4.20)$$

In the prediction program, the injection model, based on the analysis given above, is contained in a subroutine, and it is invoked when a row of holes is encountered. The empirical input is the mass shed ratio, defined as

$$\frac{\delta\dot{m}}{\dot{m}_{old}} = \text{DELMR} \qquad (4.21)$$

The DELMR expression is used in lieu of equation (4.17) for simplicity. With this input "constant", the routine processes each flow tube from the wall outward. The velocities are adjusted according to equation (4.18) to conserve momentum. The stagnation enthalpies are adjusted according to equation (4.20). The injection process is terminated when

$$\dot{m}_{jet} = \rho_2 U_2 \frac{\pi D^2}{4P^2} = \sum_i \text{DELMR} \cdot \delta\psi_i \qquad (4.22)$$

Note the introduction of P to put the flow rate on a per-unit depth basis (consistent with the dimensions of ψ). The y location where flow distribution is completed is PD , the penetration distance. This calculated distance is a significant variable in the augmented turbulent mixing model, for it is at this point that the increased mixing has its maximum.

4.3.2 Turbulence-Augmentation Model

The eddy diffusivity for momentum is modeled by the Prandtl mixing-length. To account for the jet/cross-stream interaction the mixing-length is augmented, using a variation of a model first described by Choe et al. (1976).

$$\left(\frac{\ell}{\delta}\right) = \left(\frac{\ell}{\delta}\right)_{2-d} + \left(\frac{\ell}{\delta}\right)_{a} \qquad (4.23)$$

where the "2-d" subscript refers to the two-dimensional mixing-length, and the "a" subscript denotes a departure due to discrete-hole injection. The functional form for the (ℓ/δ) expression was determined from the computed mixing-length distribution given in Section 3.4 . The functional form is depicted below.

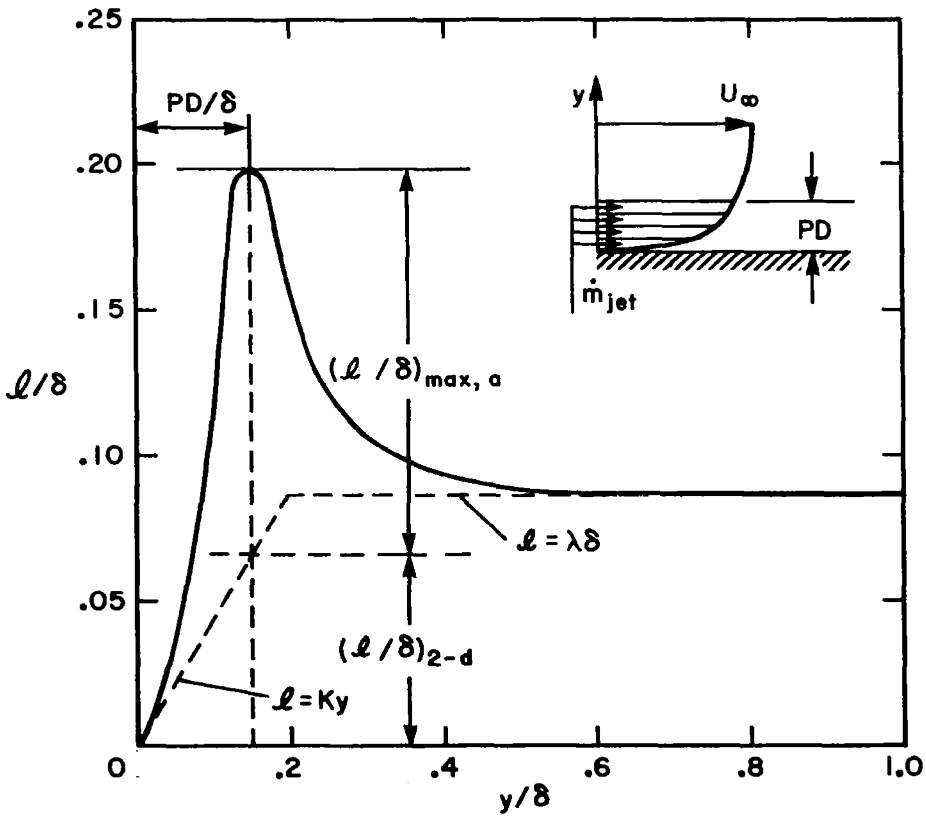

The curve represents a departure from the two-dimensional mixing-length value, with a maximum departure, $(\ell/\delta)_{max,a}$, located at PD, the penetration distance from the wall, as determined by the injection model.

The two-dimensional mixing-length is

$$\ell_{2-d} = \begin{cases} \kappa y D & \kappa y < \lambda\delta \\ \lambda\delta & \kappa y \geq \lambda\delta \end{cases} \tag{4.24}$$

where D is the Van Driest damping function,

$$D = 1 - \exp(-y^+/A^+) \tag{4.25}$$

In the predictions $\kappa = 0.41$, $\lambda = 0.085$, and $A^+ = 22$ in the blowing region for $P/D = 5$ (to account for surface roughness) and $A^+ = 25$ in the smooth, flat-plate recovery region.

The augmented mixing-length is given by

$$\ell_a = \kappa_o \delta \left(\frac{y}{\delta}\right)^2 \exp\left[-\left(\frac{y/\delta}{PD/\delta}\right)^2\right] \cdot D \tag{4.26}$$

where

$$\kappa_o = \frac{2.71828}{(PD/\delta)^2} \cdot (\ell/\delta)_{max,a} \tag{4.27}$$

In the above equations, PD is the penetration distance of the injectant, determined from the injection model. The boundary layer thickness (actually the ninty-nine percent point) is δ. The maximum mixing-length augmentation, occurring at $y = PD$, is $(\ell/\delta)_{max,a}$. This is the second input "constant" for the prediction scheme. Note that equation (4.26) contains the Van Driest damping function merely for programming convenience; the damping function approaches unity well before there is an appreciable contribution from the other terms in equation (4.26).

One of the most perplexing problems associated with the prediction scheme was in the initial blowing region and initial recovery region. In the initial blowing region A^+ changes from a smooth plate value to A^+ for the rough, discrete-hole plate, and κ_o goes from zero to its maximum value, proportional to $(\ell/\delta)_{max,a}$. The reverse transition occurs in the initial recovery region.

The A^+ transition was handled by invoking a first order lag equation similar to that described by Crawford and Kays (1975),

$$\frac{dA^+_{eff}}{dx^+} = -\frac{A^+_{eff} - A^+}{C} \tag{4.28}$$

where A^+_{eff} is the effective Van Driest damping constant, A^+ is the asymptotic value (22 for the rough, $P/D = 5$ surface; 25 for the smooth recovery region), and $C = 6000$. Thus A^+ starts out at 25, drops toward 22 when the first row of holes is encountered, and then returns to 25 in the downstream recovery region. With this lag equation, the St_o data were adequately predicted with no initial region problems.

The κ_o transition was also handled by solving an equation like (4.28) for $(\ell/\delta)_{max,a,eff}$. For the initial blowing region, the asymptote of the equation is $(\ell/\delta)_{max,a}$, and in the initial recovery region, the asymptote is zero. To simulate the beginning of the transition, the initial $(\ell/\delta)_{max,a}$ was given a step change. This method is described by Choe et al. (1976) for abrupt changes in transpiration, and it is depicted as shown below.

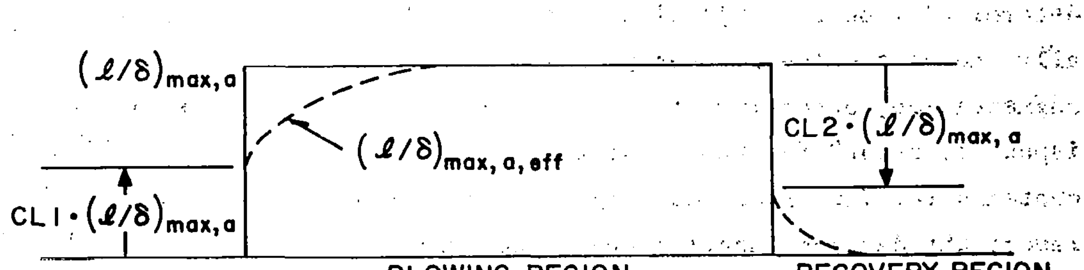

The step-change constants CL1 and CL2 were 0.3 for predictions of low M data. The CL1 value was changed to 1.0 in attempts to model the high M data. Based upon the predictions, it can be concluded that the initial region modeling was, at best, marginal. Fortunately, though, values for the step-change constants do not affect the Stanton number predictions in the region far downstream of the step location.

4.4 Numerical Prediction of the Data

Predictions of most of the P/D = 5 data have been made to assess the model outlined in the previous section. The constants DELMR and $(\ell/\delta)_{max,a}$ that successfully predicted the data are shown in Figure 4.4, plotted versus the blowing ratio. In the figure, DELMR decreases as M increases, resulting in increased penetration distance, and $(\ell/\delta)_{max,a}$ is seen to increase as M increases, indicating more intense turbulent mixing. The most interesting data point for these "computer-experiment" constants is at $M = 0.4$. Recall there were five data runs at this blowing ratio (summarized in Figure 4.4). Four of the five runs were satisfactorily predicted with the same constants. The fifth run, with a very thin initial boundary layer, required a slightly higher value of $(\ell/\delta)_{max,a}$, indicating a slightly higher turbulence level for this initial condition.

The first data set to be predicted is that discussed in Section 3.3.1 (thick initial boundary layer with heated starting length). Figure 4.5 shows Stanton number predictions for $M = 0$ and $\theta = 0$, 1 at $M = 0.4$. The $\theta = 0$ prediction spikes upward when mainstream - temperature fluid is injected into the boundary layer. Similarly, the prediction spikes downward when wall-temperature fluid is injected. Predicted velocity and temperature profiles are shown in Figures 4.6 through 4.8. They are compared to the spanwise-average profiles discussed in Section 3.4 .

To test the film-cooling model, the predictions described in the preceding paragraph were carried out for 24 rows of holes. Shown in Figure 4.9 are the finite-difference data points for prediction of 12 and 24 rows of holes. Past the first 12 rows only the average Stanton numbers per row are plotted. For $\theta = 0$, the predictions continue to exhibit an asymptotic behavior; for $\theta = 1$ the predictions continue to decrease, but at a slower rate, as if it were also approaching an asymptote.

The second data set to be predicted is the $P/D = 5$ data discussed in Section 3.3.2 (thick initial boundary layer with unheated starting length). Figures 4.10 through 4.13 shows the predictions. The two weak features of the predictions are the initial blowing region for $\theta = 0$ and the recovery region for $\theta = 1$.

The third data set to be predicted is the data discussed in Section 3.3.3 (thick initial boundary layer with change in mainstream velocity). Figures 4.14 and 4.15 show the predictions. The last data to be predicted is the $M = 0.4$ blowing ratio data at $P/D = 5$, discussed in Section 3.3.4 (thin initial boundary layer with heated starting length). Figure 4.16 shows the prediction.

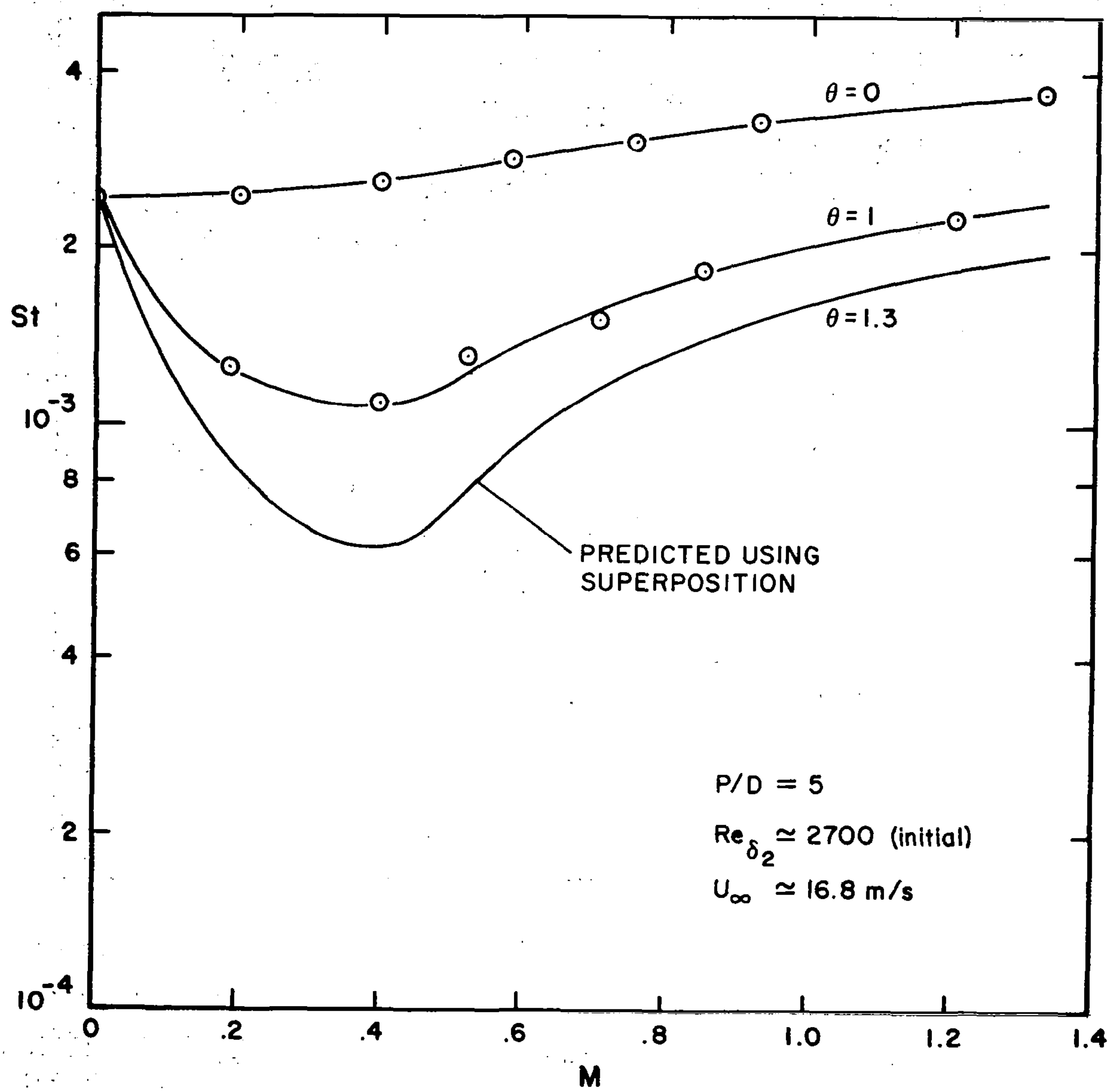

Figure 4.1 Prediction of St for θ = 1.3 by applying superposition to fundamental data sets, Figures 3.6 (plate 11)

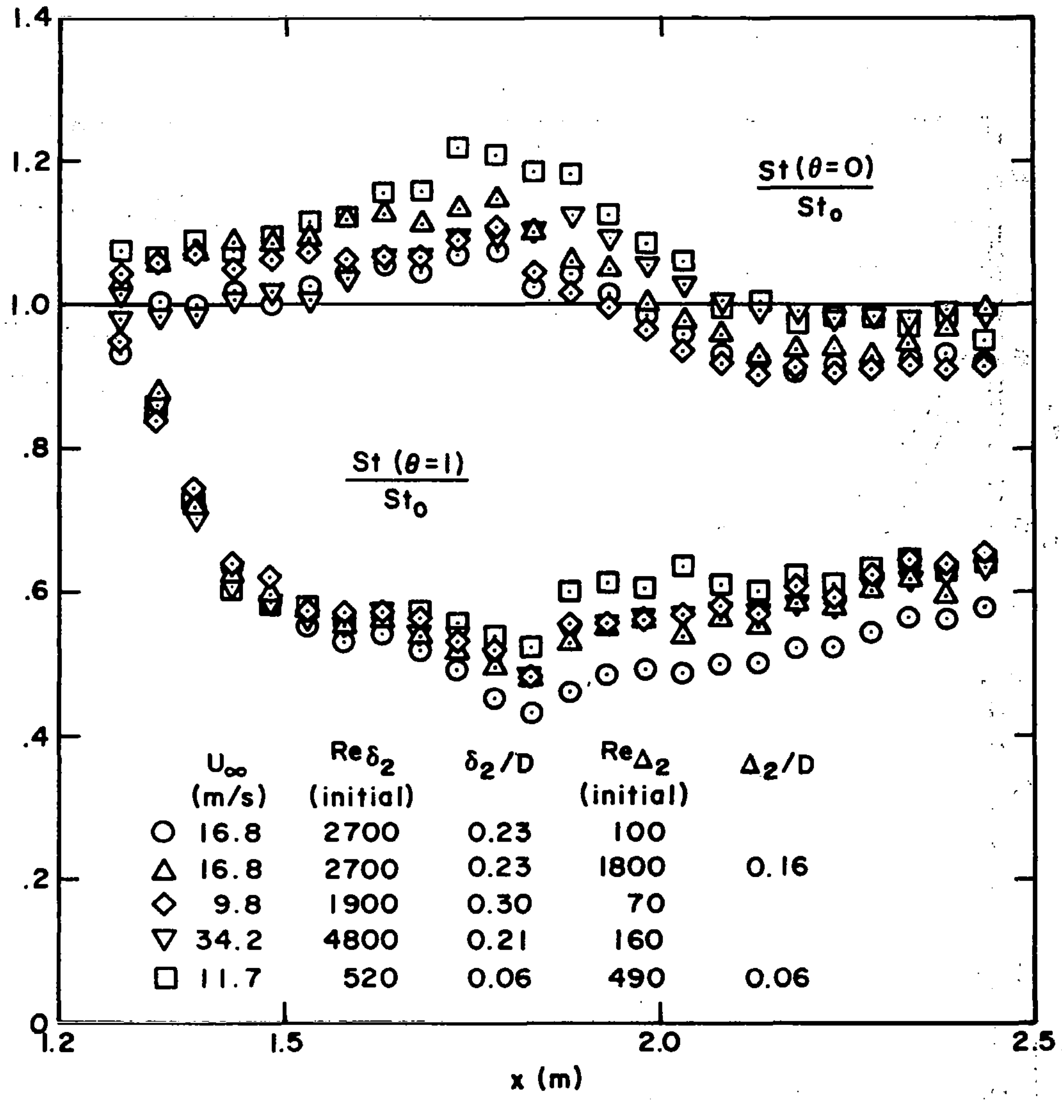

Figure 4.2 Stanton number ratios for all M ≃ 0.4 data and P/D = 5

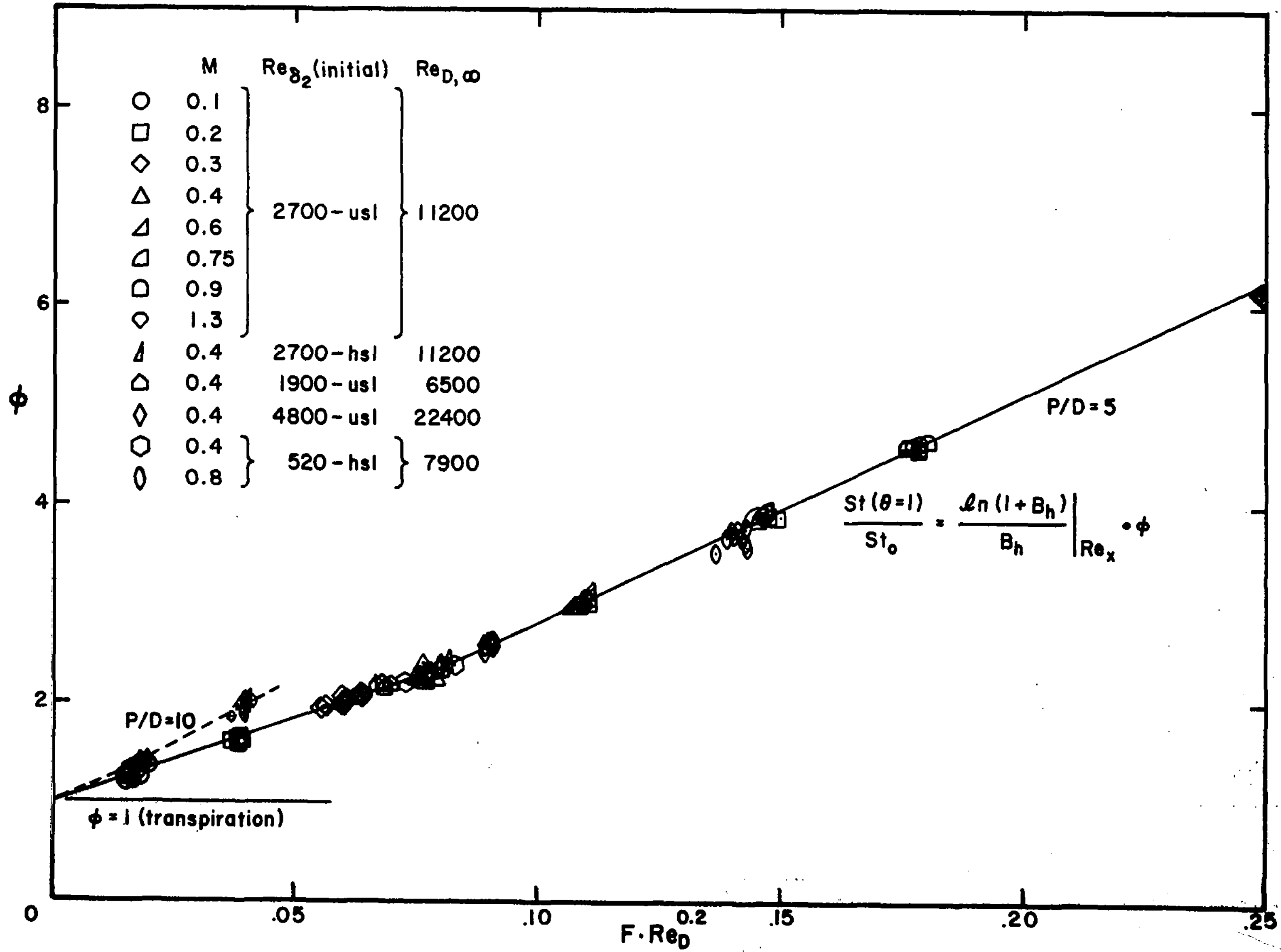

Figure 4.3 Correlation of the Stanton number data at $\theta = 1$

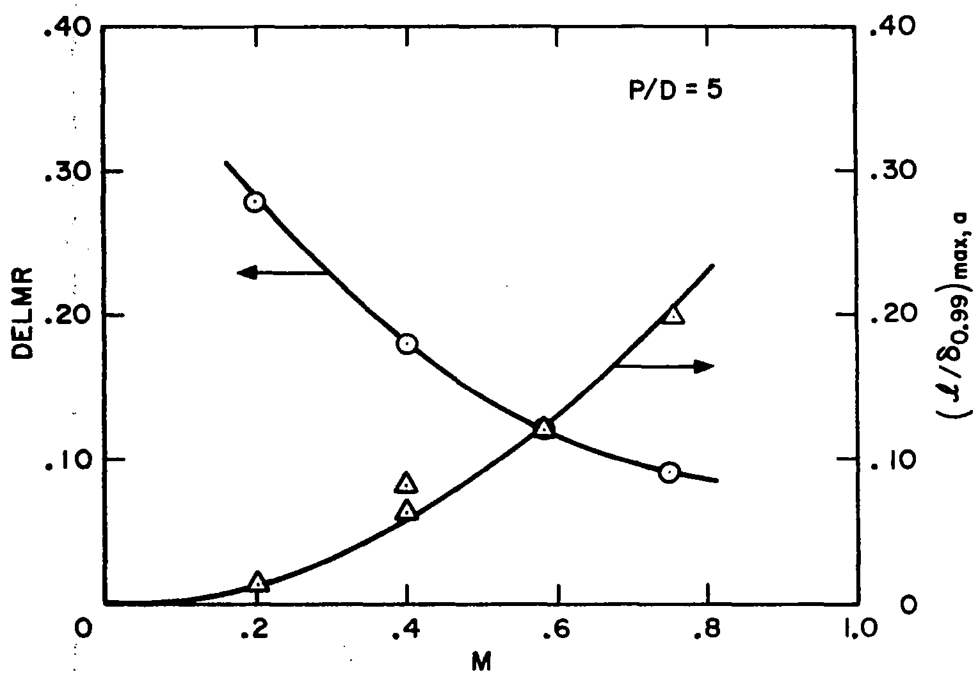

Figure 4.4 Two constants used in prediction model

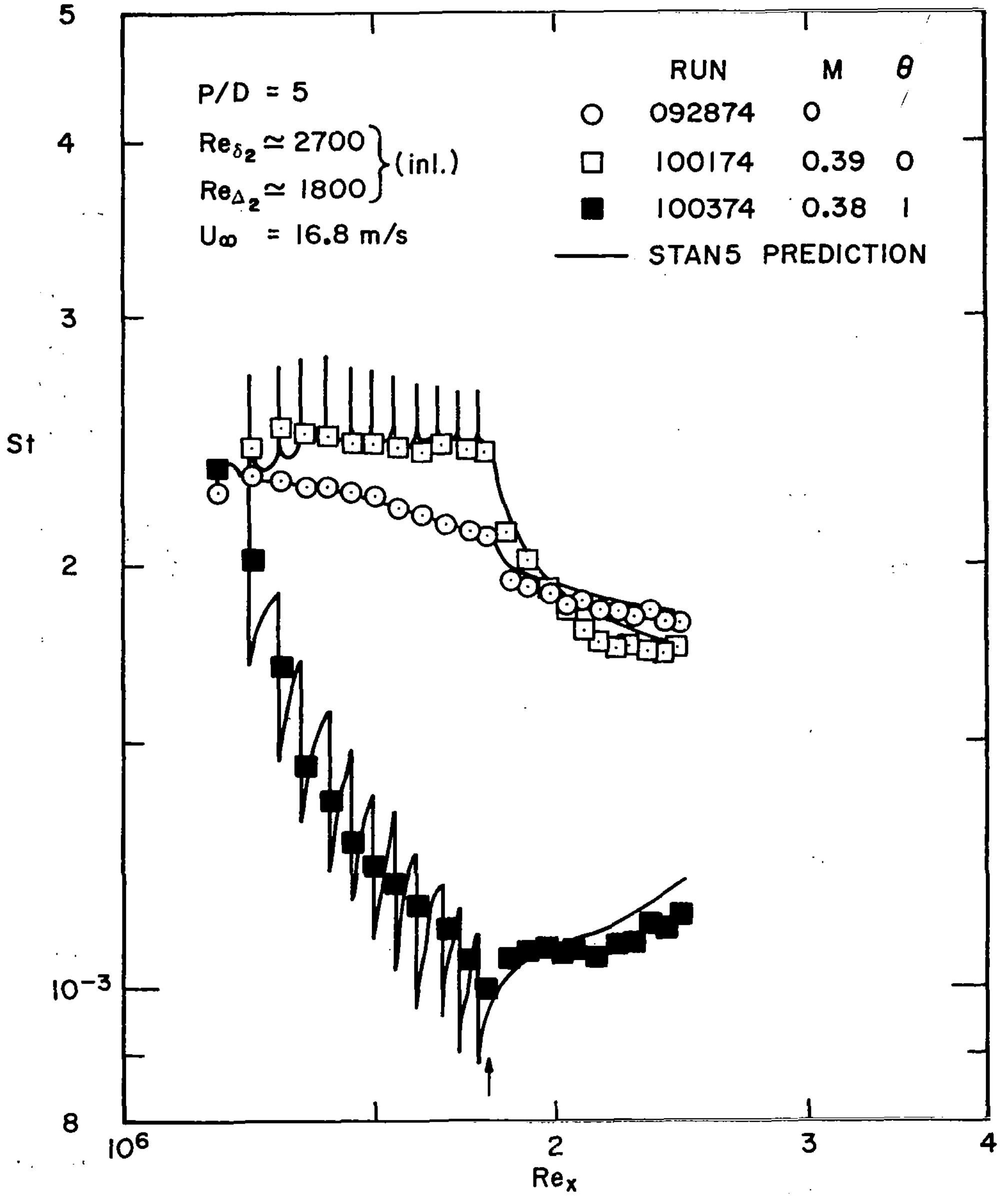

Figure 4.5 Prediction of the M = 0 and M ≃ 0.4 data from Figure 3.3

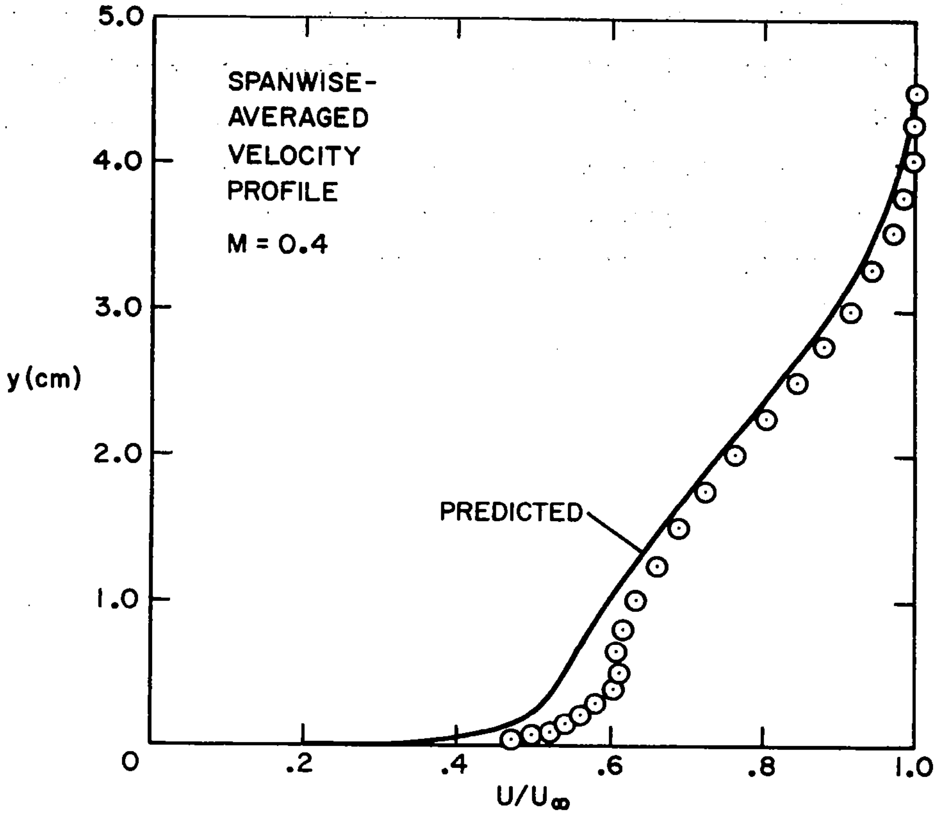

Figure 4.6 Prediction of the spanwise-averaged velocity profile from Figure 3.24

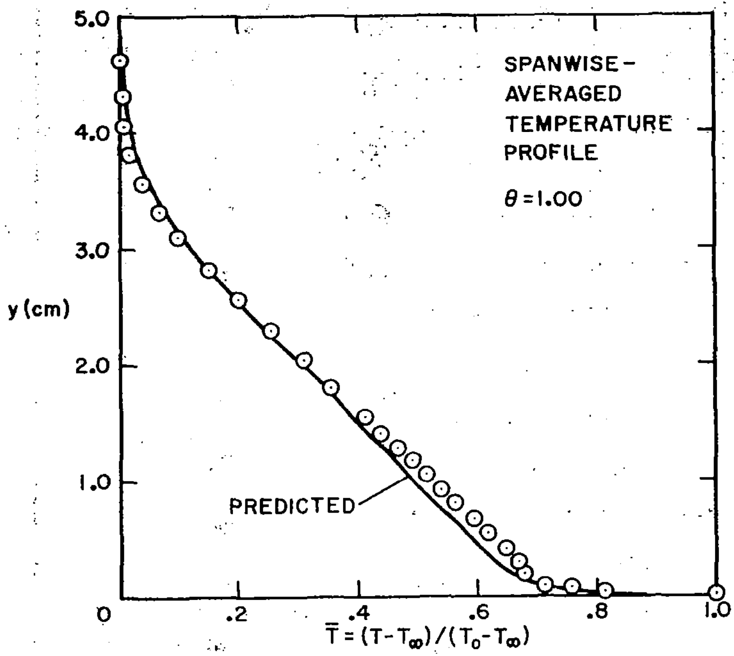

Figure 4.7 Prediction of the spanwise-averaged temperature profile (θ = 1.00) from Figure 3.29

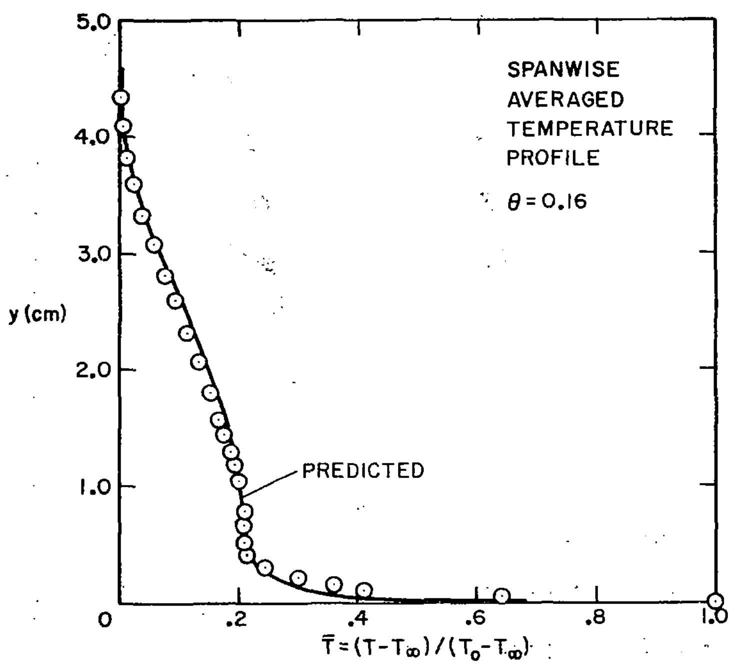

Figure 4.8 Prediction of the spanwise-averaged temperature profile (θ = 0.16) from Figure 3.30

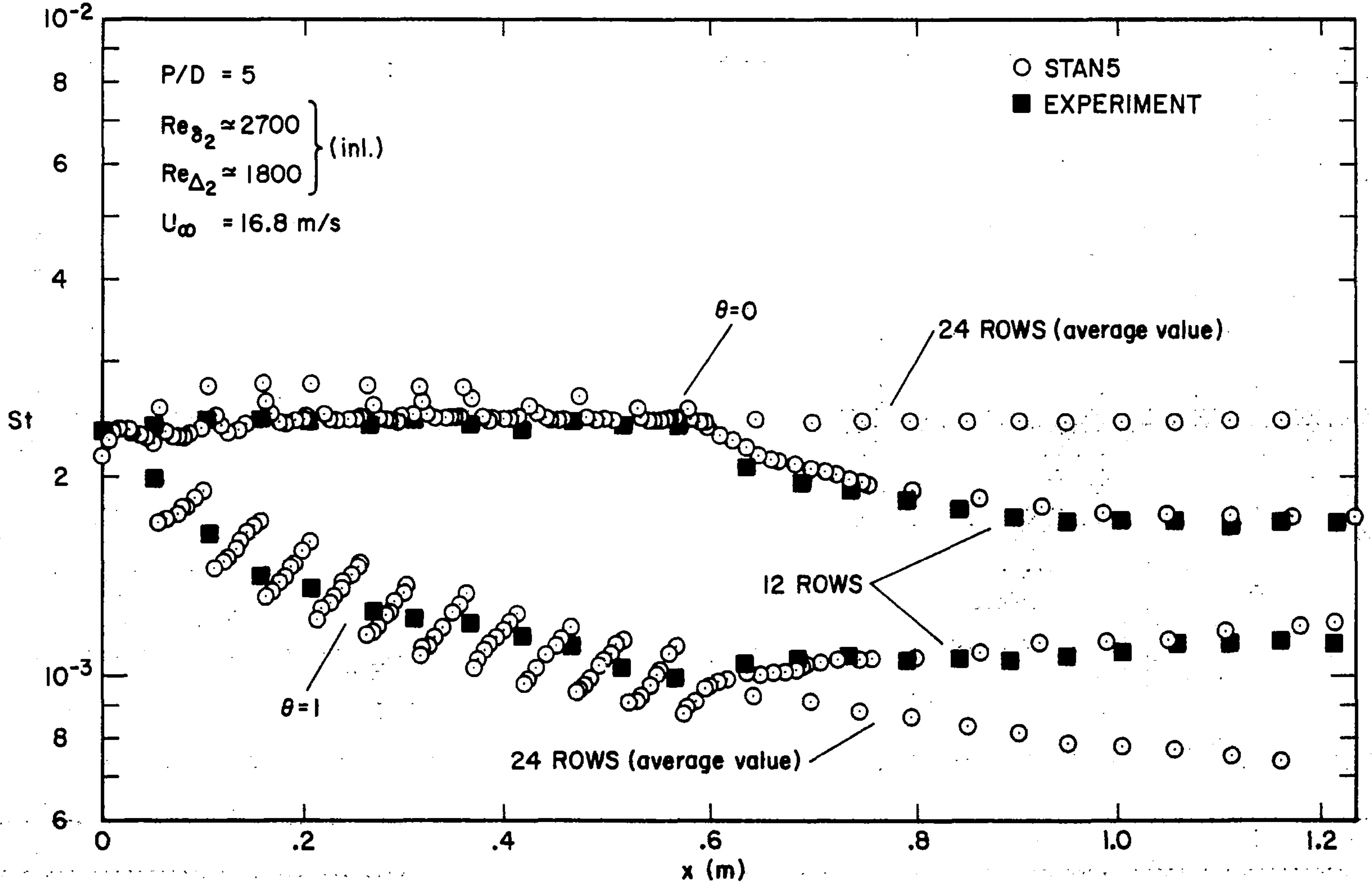

Figure 4.9 Extension of the $M = 0.4$ prediction (Figure 4.5) to 24 rows of holes to show stable behavior of injection model

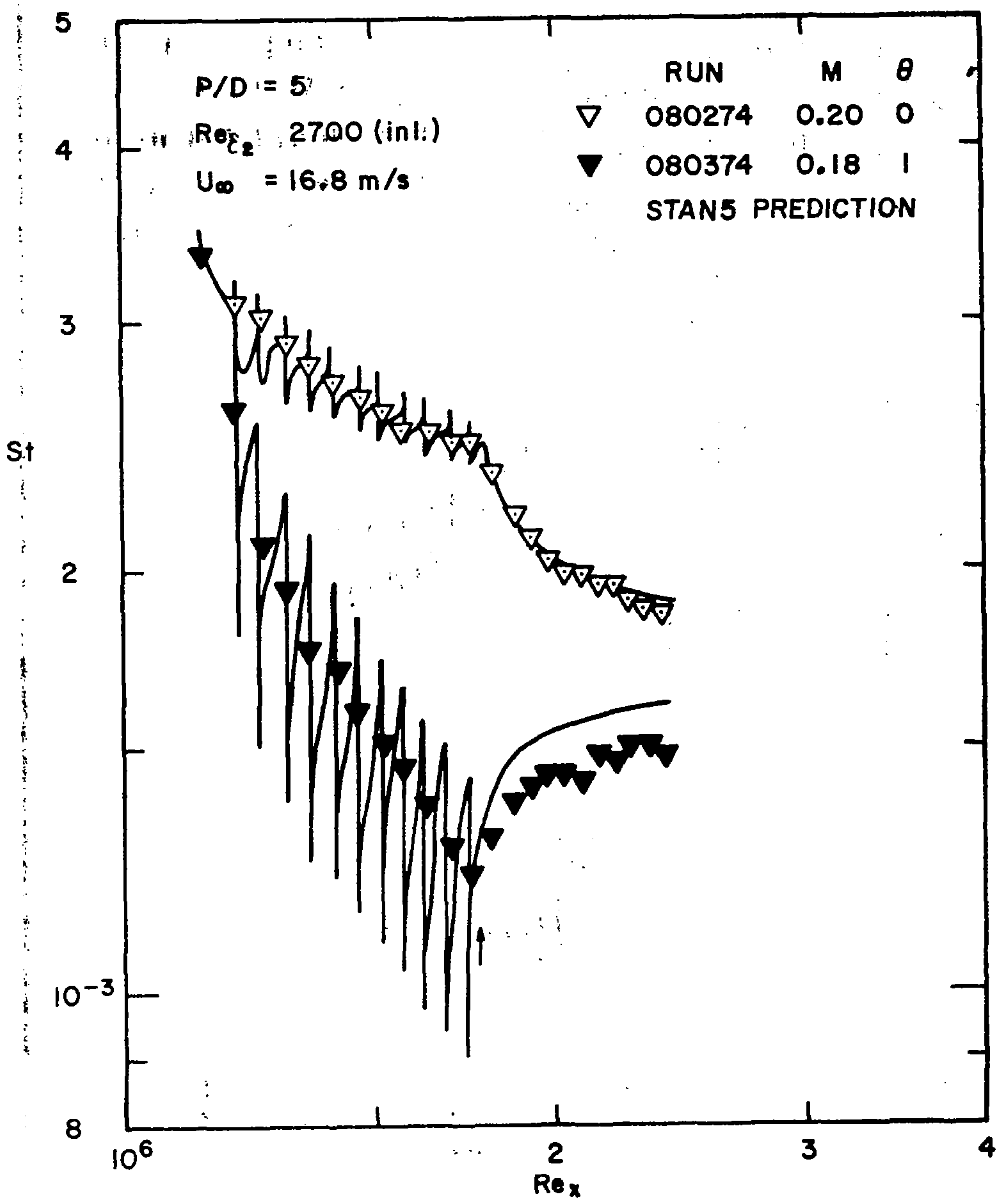

Figure 4.10 Prediction of the $M \approx 0.2$ data from Figure 3.6

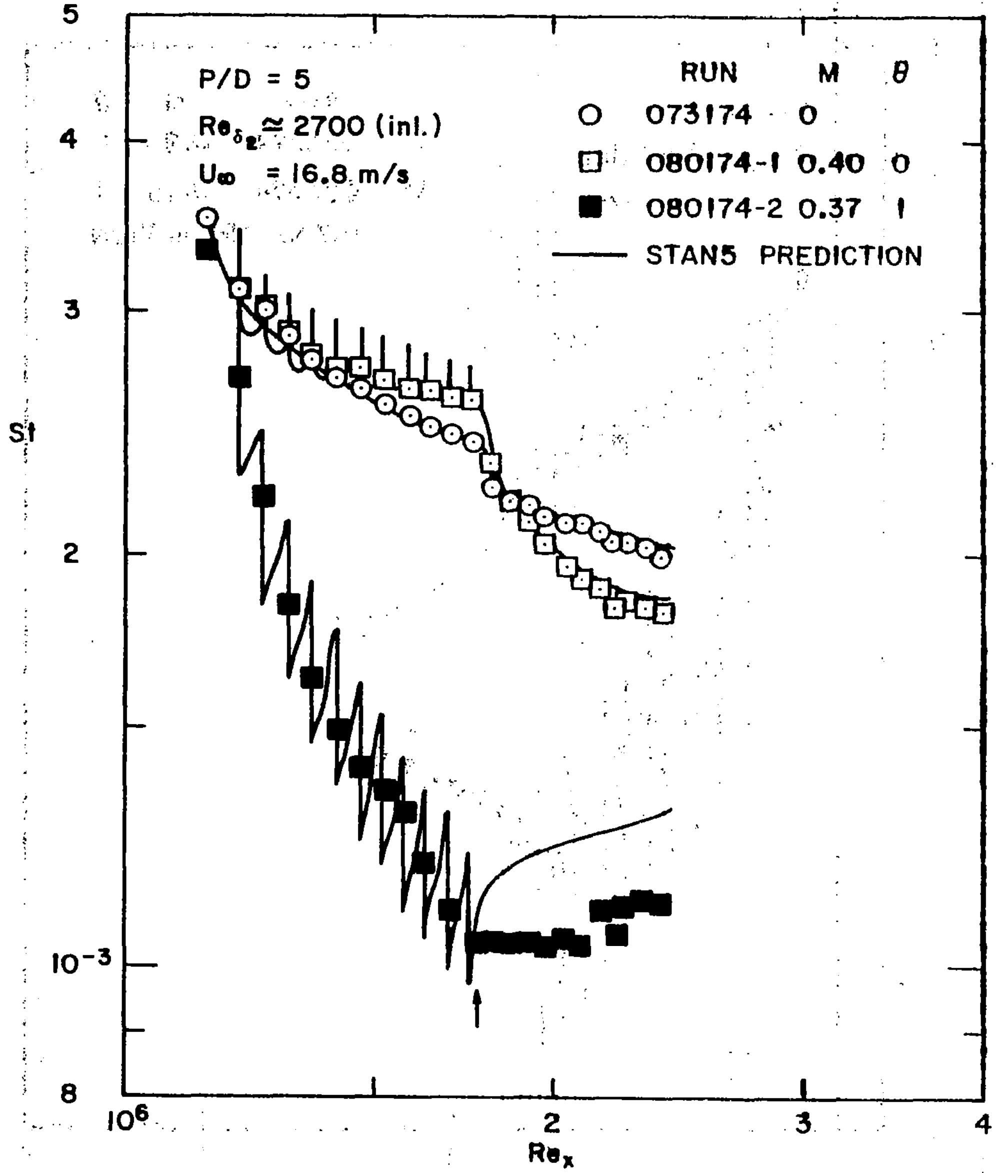

Figure 4.11 Prediction of the M ≃ 0.4 data from Figure 3.6

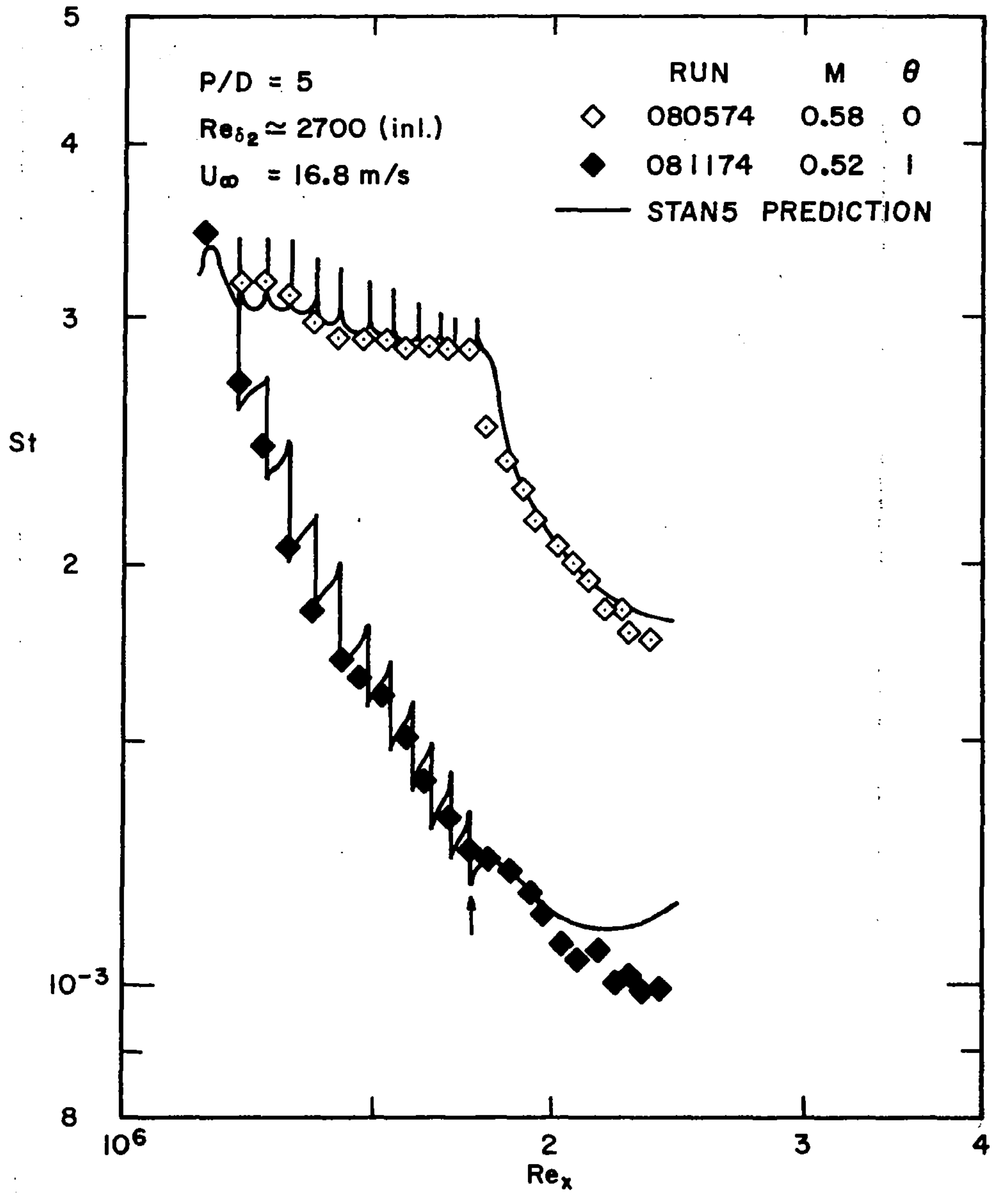

Figure 4.12 Prediction of the M ≃ 0.6 data from Figure 3.6

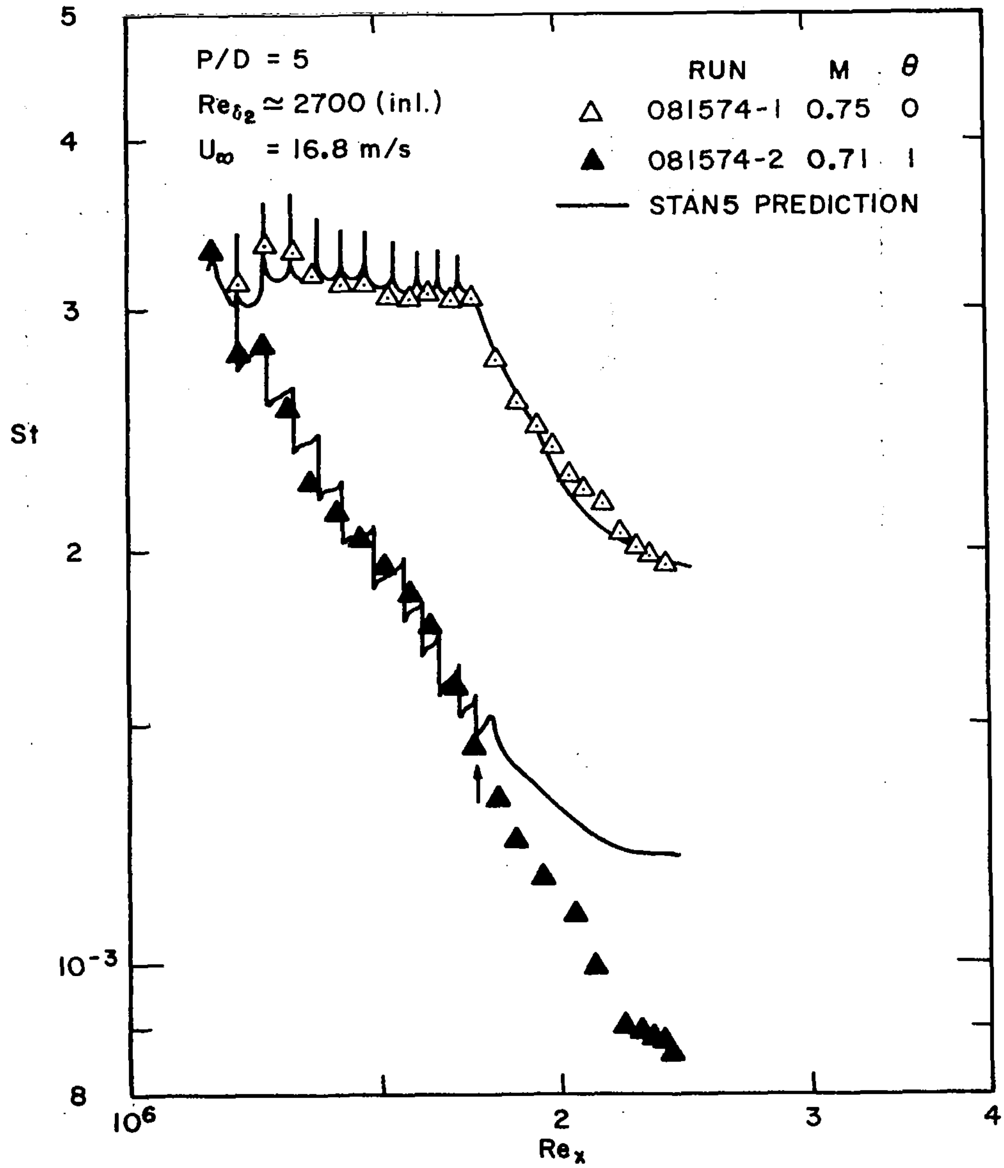

Figure 4.13 Prediction of the M ≃ 0.75 data from Figure 3.6

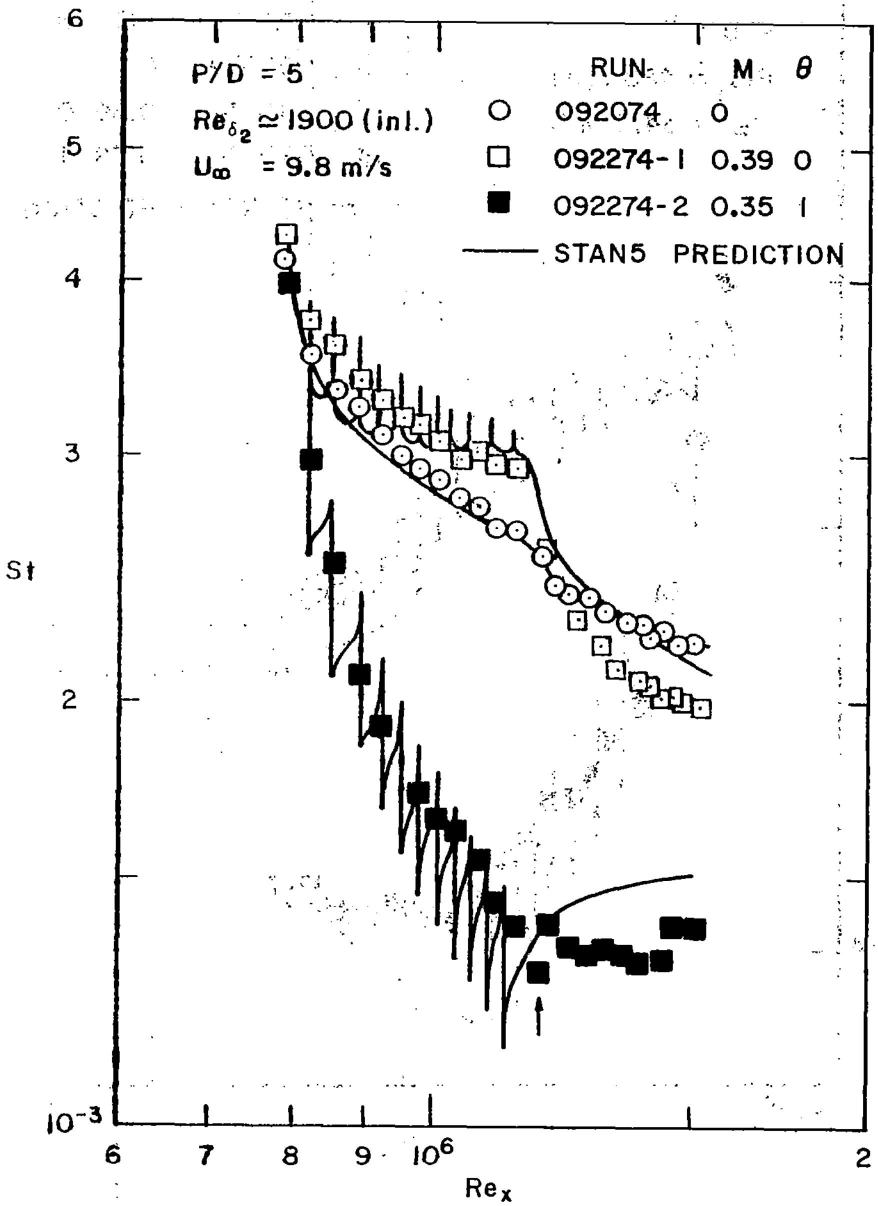

Figure 4.14 Prediction of the M = 0 and M ≃ 0.4 data from Figure 3.12

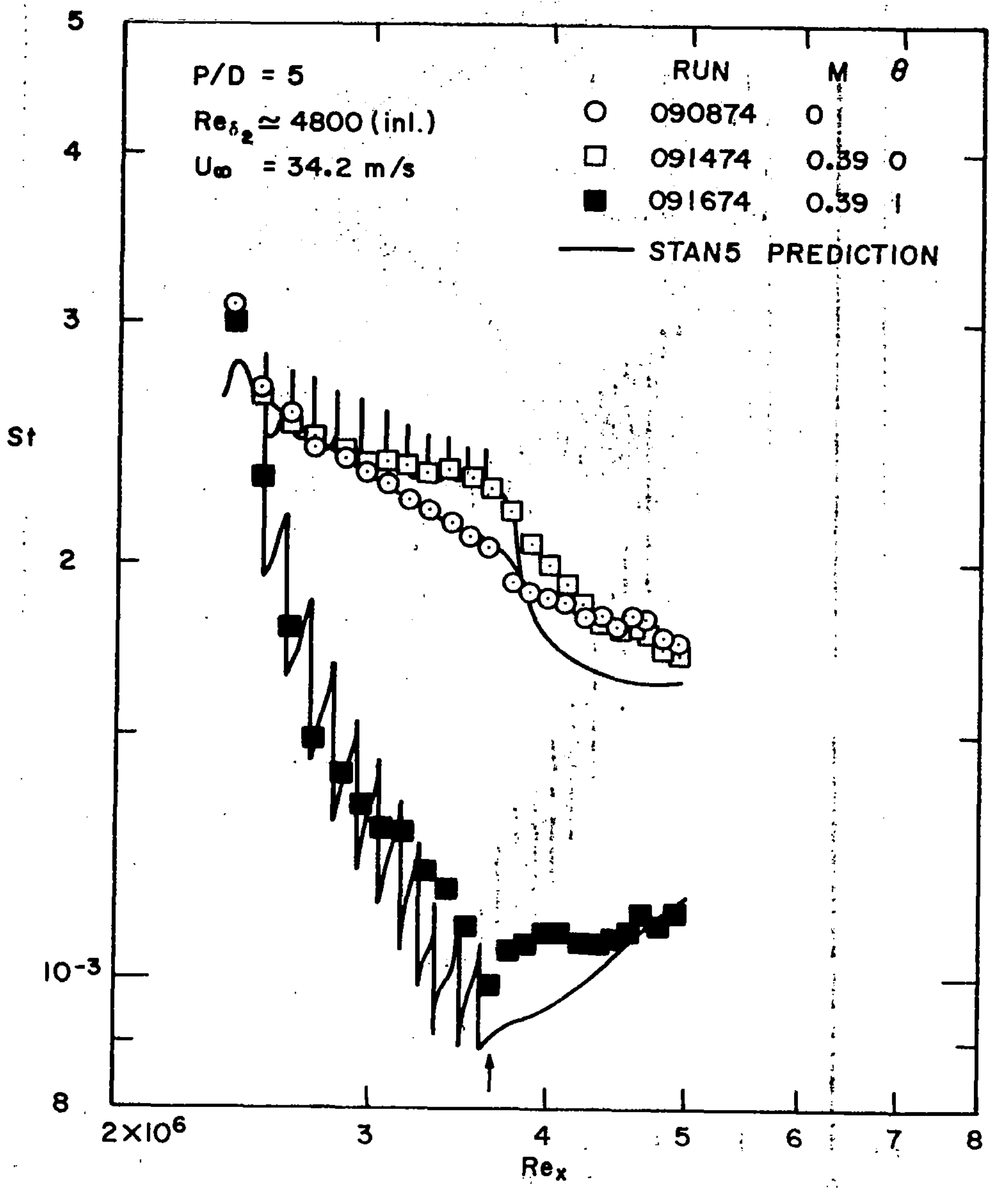

Figure 4.15 Prediction of the $M = 0$ and $M \approx 0.4$ data from Figure 3.15

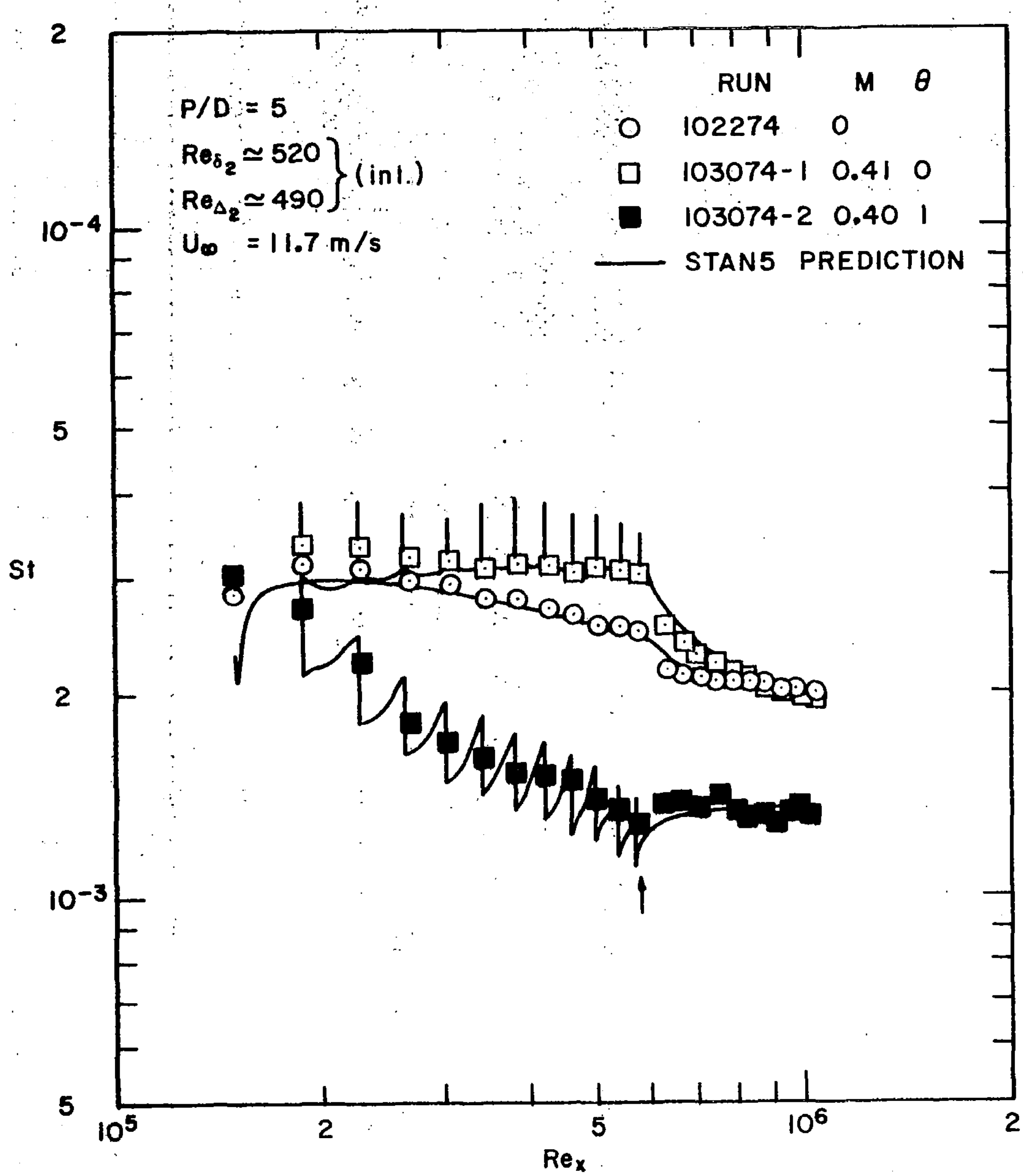

Figure 4.16 Prediction of the M = 0 and M ≃ 0.4 data from Figure 3.19

Chapter 5

SUMMARY AND RECOMMENDATIONS

An experimental and analytical investigation of heat transfer to the boundary layer over a full-coverage, film-cooled surface has been carried out. Injection was from an array of staggered holes with hole spacing-to-hole diameter ratios of 5 and 10. The holes were angled 30 degrees to the surface in the downstream direction. In summary,

1. Experimental Stanton number data have been acquired, using two temperatures at each blowing ratio to build two fundamental data sets. The data are defined using a wall temperature-to-mainstream temperature driving potential to permit direct comparison of wall heat fluxes, with and without film cooling, to describe film-cooling performance. Superposition can be applied to the two fundamental data sets to obtain Stanton number as a continuous function of injectant temperature.

2. When the injectant temperature equals plate temperature, the lowest Stanton number is produced for a blowing ratio (injectant velocity-to-mainstream velocity) of about 0.4 . Higher ratios resulted in higher Stanton numbers. The data trend indicated that for ratios above 1.5 the Stanton number could be larger than that without film cooling.

3. The major effects on Stanton number of changing either the upstream momentum thickness or the ratio of thermal-to-momentum thickness are confined to the initial blowing rows. The data showed a slight dependence upon changes in mainstream velocity.

4. Comparison of the data for the two hole spacings indicates that a wider hole spacing (10 hole diameters) produces less effect on Stanton number, for the same value of blowing ratio.

5. The data for injectant temperature equal to plate temperature were successfully correlated using the same Couette flow variables used to correlate transpiration cooling data.

6. The recovery region, 60 hole diameters downstream of the last blowing row, had two distinct data trends for the case of injectant temperature equal to plate temperature. For low velocity ratios the Stanton number immediately began to recover toward the corresponding unblown value, while for high velocity ratios the Stanton number either remained constant or dropped throughout the recovery region. This latter behavior suggests investigating an interrupted hole pattern with, say, five to ten rows of holes followed by a recovery region, before the next array begins.

7. A differential prediction model was developed to predict the experimental data. The method utilizes a two-dimensional boundary layer program with routines to model the injection process and turbulence augmentation. The program marches in the streamwise direction and, when a row of holes is encountered, stops and injects fluid into the boundary layer. The turbulence level is modeled by algebraically augmenting the mixing-length, with the augmentation keyed to a penetration distance for the injectant.

The work described in this report represents the second of three phases of experimental heat transfer investigations into full-coverage, film-cooled boundary layers at Stanford: first was normal-hole injection; the second was the slant-hole injection, and the third will be with compound-angled hole injection. Presently an experimental investigation of the slant-hole flow field is being carried out, and the compound-angled hole test section is being constructed. It is recommended that:

1. A higher-level turbulence closure model should be investigated for use in the turbulence augmentation model of the prediction program described herein. The logical choice would be a turbulence kinetic energy model. This is being pursued.

2. The effects of high mainstream turbulence level on heat transfer should be investigated. The importance of this effect may be

confined to the recovery region, and to the results described in point 6 of the summary above. The high turbulence level may promote a much faster recovery to unblown Stanton number conditions.

3. A preliminary investigation should be carried out regarding availability of three-dimensional boundary layer programs for modification to predict the full-coverage data. This recommendation is made in light of the much-improved computer execution time and core availability of the new generation of computers at Stanford. Such machines will be available to industry in the coming decade; thus it seems a justifiable course to pursue.

Appendix I

STANTON NUMBER DATA

Contained in this appendix is a numerical tabulation of the Stanton number data. Initial velocity and temperature profiles precede the data, and the sequence of data follows the discussions in Sections 3.3.1 through 3.3.4. For the Stanton number data at each blowing ratio the experimental data at $\theta \approx 1$ and $\theta \approx 0$ are given first, followed by a sheet with the superposition-adjusted data to values at $\theta = 0, 1$.

Nomenclature

CF/2	$c_f/2$, friction coefficient
CP	c_p , specific heat
DEL	velocity or thermal boundary layer thickness (see DEL99 or DELT99)
DEL1	δ_1 , displacement thickness
DEL2	δ_2 , momentum thickness
DEL99	velocity boundary layer thickness
DELT99	thermal boundary layer thickness
DREEN	uncertainty in Re_{Δ_2}
DST	uncertainty in St
DTM	uncertainty in θ
ETA	$\{1 - St(\theta = 1)\}/St(\theta = 0)$
F	blowing fraction
F-COL	F at $\theta = 0$
F-HOT	F at $\theta = 1$
H	velocity shape factor
LOGB	ϕ function in $\theta = 1$ data correlation

M	blowing parameter
PORT	topwall location where profile is obtained
PR	Pr , Prandtl number
RE DEL2 REENTH REH	Re_{Δ_2} , enthalpy thickness Reynolds number
REM	Re_{δ_2} , momentum thickness Reynolds number
REX	Re_x , x-Reynolds number
RHO	density
ST	Stanton number
STCR	$St(\theta = 0)/St_o$. Note, St_o is defined at bottom of each summary data sheet.
STHR	$St(\theta = 1)/St_o$
T	recovery temperature of temperature probe
T2	T_2 , secondary air temperature
TADB	T_∞ , r , temperature to define Stanton number
TBAR	$(T_o-T)/(T_o-T_\infty)$ (or one minus that quantity in the second tabulated data column)
THETA	θ , temperature parameter
TINF	mainstream static temperature
TO TPLATE	T_o , plate temperature
U	velocity
U+	U^+ , non-dimensional velocity
UINF	U_∞ , mainstream velocity
VISC	ν , kinematic viscosity
XLOC	x , distance from nozzle exit to probe tip

XVO x_{vo} , distance from nozzle exit to virtual origin, turbulent boundary layer

Y y , distance normal to surface

Y+ y^+ , non-dimensional y distance

Note: Some of the entries in the Stanton number data summary sheets are boxed in. These data points deviate substantially from the data trend of their surrounding points. Therefore, they were not plotted as tabulated, but adjusted and then plotted.

RUN 092874 VELOCITY AND TEMPERATURE PROFILES

REX	= 0.11787E 07	REM =	2663.	REH =	1844.
XVO =	20.98 CM.	DEL2 =	0.241 CM.	DEH2 =	0.167 CM.
UINF =	16.83 M/S	DEL99=	2.045 CM.	DELT99 =	1.894 CM.
VISC =	0.15247E-04 M2/S	DEL1 =	0.350 CM.	UINF =	16.84 M/S
PORT =	19	H =	1.450	VISC =	0.15263E-04 M2/S
XLOC =	127.76 CM.	CF/2 =	0.16794E-02	TINF =	21.96 DEG C
				TPLATE =	36.46 DEG C

Y(CM.)	Y/DEL	U(M/S)	U/UINF	Y+	U+	Y(CM.)	T(DEG C)	TBAR	TBAR
0.025	0.012	7.31	0.434	11.5	10.60	0.0165	33.33	0.218	0.782
0.028	0.014	7.56	0.449	12.6	10.96	0.0190	32.24	0.293	0.707
0.030	0.015	7.79	0.463	13.8	11.29	0.0216	31.51	0.344	0.656
0.036	0.017	8.21	0.488	16.1	11.91	0.0241	31.09	0.373	0.627
0.043	0.021	8.62	0.512	19.5	12.50	0.0292	30.21	0.434	0.566
0.053	0.026	9.15	0.544	24.1	13.26	0.0368	29.45	0.487	0.513
0.066	0.032	9.51	0.565	29.9	13.79	0.0470	28.63	0.544	0.456
0.081	0.040	9.75	0.579	36.8	14.14	0.0597	28.02	0.587	0.413
0.099	0.048	10.06	0.598	44.8	14.59	0.0775	27.45	0.627	0.373
0.119	0.058	10.31	0.612	54.0	14.94	0.0978	27.08	0.653	0.347
0.142	0.070	10.58	0.629	64.3	15.35	0.1232	26.73	0.677	0.323
0.168	0.082	10.73	0.637	75.8	15.55	0.1537	26.41	0.699	0.301
0.198	0.097	11.03	0.656	89.6	16.00	0.1892	26.07	0.722	0.278
0.234	0.114	11.27	0.670	105.7	16.34	0.2299	25.82	0.740	0.260
0.274	0.134	11.56	0.687	124.1	16.76	0.2755	25.51	0.762	0.238
0.320	0.156	11.87	0.705	144.8	17.21	0.3264	25.27	0.778	0.222
0.371	0.181	12.07	0.717	167.7	17.51	0.3899	24.97	0.799	0.201
0.432	0.211	12.38	0.735	195.3	17.94	0.4661	24.71	0.817	0.183
0.503	0.246	12.73	0.756	227.5	18.46	0.5601	24.40	0.839	0.161
0.592	0.289	13.08	0.777	267.7	18.97	0.6871	24.02	0.865	0.135
0.693	0.339	13.47	0.800	313.7	19.53	0.8141	23.68	0.888	0.112
0.818	0.400	13.86	0.823	370.0	20.09	0.9411	23.41	0.908	0.092
0.970	0.474	14.39	0.855	436.9	20.87	1.0681	23.17	0.924	0.076
1.123	0.549	14.84	0.882	507.8	21.52	1.1951	22.96	0.939	0.061
1.275	0.623	15.23	0.905	576.8	22.08	1.3221	22.78	0.952	0.048
1.427	0.698	15.68	0.932	645.7	22.73	1.4491	22.60	0.964	0.036
1.580	0.772	15.98	0.950	714.7	23.17	1.5761	22.47	0.973	0.027
1.732	0.847	16.30	0.969	783.6	23.64	1.7031	22.34	0.982	0.018
1.885	0.921	16.53	0.982	852.5	23.97	1.8301	22.27	0.987	0.013
2.037	0.996	16.68	0.991	921.5	24.16	1.9571	22.20	0.992	0.008
2.189	1.070	16.81	0.999	990.4	24.37	2.0841	22.14	0.996	0.004
2.342	1.145	16.83	1.000	1059.3	24.40	2.2111	22.11	0.998	0.002
						2.338	22.09	1.000	0.000
						2.465	22.08	1.000	0.000

RUN 092874 *** DISCRETE HOLE RIG *** NAS-3-14336 STANTON NUMBER DATA

TADB= 21.87 DEG C UINF= 16.81 M/S TINF= 21.75 DEG C
RHO= 1.187 KG/M3 VISC= 0.15243E-04 M2/S XVO= 21.0 CM
CP= 1013. J/KGK PR= 0.716

*** 2700HSLFP P/D=5 ***

PLATE	X	REX	TO	REENTH	STANTON NO	DST	DREEN	ST(THEO)	RATIO
1	127.8	0.11776E 07	36.27	0.18684E 04	0.22298E-02	0.516E-04	28.	0.20585E-02	1.083
2	132.8	0.12337E 07	36.27	0.19950E 04	0.22897E-02	0.519E-04	28.	0.20395E-02	1.123
3	137.9	0.12897E 07	36.31	0.21229E 04	0.22765E-02	0.517E-04	28.	0.20214E-02	1.126
4	143.0	0.13457E 07	36.27	0.22495E 04	0.22419E-02	0.517E-04	28.	0.20043E-02	1.119
5	148.1	0.14017E 07	36.27	0.23750E 04	0.22392E-02	0.517E-04	28.	0.19880E-02	1.126
6	153.2	0.14578E 07	36.27	0.24998E 04	0.22167E-02	0.515E-04	28.	0.19725E-02	1.124
7	158.2	0.15138E 07	36.25	0.26237E 04	0.22067E-02	0.515E-04	28.	0.19577E-02	1.127
8	163.3	0.15698E 07	36.25	0.27462E 04	0.21636E-02	0.513E-04	29.	0.19435E-02	1.113
9	168.4	0.16258E 07	36.27	0.28666E 04	0.21344E-02	0.511E-04	29.	0.19299E-02	1.106
10	173.5	0.16819E 07	36.27	0.29854E 04	0.21079E-02	0.510E-04	29.	0.19169E-02	1.100
11	178.6	0.17379E 07	36.25	0.31029E 04	0.20855E-02	0.509E-04	29.	0.19044E-02	1.095
12	183.6	0.17939E 07	36.25	0.32195E 04	0.20774E-02	0.509E-04	29.	0.18923E-02	1.098
13	187.5	0.18365E 07	36.33	0.33057E 04	0.19428E-02	0.682E-04	29.	0.18835E-02	1.032
14	190.1	0.18653E 07	36.29	0.33617E 04	0.19322E-02	0.678E-04	29.	0.18776E-02	1.029
15	192.7	0.18942E 07	36.63	0.34172E 04	0.19113E-02	0.681E-04	29.	0.18718E-02	1.021
16	195.4	0.19232E 07	36.65	0.34722E 04	0.18930E-02	0.666E-04	29.	0.18662E-02	1.014
17	198.0	0.19522E 07	36.67	0.35267E 04	0.18864E-02	0.666E-04	29.	0.18606E-02	1.014
18	200.6	0.19810E 07	36.63	0.35812E 04	0.18845E-02	0.665E-04	29.	0.18551E-02	1.016
19	203.2	0.20099E 07	36.57	0.36354E 04	0.18661E-02	0.650E-04	29.	0.18498E-02	1.009
20	205.8	0.20387E 07	36.71	0.36891E 04	0.18546E-02	0.656E-04	29.	0.18445E-02	1.005
21	208.5	0.20676E 07	36.61	0.37428E 04	0.18605E-02	0.651E-04	29.	0.18393E-02	1.012
22	211.1	0.20964E 07	36.65	0.37966E 04	0.18636E-02	0.661E-04	29.	0.18342E-02	1.016
23	213.7	0.21253E 07	36.61	0.38497E 04	0.18176E-02	0.641E-04	29.	0.18292E-02	0.994
24	216.3	0.21543E 07	36.71	0.39025E 04	0.18344E-02	0.657E-04	29.	0.18243E-02	1.006
25	218.9	0.21833E 07	36.59	0.39552E 04	0.18166E-02	0.645E-04	29.	0.18194E-02	0.998
26	221.6	0.22121E 07	36.46	0.40079E 04	0.18293E-02	0.685E-04	29.	0.18146E-02	1.008
27	224.2	0.22410E 07	35.18	0.40605E 04	0.18154E-02	0.591E-04	29.	0.18100E-02	1.003
28	226.8	0.22698E 07	36.48	0.41130E 04	0.18195E-02	0.688E-04	29.	0.18053E-02	1.008
29	229.4	0.22987E 07	36.40	0.41654E 04	0.18063E-02	0.626E-04	29.	0.18008E-02	1.003
30	232.0	0.23275E 07	36.86	0.42180E 04	0.18364E-02	0.665E-04	29.	0.17963E-02	1.022
31	234.6	0.23564E 07	36.86	0.42707E 04	0.18111E-02	0.645E-04	30.	0.17919E-02	1.011
32	237.3	0.23854E 07	36.74	0.43228E 04	0.17956E-02	0.638E-04	30.	0.17875E-02	1.005
33	239.9	0.24144E 07	36.69	0.43749E 04	0.18129E-02	0.648E-04	30.	0.17832E-02	1.017
34	242.5	0.24432E 07	36.40	0.44270E 04	0.17910E-02	0.621E-04	30.	0.17789E-02	1.007
35	245.1	0.24721E 07	36.63	0.44788E 04	0.17961E-02	0.661E-04	30.	0.17748E-02	1.012
36	247.8	0.25009E 07	36.27	0.45306E 04	0.17896E-02	0.714E-04	30.	0.17707E-02	1.011

RUN 100174-1 *** DISCRETE HOLE RIG *** NAS-3-14336 STANTON NUMBER DATA

TADB= 21.51 DEG C UINF= 16.74 M/S TINF= 21.38 DEG C
RHO= 1.188 KG/M3 VISC= 0.15229E-04 M2/S XVO= 21.0 CM
CP= 1012. J/KGK PR= 0.716

*** 2700HSL40 M=0.4 TH=0 P/D=5 ***

PLATE	X	REX	TO	REENTH	STANTON NO	DST	DREEN	M	F	T2	THETA	DTH
1	127.8	0.11738E 07	36.33	0.18177E 04	0.23449E-02	0.511E-04	28.					
2	132.8	0.12297E 07	36.36	0.19485E 04	0.23388E-02	0.509E-04	29.	0.39	0.0126	23.45	0.138	0.020
3	137.9	0.12855E 07	36.34	0.21760E 04	0.23301E-02	0.509E-04	31.	0.39	0.0128	23.72	0.156	0.020
4	143.0	0.13414E 07	36.34	0.24163E 04	0.22895E-02	0.507E-04	33.	0.39	0.0127	23.68	0.154	0.020
5	148.1	0.13972E 07	36.36	0.26528E 04	0.22665E-02	0.505E-04	35.	0.39	0.0126	23.62	0.149	0.020
6	153.2	0.14531E 07	36.40	0.28828E 04	0.22163E-02	0.501E-04	36.	0.38	0.0123	23.69	0.153	0.020
7	158.2	0.15089E 07	36.36	0.31128E 04	0.22572E-02	0.505E-04	38.	0.39	0.0126	23.86	0.165	0.020
8	163.3	0.15648E 07	36.33	0.33537E 04	0.22183E-02	0.504E-04	39.	0.39	0.0125	23.72	0.156	0.020
9	168.4	0.16206E 07	36.36	0.35856E 04	0.21767E-02	0.500E-04	41.	0.39	0.0126	23.75	0.158	0.020
10	173.5	0.16764E 07	36.34	0.38193E 04	0.21951E-02	0.502E-04	42.	0.38	0.0124	23.79	0.161	0.020
11	178.6	0.17323E 07	36.34	0.40522E 04	0.21703E-02	0.500E-04	44.	0.39	0.0126	23.79	0.161	0.020
12	183.6	0.17881E 07	36.36	0.42847E 04	0.20850E-02	0.495E-04	45.	0.39	0.0125	23.73	0.157	0.020
13	187.5	0.18306E 07	35.79	0.44818E 04	0.20382E-02	0.688E-04	46.					
14	190.1	0.18593E 07	35.79	0.45388E 04	0.19243E-02	0.677E-04	46.					
15	192.7	0.18881E 07	36.15	0.45937E 04	0.18876E-02	0.673E-04	46.					
16	195.4	0.19170E 07	36.21	0.46475E 04	0.18493E-02	0.653E-04	46.					
17	198.0	0.19459E 07	36.27	0.47003E 04	0.18176E-02	0.644E-04	46.					
18	200.6	0.19747E 07	36.27	0.47521E 04	0.17824E-02	0.633E-04	46.					
19	203.2	0.20034E 07	36.27	0.48005E 04	0.15769E-02	0.609E-04	46.					
20	205.8	0.20322E 07	34.68	0.48563E 04	0.23008E-02	0.723E-04	46.					
21	208.5	0.20609E 07	36.34	0.49119E 04	0.15608E-02	0.601E-04	46.					
22	211.1	0.20897E 07	36.44	0.49584E 04	0.16724E-02	0.603E-04	46.					
23	213.7	0.21185E 07	36.40	0.50062E 04	0.16460E-02	0.586E-04	46.					
24	216.3	0.21474E 07	36.55	0.50535E 04	0.16386E-02	0.599E-04	46.					
25	218.9	0.21763E 07	36.40	0.51009E 04	0.16558E-02	0.592E-04	46.					
26	221.6	0.22050E 07	36.33	0.51480E 04	0.16179E-02	0.616E-04	46.					
27	224.2	0.22338E 07	35.14	0.51947E 04	0.16207E-02	0.537E-04	46.					
28	226.8	0.22625E 07	36.31	0.52415E 04	0.16311E-02	0.622E-04	46.					
29	229.4	0.22913E 07	36.31	0.52881E 04	0.16040E-02	0.565E-04	46.					
30	232.0	0.23201E 07	36.74	0.53346E 04	0.16302E-02	0.601E-04	46.					
31	234.6	0.23488E 07	36.69	0.53815E 04	0.16291E-02	0.587E-04	46.					
32	237.3	0.23777E 07	36.55	0.54283E 04	0.16166E-02	0.581E-04	46.					
33	239.9	0.24066E 07	36.53	0.54750E 04	0.16280E-02	0.592E-04	46.					
34	242.5	0.24354E 07	36.21	0.55219E 04	0.16290E-02	0.570E-04	46.					
35	245.1	0.24641E 07	36.44	0.55686E 04	0.16141E-02	0.604E-04	46.					
36	247.8	0.24929E 07	36.06	0.56150E 04	0.16124E-02	0.658E-04	46.					

UNCERTAINTY IN REX=27922. UNCERTAINTY IN F=0.05036 IN RATIO

RUN 100374 *** DISCRETE HOLE RIG *** NAS-3-14336 STANTON NUMBER DATA

TADB= 20.81 DEG C UINF= 16.70 M/S TINF= 20.69 DEG C
RHO= 1.194 KG/M3 VISC= 0.15125E-04 M2/S XVO= 21.0 CM
CP= 1012. J/KGK PR= 0.716

*** 2700HSL40 M=0.4 TH=1 P/D=5 ***

PLATE	X	REX	TO	REENTH	STANTON NO	DST	DREEN	M	F	T2	THETA	DTH
1	127.8	0.11790E 07	36.33	0.18258E 04	0.23403E-02	0.488E-04	28.					
2	132.8	0.12351E 07	36.36	0.19478E 04	0.20106E-02	0.470E-04	33.	0.37	0.0120	35.59	0.951	0.020
3	137.9	0.12912E 07	36.38	0.26887E 04	0.16555E-02	0.453E-04	42.	0.37	0.0120	36.47	1.006	0.020
4	143.0	0.13473E 07	36.34	0.34518E 04	0.13919E-02	0.444E-04	49.	0.38	0.0122	36.87	1.034	0.020
5	148.1	0.14034E 07	36.31	0.42343E 04	0.13162E-02	0.443E-04	56.	0.37	0.0120	36.53	1.014	0.020
6	153.2	0.14595E 07	36.33	0.49864E 04	0.12416E-02	0.440E-04	62.	0.39	0.0127	36.35	1.002	0.020
7	158.2	0.15156E 07	36.33	0.57716E 04	0.12191E-02	0.439E-04	68.	0.38	0.0124	36.21	0.992	0.020
8	163.3	0.15717E 07	36.33	0.65274E 04	0.11969E-02	0.438E-04	73.	0.36	0.0118	36.76	1.028	0.020
9	168.4	0.16278E 07	36.34	0.72728E 04	0.11419E-02	0.436E-04	77.	0.37	0.0120	36.24	0.993	0.020
10	173.5	0.16839E 07	36.31	0.80028E 04	0.11287E-02	0.437E-04	82.	0.38	0.0123	35.81	0.968	0.020
11	178.6	0.17400E 07	36.34	0.87338E 04	0.10889E-02	0.434E-04	86.	0.39	0.0125	35.59	0.952	0.020
12	183.6	0.17960E 07	36.36	0.94645E 04	0.10709E-02	0.433E-04	89.	0.37	0.0120	35.31	0.933	0.020
13	187.5	0.18387E 07	36.23	0.10136E 05	0.10778E-02	0.406E-04	91.					
14	190.1	0.18676E 07	36.13	0.10168E 05	0.11053E-02	0.427E-04	91.					
15	192.7	0.18964E 07	36.36	0.10200E 05	0.11136E-02	0.431E-04	91.					
16	195.4	0.19255E 07	36.36	0.10232E 05	0.11104E-02	0.424E-04	91.					
17	198.0	0.19545E 07	36.36	0.10264E 05	0.11164E-02	0.427E-04	91.					
18	200.6	0.19834E 07	36.33	0.10297E 05	0.11219E-02	0.429E-04	91.					
19	203.2	0.20123E 07	36.29	0.10329E 05	0.10931E-02	0.412E-04	91.					
20	205.8	0.20412E 07	36.36	0.10361E 05	0.11041E-02	0.419E-04	91.					
21	208.5	0.20701E 07	36.33	0.10392E 05	0.10947E-02	0.415E-04	91.					
22	211.1	0.20989E 07	36.34	0.10424E 05	0.10978E-02	0.424E-04	91.					
23	213.7	0.21278E 07	36.33	0.10456E 05	0.10804E-02	0.415E-04	91.					
24	216.3	0.21569E 07	36.44	0.10487E 05	0.10914E-02	0.430E-04	91.					
25	218.9	0.21859E 07	36.31	0.10519E 05	0.11007E-02	0.425E-04	91.					
26	221.6	0.22148E 07	36.17	0.10551E 05	0.11104E-02	0.446E-04	91.					
27	224.2	0.22437E 07	35.39	0.10582E 05	0.10595E-02	0.388E-04	91.					
28	226.8	0.22725E 07	36.23	0.10613E 05	0.11131E-02	0.452E-04	91.					
29	229.4	0.23014E 07	36.19	0.10646E 05	0.11054E-02	0.417E-04	91.					
30	232.0	0.23303E 07	36.44	0.10678E 05	0.11589E-02	0.450E-04	91.					
31	234.6	0.23592E 07	36.44	0.10711E 05	0.11346E-02	0.438E-04	91.					
32	237.3	0.23882E 07	36.27	0.10744E 05	0.11522E-02	0.440E-04	91.					
33	239.9	0.24173E 07	36.23	0.10778E 05	0.11711E-02	0.448E-04	91.					
34	242.5	0.24461E 07	36.02	0.10811E 05	0.11055E-02	0.416E-04	91.					
35	245.1	0.24750E 07	36.13	0.10844E 05	0.11699E-02	0.463E-04	91.					
36	247.8	0.25039E 07	35.83	0.10878E 05	0.11610E-02	0.500E-04	91.					

UNCERTAINTY IN REX=28046. UNCERTAINTY IN F=0.05036 IN RATIO

RUN 100174-1 *** DISCRETE HOLE RIG *** NAS-3-14336 STANTON NUMBER DATA

*** 2700HSL40 M=0.4 TH=0 P/D=5 ***

RUN 100374 *** DISCRETE HOLE RIG *** NAS-3-14336 STANTON NUMBER DATA

*** 2700HSL40 M=0.4 TH=1 P/D=5 ***

LINEAR SUPERPOSITION IS APPLIED TO STANTON NUMBER DATA FROM
RUN NUMBERS 100174-1 AND 100374 TO OBTAIN STANTON NUMBER DATA AT TH=0 AND TH=1

PLATE	REXCOL	RE DEL2	ST(TH=0)	REXHOT	RE DEL2	ST(TH=1)	ETA	STCR	F-COL	STHR	F-HOT	LOGB
1	1173846.0	1817.7	0.002345	1179040.0	1825.8	0.002340	UUUUU	1.040	0.0000	1.038	0.0000	1.038
2	1229690.0	1950.1	0.002395	1235131.0	1947.2	0.001991	0.169	1.057	0.0126	0.879	0.0120	2.713
3	1285534.0	2085.3	0.002450	1291222.0	2720.1	0.001638	0.331	1.077	0.0128	0.720	0.0120	2.491
4	1341379.0	2222.1	0.002450	1347314.0	3479.4	0.001412	0.424	1.088	0.0127	0.627	0.0122	2.390
5	1397223.0	2358.4	0.002431	1403405.0	4240.2	0.001342	0.448	1.086	0.0126	0.599	0.0120	2.329
6	1453067.0	2493.0	0.002388	1459496.0	4983.7	0.001251	0.476	1.094	0.0123	0.573	0.0127	2.417
7	1508912.0	2628.2	0.002455	1515588.0	5767.9	0.001215	0.505	1.118	0.0126	0.554	0.0124	2.333
8	1564756.0	2764.1	0.002411	1571679.0	6529.2	0.001209	0.499	1.125	0.0125	0.564	0.0118	2.316
9	1620600.0	2897.5	0.002367	1627770.0	7256.8	0.001155	0.512	1.106	0.0126	0.540	0.0120	2.299
10	1676444.0	3030.7	0.002402	1683862.0	7990.9	0.001104	0.540	1.132	0.0124	0.520	0.0123	2.323
11	1732289.0	3164.5	0.002388	1739953.0	8741.7	0.001035	0.567	1.148	0.0126	0.497	0.0125	2.342
12	1788133.0	3295.1	0.002291	1796044.0	9502.4	0.000996	0.565	1.100	0.0125	0.478	0.0120	2.240
13	1830575.0	3391.2	0.002233	1838674.0	10216.3	0.001007	0.549	1.142		0.515		
14	1859334.0	3453.5	0.002090	1867561.0	10246.0	0.001045	0.500	1.061		0.531		
15	1888094.0	3513.0	0.002045	1896448.0	10276.4	0.001057	0.483	1.057		0.547		
16	1916993.0	3571.2	0.001999	1925475.0	10306.9	0.001056	0.472	1.051		0.555		
17	1945893.0	3628.2	0.001960	1954502.0	10337.6	0.001065	0.457	1.034		0.562		
18	1974653.0	3684.0	0.001916	1983389.0	10368.5	0.001073	0.440	1.004		0.562		
19	2003412.0	3735.7	0.001675	2012276.0	10399.4	0.001058	0.369	0.889		0.561		
20	2032172.0	3796.4	0.002542	2041163.0	10429.3	0.001016	0.600	1.354		0.541		
21	2060932.0	3856.9	0.001654	2070051.0	10459.4	0.001060	0.359	0.886		0.568		
22	2089692.0	3906.4	0.001789	2098938.0	10490.0	0.001056	0.410	0.958		0.565		
23	2118452.0	3957.5	0.001761	2127825.0	10520.3	0.001039	0.410	0.966		0.570		
24	2147351.0	4008.1	0.001750	2156852.0	10550.5	0.001051	0.399	0.930		0.559		
25	2176250.0	4058.7	0.001768	2185879.0	10581.0	0.001060	0.401	0.961		0.576		
26	2205010.0	4108.9	0.001721	2214766.0	10611.9	0.001073	0.376	0.937		0.584		
27	2233770.0	4158.7	0.001735	2243653.0	10642.1	0.001018	0.413	0.942		0.553		
28	2262530.0	4208.7	0.001736	2272540.0	10672.4	0.001075	0.381	0.944		0.584		
29	2291290.0	4258.2	0.001705	2301428.0	10703.4	0.001069	0.373	0.912		0.572		
30	2320050.0	4307.6	0.001726	2330315.0	10735.1	0.001124	0.349	0.928		0.605		
31	2348810.0	4357.3	0.001729	2359202.0	10767.2	0.001098	0.365	0.950		0.603		
32	2377709.0	4406.9	0.001711	2388229.0	10799.3	0.001118	0.346	0.948		0.620		
33	2406608.0	4456.3	0.001721	2417256.0	10831.9	0.001138	0.339	0.950		0.628		
34	2435368.0	4506.0	0.001735	2446143.0	10863.8	0.001067	0.385	0.967		0.595		
35	2464128.0	4555.5	0.001704	2475030.0	10895.7	0.001137	0.333	0.960		0.641		
36	2492887.0	4604.6	0.001704	2503917.0	10928.4	0.001128	0.338	0.997		0.660		

STANTON NUMBER RATIO BASED ON EXPERIMENTAL FLAT PLATE VALUE AT SAME X LOCATION

STANTON NUMBER RATIO FOR TH=1 IS CONVERTED TO COMPARABLE TRANSPIRATION VALUE
USING ALOG(1 + B)/B EXPRESSION IN THE BLOWN SECTION

RUN 073174 VELOCITY PROFILE

REX =	0.11423E 07	REM =	2597.
XVO =	22.35 CM.	DEL2 =	0.240 CM.
UINF =	16.80 M/S	DEL99=	2.000 CM.
VISC =	0.15498E-04 M2/S	DEL1 =	0.334 CM.
PORT =	19	H =	1.392
XLOC =	127.76 CM.	CF/2 =	0.17156E-02

Y(CM.)	Y/DEL	U(M/S)	U/UINF	Y+	U+
0.025	0.013	7.25	0.431	11.4	10.42
0.028	0.014	7.41	0.441	12.5	10.65
0.030	0.015	7.63	0.454	13.7	10.97
0.033	0.017	7.84	0.467	14.8	11.26
0.036	0.018	8.16	0.486	16.0	11.72
0.041	0.020	8.50	0.506	18.2	12.22
0.048	0.024	8.90	0.530	21.7	12.79
0.051	0.025	8.96	0.534	22.8	12.88
0.058	0.029	9.31	0.555	26.2	13.39
0.066	0.033	9.45	0.563	29.6	13.59
0.076	0.038	9.70	0.578	34.2	13.94
0.089	0.044	9.96	0.593	39.9	14.31
0.114	0.057	10.31	0.614	51.3	14.83
0.152	0.076	10.69	0.637	68.4	15.37
0.203	0.102	11.15	0.664	91.2	16.03
0.267	0.133	11.58	0.689	119.7	16.64
0.343	0.171	12.01	0.715	153.9	17.26
0.432	0.216	12.40	0.738	193.8	17.82
0.533	0.267	12.84	0.764	239.4	18.45
0.648	0.324	13.34	0.795	290.7	19.18
0.800	0.400	13.85	0.825	359.1	19.91
0.978	0.489	14.45	0.860	438.9	20.77
1.181	0.590	15.06	0.897	530.1	21.66
1.440	0.720	15.71	0.936	646.4	22.59
1.664	0.832	16.19	0.964	746.8	23.28
1.981	0.990	16.61	0.989	889.3	23.88
2.362	1.181	16.80	1.000	1060.3	24.14
3.028	1.514	16.80	1.000	1359.0	24.14

RUN 073174 *** DISCRETE HOLE RIG *** NAS-3-14336 STANTON NUMBER DATA

TADB= 26.81 DEG C UINF= 16.80 M/S TINF= 26.68 DEG C
RHO= 1.171 KG/M3 VISC= 0.15622E-04 M2/S XVO= 22.4 CM
CP= 1015. J/KGK PR= 0.717

*** 2700STEPFP P/D =5 ***

PLATE	X	REX	TO	REENTH	STANTON NO	DST	DREEN	ST(THEO)	RATIO
1	127.8	0.11335E 07	39.35	0.95676E 02	0.35028E-02	0.683E-04	2.	0.31739E-02	1.104
2	132.8	0.11882E 07	39.39	0.27670E 03	0.31248E-02	0.652E-04	3.	0.27968E-02	1.117
3	137.9	0.12428E 07	39.39	0.44390E 03	0.29964E-02	0.642E-04	4.	0.26313E-02	1.139
4	143.0	0.12974E 07	39.31	0.60297E 03	0.28270E-02	0.634E-04	5.	0.25245E-02	1.120
5	148.1	0.13521E 07	39.37	0.75534E 03	0.27515E-02	0.626E-04	5.	0.24454E-02	1.125
6	153.2	0.14067E 07	39.43	0.90327E 03	0.26641E-02	0.617E-04	6.	0.23826E-02	1.118
7	158.2	0.14613E 07	39.39	0.10475E 04	0.26161E-02	0.616E-04	6.	0.23305E-02	1.123
8	163.3	0.15159E 07	39.41	0.11884E 04	0.25417E-02	0.610E-04	7.	0.22858E-02	1.112
9	168.4	0.15706E 07	39.41	0.13265E 04	0.25137E-02	0.608E-04	7.	0.22468E-02	1.119
10	173.5	0.16252E 07	39.44	0.14621E 04	0.24535E-02	0.603E-04	8.	0.22120E-02	1.109
11	178.6	0.16798E 07	39.46	0.15952E 04	0.24171E-02	0.600E-04	8.	0.21808E-02	1.108
12	183.6	0.17345E 07	39.54	0.17268E 04	0.24016E-02	0.595E-04	8.	0.21524E-02	1.116
13	187.5	0.17760E 07	39.44	0.18241E 04	0.22480E-02	0.795E-04	9.	0.21324E-02	1.054
14	190.1	0.18041E 07	39.41	0.18869E 04	0.22150E-02	0.791E-04	9.	0.21196E-02	1.045
15	192.7	0.18322E 07	39.75	0.19489E 04	0.21877E-02	0.792E-04	9.	0.21073E-02	1.038
16	195.4	0.18605E 07	39.77	0.20102E 04	0.21648E-02	0.774E-04	9.	0.20953E-02	1.033
17	198.0	0.18888E 07	39.81	0.20709E 04	0.21431E-02	0.770E-04	9.	0.20838E-02	1.028
18	200.6	0.19169E 07	39.75	0.21313E 04	0.21446E-02	0.769E-04	9.	0.20728E-02	1.035
19	203.2	0.19451E 07	39.69	0.21913E 04	0.21180E-02	0.751E-04	9.	0.20622E-02	1.027
20	205.8	0.19732E 07	39.82	0.22509E 04	0.21150E-02	0.759E-04	10.	0.20519E-02	1.031
21	208.5	0.20013E 07	39.79	0.23102E 04	0.20941E-02	0.748E-04	10.	0.20419E-02	1.026
22	211.1	0.20295E 07	39.81	0.23691E 04	0.20913E-02	0.756E-04	10.	0.20322E-02	1.029
23	213.7	0.20576E 07	39.73	0.24274E 04	0.20465E-02	0.733E-04	10.	0.20229E-02	1.012
24	216.3	0.20859E 07	39.84	0.24855E 04	0.20762E-02	0.754E-04	10.	0.20137E-02	1.031
25	218.9	0.21141E 07	39.84	0.25435E 04	0.20436E-02	0.739E-04	10.	0.20048E-02	1.019
26	221.6	0.21423E 07	39.81	0.26018E 04	0.20973E-02	0.766E-04	10.	0.19963E-02	1.051
27	224.2	0.21704E 07	39.43	0.26628E 04	$\boxed{0.22334E-02}$	0.778E-04	10.	0.19879E-02	1.123
28	226.8	0.21985E 07	39.86	0.27222E 04	0.19834E-02	0.738E-04	11.	0.19798E-02	1.002
29	229.4	0.22267E 07	39.67	0.27782E 04	0.19925E-02	0.702E-04	11.	0.19718E-02	1.010
30	232.0	0.22548E 07	40.09	0.28347E 04	0.20210E-02	0.746E-04	11.	0.19641E-02	1.029
31	234.6	0.22829E 07	40.05	0.28916E 04	0.20168E-02	0.730E-04	11.	0.19566E-02	1.031
32	237.3	0.23112E 07	39.94	0.29479E 04	0.19831E-02	0.720E-04	11.	0.19492E-02	1.017
33	239.9	0.23395E 07	39.86	0.30042E 04	0.20099E-02	0.731E-04	11.	0.19420E-02	1.035
34	242.5	0.23676E 07	39.62	0.30601E 04	0.19633E-02	0.697E-04	11.	0.19349E-02	1.015
35	245.1	0.23957E 07	39.82	0.31160E 04	0.20032E-02	0.748E-04	11.	0.19281E-02	1.039
36	247.8	0.24239E 07	39.54	0.31717E 04	0.19498E-02	0.796E-04	11.	0.19214E-02	1.015

RUN 090574 *** DISCRETE HOLE RIG *** NAS-3-14336 STANTON NUMBER DATA

TADB= 27.69 DEG C UINF= 16.81 M/S TINF= 27.56 DEG C
RHO= 1.161 KG/M3 VISC= 0.15796E-04 M2/S XVO= 22.4 CM
CP= 1015. J/KGK PR= 0.717

*** 2700STEP10 M=0.1 TH=0 P/D=5 ***

PLATE	X	REX	TO	REENTH	STANTON NO	DST	DREEN	M	F	T2	THETA	DTH
1	127.8	0.11218E 07	38.19	0.96243E 02	0.35604E-02	0.813E-04	2.					
2	132.8	0.11759E 07	38.19	0.27581E 03	0.30823E-02	0.772E-04	5.	0.11	0.0035	28.02	0.043	0.029
3	137.9	0.12299E 07	38.19	0.44916E 03	0.30353E-02	0.768E-04	7.	0.10	0.0033	28.69	0.106	0.029
4	143.0	0.12840E 07	38.23	0.62760E 03	0.28675E-02	0.752E-04	8.	0.10	0.0033	28.55	0.093	0.029
5	148.1	0.13381E 07	38.23	0.79750E 03	0.27960E-02	0.746E-04	9.	0.10	0.0033	28.45	0.083	0.029
6	153.2	0.13921E 07	38.23	0.96012E 03	0.26709E-02	0.736E-04	11.	0.10	0.0033	28.51	0.088	0.029
7	158.2	0.14462E 07	38.21	0.11195E 04	0.26431E-02	0.736E-04	12.	0.10	0.0032	28.68	0.105	0.029
8	163.3	0.15003E 07	38.19	0.12779E 04	0.25381E-02	0.729E-04	12.	0.10	0.0032	28.62	0.100	0.029
9	168.4	0.15543E 07	38.21	0.14296E 04	0.24392E-02	0.721E-04	13.	0.10	0.0033	28.58	0.095	0.029
10	173.5	0.16084E 07	38.21	0.15773E 04	0.23974E-02	0.718E-04	14.	0.11	0.0035	28.56	0.094	0.029
11	178.6	0.16624E 07	38.23	0.17223E 04	0.23143E-02	0.711E-04	15.	0.10	0.0034	28.68	0.105	0.029
12	183.6	0.17165E 07	38.27	0.18637E 04	0.22062E-02	0.702E-04	15.	0.10	0.0034	28.61	0.098	0.029
13	187.5	0.17576E 07	37.73	0.19724E 04	0.22441E-02	0.812E-04	16.					
14	190.1	0.17854E 07	37.64	0.20346E 04	0.22175E-02	0.835E-04	16.					
15	192.7	0.18133E 07	37.94	0.20952E 04	0.21296E-02	0.814E-04	16.					
16	195.4	0.18413E 07	37.96	0.21540E 04	0.20915E-02	0.790E-04	16.					
17	198.0	0.18692E 07	37.98	0.22120E 04	0.20668E-02	0.784E-04	16.					
18	200.6	0.18971E 07	37.96	0.22694E 04	0.20517E-02	0.779E-04	16.					
19	203.2	0.19249E 07	37.94	0.23260E 04	0.20097E-02	0.755E-04	16.					
20	205.8	0.19528E 07	38.04	0.23822E 04	0.20200E-02	0.765E-04	16.					
21	208.5	0.19806E 07	37.98	0.24383E 04	0.20106E-02	0.754E-04	17.					
22	211.1	0.20084E 07	38.10	0.24938E 04	0.19678E-02	0.759E-04	17.					
23	213.7	0.20363E 07	38.04	0.25482E 04	0.19378E-02	0.739E-04	17.					
24	216.3	0.20643E 07	38.11	0.26028E 04	0.19767E-02	0.762E-04	17.					
25	218.9	0.20922E 07	38.10	0.26577E 04	0.19623E-02	0.753E-04	17.					
26	221.6	0.21201E 07	38.02	0.27120E 04	0.19357E-02	0.781E-04	17.					
27	224.2	0.21479E 07	37.05	0.27662E 04	0.19526E-02	0.710E-04	17.					
28	226.8	0.21758E 07	38.02	0.28205E 04	0.19416E-02	0.788E-04	17.					
29	229.4	0.22036E 07	37.96	0.28743E 04	0.19168E-02	0.722E-04	17.					
30	232.0	0.22315E 07	38.29	0.29281E 04	0.19465E-02	0.760E-04	17.					
31	234.6	0.22593E 07	38.29	0.29822E 04	0.19282E-02	0.741E-04	17.					
32	237.3	0.22873E 07	38.19	0.30355E 04	0.18998E-02	0.733E-04	17.					
33	239.9	0.23153E 07	38.13	0.30886E 04	0.19113E-02	0.738E-04	17.					
34	242.5	0.23431E 07	37.92	0.31416E 04	0.18849E-02	0.712E-04	17.					
35	245.1	0.23709E 07	38.08	0.31944E 04	0.19101E-02	0.759E-04	17.					
36	247.8	0.23988E 07	37.85	0.32472E 04	0.18734E-02	0.813E-04	18.					

UNCERTAINTY IN REX=27032. UNCERTAINTY IN F=0.05037 IN RATIO

RUN 090674 *** DISCRETE HOLE RIG *** NAS-3-14336 STANTON NUMBER DATA

TADB= 27.36 DEG C UINF= 16.87 M/S TINF= 27.24 DEG C
RHO= 1.162 KG/M3 VISC= 0.15755E-04 M2/S XVO= 22.4 CM
CP= 1016. J/KGK PR= 0.717

*** 2700STEP10 M=0.1 TH=1 P/D=5 ***

PLATE	X	REX	TO	REENTH	STANTON NO	DST	DREEN	M	F	T2	THETA	DTH
1	127.8	0.11285E 07	39.37	0.90674E 02	0.33346E-02	0.698E-04	2.					
2	132.8	0.11828E 07	39.37	0.25571E 03	0.27347E-02	0.653E-04	5.	0.10	0.0031	36.68	0.779	0.025
3	137.9	0.12372E 07	39.39	0.52671E 03	0.24412E-02	0.632E-04	8.	0.08	0.0024	36.86	0.792	0.025
4	143.0	0.12916E 07	39.35	0.76178E 03	0.23350E-02	0.627E-04	9.	0.08	0.0027	36.81	0.790	0.025
5	148.1	0.13460E 07	39.35	0.10024E 04	0.21869E-02	0.618E-04	11.	0.07	0.0024	36.83	0.792	0.025
6	153.2	0.14004E 07	39.35	0.12199E 04	0.20747E-02	0.612E-04	12.	0.08	0.0027	36.64	0.777	0.025
7	158.2	0.14548E 07	39.35	0.14446E 04	0.20051E-02	0.608E-04	13.	0.07	0.0022	36.65	0.777	0.025
8	163.3	0.15091E 07	39.35	0.16460E 04	0.19296E-02	0.604E-04	14.	0.07	0.0024	37.01	0.806	0.025
9	168.4	0.15635E 07	39.37	0.18520E 04	0.18394E-02	0.598E-04	15.	0.08	0.0025	36.85	0.792	0.025
10	173.5	0.16179E 07	39.41	0.20568E 04	0.17525E-02	0.592E-04	16.	0.09	0.0029	36.65	0.773	0.025
11	178.6	0.16723E 07	39.41	0.22713E 04	0.16776E-02	0.588E-04	16.	0.08	0.0026	36.72	0.780	0.025
12	183.6	0.17267E 07	39.41	0.24723E 04	0.16258E-02	0.586E-04	17.	0.08	0.0026	36.87	0.792	0.025
13	187.5	0.17680E 07	39.29	0.26543E 04	0.17220E-02	0.642E-04	18.					
14	190.1	0.17960E 07	39.10	0.27042E 04	0.18322E-02	0.680E-04	18.					
15	192.7	0.18240E 07	39.41	0.27550E 04	0.17910E-02	0.678E-04	18.					
16	195.4	0.18522E 07	39.41	0.28051E 04	0.17839E-02	0.666E-04	18.					
17	198.0	0.18803E 07	39.39	0.28554E 04	0.18041E-02	0.672E-04	18.					
18	200.6	0.19083E 07	39.39	0.29057E 04	0.17888E-02	0.669E-04	18.					
19	203.2	0.19363E 07	39.37	0.29555E 04	0.17589E-02	0.651E-04	18.					
20	205.8	0.19643E 07	39.43	0.30054E 04	0.17984E-02	0.666E-04	18.					
21	208.5	0.19923E 07	39.43	0.30551E 04	0.17517E-02	0.654E-04	18.					
22	211.1	0.20203E 07	39.37	0.31049E 04	0.17949E-02	0.672E-04	18.					
23	213.7	0.20483E 07	39.31	0.31548E 04	0.17684E-02	0.657E-04	18.					
24	216.3	0.20765E 07	39.48	0.32043E 04	0.17623E-02	0.674E-04	18.					
25	218.9	0.21046E 07	39.37	0.32544E 04	0.18058E-02	0.677E-04	18.					
26	221.6	0.21326E 07	39.24	0.33050E 04	0.18058E-02	0.705E-04	18.					
27	224.2	0.21606E 07	38.36	0.33549E 04	0.17519E-02	0.622E-04	18.					
28	226.8	0.21887E 07	39.29	0.34044E 04	0.17801E-02	0.706E-04	18.					
29	229.4	0.22167E 07	39.20	0.34540E 04	0.17578E-02	0.649E-04	19.					
30	232.0	0.22447E 07	39.46	0.35043E 04	0.18330E-02	0.695E-04	19.					
31	234.6	0.22727E 07	39.50	0.35548E 04	0.17671E-02	0.672E-04	19.					
32	237.3	0.23008E 07	39.27	0.36050E 04	0.18104E-02	0.675E-04	19.					
33	239.9	0.23290E 07	39.27	0.36556E 04	0.18020E-02	0.682E-04	19.					
34	242.5	0.23570E 07	39.05	0.37058E 04	0.17756E-02	0.654E-04	19.					
35	245.1	0.23850E 07	39.22	0.37560E 04	0.18084E-02	0.700E-04	19.					
36	247.8	0.24130E 07	39.01	0.38064E 04	0.17810E-02	0.747E-04	19.					

UNCERTAINTY IN REX=27192. UNCERTAINTY IN F=0.05036 IN RATIO

RUN 090574 *** DISCRETE HOLE RIG *** NAS-3-14336 STANTON NUMBER DATA

*** 2700STEP10 M=0.1 TH=0 P/D=5 ***

RUN 090674 *** DISCRETE HOLE RIG *** NAS-3-14336 STANTON NUMBER DATA

*** 2700STEP10 M=0.1 TH=1 P/D=5 ***

LINEAR SUPERPOSITION IS APPLIED TO STANTON NUMBER DATA FROM
RUN NUMBERS 090574 AND 090674 TO OBTAIN STANTON NUMBER DATA AT TH=0 AND TH=1

PLATE	REXCOL	RE DEL2	ST(TH=0)	REXHOT	RE DEL2	ST(TH=1)	ETA	STCR	F-COL	STHR	F-HOT	LOGB
1	1121810.0	96.2	0.003560	1128452.0	90.7	0.003335	UUUUU	1.016	0.0000	0.952	0.0000	0.952
2	1175873.0	276.4	0.003103	1182835.0	252.9	0.002630	0.152	0.814	0.0035	0.940	0.0031	1.419
3	1229936.0	444.0	0.003098	1237218.0	553.2	0.002262	0.270	0.909	0.0033	0.859	0.0024	1.267
4	1283999.0	607.3	0.002944	1291602.0	806.7	0.002174	0.262	0.931	0.0033	0.861	0.0027	1.330
5	1338063.0	764.5	0.002872	1345985.0	1069.2	0.002006	0.302	0.960	0.0033	0.820	0.0024	1.240
6	1392126.0	916.3	0.002744	1400368.0	1303.4	0.001891	0.311	0.958	0.0033	0.793	0.0027	1.276
7	1446189.0	1064.4	0.002734	1454751.0	1550.2	0.001796	0.343	0.990	0.0032	0.770	0.0022	1.185
8	1500252.0	1209.3	0.002628	1509134.0	1768.1	0.001746	0.336	0.983	0.0032	0.763	0.0024	1.207
9	1554315.0	1348.6	0.002522	1563518.0	1989.2	0.001668	0.339	0.969	0.0033	0.742	0.0025	1.212
10	1608378.0	1483.9	0.002486	1617901.0	2211.9	0.001549	0.377	0.979	0.0035	0.700	0.0029	1.239
11	1662442.0	1616.2	0.002407	1672284.0	2450.7	0.001467	0.390	0.969	0.0034	0.673	0.0026	1.173
12	1716505.0	1743.3	0.002292	1726667.0	2672.5	0.001444	0.370	0.941	0.0034	0.671	0.0026	1.179
13	1757593.0	1837.6	0.002321	1767999.0	2877.2	0.001559	0.329	0.966		0.730		
14	1785435.0	1901.6	0.002274	1796006.0	2923.0	0.001712	0.247	0.955		0.807		
15	1813278.0	1963.7	0.002180	1824013.0	2970.6	0.001685	0.227	0.923		0.799		
16	1841255.0	2023.9	0.002137	1852157.0	3017.9	0.001688	0.210	0.913		0.805		
17	1869233.0	2083.0	0.002106	1880300.0	3065.7	0.001722	0.182	0.907		0.826		
18	1897075.0	2141.5	0.002091	1908307.0	3113.8	0.001706	0.184	0.907		0.823		
19	1924918.0	2199.2	0.002047	1936315.0	3161.3	0.001680	0.179	0.895		0.814		
20	1952760.0	2256.3	0.002053	1964322.0	3209.1	0.001729	0.158	0.904		0.842		
21	1980603.0	2313.5	0.002049	1992330.0	3256.8	0.001671	0.185	0.908		0.818		
22	2008446.0	2369.8	0.001993	2020337.0	3304.6	0.001741	0.127	0.889		0.856		
23	2036288.0	2424.9	0.001963	2048344.0	3353.0	0.001715	0.126	0.882		0.848		
24	2064266.0	2480.3	0.002008	2076487.0	3400.9	0.001695	0.156	0.908		0.841		
25	2092243.0	2536.0	0.001985	2104631.0	3449.3	0.001757	0.115	0.903		0.876		
26	2120086.0	2590.9	0.001955	2132638.0	3498.6	0.001765	0.097	0.894		0.884		
27	2147928.0	2645.8	0.001982	2160645.0	3547.1	0.001689	0.148	0.912		0.849		
28	2175771.0	2700.8	0.001965	2188653.0	3595.0	0.001730	0.120	0.909		0.873		
29	2203614.0	2755.2	0.001940	2216661.0	3643.2	0.001708	0.120	0.903		0.866		
30	2231456.0	2809.7	0.001966	2244668.0	3692.3	0.001797	0.086	0.919		0.914		
31	2259299.0	2864.3	0.001952	2272675.0	3741.6	0.001717	0.121	0.918		0.877		
32	2287276.0	2918.1	0.001913	2300818.0	3790.7	0.001782	0.068	0.904		0.914		
33	2315254.0	2971.7	0.001927	2328962.0	3840.4	0.001768	0.083	0.915		0.910		
34	2343096.0	3025.0	0.001901	2356969.0	3889.6	0.001741	0.084	0.907		0.899		
35	2370939.0	3078.3	0.001925	2384976.0	3938.9	0.001777	0.077	0.923		0.921		
36	2398781.0	3131.5	0.001687	2412984.0	3988.4	0.001752	0.072	0.909		0.911		

STANTON NUMBER RATIO BASED ON ST*PR**0.4=0.0295*REX**(-.2)*(1.-(XI/(X-XVO))**0.9)**(-1./9.)

STANTON NUMBER RATIO FOR TH=1 IS CONVERTED TO COMPARABLE TRANSPIRATION VALUE
USING ALOG(1 + B)/B EXPRESSION IN THE BLOWN SECTION

RUN 080274 *** DISCRETE HOLE RIG *** NAS-3-14336 STANTON NUMBER DATA

TADB= 28.65 DEG C UINF= 16.80 M/S TINF= 28.53 DEG C
RHO= 1.164 KG/M3 VISC= 0.15775E-04 M2/S XVO= 22.4 CM
CP= 1016. J/KGK PR= 0.717

*** 2700STEP20 M=0.2 TH=0 P/D=5 ***

PLATE	X	REX	TO	REENTH	STANTON NO	DST	DREEN	M	F	T2	THETA	DTH
1	127.8	0.11225E 07	40.03	0.89744E 02	0.33179E-02	0.733E-04	2.					
2	132.8	0.11766E 07	39.96	0.26141E 03	0.30285E-02	0.714E-04	6.	0.20	0.0066	29.12	0.052	0.027
3	137.9	0.12307E 07	39.98	0.44003E 03	0.28841E-02	0.702E-04	9.	0.20	0.0065	29.50	0.085	0.027
4	143.0	0.12848E 07	39.98	0.62375E 03	0.27989E-02	0.696E-04	12.	0.20	0.0064	29.51	0.086	0.027
5	148.1	0.13389E 07	39.94	0.80229E 03	0.26996E-02	0.690E-04	14.	0.20	0.0064	29.41	0.077	0.027
6	153.2	0.13930E 07	39.96	0.97262E 03	0.26049E-02	0.683E-04	16.	0.20	0.0064	29.50	0.085	0.027
7	158.2	0.14471E 07	39.96	0.11415E 04	0.25536E-02	0.679E-04	17.	0.20	0.0064	29.59	0.093	0.027
8	163.3	0.15012E 07	39.96	0.13097E 04	0.24723E-02	0.674E-04	19.	0.20	0.0065	29.57	0.091	0.027
9	168.4	0.15553E 07	39.96	0.14740E 04	0.24100E-02	0.669E-04	20.	0.20	0.0065	29.52	0.087	0.027
10	173.5	0.16094E 07	39.98	0.16341E 04	0.23882E-02	0.667E-04	21.	0.20	0.0063	29.46	0.082	0.027
11	178.6	0.16635E 07	39.96	0.17905E 04	0.23551E-02	0.666E-04	22.	0.20	0.0065	29.50	0.085	0.027
12	183.6	0.17176E 07	40.00	0.19447E 04	0.22403E-02	0.656E-04	23.	0.20	0.0064	29.51	0.086	0.027
13	187.5	0.17587E 07	39.50	0.20659E 04	0.22006E-02	0.792E-04	24.					
14	190.1	0.17866E 07	39.33	0.21278E 04	0.22410E-02	0.824E-04	24.					
15	192.7	0.18144E 07	39.67	0.21892E 04	0.21609E-02	0.811E-04	24.					
16	195.4	0.18424E 07	39.73	0.22487E 04	0.21029E-02	0.781E-04	24.					
17	198.0	0.18704E 07	39.79	0.23068E 04	0.20635E-02	0.771E-04	24.					
18	200.6	0.18983E 07	39.75	0.23642E 04	0.20518E-02	0.765E-04	24.					
19	203.2	0.19261E 07	39.73	0.24207E 04	0.20044E-02	0.741E-04	24.					
20	205.8	0.19540E 07	39.84	0.24764E 04	0.19875E-02	0.742E-04	24.					
21	208.5	0.19819E 07	39.81	0.25316E 04	0.19716E-02	0.731E-04	24.					
22	211.1	0.20097E 07	39.88	0.25861E 04	0.19319E-02	0.733E-04	25.					
23	213.7	0.20376E 07	39.81	0.26396E 04	0.19102E-02	0.716E-04	25.					
24	216.3	0.20656E 07	39.90	0.26933E 04	0.19336E-02	0.735E-04	25.					
25	218.9	0.20936E 07	39.90	0.27468E 04	0.19024E-02	0.721E-04	25.					
26	221.6	0.21214E 07	39.84	0.28005E 04	0.19539E-02	0.746E-04	25.					
27	224.2	0.21493E 07	39.52	0.28568E 04	0.20767E-02	0.756E-04	25.					
28	226.8	0.21772E 07	39.94	0.29116E 04	0.18586E-02	0.726E-04	25.					
29	229.4	0.22050E 07	39.73	0.29638E 04	0.18828E-02	0.692E-04	25.					
30	232.0	0.22329E 07	40.09	0.30162E 04	0.18746E-02	0.725E-04	25.					
31	234.6	0.22607E 07	40.07	0.30684E 04	0.18692E-02	0.710E-04	25.					
32	237.3	0.22887E 07	39.96	0.31203E 04	0.18524E-02	0.705E-04	25.					
33	239.9	0.23167E 07	39.88	0.31724E 04	0.18818E-02	0.717E-04	25.					
34	242.5	0.23446E 07	39.64	0.32245E 04	0.18540E-02	0.688E-04	25.					
35	245.1	0.23725E 07	39.82	0.32764E 04	0.18683E-02	0.734E-04	25.					
36	247.8	0.24003E 07	39.58	0.33276E 04	0.18182E-02	0.783E-04	25.					

UNCERTAINTY IN REX=27049. UNCERTAINTY IN F=0.05037 IN RATIO

RUN 080374 *** DISCRETE HOLE RIG *** NAS-3-14336 STANTON NUMBER DATA

TADB= 26.81 DEG C UINF= 16.71 M/S TINF= 26.68 DEG C
RHO= 1.173 KG/M3 VISC= 0.15612E-04 M2/S XVO= 22.4 CM
CP= 1013. J/KGK PR= 0.715

*** 2700STEP20 M=0.2 TH=1 P/D=5 ***

PLATE	X	REX	TO	REENTH	STANTON NO	DST	DREEN	M	F	T2	THETA	DTH
1	127.8	0.11280E 07	41.32	0.88229E 02	0.32461E-02	0.584E-04	2.					
2	132.8	0.11823E 07	41.36	0.24652E 03	0.25778E-02	0.538E-04	9.	0.19	0.0062	41.00	0.975	0.021
3	137.9	0.12367E 07	41.38	0.69896E 03	0.20407E-02	0.508E-04	16.	0.18	0.0060	41.42	1.002	0.021
4	143.0	0.12911E 07	41.32	0.11301E 04	0.18855E-02	0.502E-04	20.	0.18	0.0058	41.83	1.035	0.021
5	148.1	0.13454E 07	41.32	0.15552E 04	0.17385E-02	0.495E-04	24.	0.18	0.0058	41.34	1.001	0.021
6	153.2	0.13998E 07	41.31	0.19633E 04	0.16639E-02	0.493E-04	27.	0.18	0.0057	41.46	1.011	0.021
7	158.2	0.14541E 07	41.34	0.23666E 04	0.15628E-02	0.487E-04	30.	0.18	0.0059	41.29	0.996	0.021
8	163.3	0.15085E 07	41.31	0.27690E 04	0.15242E-02	0.487E-04	32.	0.19	0.0060	42.43	1.077	0.022
9	168.4	0.15629E 07	41.36	0.32002E 04	0.14368E-02	0.482E-04	35.	0.18	0.0060	41.29	0.995	0.021
10	173.5	0.16172E 07	41.31	0.35997E 04	0.14075E-02	0.482E-04	37.	0.18	0.0059	40.39	0.938	0.021
11	178.6	0.16716E 07	41.34	0.39756E 04	0.13603E-02	0.479E-04	39.	0.18	0.0060	40.04	0.911	0.021
12	183.6	0.17259E 07	41.36	0.43442E 04	0.13454E-02	0.478E-04	41.	0.19	0.0061	40.41	0.935	0.021
13	187.5	0.17672E 07	40.28	0.47082E 04	0.12055E-02	0.441E-04	42.					
14	190.1	0.17952E 07	39.88	0.47443E 04	0.13684E-02	0.522E-04	42.					
15	192.7	0.18232E 07	40.05	0.47831E 04	0.14015E-02	0.542E-04	42.					
16	195.4	0.18514E 07	40.03	0.48227E 04	0.14214E-02	0.542E-04	42.					
17	198.0	0.18795E 07	40.01	0.48629E 04	0.14528E-02	0.553E-04	42.					
18	200.6	0.19075E 07	39.96	0.49037E 04	0.14539E-02	0.554E-04	42.					
19	203.2	0.19355E 07	39.90	0.49443E 04	0.14453E-02	0.542E-04	42.					
20	205.8	0.19635E 07	39.96	0.49853E 04	0.14778E-02	0.555E-04	42.					
21	208.5	0.19915E 07	39.98	0.50262E 04	0.14401E-02	0.548E-04	42.					
22	211.1	0.20195E 07	39.90	0.50672E 04	0.14850E-02	0.563E-04	42.					
23	213.7	0.20475E 07	39.90	0.51084E 04	0.14585E-02	0.552E-04	42.					
24	216.3	0.20756E 07	40.07	0.51492E 04	0.14539E-02	0.567E-04	42.					
25	218.9	0.21037E 07	39.94	0.51905E 04	0.14897E-02	0.564E-04	42.					
26	221.6	0.21317E 07	39.90	0.52329E 04	0.15349E-02	0.584E-04	42.					
27	224.2	0.21597E 07	39.77	0.52772E 04	0.16278E-02	0.601E-04	42.					
28	226.8	0.21877E 07	40.01	0.53207E 04	0.14766E-02	0.574E-04	42.					
29	229.4	0.22157E 07	39.84	0.53618E 04	0.14538E-02	0.544E-04	42.					
30	232.0	0.22437E 07	40.01	0.54038E 04	0.15463E-02	0.591E-04	42.					
31	234.6	0.22717E 07	40.03	0.54465E 04	0.15022E-02	0.577E-04	42.					
32	237.3	0.22998E 07	39.81	0.54892E 04	0.15420E-02	0.580E-04	42.					
33	239.9	0.23280E 07	39.82	0.55322E 04	0.15275E-02	0.585E-04	42.					
34	242.5	0.23560E 07	39.60	0.55747E 04	0.15036E-02	0.559E-04	42.					
35	245.1	0.23840E 07	39.73	0.56175E 04	0.15525E-02	0.608E-04	42.					
36	247.8	0.24120E 07	39.48	0.56605E 04	0.15165E-02	0.648E-04	42.					

UNCERTAINTY IN REX=27180. UNCERTAINTY IN F=0.05037 IN RATIO

RUN 080274 *** DISCRETE HOLE RIG *** NAS-3-14336 STANTON NUMBER DATA

*** 2700STEP20 M=0.2 TH=0 P/D=5 ***

RUN 080374 *** DISCRETE HOLE RIG *** NAS-3-14336 STANTON NUMBER DATA

*** 2700STEP20 M=0.2 TH=1 P/D=5 ***

LINEAR SUPERPOSITION IS APPLIED TO STANTON NUMBER DATA FROM
RUN NUMBERS 080274 AND 080374 TO OBTAIN STANTON NUMBER DATA AT TH=0 AND TH=1

PLATE	REXCOL	RE DEL2	ST(TH=0)	REXHOT	RE DEL2	ST(TH=1)	ETA	STCR	F-COL	STHR	F-HOT	LOGB
1	1122526.0	89.7	0.003318	1127970.0	88.2	0.003246	UUUUU	0.947	0.0000	0.927	0.0000	0.927
2	1176624.0	262.1	0.003054	1182330.0	246.2	0.002566	0.160	0.800	0.0066	0.916	0.0062	1.797
3	1230722.0	424.4	0.002947	1236690.0	706.3	0.002030	0.311	0.864	0.0065	0.770	0.0060	1.650
4	1284819.0	582.1	0.002883	1291050.0	1136.9	0.001904	0.340	0.911	0.0064	0.753	0.0058	1.642
5	1338917.0	735.4	0.002783	1345410.0	1552.1	0.001757	0.369	0.929	0.0064	0.717	0.0058	1.623
6	1393015.0	883.4	0.002688	1399770.0	1960.5	0.001670	0.379	0.938	0.0064	0.700	0.0057	1.615
7	1447112.0	1027.7	0.002650	1454130.0	2360.7	0.001567	0.409	0.959	0.0064	0.671	0.0059	1.616
8	1501210.0	1168.8	0.002565	1508490.0	2765.3	$\boxed{0.001561}$	0.391	0.958	0.0065	0.682	0.0060	1.660
9	1555308.0	1305.8	0.002502	1562850.0	3173.5	0.001474	0.411	0.960	0.0065	0.655	0.0060	1.636
10	1609405.0	1440.6	0.002482	1617210.0	3574.6	0.001370	0.448	0.976	0.0063	0.618	0.0059	1.595
11	1663503.0	1574.1	0.002454	1671570.0	3967.1	0.001271	0.482	0.986	0.0065	0.582	0.0060	1.569
12	1717601.0	1703.6	$\boxed{0.002332}$	1725930.0	4359.8	$\boxed{0.001263}$	0.458	0.956	0.0064	0.586	0.0061	1.606
13	1758715.0	1798.8	0.002302	1767244.0	4741.9	0.001114	0.516	0.957		0.522		
14	1786575.0	1863.4	0.002330	1795239.0	4775.6	0.001288	0.447	0.977		0.607		
15	1814435.0	1927.1	0.002238	1823235.0	4812.3	0.001332	0.405	0.947		0.631		
16	1842431.0	1988.6	0.002172	1851366.0	4850.0	0.001359	0.375	0.927		0.647		
17	1870426.0	2048.5	0.002126	1879497.0	4888.6	0.001397	0.343	0.914		0.669		
18	1898287.0	2107.6	0.002112	1907493.0	4927.8	0.001399	0.338	0.915		0.674		
19	1926147.0	2165.8	0.002061	1935488.0	4967.0	0.001394	0.324	0.900		0.675		
20	1954007.0	2223.0	0.002039	1963483.0	5006.5	0.001431	0.298	0.897		0.696		
21	1981868.0	2279.7	0.002026	1991479.0	5046.1	0.001391	0.313	0.897		0.680		
22	2009728.0	2335.6	0.001977	2019474.0	5085.8	0.001444	0.270	0.881		0.709		
23	2037588.0	2390.4	0.001956	2047470.0	5125.9	0.001417	0.276	0.878		0.699		
24	2065584.0	2445.4	0.001983	2075601.0	5165.5	0.001410	0.289	0.895		0.699		
25	2093579.0	2500.1	0.001944	2103732.0	5205.6	0.001452	0.253	0.883		0.723		
26	2121440.0	2555.1	0.001997	2131728.0	5247.0	0.001496	0.251	0.912		0.748		
27	2149300.0	2612.5	0.002123	2159723.0	5290.2	0.001587	0.253	0.976		0.797		
28	2177160.0	2668.6	0.001898	2187718.0	5332.6	0.001441	0.240	0.877		0.727		
29	2205021.0	2721.9	0.001927	2215714.0	5372.6	0.001414	0.266	0.895		0.716		
30	2232881.0	2775.4	0.001908	2243710.0	5413.7	0.001516	0.205	0.892		0.771		
31	2260741.0	2828.6	0.001907	2271705.0	5455.5	0.001468	0.230	0.896		0.749		
32	2288736.0	2881.5	0.001884	2299836.0	5497.3	0.001513	0.197	0.890		0.775		
33	2316732.0	2934.5	0.001918	2327967.0	5539.5	0.001495	0.221	0.910		0.768		
34	2344592.0	2987.6	0.001890	2355963.0	5581.0	0.001471	0.221	0.901		0.759		
35	2372453.0	3040.5	0.001900	2383958.0	5623.0	0.001523	0.198	0.910		0.789		
36	2400313.0	3092.8	0.001849	2411953.0	5665.2	0.001489	0.195	0.890		0.774		

STANTON NUMBER RATIO BASED ON ST*PR**0.4=0.0295*REX**(-.2)*(1.-(XI/(X-XVO))**0.9)**(-1./9.)

STANTON NUMBER RATIO FOR TH=1 IS CONVERTED TO COMPARABLE TRANSPIRATION VALUE
USING ALOG(1 + B)/B EXPRESSION IN THE BLOWN SECTION

RUN 090374 *** DISCRETE HOLE RIG *** NAS-3-14336 STANTON NUMBER DATA

TADB= 26.08 DEG C UINF= 16.87 M/S TINF= 25.95 DEG C
RHO= 1.167 KG/M3 VISC= 0.15649E-04 M2/S XVO= 22.4 CM
CP= 1015. J/KGK PR= 0.717

*** 2700STEP30 M=0.3 TH=0 P/D=5 ***

PLATE	X	REX	TO	REENTH	STANTON NO	DST	DREEN	M	F	T2	THETA	DTH
1	127.8	0.11361E 07	37.51	0.99709E 02	0.36423E-02	0.755E-04	2.					
2	132.8	0.11908E 07	37.56	0.28704E 03	0.32007E-02	0.714E-04	8.	0.29	0.0093	26.31	0.031	0.027
3	137.9	0.12456E 07	37.54	0.47214E 03	0.29776E-02	0.698E-04	13.	0.29	0.0094	26.65	0.060	0.026
4	143.0	0.13003E 07	37.54	0.66340E 03	0.28666E-02	0.690E-04	16.	0.29	0.0095	26.64	0.059	0.026
5	148.1	0.13551E 07	37.54	0.84888E 03	0.27846E-02	0.684E-04	19.	0.29	0.0095	26.64	0.060	0.026
6	153.2	0.14098E 07	37.56	0.10308E 04	0.27331E-02	0.679E-04	22.	0.29	0.0093	26.65	0.060	0.026
7	158.2	0.14646E 07	37.56	0.12097E 04	0.26837E-02	0.675E-04	24.	0.29	0.0093	26.74	0.068	0.026
8	163.3	0.15194E 07	37.58	0.13889E 04	0.26049E-02	0.669E-04	26.	0.29	0.0094	26.79	0.072	0.026
9	168.4	0.15741E 07	37.58	0.15673E 04	0.25524E-02	0.665E-04	28.	0.29	0.0095	26.74	0.067	0.026
10	173.5	0.16289E 07	37.58	0.17425E 04	0.25670E-02	0.666E-04	29.	0.29	0.0093	26.68	0.062	0.026
11	178.6	0.16836E 07	37.58	0.19132E 04	0.25053E-02	0.662E-04	31.	0.29	0.0093	26.74	0.068	0.026
12	183.6	0.17384E 07	37.58	0.20815E 04	0.23768E-02	0.653E-04	33.	0.29	0.0093	26.71	0.065	0.026
13	187.5	0.17800E 07	36.99	0.22130E 04	0.23355E-02	0.821E-04	33.					
14	190.1	0.18082E 07	36.90	0.22782E 04	0.22806E-02	0.833E-04	33.					
15	192.7	0.18364E 07	37.22	0.23417E 04	0.22186E-02	0.822E-04	33.					
16	195.4	0.18647E 07	37.26	0.24034E 04	0.21553E-02	0.790E-04	34.					
17	198.0	0.18930E 07	37.31	0.24638E 04	0.21224E-02	0.782E-04	34.					
18	200.6	0.19212E 07	37.31	0.25231E 04	0.20817E-02	0.768E-04	34.					
19	203.2	0.19494E 07	37.33	0.25809E 04	0.20087E-02	0.737E-04	34.					
20	205.8	0.19776E 07	37.43	0.26375E 04	0.20042E-02	0.740E-04	34.					
21	208.5	0.20058E 07	37.37	0.26940E 04	0.19963E-02	0.731E-04	34.					
22	211.1	0.20340E 07	37.47	0.27496E 04	0.19435E-02	0.730E-04	34.					
23	213.7	0.20622E 07	37.39	0.28042E 04	0.19251E-02	0.713E-04	34.					
24	216.3	0.20905E 07	37.51	0.28586E 04	0.19304E-02	0.729E-04	34.					
25	218.9	0.21189E 07	37.45	0.29130E 04	0.19222E-02	0.721E-04	34.					
26	221.6	0.21471E 07	37.33	0.29671E 04	0.19072E-02	0.752E-04	34.					
27	224.2	0.21753E 07	36.27	0.30215E 04	0.19522E-02	0.683E-04	34.					
28	226.8	0.22035E 07	37.37	0.30759E 04	0.19003E-02	0.758E-04	34.					
29	229.4	0.22317E 07	37.28	0.31296E 04	0.19066E-02	0.697E-04	34.					
30	232.0	0.22599E 07	37.66	0.31835E 04	0.19083E-02	0.730E-04	34.					
31	234.6	0.22881E 07	37.62	0.32373E 04	0.19024E-02	0.713E-04	34.					
32	237.3	0.23164E 07	37.51	0.32908E 04	0.18887E-02	0.709E-04	34.					
33	239.9	0.23447E 07	37.47	0.33441E 04	0.18885E-02	0.713E-04	34.					
34	242.5	0.23729E 07	37.22	0.33974E 04	0.18856E-02	0.691E-04	34.					
35	245.1	0.24011E 07	37.41	0.34509E 04	0.19042E-02	0.737E-04	34.					
36	247.8	0.24293E 07	37.16	0.35041E 04	0.18632E-02	0.792E-04	34.					

UNCERTAINTY IN REX=27376. UNCERTAINTY IN F=0.05036 IN RATIO

RUN 090474 *** DISCRETE HOLE RIG *** NAS-3-14336 STANTON NUMBER DATA

TADB= 26.90 DEG C UINF= 16.84 M/S TINF= 26.78 DEG C
RHO= 1.160 KG/M3 VISC= 0.15753E-04 M2/S XVO= 22.4 CM
CP= 1017. J/KGK PR= 0.718

*** 2700STEP 30 M=0.3 TH=1 P/D=5 ***

PLATE	X	REX	TO	REENTH	STANTON NO	DST	DREEN	M	F	T2	THETA	DTH
1	127.8	0.11270E 07	43.11	0.94222E 02	0.34694E-02	0.545E-04	2.					
2	132.8	0.11814E 07	43.09	0.26167E 03	0.26963E-02	0.496E-04	12.	0.28	0.0090	41.14	0.881	0.019
3	137.9	0.12357E 07	43.09	0.82573E 03	0.21395E-02	0.465E-04	21.	0.29	0.0093	42.06	0.937	0.019
4	143.0	0.12900E 07	43.03	0.14073E 04	0.18765E-02	0.454E-04	28.	0.28	0.0092	42.20	0.949	0.019
5	148.1	0.13443E 07	43.05	0.19786E 04	0.17874E-02	0.450E-04	34.	0.29	0.0095	41.88	0.928	0.019
6	153.2	0.13986E 07	43.07	0.25502E 04	0.16701E-02	0.444E-04	39.	0.31	0.0100	41.72	0.917	0.019
7	158.2	0.14529E 07	43.07	0.31368E 04	0.16152E-02	0.442E-04	43.	0.29	0.0093	41.59	0.909	0.019
8	163.3	0.15073E 07	43.05	0.36811E 04	0.15653E-02	0.441E-04	46.	0.27	0.0087	42.46	0.964	0.019
9	168.4	0.15616E 07	43.03	0.42181E 04	0.14709E-02	0.438E-04	49.	0.27	0.0087	41.70	0.918	0.019
10	173.5	0.16159E 07	43.07	0.47287E 04	0.14365E-02	0.435E-04	52.	0.30	0.0097	41.00	0.873	0.019
11	178.6	0.16702E 07	43.07	0.52670E 04	0.13962E-02	0.434E-04	55.	0.29	0.0094	40.90	0.867	0.019
12	183.6	0.17245E 07	43.07	0.57848E 04	0.13624E-02	0.433E-04	58.	0.31	0.0100	40.84	0.863	0.019
13	187.5	0.17658E 07	42.61	0.63117E 04	0.13734E-02	0.493E-04	59.					
14	190.1	0.17938E 07	42.42	0.63509E 04	0.14227E-02	0.521E-04	59.					
15	192.7	0.18217E 07	42.73	0.63908E 04	0.14254E-02	0.532E-04	59.					
16	195.4	0.18498E 07	42.73	0.64308E 04	0.14326E-02	0.526E-04	60.					
17	198.0	0.18780E 07	42.73	0.64710E 04	0.14358E-02	0.529E-04	60.					
18	200.6	0.19059E 07	42.67	0.65111E 04	0.14332E-02	0.528E-04	60.					
19	203.2	0.19339E 07	42.63	0.65509E 04	0.14096E-02	0.513E-04	60.					
20	205.8	0.19619E 07	42.75	0.65906E 04	0.14227E-02	0.522E-04	60.					
21	208.5	0.19898E 07	42.73	0.66302E 04	0.14057E-02	0.516E-04	60.					
22	211.1	0.20178E 07	42.73	0.66699E 04	0.14255E-02	0.527E-04	60.					
23	213.7	0.20458E 07	42.71	0.67094E 04	0.13979E-02	0.514E-04	60.					
24	216.3	0.20739E 07	42.86	0.67486E 04	0.14019E-02	0.528E-04	60.					
25	218.9	0.21020E 07	42.76	0.67880E 04	0.14108E-02	0.524E-04	60.					
26	221.6	0.21300E 07	42.59	0.68278E 04	0.14294E-02	0.553E-04	60.					
27	224.2	0.21580E 07	41.61	0.68671E 04	0.13778E-02	0.474E-04	60.					
28	226.8	0.21859E 07	42.63	0.69064E 04	0.14325E-02	0.560E-04	60.					
29	229.4	0.22139E 07	42.58	0.69460E 04	0.13955E-02	0.506E-04	60.					
30	232.0	0.22419E 07	42.90	0.69861E 04	0.14636E-02	0.549E-04	60.					
31	234.6	0.22698E 07	42.88	0.70268E 04	0.14453E-02	0.538E-04	60.					
32	237.3	0.22979E 07	42.65	0.70678E 04	0.14821E-02	0.542E-04	60.					
33	239.9	0.23261E 07	42.63	0.71093E 04	0.14832E-02	0.550E-04	60.					
34	242.5	0.23540E 07	42.37	0.71504E 04	0.14509E-02	0.522E-04	60.					
35	245.1	0.23820E 07	42.54	0.71917E 04	0.15014E-02	0.571E-04	60.					
36	247.8	0.24100E 07	42.20	0.72338E 04	0.15048E-02	0.624E-04	60.					

UNCERTAINTY IN REX=27158. UNCERTAINTY IN F=0.05036 IN RATIO

RUN 090374 *** DISCRETE HOLE RIG *** NAS-3-14336 STANTON NUMBER DATA

*** 2700STEP30 M=0.3 TH=0 P/D=5 ***

RUN 090474 *** DISCRETE HOLE RIG *** NAS-3-14336 STANTON NUMBER DATA

*** 2700STEP30 M=0.3 TH=1 P/D=5 ***

LINEAR SUPERPOSITION IS APPLIED TO STANTON NUMBER DATA FROM
RUN NUMBERS 090374 AND 090474 TO OBTAIN STANTON NUMBER DATA AT TH=0 AND TH=1

PLATE	REXCOL	RE DEL2	ST(TH=0)	REXHOT	RE DEL2	ST(TH=1)	ETA	STCR	F-COL	STHR	F-HOT	LOGB
1	1136091.0	99.7	0.003642	1127044.0	94.2	0.003469	UUUUU	1.040	0.0000	0.990	0.0000	0.990
2	1190843.0	287.5	0.003219	1181359.0	259.7	0.002625	0.184	0.847	0.0093	0.938	0.0090	2.167
3	1245594.0	458.4	0.003022	1235675.0	878.2	0.002051	0.321	0.890	0.0094	0.779	0.0093	2.063
4	1300345.0	621.5	0.002934	1289990.0	1467.4	0.001812	0.382	0.930	0.0095	0.718	0.0092	2.014
5	1355097.0	779.9	0.002852	1344305.0	2080.6	0.001717	0.398	0.956	0.0095	0.702	0.0095	2.067
6	1409848.0	934.8	0.002807	1398621.0	2684.8	0.001575	0.439	0.983	0.0093	0.661	0.0100	2.102
7	1464600.0	1087.3	0.002764	1452936.0	3310.8	0.001506	0.455	1.005	0.0093	0.646	0.0093	2.021
8	1519351.0	1236.6	0.002689	1507252.0	3895.7	0.001485	0.446	1.008	0.0094	0.651	0.0087	1.976
9	1574102.0	1382.4	0.002639	1561567.0	4445.6	0.001398	0.470	1.017	0.0095	0.622	0.0087	1.952
10	1628854.0	1527.4	0.002655	1615882.0	4988.9	0.001294	0.513	1.049	0.0093	0.585	0.0097	2.052
11	1683605.0	1671.1	0.002595	1670198.0	5585.4	0.001217	0.531	1.047	0.0093	0.558	0.0094	1.990
12	1738357.0	1809.5	0.002461	1724513.0	6161.7	0.001191	0.516	1.013	0.0093	0.553	0.0100	2.078
13	1779968.0	1911.0	0.002416	1765793.0	6756.2	0.001211	0.499	1.008		0.568		
14	1808165.0	1978.3	0.002352	1793765.0	6791.1	0.001278	0.457	0.991		0.603		
15	1836362.0	2043.8	0.002285	1821738.0	6827.1	0.001291	0.435	0.971		0.613		
16	1864695.0	2107.3	0.002215	1849846.0	6863.5	0.001311	0.408	0.949		0.625		
17	1893029.0	2169.3	0.002180	1877954.0	6900.3	0.001320	0.394	0.941		0.633		
18	1921226.0	2230.2	0.002136	1905926.0	6937.3	0.001324	0.380	0.929		0.638		
19	1949423.0	2289.4	0.002059	1933899.0	6974.2	0.001308	0.364	0.902		0.634		
20	1977620.0	2347.5	0.002053	1961871.0	7011.1	0.001324	0.355	0.906		0.645		
21	2005817.0	2405.3	0.002046	1989844.0	7047.9	0.001306	0.362	0.909		0.639		
22	2034014.0	2462.2	0.001987	2017816.0	7084.9	0.001338	0.326	0.889		0.658		
23	2062211.0	2518.1	0.001969	2045789.0	7122.0	0.001309	0.335	0.887		0.647		
24	2090545.0	2573.7	0.001974	2073897.0	7158.7	0.001313	0.335	0.895		0.652		
25	2118879.0	2629.3	0.001965	2102005.0	7195.6	0.001325	0.326	0.896		0.660		
26	2147076.0	2684.6	0.001947	2129977.0	7233.1	0.001349	0.307	0.893		0.675		
27	2175273.0	2740.3	0.002000	2157950.0	7269.9	0.001281	0.360	0.923		0.644		
28	2203470.0	2795.9	0.001939	2185922.0	7306.8	0.001354	0.302	0.900		0.683		
29	2231667.0	2850.8	0.001949	2213895.0	7344.1	0.001309	0.328	0.909		0.664		
30	2259864.0	2905.7	0.001945	2241867.0	7381.8	0.001389	0.286	0.913		0.707		
31	2288061.0	2960.6	0.001940	2269840.0	7420.4	0.001368	0.295	0.915		0.699		
32	2316394.0	3015.1	0.001923	2297948.0	7459.4	0.001413	0.265	0.911		0.725		
33	2344728.0	3069.4	0.001922	2326056.0	7498.0	0.001415	0.264	0.916		0.728		
34	2372925.0	3123.7	0.001922	2354028.0	7538.1	0.001378	0.283	0.920		0.712		
35	2401122.0	3178.1	0.001938	2382001.0	7577.4	0.001433	0.260	0.932		0.743		
36	2429319.0	3232.2	0.001893	2409973.0	7617.7	0.001444	0.237	0.915		0.751		

STANTON NUMBER RATIO BASED ON ST*PR**0.4=0.0295*REX**(-.2)*(1.-(XI/(X-XVO))**0.9)**(-1./9.)

STANTON NUMBER RATIO FOR TH=1 IS CONVERTED TO COMPARABLE TRANSPIRATION VALUE
USING ALOG(1 + B)/B EXPRESSION IN THE BLOWN SECTION

RUN 090474-1 *** DISCRETE HOLE RIG *** NAS-3-14336 STANTON NUMBER DATA

TADB= 26.88 DEG C UINF= 16.83 M/S TINF= 26.76 DEG C
RHO= 1.160 KG/M3 VISC= 0.15751E-04 M2/S XVO= 22.4 CM
CP= 1017. J/KGK PR= 0.718

*** 27COSTEP30 M=0.3 TH=1.25 P/D=5 ***

PLATE	X	REX	TO	REENTH	STANTON NO	DST	DREEN	M	F	T2	THETA	DTH
1	127.8	0.11263E 07	43.52	0.90115E 02	0.33205E-02	0.523E-04	1.					
2	132.8	0.11806E 07	43.54	0.24816E 03	0.25029E-02	0.473E-04	15.	0.26	0.0084	47.46	1.234	0.020
3	137.9	0.12348E 07	43.56	0.92537E 03	0.17805E-02	0.436E-04	27.	0.27	0.0087	48.39	1.288	0.020
4	143.0	0.12891E 07	43.58	0.16225E 04	0.14718E-02	0.424E-04	35.	0.27	0.0086	48.63	1.300	0.020
5	148.1	0.13434E 07	43.56	0.23082E 04	0.13638E-02	0.420E-04	42.	0.27	0.0089	48.17	1.275	0.020
6	153.2	0.13977E 07	43.56	0.29935E 04	0.12920E-02	0.418E-04	48.	0.27	0.0088	48.12	1.271	0.020
7	158.2	0.14519E 07	43.56	0.36646E 04	0.11671E-02	0.414E-04	52.	0.25	0.0081	47.84	1.255	0.020
8	163.3	0.15062E 07	43.56	0.42797E 04	0.11297E-02	0.413E-04	57.	0.25	0.0081	49.21	1.336	0.020
9	168.4	0.15605E 07	43.56	0.49262E 04	0.10424E-02	0.411E-04	61.	0.25	0.0082	48.03	1.266	0.020
10	173.5	0.16148E 07	43.58	0.55424E 04	0.10200E-02	0.409E-04	64.	0.28	0.0091	47.23	1.217	0.019
11	178.6	0.16691E 07	43.58	0.61993E 04	0.95298E-03	0.408E-04	68.	0.27	0.0086	47.03	1.205	0.019
12	183.6	0.17233E 07	43.56	0.68119E 04	0.92813E-03	0.408E-04	71.	0.28	0.0090	46.93	1.200	0.019
13	187.5	0.17646E 07	43.35	0.74403E 04	0.10193E-02	0.392E-04	73.					
14	190.1	0.17925E 07	43.12	0.74701E 04	0.11118E-02	0.426E-04	73.					
15	192.7	0.18205E 07	43.35	0.75016E 04	0.11349E-02	0.439E-04	73.					
16	195.4	0.18486E 07	43.33	0.75337E 04	0.11577E-02	0.440E-04	73.					
17	198.0	0.18767E 07	43.31	0.75664E 04	0.11836E-02	0.449E-04	73.					
18	200.6	0.19046E 07	43.28	0.75996E 04	0.11833E-02	0.450E-04	73.					
19	203.2	0.19326E 07	43.22	0.76327E 04	0.11855E-02	0.442E-04	73.					
20	205.8	0.19605E 07	43.31	0.76661E 04	0.12048E-02	0.452E-04	73.					
21	208.5	0.19885E 07	43.31	0.76995E 04	0.11777E-02	0.447E-04	73.					
22	211.1	0.20164E 07	43.20	0.77331E 04	0.12246E-02	0.461E-04	73.					
23	213.7	0.20444E 07	43.16	0.77672E 04	0.12147E-02	0.454E-04	73.					
24	216.3	0.20725E 07	43.39	0.78009E 04	0.11947E-02	0.466E-04	73.					
25	218.9	0.21006E 07	43.22	0.78350E 04	0.12368E-02	0.468E-04	73.					
26	221.6	0.21285E 07	43.03	0.78700E 04	0.12627E-02	0.492E-04	73.					
27	224.2	0.21565E 07	42.25	0.79042E 04	0.11854E-02	0.422E-04	73.					
28	226.8	0.21844E 07	43.14	0.79384E 04	0.12561E-02	0.500E-04	73.					
29	229.4	0.22124E 07	43.03	0.79732E 04	0.12340E-02	0.457E-04	73.					
30	232.0	0.22403E 07	43.22	0.80091E 04	0.13296E-02	0.501E-04	73.					
31	234.6	0.22683E 07	43.26	0.80457E 04	0.12862E-02	0.490E-04	73.					
32	237.3	0.22964E 07	42.95	0.80825E 04	0.13422E-02	0.495E-04	73.					
33	239.9	0.23245E 07	42.97	0.81198E 04	0.13226E-02	0.500E-04	73.					
34	242.5	0.23524E 07	42.73	0.81567E 04	0.13139E-02	0.480E-04	73.					
35	245.1	0.23804E 07	42.86	0.81941E 04	0.13651E-02	0.524E-04	73.					
36	247.8	0.24083E 07	42.59	0.82322E 04	0.13533E-02	0.566E-04	73.					

UNCERTAINTY IN REX=27139. UNCERTAINTY IN F=0.05037 IN RATIO

RUN C80174-1 *** DISCRETE HOLE RIG *** NAS-3-14336 STANTON NUMBER DATA

TADB= 25.96 DEG C UINF= 16.87 M/S TINF= 25.83 DEG C
RHO= 1.176 KG/M3 VISC= 0.15539E-04 M2/S XVO= 22.4 CM
CP= 1014. J/KGK PR= 0.716

*** 2700STEP40 M=0.4 TH=0 P/D=5 ***

PLATE	X	REX	TO	REENTH	STANTON NO	CST	DREEN	M	F	T2	THETA	DTH
1	127.8	0.11441E 07	38.00	0.99311E 02	0.36022E-02	0.713E-04	2.					
2	132.8	0.11993E 07	37.96	0.28488E 03	0.31286E-02	0.677E-04	10.	0.42	0.0135	26.02	0.015	0.026
3	137.9	0.12544E 07	37.92	0.46447E 03	0.29735E-02	0.667E-04	17.	0.40	0.0129	26.31	0.040	0.025
4	143.0	0.13095E 07	37.94	0.65318E 03	0.28453E-02	0.657E-04	21.	0.41	0.0133	26.23	0.033	0.025
5	148.1	0.13647E 07	37.94	0.83096E 03	0.27331E-02	0.649E-04	25.	0.40	0.0129	26.21	0.031	0.025
6	153.2	0.14198E 07	37.94	0.10028E 04	0.26999E-02	0.647E-04	28.	0.40	0.0131	26.23	0.032	0.025
7	158.2	0.14750E 07	37.92	0.11742E 04	0.26709E-02	0.646E-04	31.	0.40	0.0129	26.36	0.044	0.025
8	163.3	0.15301E 07	37.92	0.13511E 04	0.26193E-02	0.642E-04	34.	0.41	0.0132	26.36	0.043	0.025
9	168.4	0.15852E 07	37.98	0.15257E 04	0.25694E-02	0.636E-04	37.	0.40	0.0130	26.35	0.042	0.025
10	173.5	0.16404E 07	37.96	0.16976E 04	0.25639E-02	0.636E-04	39.	0.40	0.0129	26.32	0.040	0.025
11	178.6	0.16955E 07	37.98	0.18666E 04	0.25255E-02	0.633E-04	41.	0.40	0.0129	26.37	0.044	0.025
12	183.6	0.17507E 07	38.02	0.20335E 04	0.23908E-02	0.622E-04	43.	0.39	0.0128	26.36	0.043	0.025
13	187.5	0.17926E 07	37.24	0.21639E 04	0.23811E-02	0.820E-04	44.					
14	190.1	0.18210E 07	37.18	0.22298E 04	0.22544E-02	0.818E-04	44.					
15	192.7	0.18494E 07	37.52	0.22931E 04	0.21989E-02	0.808E-04	44.					
16	195.4	0.18779E 07	37.58	0.23548E 04	0.21435E-02	0.780E-04	44.					
17	198.0	0.19064E 07	37.64	0.24151E 04	0.20975E-02	0.768E-04	44.					
18	200.6	0.19348E 07	37.62	0.24743E 04	0.20677E-02	0.757E-04	44.					
19	203.2	0.19632E 07	37.60	0.25323E 04	0.20088E-02	0.729E-04	44.					
20	205.8	0.19916E 07	37.71	0.25892E 04	0.19945E-02	0.730E-04	44.					
21	208.5	0.20200E 07	37.71	0.26453E 04	0.19567E-02	0.713E-04	44.					
22	211.1	0.20484E 07	37.81	0.27002E 04	0.19056E-02	0.710E-04	44.					
23	213.7	0.20768E 07	37.77	0.27539E 04	0.18680E-02	0.688E-04	44.					
24	216.3	0.21053E 07	37.90	0.28071E 04	0.18785E-02	0.706E-04	44.					
25	218.9	0.21339E 07	37.83	0.28607E 04	0.18905E-02	0.697E-04	44.					
26	221.6	0.21623E 07	37.87	0.29142E 04	0.18730E-02	0.707E-04	44.					
27	224.2	0.21907E 07	37.54	0.29695E 04	0.20182E-02	0.725E-04	44.					
28	226.8	0.22191E 07	37.89	0.30237E 04	0.17923E-02	0.685E-04	44.					
29	229.4	0.22475E 07	37.75	0.30749E 04	0.18099E-02	0.658E-04	44.					
30	232.0	0.22758E 07	38.10	0.31266E 04	0.18253E-02	0.693E-04	44.					
31	234.6	0.23042E 07	38.06	0.31783E 04	0.18173E-02	0.677E-04	44.					
32	237.3	0.23328E 07	37.96	0.32298E 04	0.17999E-02	0.673E-04	44.					
33	239.9	0.23613E 07	37.92	0.32811E 04	0.18087E-02	0.680E-04	44.					
34	242.5	0.23897E 07	37.66	0.33323E 04	0.17971E-02	0.654E-04	44.					
35	245.1	0.24181E 07	37.87	0.33836E 04	0.18070E-02	0.699E-04	44.					
36	247.8	0.24465E 07	37.58	0.34343E 04	0.17632E-02	0.749E-04	45.					

UNCERTAINTY IN REX=27569. UNCERTAINTY IN F=0.05035 IN RATIO

RUN 080174-2 *** DISCRETE HOLE RIG *** NAS-3-14336 STANTON NUMBER DATA

TADB= 27.38 DEG C UINF= 16.81 M/S TINF= 27.26 DEG C
RHO= 1.169 KG/M3 VISC= 0.15668E-04 M2/S XVO= 22.4 CM
CP= 1015. J/KGK PR= 0.716

*** 270STEP40 M=0.4 TH=1 P/D=5 ***

PLATE	X	REX	TO	REENTH	STANTON NO	DST	DREEN	M	F	T2	THETA	DTH
1	127.8	0.11310E 07	43.52	0.89313E 02	0.32773E-02	0.532E-04	2.					
2	132.8	0.11855E 07	43.62	0.25211E 03	0.26963E-02	0.493E-04	17.	0.38	0.0124	41.75	0.886	0.019
3	137.9	0.12400E 07	43.56	0.98511E 03	0.22038E-02	0.467E-04	29.	0.37	0.0118	42.95	0.963	0.019
4	143.0	0.12945E 07	43.58	0.17150E 04	0.18070E-02	0.448E-04	38.	0.37	0.0121	43.68	1.006	0.019
5	148.1	0.13490E 07	43.58	0.24704E 04	0.16427E-02	0.441E-04	45.	0.37	0.0119	42.93	0.960	0.019
6	153.2	0.14035E 07	43.58	0.31782E 04	0.15277E-02	0.436E-04	51.	0.38	0.0122	42.86	0.956	0.019
7	158.2	0.14580E 07	43.60	0.38931E 04	0.14659E-02	0.433E-04	57.	0.37	0.0120	42.50	0.933	0.019
8	163.3	0.15125E 07	43.60	0.45846E 04	0.14484E-02	0.433E-04	61.	0.36	0.0118	43.07	0.968	0.019
9	168.4	0.15670E 07	43.58	0.52817E 04	0.13812E-02	0.431E-04	66.	0.37	0.0118	42.32	0.923	0.019
10	173.5	0.16215E 07	43.56	0.59519E 04	0.13541E-02	0.430E-04	69.	0.36	0.0117	41.41	0.868	0.019
11	178.6	0.16760E 07	43.54	0.65787E 04	0.13125E-02	0.429E-04	73.	0.38	0.0123	41.05	0.847	0.019
12	183.6	0.17305E 07	43.54	0.72181E 04	0.12784E-02	0.428E-04	76.	0.37	0.0119	40.52	0.814	0.018
13	187.5	0.17719E 07	42.95	0.77993E 04	0.12314E-02	0.446E-04	77.					
14	190.1	0.18000E 07	42.78	0.78341E 04	0.12471E-02	0.471E-04	77.					
15	192.7	0.18281E 07	43.05	0.78692E 04	0.12496E-02	0.479E-04	77.					
16	195.4	0.18563E 07	43.05	0.79043E 04	0.12456E-02	0.471E-04	77.					
17	198.0	0.18845E 07	43.05	0.79393E 04	0.12449E-02	0.471E-04	77.					
18	200.6	0.19126E 07	43.03	0.79741E 04	0.12320E-02	0.468E-04	77.					
19	203.2	0.19406E 07	43.01	0.80084E 04	0.12121E-02	0.454E-04	77.					
20	205.8	0.19687E 07	43.12	0.80424E 04	0.12066E-02	0.457E-04	77.					
21	208.5	0.19968E 07	43.09	0.80763E 04	0.12061E-02	0.455E-04	77.					
22	211.1	0.20248E 07	43.09	0.81102E 04	0.12038E-02	0.461E-04	77.					
23	213.7	0.20529E 07	43.07	0.81437E 04	0.11802E-02	0.450E-04	77.					
24	216.3	0.20811E 07	43.18	0.81770E 04	0.11921E-02	0.464E-04	77.					
25	218.9	0.21093E 07	43.11	0.82105E 04	0.11939E-02	0.458E-04	77.					
26	221.6	0.21374E 07	43.03	0.82446E 04	0.12354E-02	0.474E-04	77.					
27	224.2	0.21655E 07	42.82	0.82803E 04	0.13043E-02	0.483E-04	77.					
28	226.8	0.21935E 07	43.09	0.83152E 04	0.11748E-02	0.462E-04	77.					
29	229.4	0.22216E 07	42.94	0.83483E 04	0.11810E-02	0.442E-04	77.					
30	232.0	0.22497E 07	43.18	0.83822E 04	0.12367E-02	0.479E-04	77.					
31	234.6	0.22777E 07	43.18	0.84168E 04	0.12255E-02	0.472E-04	77.					
32	237.3	0.23059E 07	42.99	0.84516E 04	0.12455E-02	0.473E-04	77.					
33	239.9	0.23341E 07	42.95	0.84867E 04	0.12540E-02	0.480E-04	77.					
34	242.5	0.23622E 07	42.73	0.85216E 04	0.12330E-02	0.459E-04	77.					
35	245.1	0.23903E 07	42.86	0.85568E 04	0.12718E-02	0.501E-04	77.					
36	247.8	0.24184E 07	42.56	0.85922E 04	0.12476E-02	0.540E-04	77.					

UNCERTAINTY IN REX=27252. UNCERTAINTY IN F=0.05036 IN RATIO

RUN 080174-1 *** DISCRETE HOLE RIG *** NAS-3-14336 STANTON NUMBER DATA

*** 2700STEP40 M=0.4 TH=0 P/D=5 ***

RUN 080174-2 *** DISCRETE HOLE RIG *** NAS-3-14336 STANTON NUMBER DATA

*** 2700STEP40 M=0.4 TH=1 P/D=5 ***

LINEAR SUPERPOSITION IS APPLIED TO STANTON NUMBER DATA FROM
RUN NUMBERS 080174-1 AND 080174-2 TO OBTAIN STANTON NUMBER DATA AT TH=0 AND TH=1

PLATE	REXCOL	RE DEL2	ST(TH=0)	REXHOT	RE DEL2	ST(TH=1)	ETA	STCR	F-COL	STHR	F-HOT	LOGB
1	1144127.0	99.3	0.003602	1130962.0	89.3	0.003277	UUUUJ	1.028	0.0000	0.936	0.0000	0.936
2	1199266.0	285.1	0.003136	1185467.0	250.6	0.002640	0.158	0.825	0.0135	0.943	0.0124	2.548
3	1254405.0	454.2	0.002997	1239971.0	1057.3	0.002139	0.286	0.883	0.0129	0.812	0.0118	2.394
4	1309544.0	616.3	0.002885	1294475.0	1808.9	0.001790	0.380	0.915	0.0133	0.709	0.0121	2.334
5	1364682.0	772.2	0.002770	1348979.0	2559.3	0.001623	0.414	0.929	0.0129	0.663	0.0119	2.291
6	1419821.0	924.1	0.002740	1403484.0	3290.8	0.001475	0.462	0.960	0.0131	0.619	0.0122	2.293
7	1474960.0	1074.7	0.002722	1457988.0	4031.6	0.001392	0.489	0.989	0.0129	0.597	0.0120	2.277
8	1530098.0	1223.5	0.002675	1512492.0	4763.4	0.001384	0.483	1.004	0.0132	0.605	0.0118	2.284
9	1585237.0	1369.7	0.002626	1566996.0	5477.4	0.001309	0.501	1.012	0.0130	0.582	0.0118	2.283
10	1640376.0	1514.3	0.002623	1621500.0	6191.3	0.001206	0.540	1.036	0.0129	0.545	0.0117	2.231
11	1695514.0	1658.0	0.002588	1676005.0	6892.4	0.001101	0.575	1.045	0.0129	0.504	0.0123	2.258
12	1750653.0	1797.0	0.002453	1730509.0	7622.3	0.001039	0.576	1.010	0.0128	0.482	0.0119	2.193
13	1792559.0	1899.3	0.002445	1771932.0	8314.1	0.000984	0.598	1.021		0.461		
14	1820955.0	1966.9	0.002310	1800002.0	8342.4	0.001030	0.554	0.973		0.486		
15	1849351.0	2031.8	0.002252	1828072.0	8371.6	0.001045	0.536	0.957		0.496		
16	1877885.0	2095.0	0.002193	1856277.0	8401.1	0.001052	0.520	0.940		0.502		
17	1906420.0	2156.6	0.002145	1884483.0	8430.8	0.001061	0.505	0.927		0.509		
18	1934816.0	2217.2	0.002114	1912553.0	8460.5	0.001052	0.502	0.920		0.507		
19	1963213.0	2276.4	0.002053	1940623.0	8489.9	0.001041	0.493	0.900		0.504		
20	1991609.0	2334.6	0.002038	1968692.0	8519.1	0.001037	0.491	0.900		0.505		
21	2020006.0	2392.0	0.001958	1996762.0	8548.3	0.001045	0.477	0.889		0.511		
22	2048402.0	2448.0	0.001945	2024832.0	8577.8	0.001053	0.459	0.871		0.519		
23	2076799.0	2502.8	0.001906	2052902.0	8607.1	0.001032	0.459	0.859		0.510		
24	2105332.0	2557.1	0.001917	2081107.0	8636.3	0.001044	0.455	0.869		0.518		
25	2133867.0	2611.8	0.001929	2109313.0	8665.6	0.001044	0.459	0.880		0.520		
26	2162263.0	2666.3	0.001908	2137383.0	8695.7	0.001098	0.425	0.876		0.550		
27	2190660.0	2722.7	0.002058	2165452.0	8727.3	0.001151	0.441	0.950		0.578		
28	2219056.0	2777.9	0.001827	2193522.0	8758.1	0.001042	0.430	0.848		0.526		
29	2247453.0	2830.1	0.001845	2221592.0	8787.5	0.001046	0.433	0.861		0.530		
30	2275849.0	2882.7	0.001858	2249662.0	8817.8	0.001110	0.403	0.872		0.565		
31	2304246.0	2935.5	0.001850	2277732.0	8848.8	0.001098	0.406	0.873		0.561		
32	2332780.0	2987.8	0.001831	2305937.0	8880.0	0.001126	0.385	0.868		0.577		
33	2361314.0	3039.9	0.001840	2334143.0	8911.8	0.001135	0.383	0.877		0.584		
34	2389710.0	3092.1	0.001828	2362213.0	8943.4	0.001112	0.392	0.876		0.574		
35	2418107.0	3144.2	0.001837	2390282.0	8975.2	0.001157	0.370	0.884		0.599		
36	2446503.0	3195.8	0.001792	2418352.0	9007.5	0.001137	0.366	0.866		0.591		

STANTON NUMBER RATIO BASED ON ST*PR**0.4=0.0295*REX**(-.2)*(1.-(XI/(X-XVO))**0.9)**(-1./9.)

STANTON NUMBER RATIO FOR TH=1 IS CONVERTED TO COMPARABLE TRANSPIRATION VALUE
USING ALOG(1 + B)/B EXPRESSION IN THE BLOWN SECTION

RUN 080574 *** DISCRETE HOLE RIG *** NAS-3-14336 STANTON NUMBER DATA

TADB= 27.67 DEG C   UINF= 17.12 M/S   TINF= 27.54 DEG C
RHO= 1.168 KG/M3   VISC= 0.15699E-04 M2/S   XVO= 22.4 CM
CP= 1015. J/KGK   PR= 0.716

*** 2700STEP60 M=0.6 TH=0 P/D=5 ***

PLATE	X	REX	TO	REENTH	STANTON NO	DST	DREEN	M	F	T2	THETA	DTH
1	127.8	0.11497E 07	39.39	0.95295E 02	0.34398E-02	0.712E-04	2.					
2	132.8	0.12051E 07	39.37	0.27748E 03	0.31364E-02	0.689E-04	14.	0.58	0.0189	28.26	0.060	0.026
3	137.9	0.12605E 07	39.37	0.51479E 03	0.31420E-02	0.689E-04	24.	0.58	0.0188	28.41	0.073	0.026
4	143.0	0.13159E 07	39.39	0.76200E 03	0.30325E-02	0.680E-04	31.	0.57	0.0184	28.41	0.073	0.026
5	148.1	0.13713E 07	39.39	0.10006E 04	0.28998E-02	0.670E-04	36.	0.56	0.0181	28.38	0.070	0.026
6	153.2	0.14267E 07	39.39	0.12291E 04	0.28067E-02	0.663E-04	41.	0.58	0.0189	28.46	0.077	0.026
7	158.2	0.14821E 07	39.41	0.14655E 04	0.28003E-02	0.661E-04	45.	0.59	0.0189	28.59	0.088	0.026
8	163.3	0.15375E 07	39.39	0.17120E 04	0.27594E-02	0.659E-04	49.	0.58	0.0189	28.65	0.093	0.026
9	168.4	0.15929E 07	39.39	0.19611E 04	0.27087E-02	0.656E-04	53.	0.57	0.0186	28.72	0.100	0.026
10	173.5	0.16484E 07	39.39	0.22142E 04	0.27237E-02	0.657E-04	56.	0.57	0.0185	28.68	0.096	0.026
11	178.6	0.17038E 07	39.37	0.24621E 04	0.26818E-02	0.655E-04	60.	0.57	0.0186	28.90	0.115	0.026
12	183.6	0.17592E 07	39.39	0.27276E 04	0.26299E-02	0.650E-04	63.	0.57	0.0186	28.87	0.112	0.026
13	187.5	0.18013E 07	38.89	0.29529E 04	0.25950E-02	0.900E-04	64.					
14	190.1	0.18298E 07	38.95	0.30241E 04	0.23908E-02	0.866E-04	64.					
15	192.7	0.18583E 07	39.29	0.30918E 04	0.23442E-02	0.855E-04	64.					
16	195.4	0.18870E 07	39.37	0.31575E 04	0.22582E-02	0.816E-04	64.					
17	198.0	0.19157E 07	39.46	0.32211E 04	0.21968E-02	0.799E-04	64.					
18	200.6	0.19442E 07	39.48	0.32832E 04	0.21500E-02	0.782E-04	64.					
19	203.2	0.19728E 07	39.50	0.33437E 04	0.20806E-02	0.752E-04	64.					
20	205.8	0.20013E 07	39.62	0.34028E 04	0.20593E-02	0.750E-04	64.					
21	208.5	0.20298E 07	39.60	0.34610E 04	0.20161E-02	0.731E-04	64.					
22	211.1	0.20584E 07	39.69	0.35179E 04	0.19665E-02	0.727E-04	64.					
23	213.7	0.20869E 07	39.67	0.35732E 04	0.19047E-02	0.699E-04	64.					
24	216.3	0.21156E 07	39.81	0.36277E 04	0.19103E-02	0.712E-04	64.					
25	218.9	0.21442E 07	39.79	0.36818E 04	0.18755E-02	0.692E-04	64.					
26	221.6	0.21728E 07	39.82	0.37354E 04	0.18801E-02	0.708E-04	64.					
27	224.2	0.22013E 07	39.48	0.37909E 04	0.20045E-02	0.715E-04	64.					
28	226.8	0.22298E 07	39.92	0.38450E 04	0.17813E-02	0.683E-04	64.					
29	229.4	0.22584E 07	39.73	0.38958E 04	0.17755E-02	0.643E-04	64.					
30	232.0	0.22869E 07	40.11	0.39466E 04	0.17793E-02	0.676E-04	64.					
31	234.6	0.23155E 07	40.11	0.39970E 04	0.17493E-02	0.656E-04	65.					
32	237.3	0.23441E 07	39.98	0.40468E 04	0.17368E-02	0.649E-04	65.					
33	239.9	0.23728E 07	39.94	0.40963E 04	0.17321E-02	0.652E-04	65.					
34	242.5	0.24013E 07	39.71	0.41455E 04	0.17139E-02	0.627E-04	65.					
35	245.1	0.24299E 07	39.92	0.41946E 04	0.17174E-02	0.667E-04	65.					
36	247.8	0.24584E 07	39.65	0.42429E 04	0.16664E-02	0.711E-04	65.					

UNCERTAINTY IN REX=27703.   UNCERTAINTY IN F=0.05034 IN RATIO

RUN 081174-1 *** DISCRETE HOLE RIG *** NAS-3-14336 STANTON NUMBER DATA

TADB= 26.90 DEG C UINF= 17.05 M/S TINF= 26.77 DEG C
RHO= 1.167 KG/M3 VISC= 0.15669E-04 M2/S XVO= 22.4 CM
CP= 1015. J/KGK PR= 0.717

*** 2700STEP60 M=0.6 TH=1 P/C*5 ***

PLATE	X	REX	TO	REENTH	STANTON NO	DST	DREEN	M	F	T2	THETA	DTH
1	127.8	0.11473E 07	40.70	0.92461E 02	0.33445E-02	0.609E-04	2.					
2	132.8	0.12026E 07	40.68	0.26118E 03	0.27586E-02	0.569E-04	23.	0.53	0.0173	38.23	0.824	0.022
3	137.9	0.12579E 07	40.68	0.11936E 04	0.25335E-02	0.555E-04	39.	0.53	0.0171	38.56	0.848	0.022
4	143.0	0.13132E 07	40.70	0.21262E 04	0.21633E-02	0.533E-04	51.	0.53	0.0171	39.25	0.896	0.022
5	148.1	0.13684E 07	40.70	0.30887E 04	0.19505E-02	0.522E-04	61.	0.52	0.0168	39.29	0.899	0.022
6	153.2	0.14237E 07	40.70	0.40281E 04	0.18043E-02	0.515E-04	70.	0.52	0.0170	39.49	0.913	0.022
7	158.2	0.14790E 07	40.72	0.49838E 04	0.17563E-02	0.512E-04	78.	0.53	0.0172	39.64	0.922	0.022
8	163.3	0.15343E 07	40.70	0.59537E 04	0.16617E-02	0.508E-04	85.	0.53	0.0172	40.02	0.951	0.022
9	168.4	0.15896E 07	40.70	0.69457E 04	0.15815E-02	0.505E-04	92.	0.51	0.0166	39.80	0.935	0.022
10	173.5	0.16449E 07	40.68	0.78896E 04	0.15156E-02	0.503E-04	98.	0.51	0.0164	39.36	0.905	0.022
11	178.6	0.17002E 07	40.68	0.87937E 04	0.14745E-02	0.501E-04	103.	0.52	0.0168	39.22	0.895	0.022
12	183.6	0.17555E 07	40.68	0.97040E 04	0.14402E-02	0.500E-04	108.	0.52	0.0169	38.91	0.873	0.022
13	187.5	0.17975E 07	40.26	0.10579E 05	0.14473E-02	0.523E-04	111.					
14	190.1	0.18260E 07	40.24	0.10620E 05	0.13952E-02	0.534E-04	111.					
15	192.7	0.18545E 07	40.55	0.10660E 05	0.13762E-02	0.530E-04	111.					
16	195.4	0.18831E 07	40.58	0.10698E 05	0.13485E-02	0.513E-04	111.					
17	198.0	0.19117E 07	40.64	0.10736E 05	0.13185E-02	0.506E-04	111.					
18	200.6	0.19402E 07	40.64	0.10774E 05	0.12957E-02	0.499E-04	111.					
19	203.2	0.19686E 07	40.64	0.10810E 05	0.12602E-02	0.479E-04	111.					
20	205.8	0.19971E 07	40.77	0.10846E 05	0.12438E-02	0.479E-04	111.					
21	208.5	0.20256E 07	40.77	0.10881E 05	0.12089E-02	0.466E-04	111.					
22	211.1	0.20541E 07	40.81	0.10915E 05	0.11891E-02	0.469E-04	111.					
23	213.7	0.20825E 07	40.79	0.10948E 05	0.11629E-02	0.456E-04	111.					
24	216.3	0.21111E 07	40.93	0.10982E 05	0.11586E-02	0.466E-04	111.					
25	218.9	0.21398E 07	40.89	0.11014E 05	0.11534E-02	0.456E-04	111.					
26	221.6	0.21682E 07	40.89	0.11048E 05	0.11650E-02	0.466E-04	111.					
27	224.2	0.21967E 07	40.68	0.11081E 05	0.12120E-02	0.465E-04	111.					
28	226.8	0.22252E 07	40.98	0.11114E 05	0.11082E-02	0.454E-04	111.					
29	229.4	0.22537E 07	40.85	0.11146E 05	0.10917E-02	0.426E-04	111.					
30	232.0	0.22821E 07	41.12	0.11177E 05	0.11172E-02	0.456E-04	111.					
31	234.6	0.23106E 07	41.10	0.11209E 05	0.11051E-02	0.444E-04	111.					
32	237.3	0.23392E 07	40.98	0.11240E 05	0.11001E-02	0.443E-04	111.					
33	239.9	0.23678E 07	40.94	0.11272E 05	0.11097E-02	0.446E-04	111.					
34	242.5	0.23963E 07	40.76	0.11303E 05	0.10909E-02	0.427E-04	111.					
35	245.1	0.24248E 07	40.89	0.11335E 05	0.11050E-02	0.462E-04	111.					
36	247.8	0.24533E 07	40.64	0.11366E 05	0.10664E-02	0.491E-04	111.					

UNCERTAINTY IN REX=27645. UNCERTAINTY IN F=0.05034 IN RATIO

RUN 080574 *** DISCRETE HOLE RIG *** NAS-3-14336 STANTON NUMBER DATA

*** 2700STEP60 M=0.6 TH=0 P/D=5 ***

RUN 081174-1 *** DISCRETE HOLE RIG *** NAS-3-14336 STANTON NUMBER DATA

*** 2700STEP60 M=0.6 TH=1 P/D=5 ***

LINEAR SUPERPOSITION IS APPLIED TO STANTON NUMBER DATA FROM
RUN NUMBERS 080574 AND 081174-1 TO OBTAIN STANTON NUMBER DATA AT TH=0 AND TH=1

PLATE	REXCOL	RE DEL2	ST(TH=0)	REXHOT	RE DEL2	ST(TH=1)	ETA	STCR	F-COL	STHR	F-HOT	LOGB
1	1149692.0	95.3	0.003440	1147284.0	92.5	0.003345	UUUUU	0.982	0.0000	0.955	0.0000	0.955
2	1205099.0	278.3	0.003166	1202574.0	258.8	0.002671	0.156	0.834	0.0189	0.958	0.0173	3.079
3	1260506.0	454.5	0.003195	1257865.0	1353.1	0.002404	0.248	0.942	0.0188	0.916	0.0171	3.115
4	1315913.0	629.3	0.003112	1313156.0	2422.4	0.002024	0.350	0.989	0.0184	0.804	0.0171	3.027
5	1371320.0	798.1	0.002982	1368447.0	3476.0	0.001833	0.385	1.002	0.0181	0.751	0.0168	2.972
6	1426727.0	960.9	0.002896	1423738.0	4503.0	0.001691	0.416	1.016	0.0189	0.712	0.0170	2.975
7	1482134.0	1121.6	0.002904	1479028.0	5534.1	0.001654	0.431	1.057	0.0189	0.711	0.0172	3.037
8	1537540.0	1281.7	0.002877	1534319.0	6572.5	0.001580	0.451	1.081	0.0189	0.693	0.0172	3.043
9	1592947.0	1440.0	0.002837	1589610.0	7606.6	0.001506	0.469	1.095	0.0186	0.672	0.0166	2.978
10	1648354.0	1598.1	0.002867	1644901.0	8604.4	0.001399	0.512	1.134	0.0185	0.634	0.0164	2.923
11	1703761.0	1756.2	0.002842	1700192.0	9586.9	0.001323	0.534	1.149	0.0186	0.608	0.0168	2.947
12	1759168.0	1912.7	$\boxed{0.002805}$	1755482.0	10585.4	0.001261	0.550	1.157	0.0186	0.587	0.0169	2.950
13	1801277.0	2029.9	0.002764	1797503.0	11572.1	0.001274	0.539	1.156		0.599		
14	1829812.0	2105.6	0.002538	1825978.0	11608.0	0.001245	0.509	1.071		0.589		
15	1858346.0	2177.4	0.002487	1854453.0	11643.3	0.001230	0.505	1.058		0.585		
16	1887019.0	2247.1	0.002392	1883066.0	11678.1	0.001211	0.494	1.027		0.580		
17	1915692.0	2314.5	0.002326	1911679.0	11712.3	0.001186	0.490	1.006		0.571		
18	1944227.0	2380.2	0.002276	1940153.0	11745.9	0.001167	0.487	0.992		0.565		
19	1972761.0	2444.2	0.002202	1968628.0	11778.7	0.001137	0.484	0.967		0.553		
20	2001296.0	2506.7	0.002179	1997103.0	11810.9	0.001121	0.486	0.964		0.548		
21	2029831.0	2568.4	0.002135	2025578.0	11842.4	0.001087	0.491	0.951		0.534		
22	2058365.0	2628.6	0.002081	2054053.0	11873.1	0.001072	0.485	0.933		0.529		
23	2086900.0	2687.1	0.002014	2082527.0	11903.4	0.001051	0.478	0.909		0.521		
24	2115573.0	2744.7	0.002021	2111140.0	11933.3	0.001045	0.483	0.918		0.521		
25	2144246.0	2801.9	0.001982	2139753.0	11963.1	0.001045	0.473	0.906		0.522		
26	2172780.0	2858.6	0.001986	2168228.0	11993.0	0.001057	0.468	0.913		0.531		
27	2201315.0	2917.2	0.002121	2196703.0	12023.7	0.001093	0.485	0.981		0.551		
28	2229849.0	2974.4	0.001880	2225177.0	12053.6	0.001007	0.465	0.874		0.510		
29	2258384.0	3028.1	0.001876	2253652.0	12082.1	0.000989	0.473	0.877		0.503		
30	2286919.0	3081.7	0.001877	2282127.0	12110.6	0.001017	0.458	0.882		0.519		
31	2315453.0	3134.3	0.001844	2310602.0	12139.5	0.001008	0.453	0.871		0.517		
32	2344126.0	3187.3	0.001831	2339215.0	12168.2	0.001004	0.451	0.869		0.517		
33	2372799.0	3239.5	0.001824	2367828.0	12197.0	0.001016	0.443	0.870		0.525		
34	2401334.0	3291.4	0.001806	2396302.0	12225.7	0.000997	0.448	0.866		0.517		
35	2429868.0	3343.0	0.001808	2424777.0	12254.3	0.001013	0.440	0.871		0.527		
36	2458403.0	3393.9	0.001755	2453252.0	12282.7	0.000976	0.444	0.849		0.509		

STANTON NUMBER RATIO BASED ON ST*PR**0.4=0.0295*REX**(-.2)*(1.-(XI/(X-XVO))**0.9)**(-1./9.)

STANTON NUMBER RATIO FOR TH=1 IS CONVERTED TO COMPARABLE TRANSPIRATION VALUE
USING ALOG(1 + B)/B EXPRESSION IN THE BLOWN SECTION

RUN 081574-1 *** DISCRETE HOLE RIG *** NAS-3-14336 STANTON NUMBER DATA

TADB= 26.88 DEG C UINF= 17.12 M/S TINF= 26.75 DEG C
RHO= 1.166 KG/M3 VISC= 0.15689E-04 M2/S XVO= 22.4 CM
CP= 1015. J/KGK PR= 0.717

*** 2700STEP75 M=0.75 TH=0 P/D=5 ***

PLATE	X	REX	TO	REENTH	STANTON NO	DST	DREEN	M	F	T2	THETA	DTH
1	127.8	0.11504E 07	37.22	0.99736E 02	0.35979E-02	0.815E-04	2.					
2	132.8	0.12058E 07	37.16	0.28746E 03	0.31739E-02	0.781E-04	21.	0.77	0.0250	26.72	-0.003	0.030
3	137.9	0.12613E 07	37.22	0.46340E 03	0.33393E-02	0.791E-04	36.	0.76	0.0245	26.90	0.014	0.030
4	143.0	0.13167E 07	37.24	0.66733E 03	0.33265E-02	0.789E-04	46.	0.77	0.0250	26.92	0.016	0.030
5	148.1	0.13722E 07	37.24	0.86954E 03	0.31859E-02	0.777E-04	54.	0.76	0.0246	26.89	0.013	0.030
6	153.2	0.14276E 07	37.22	0.10618E 04	0.31288E-02	0.773E-04	62.	0.76	0.0247	26.91	0.014	0.030
7	158.2	0.14831E 07	37.22	0.12546E 04	0.31096E-02	0.772E-04	68.	0.76	0.0246	27.02	0.025	0.030
8	163.3	0.15385E 07	37.24	0.14591E 04	0.30245E-02	0.763E-04	74.	0.77	0.0251	27.07	0.030	0.029
9	168.4	0.15939E 07	37.22	0.16691E 04	0.30375E-02	0.766E-04	79.	0.76	0.0246	27.02	0.025	0.030
10	173.5	0.16494E 07	37.24	0.18718E 04	0.30270E-02	0.763E-04	84.	0.76	0.0247	26.97	0.020	0.030
11	178.6	0.17048E 07	37.20	0.20681E 04	0.30427E-02	0.767E-04	89.	0.75	0.0244	27.01	0.025	0.030
12	183.6	0.17603E 07	37.24	0.22668E 04	0.29212E-02	0.755E-04	94.	0.77	0.0251	26.99	0.023	0.029
13	187.5	0.18024E 07	36.46	0.24212E 04	0.29245E-02	0.102E-03	96.					
14	190.1	0.18310E 07	36.42	0.25023E 04	0.27485E-02	0.101E-03	96.					
15	192.7	0.18595E 07	36.80	0.25795E 04	0.26504E-02	0.984E-04	96.					
16	195.4	0.18882E 07	36.88	0.26539E 04	0.25576E-02	0.940E-04	96.					
17	198.0	0.19169E 07	36.95	0.27262E 04	0.24965E-02	0.922E-04	96.					
18	200.6	0.19454E 07	36.95	0.27969E 04	0.24527E-02	0.905E-04	96.					
19	203.2	0.19740E 07	36.97	0.28657E 04	0.23623E-02	0.867E-04	96.					
20	205.8	0.20025E 07	37.07	0.29333E 04	0.23613E-02	0.871E-04	96.					
21	208.5	0.20311E 07	37.05	0.29997E 04	0.22860E-02	0.841E-04	96.					
22	211.1	0.20596E 07	37.16	0.30641E 04	0.22222E-02	0.836E-04	96.					
23	213.7	0.20882E 07	37.11	0.31272E 04	0.21890E-02	0.812E-04	96.					
24	216.3	0.21169E 07	37.26	0.31898E 04	0.21898E-02	0.828E-04	96.					
25	218.9	0.21456E 07	37.24	0.32519E 04	0.21542E-02	0.806E-04	96.					
26	221.6	0.21741E 07	37.26	0.33132E 04	0.21409E-02	0.816E-04	96.					
27	224.2	0.22027E 07	36.93	0.33763E 04	0.22711E-02	0.825E-04	96.					
28	226.8	0.22312E 07	37.39	0.34377E 04	0.20226E-02	0.786E-04	96.					
29	229.4	0.22598E 07	37.22	0.34953E 04	0.20090E-02	0.739E-04	96.					
30	232.0	0.22883E 07	37.58	0.35527E 04	0.20086E-02	0.772E-04	96.					
31	234.6	0.23169E 07	37.58	0.36095E 04	0.19604E-02	0.744E-04	96.					
32	237.3	0.23456E 07	37.49	0.36651E 04	0.19318E-02	0.734E-04	96.					
33	239.9	0.23743E 07	37.47	0.37202E 04	0.19223E-02	0.736E-04	96.					
34	242.5	0.24028E 07	37.24	0.37747E 04	0.18932E-02	0.705E-04	96.					
35	245.1	0.24314E 07	37.45	0.38285E 04	0.18710E-02	0.740E-04	96.					
36	247.8	0.24599E 07	37.22	0.38811E 04	0.18061E-02	0.779E-04	96.					

UNCERTAINTY IN REX=27721. UNCERTAINTY IN F=0.05034 IN RATIO

RUN 081574-2 *** DISCRETE HOLE RIG *** NAS-3-14336 STANTON NUMBER DATA

TADB= 27.84 DEG C UINF= 17.14 M/S TINF= 27.72 DEG C
RHO= 1.162 KG/M3 VISC= 0.15776E-04 M2/S XVO= 22.4 CM
CP= 1015. J/KGK PR= 0.717

*** 2700STEP75 M=0.75 TH=1 P/D=5 ***

PLATE	X	REX	TO	REENTH	STANTON NO	DST	DREEN	M	F	T2	THETA	DTH
1	127.8	0.11453E 07	40.28	0.92838E 02	0.33639E-02	0.670E-04	2.					
2	132.8	0.12005E 07	40.26	0.26297E 03	0.28007E-02	0.629E-04	35.	0.71	0.0231	39.98	0.978	0.025
3	137.9	0.12557E 07	40.28	0.16658E 04	0.28338E-02	0.630E-04	61.	0.70	0.0227	39.95	0.974	0.025
4	143.0	0.13109E 07	40.28	0.30314E 04	0.25184E-02	0.609E-04	78.	0.70	0.0228	40.33	1.004	0.025
5	148.1	0.13661E 07	40.28	0.44256E 04	0.22530E-02	0.593E-04	93.	0.71	0.0230	39.97	0.975	0.025
6	153.2	0.14213E 07	40.26	0.57862E 04	0.21482E-02	0.587E-04	105.	0.71	0.0230	39.78	0.962	0.025
7	158.2	0.14765E 07	40.28	0.71236E 04	0.20589E-02	0.582E-04	116.	0.71	0.0229	39.75	0.958	0.025
8	163.3	0.15317E 07	40.26	0.84462E 04	0.20255E-02	0.581E-04	126.	0.70	0.0227	39.98	0.978	0.025
9	168.4	0.15869E 07	40.28	0.97825E 04	0.19362E-02	0.575E-04	135.	0.69	0.0223	39.36	0.927	0.024
10	173.5	0.16421E 07	40.26	0.11030E 05	0.19066E-02	0.574E-04	142.	0.70	0.0226	38.69	0.875	0.024
11	178.6	0.16973E 07	40.30	0.12222E 05	0.18412E-02	0.569E-04	148.	0.70	0.0226	37.67	0.791	0.024
12	183.6	0.17525E 07	40.30	0.13308E 05	0.17958E-02	0.567E-04	154.	0.72	0.0233	37.21	0.755	0.024
13	187.5	0.17944E 07	39.44	0.14352E 05	0.16988E-02	0.603E-04	157.					
14	190.1	0.18228E 07	39.31	0.14399E 05	0.16490E-02	0.628E-04	157.					
15	192.7	0.18513E 07	39.64	0.14446E 05	0.15942E-02	0.618E-04	157.					
16	195.4	0.18798E 07	39.69	0.14490E 05	0.15393E-02	0.591E-04	157.					
17	198.0	0.19084E 07	39.75	0.14533E 05	0.15001E-02	0.580E-04	157.					
18	200.6	0.19368E 07	39.77	0.14575E 05	0.14582E-02	0.568E-04	157.					
19	203.2	0.19653E 07	39.79	0.14616E 05	0.14061E-02	0.541E-04	157.					
20	205.8	0.19937E 07	39.94	0.14656E 05	0.13811E-02	0.539E-04	157.					
21	208.5	0.20221E 07	39.92	0.14695E 05	0.13327E-02	0.522E-04	157.					
22	211.1	0.20505E 07	39.94	0.14732E 05	0.13151E-02	0.525E-04	157.					
23	213.7	0.20790E 07	39.94	0.14769E 05	0.12753E-02	0.509E-04	157.					
24	216.3	0.21075E 07	40.09	0.14805E 05	0.12554E-02	0.515E-04	157.					
25	218.9	0.21361E 07	40.05	0.14840E 05	0.12274E-02	0.499E-04	157.					
26	221.6	0.21645E 07	40.00	0.14876E 05	0.12644E-02	0.514E-04	157.					
27	224.2	0.21929E 07	39.82	0.14912E 05	0.12706E-02	0.503E-04	157.					
28	226.8	0.22214E 07	40.15	0.14947E 05	0.11654E-02	0.493E-04	157.					
29	229.4	0.22498E 07	40.00	0.14980E 05	0.11728E-02	0.467E-04	157.					
30	232.0	0.22782E 07	40.28	0.15013E 05	0.11681E-02	0.492E-04	157.					
31	234.6	0.23066E 07	40.28	0.15046E 05	0.11438E-02	0.476E-04	157.					
32	237.3	0.23352E 07	40.17	0.15078E 05	0.11338E-02	0.472E-04	157.					
33	239.9	0.23638E 07	40.15	0.15111E 05	0.11349E-02	0.473E-04	157.					
34	242.5	0.23922E 07	39.98	0.15143E 05	0.11053E-02	0.450E-04	157.					
35	245.1	0.24206E 07	40.13	0.15174E 05	0.11046E-02	0.484E-04	157.					
36	247.8	0.24490E 07	39.92	0.15205E 05	0.10650E-02	0.507E-04	157.					

UNCERTAINTY IN REX=2759. UNCERTAINTY IN F=0.05034 IN RATIO

RUN 081574-1 *** DISCRETE HOLE RIG *** NAS-3-14336 STANTON NUMBER DATA

*** 2700STEP75 M=0.75 TH=0 P/D=5 ***

RUN 081574-2 *** DISCRETE HOLE RIG *** NAS-3-14336 STANTON NUMBER DATA

*** 2700STEP75 M=0.75 TH=1 P/D=5 ***

LINEAR SUPERPOSITION IS APPLIED TO STANTON NUMBER DATA FROM
RUN NUMBERS 081574-1 AND 081574-2 TO OBTAIN STANTON NUMBER DATA AT TH=0 AND TH=1

PLATE	REXCOL	RE DEL2	ST(TH=0)	REXHOT	RE DEL2	ST(TH=1)	ETA	STCR	F-COL	STHR	F-HOT	LOGB
1	1150408.0	99.7	0.003598	1145315.0	92.8	0.003364	ULUUU	1.027	0.0000	0.960	0.0000	0.960
2	1205849.0	287.4	0.003173	1200511.0	262.7	0.002792	0.120	0.836	0.0250	1.001	0.0231	3.718
3	1261291.0	468.0	0.003342	1255707.0	1693.2	0.002821	0.156	0.986	0.0245	1.075	0.0227	3.921
4	1316732.0	653.2	0.003339	1310903.0	3090.8	0.002509	0.248	1.061	0.0250	0.996	0.0228	3.914
5	1372173.0	834.5	0.003199	1366099.0	4479.4	0.002243	0.299	1.074	0.0246	0.919	0.0230	3.896
6	1427615.0	1010.3	0.003143	1421295.0	5870.6	0.002116	0.327	1.103	0.0247	0.890	0.0230	3.911
7	1483056.0	1184.2	0.003132	1476491.0	7254.3	0.002014	0.357	1.140	0.0246	0.866	0.0229	3.914
8	1538497.0	1355.7	0.003054	1531687.0	8628.2	0.001991	0.348	1.147	0.0251	0.873	0.0227	3.957
9	1593939.0	1525.5	0.003071	1586883.0	9990.0	0.001879	0.388	1.186	0.0246	0.838	0.0223	3.894
10	1649380.0	1695.3	0.003056	1642079.0	11322.0	0.001780	0.418	1.209	0.0247	0.806	0.0226	3.907
11	1704822.0	1865.3	0.003076	1697275.0	12659.8	0.001593	0.482	1.244	0.0244	0.732	0.0226	3.816
12	1760263.0	2032.5	0.002957	1752471.0	13990.5	0.001454	0.508	1.219	0.0251	0.677	0.0233	3.826
13	1802398.0	2156.9	0.002963	1794420.0	15334.8	0.001327	0.552	1.239		0.624		
14	1830951.0	2239.0	0.002783	1822846.0	15372.4	0.001315	0.527	1.174		0.622		
15	1859503.0	2317.1	0.002684	1851272.0	15409.2	0.001274	0.525	1.142		0.606		
16	1888194.0	2392.5	0.002590	1879835.0	15444.8	0.001230	0.525	1.111		0.588		
17	1916885.0	2465.7	0.002528	1908399.0	15479.4	0.001198	0.526	1.094		0.576		
18	1945437.0	2537.3	0.002484	1936825.0	15512.9	0.001156	0.534	1.083		0.559		
19	1973989.0	2607.0	0.002393	1965251.0	15545.2	0.001116	0.534	1.051		0.542		
20	2002541.0	2675.4	0.002392	1993677.0	15576.5	0.001084	0.547	1.058		0.529		
21	2031094.0	2742.7	0.002316	2022103.0	15606.8	0.001043	0.550	1.032		0.512		
22	2059646.0	2808.0	0.002251	2050529.0	15636.4	0.001040	0.538	1.009		0.513		
23	2088199.0	2871.9	0.002218	2078955.0	15665.4	0.000998	0.550	1.001		0.494		
24	2116889.0	2935.3	0.002220	2107518.0	15693.5	0.000972	0.562	1.008		0.484		
25	2145580.0	2998.3	0.002184	2136082.0	15720.8	0.000946	0.567	0.998		0.473		
26	2174133.0	3060.5	0.002169	2164508.0	15748.4	0.000998	0.540	0.997		0.501		
27	2202685.0	3124.4	0.002303	2192934.0	15776.4	0.000967	0.580	1.065		0.488		
28	2231237.0	3186.6	0.002050	2221360.0	15803.0	0.000905	0.558	0.953		0.458		
29	2259790.0	3245.0	0.002036	2249786.0	15829.0	0.000919	0.549	0.952		0.467		
30	2288342.0	3303.2	0.002035	2278212.0	15855.1	0.000913	0.551	0.957		0.466		
31	2316894.0	3360.6	0.001986	2306638.0	15880.8	0.000896	0.549	0.938		0.459		
32	2345585.0	3417.0	0.001957	2335202.0	15906.3	0.000892	0.544	0.929		0.458		
33	2374276.0	3472.8	0.001947	2363766.0	15931.7	0.000896	0.540	0.929		0.462		
34	2402828.0	3528.1	0.001918	2392192.0	15956.8	0.000866	0.548	0.920		0.449		
35	2431380.0	3582.6	0.001895	2420617.0	15981.5	0.000872	0.540	0.913		0.453		
36	2459933.0	3635.8	0.001830	2449043.0	16005.9	0.000840	0.541	0.886		0.438		

STANTON NUMBER RATIO BASED ON ST*PR**0.4=0.0295*REX**(-.2)*(1.-(XI/(X-XVO))**0.9)**(-1./9.)

STANTON NUMBER RATIO FOR TH=1 IS CONVERTED TO COMPARABLE TRANSPIRATION VALUE
USING ALOG(1 + B)/B EXPRESSION IN THE BLOWN SECTION

RUN 081974-1 *** DISCRETE HOLE RIG *** NAS-3-14336 STANTON NUMBER DATA

TADB= 25.27 DEG C UINF= 13.14 M/S TINF= 25.14 DEG C
RHO= 1.173 KG/M3 VISC= 0.15580E-04 M2/S XVO= 22.4 CM
CP= 1011. J/KGK PR= 0.715

*** 2700STEP90 M=0.9 TH=0 P/D=5 ***

PLATE	X	REX	TO	REENTH	STANTON NO	DST	DREEN	M	F	T2	THETA	DTH
1	127.8	0.11594E 07	36.33	0.10006E 03	0.35817E-02	0.762E-04	2.					
2	132.8	0.12153E 07	36.31	0.28926E 03	0.31907E-02	0.730E-04	24.	0.93	0.0301	25.36	0.020	0.028
3	137.9	0.12711E 07	36.33	0.50661E 03	0.33762E-02	0.745E-04	41.	0.93	0.0301	25.56	0.038	0.028
4	143.0	0.13270E 07	36.33	0.76421E 03	0.35661E-02	0.761E-04	52.	0.94	0.0303	25.54	0.036	0.028
5	148.1	0.13829E 07	36.33	0.10231E 04	0.35176E-02	0.757E-04	62.	0.93	0.0300	25.55	0.036	0.028
6	153.2	0.14388E 07	36.34	0.12760E 04	0.33505E-02	0.741E-04	70.	0.93	0.0302	25.53	0.035	0.028
7	158.2	0.14946E 07	36.34	0.15233E 04	0.33942E-02	0.745E-04	78.	0.94	0.0303	25.66	0.047	0.027
8	163.3	0.15505E 07	36.34	0.17906E 04	0.33548E-02	0.742E-04	84.	0.94	0.0303	25.68	0.048	0.027
9	168.4	0.16064E 07	36.34	0.20576E 04	0.32798E-02	0.735E-04	91.	0.93	0.0299	25.68	0.048	0.027
10	173.5	0.16623E 07	36.31	0.23226E 04	0.33021E-02	0.740E-04	96.	0.91	0.0295	25.63	0.044	0.028
11	178.6	0.17181E 07	36.31	0.25787E 04	0.32567E-02	0.736E-04	102.	0.92	0.0298	25.67	0.048	0.028
12	183.6	0.17740E 07	36.33	0.28373E 04	0.31681E-02	0.727E-04	107.	0.92	0.0298	25.62	0.043	0.028
13	187.5	0.18165E 07	35.56	0.30434E 04	0.32087E-02	0.110E-03	109.					
14	190.1	0.18453E 07	35.51	0.31336E 04	0.30504E-02	0.108E-03	109.					
15	192.7	0.18740E 07	35.96	0.32194E 04	0.29115E-02	0.105E-03	109.					
16	195.4	0.19029E 07	36.06	0.33019E 04	0.28102E-02	0.100E-03	109.					
17	198.0	0.19319E 07	36.17	0.33815E 04	0.27198E-02	0.976E-04	109.					
18	200.6	0.19606E 07	36.17	0.34592E 04	0.26757E-02	0.958E-04	109.					
19	203.2	0.19894E 07	36.19	0.35349E 04	0.25753E-02	0.918E-04	109.					
20	205.8	0.20182E 07	36.29	0.36093E 04	0.25926E-02	0.927E-04	109.					
21	208.5	0.20470E 07	36.31	0.36825E 04	0.24881E-02	0.889E-04	109.					
22	211.1	0.20757E 07	36.42	0.37536E 04	0.24452E-02	0.887E-04	109.					
23	213.7	0.21045E 07	36.40	0.38229E 04	0.23666E-02	0.852E-04	109.					
24	216.3	0.21334E 07	36.53	0.38916E 04	0.24042E-02	0.875E-04	109.					
25	218.9	0.21623E 07	36.53	0.39605E 04	0.23778E-02	0.859E-04	109.					
26	221.6	0.21911E 07	36.55	0.40287E 04	0.23543E-02	0.865E-04	110.					
27	224.2	0.22199E 07	36.21	0.40985E 04	0.24904E-02	0.874E-04	110.					
28	226.8	0.22487E 07	36.69	0.41665E 04	0.22346E-02	0.835E-04	110.					
29	229.4	0.22774E 07	36.50	0.42305E 04	0.22083E-02	0.784E-04	110.					
30	232.0	0.23062E 07	36.88	0.42945E 04	0.22328E-02	0.823E-04	110.					
31	234.6	0.23350E 07	36.92	0.43579E 04	0.21717E-02	0.795E-04	110.					
32	237.3	0.23639E 07	36.78	0.44199E 04	0.21317E-02	0.778E-04	110.					
33	239.9	0.23928E 07	36.74	0.44813E 04	0.21299E-02	0.783E-04	110.					
34	242.5	0.24216E 07	36.50	0.45420E 04	0.20792E-02	0.745E-04	110.					
35	245.1	0.24504E 07	36.72	0.46017E 04	0.20690E-02	0.783E-04	110.					
36	247.8	0.24791E 07	36.48	0.46604E 04	0.20042E-02	0.824E-04	110.					

UNCERTAINTY IN REX=27937. UNCERTAINTY IN F=0.05033 IN RATIO

RUN 081974-2 *** DISCRETE HOLE RIG *** NAS-3-14336 STANTON NUMBER DATA

TADB= 26.63 DEG C UINF= 17.05 M/S TINF= 26.51 DEG C
RHO= 1.166 KG/M3 VISC= 0.15703E-04 M2/S XVO= 22.4 CM
CP= 1013. J/KGK PR= 0.715

*** 2700STEP90 M=0.9 TH=1 P/D=5 ***

PLATE	X	REX	TO	REENTH	STANTON NO	DST	DREEN	M	F	T2	THETA	DTH
1	127.8	0.11442E 07	40.20	0.92159E 02	0.33425E-02	0.619E-04	2.					
2	132.8	0.11994E 07	40.19	0.26105E 03	0.27830E-02	0.581E-04	43.	0.85	0.0275	40.52	1.024	0.023
3	137.9	0.12545E 07	40.19	0.19703E 04	0.29599E-02	0.593E-04	74.	0.85	0.0276	40.33	1.011	0.023
4	143.0	0.13097E 07	40.19	0.36668E 04	0.28056E-02	0.583E-04	95.	0.84	0.0273	40.41	1.017	0.023
5	148.1	0.13648E 07	40.19	0.53470E 04	0.25668E-02	0.567E-04	113.	0.85	0.0274	40.29	1.007	0.023
6	153.2	0.14200E 07	40.20	0.70037E 04	0.23464E-02	0.553E-04	127.	0.85	0.0276	39.85	0.974	0.023
7	158.2	0.14751E 07	40.20	0.86169E 04	0.23251E-02	0.552E-04	140.	0.86	0.0279	39.70	0.963	0.023
8	163.3	0.15303E 07	40.22	0.10223E 05	0.22408E-02	0.546E-04	151.	0.84	0.0272	39.79	0.969	0.023
9	168.4	0.15854E 07	40.20	0.11800E 05	0.21477E-02	0.542E-04	162.	0.85	0.0276	39.55	0.953	0.022
10	173.5	0.16405E 07	40.19	0.13365E 05	0.20888E-02	0.540E-04	171.	0.84	0.0271	39.19	0.927	0.022
11	178.6	0.16957E 07	40.19	0.14863E 05	0.20024E-02	0.535E-04	180.	0.85	0.0275	38.78	0.898	0.022
12	183.6	0.17508E 07	40.19	0.16334E 05	0.19490E-02	0.532E-04	188.	0.85	0.0275	38.14	0.851	0.022
13	187.5	0.17927E 07	39.43	0.17705E 05	0.18659E-02	0.647E-04	191.					
14	190.1	0.18211E 07	39.31	0.17757E 05	0.18074E-02	0.659E-04	191.					
15	192.7	0.18495E 07	39.67	0.17808E 05	0.17504E-02	0.651E-04	191.					
16	195.4	0.18781E 07	39.75	0.17857E 05	0.16826E-02	0.620E-04	191.					
17	198.0	0.19066E 07	39.82	0.17904E 05	0.16327E-02	0.606E-04	191.					
18	200.6	0.19350E 07	39.86	0.17949E 05	0.15896E-02	0.593E-04	191.					
19	203.2	0.19634E 07	39.88	0.17994E 05	0.15238E-02	0.562E-04	191.					
20	205.8	0.19918E 07	40.03	0.18037E 05	0.15024E-02	0.561E-04	191.					
21	208.5	0.20202E 07	40.03	0.18079E 05	0.14493E-02	0.542E-04	191.					
22	211.1	0.20486E 07	40.09	0.18119E 05	0.14166E-02	0.541E-04	191.					
23	213.7	0.20770E 07	40.07	0.18159E 05	0.13730E-02	0.521E-04	191.					
24	216.3	0.21055E 07	40.22	0.18198E 05	0.13722E-02	0.532E-04	191.					
25	218.9	0.21341E 07	40.22	0.18237E 05	0.13287E-02	0.514E-04	191.					
26	221.6	0.21625E 07	40.17	0.18275E 05	0.13566E-02	0.526E-04	191.					
27	224.2	0.21909E 07	39.96	0.18314E 05	0.13822E-02	0.517E-04	191.					
28	226.8	0.22193E 07	40.32	0.18351E 05	0.12616E-02	0.505E-04	191.					
29	229.4	0.22477E 07	40.19	0.18387E 05	0.12423E-02	0.472E-04	191.					
30	232.0	0.22761E 07	40.49	0.18422E 05	0.12512E-02	0.499E-04	191.					
31	234.6	0.23045E 07	40.49	0.18458E 05	0.12284E-02	0.484E-04	191.					
32	237.3	0.23330E 07	40.38	0.18492E 05	0.12060E-02	0.476E-04	191.					
33	239.9	0.23616E 07	40.36	0.18526E 05	0.11984E-02	0.476E-04	191.					
34	242.5	0.23900E 07	40.17	0.18560E 05	0.11732E-02	0.453E-04	191.					
35	245.1	0.24184E 07	40.34	0.18593E 05	0.11668E-02	0.483E-04	191.					
36	247.8	0.24468E 07	40.13	0.18626E 05	0.11215E-02	0.504E-04	191.					

UNCERTAINTY IN REX=27572. UNCERTAINTY IN F=0.05034 IN RATIO

RUN 081974-1 *** DISCRETE HOLE RIG *** NAS-3-14336 STANTON NUMBER DATA

*** 2700STEP90 M=0.9 TH=0 P/D=5 ***

RUN 081974-2 *** DISCRETE HOLE RIG *** NAS-3-14336 STANTON NUMBER DATA

*** 2700STEP90 M=0.9 TH=1 P/D=5 ***

LINEAR SUPERPOSITION IS APPLIED TO STANTON NUMBER DATA FROM
RUN NUMBERS 081974-1 AND 081974-2 TO OBTAIN STANTON NUMBER DATA AT TH=0 AND TH=1

PLATE	REXCOL	RE DEL2	ST(TH=0)	REXHOT	RE DEL2	ST(TH=1)	ETA	STCR	F-COL	STHR	F-HOT	LOGB
1	1159394.0	100.1	0.003582	1144244.0	92.2	0.003342	UUUUU	1.023	0.0000	0.954	0.0000	0.954
2	1215269.0	289.5	0.003199	1199388.0	261.3	0.002793	0.127	0.843	0.0301	1.000	0.0275	4.125
3	1271143.0	473.5	0.003388	1254532.0	1934.2	0.002967	0.124	1.000	0.0301	1.129	0.0276	4.501
4	1327018.0	668.6	0.003595	1309677.0	3614.9	0.002816	0.217	1.143	0.0303	1.117	0.0273	4.571
5	1382892.0	868.3	0.003553	1364821.0	5270.6	0.002578	0.274	1.194	0.0300	1.055	0.0274	4.570
6	1438766.0	1062.2	$\boxed{0.003388}$	1419965.0	6916.3	$\boxed{0.002337}$	0.310	1.190	0.0302	0.982	0.0276	4.550
7	1494641.0	1253.0	0.003441	1475109.0	8567.9	0.002289	0.335	1.253	0.0303	0.983	0.0279	4.643
8	1550515.0	1444.4	0.003412	1530254.0	10228.7	0.002199	0.355	1.283	0.0303	0.963	0.0272	4.599
9	1606390.0	1633.1	0.003340	1585398.0	11849.8	0.002099	0.372	1.290	0.0299	0.935	0.0276	4.637
10	1662264.0	1820.4	0.003365	1640542.0	13483.2	0.002007	0.404	1.332	0.0295	0.908	0.0271	4.586
11	1718139.0	2007.2	0.003323	1695687.0	15084.9	0.001875	0.436	1.344	0.0298	0.861	0.0275	4.589
12	1774013.0	2190.4	$\boxed{0.003235}$	1750831.0	16702.5	0.001764	0.455	1.335	0.0298	0.820	0.0275	4.555
13	1816478.0	2328.1	0.003282	1792741.0	18292.0	0.001662	0.494	1.373		0.780		
14	1845253.0	2420.3	0.003118	1821140.0	18338.6	0.001619	0.481	1.316		0.764		
15	1874028.0	2508.0	0.002975	1849539.0	18384.0	0.001574	0.471	1.267		0.748		
16	1902943.0	2592.3	0.002872	1878076.0	18427.9	0.001511	0.474	1.233		0.722		
17	1931858.0	2673.7	0.002779	1906613.0	18470.3	0.001468	0.472	1.203		0.705		
18	1960634.0	2753.1	0.002735	1935013.0	18511.4	0.001425	0.479	1.193		0.688		
19	1989409.0	2830.4	0.002638	1963412.0	18551.0	0.001364	0.482	1.157		0.662		
20	2018184.0	2906.5	0.002652	1991811.0	18589.4	0.001337	0.496	1.174		0.652		
21	2046960.0	2981.4	0.002545	2020211.0	18626.8	0.001292	0.492	1.134		0.633		
22	2075735.0	3054.1	0.002501	2048610.0	18663.1	0.001260	0.496	1.122		0.621		
23	2104511.0	3125.0	0.002421	2077009.0	18698.4	0.001222	0.495	1.093		0.605		
24	2133425.0	3195.3	0.002460	2105546.0	18733.0	0.001216	0.506	1.118		0.604		
25	2162340.0	3265.8	0.002435	2134084.0	18766.9	0.001169	0.520	1.113		0.584		
26	2191116.0	3335.6	0.002409	2162483.0	18800.7	0.001205	0.500	1.108		0.604		
27	2219891.0	3407.0	0.002551	2190882.0	18835.1	0.001214	0.524	1.180		0.611		
28	2248666.0	3476.7	0.002288	2219281.0	18868.2	0.001114	0.513	1.064		0.563		
29	2277442.0	3542.3	0.002261	2247681.0	18899.6	0.001096	0.515	1.057		0.556		
30	2306217.0	3607.8	0.002286	2276080.0	18930.8	0.001102	0.518	1.075		0.562		
31	2334993.0	3672.7	0.002223	2304480.0	18961.9	0.001085	0.512	1.051		0.555		
32	2363907.0	3736.2	0.002182	2333017.0	18992.5	0.001065	0.512	1.037		0.547		
33	2392822.0	3799.0	0.002181	2361554.0	19022.7	0.001057	0.515	1.041		0.545		
34	2421598.0	3861.1	0.002129	2389953.0	19052.4	0.001036	0.513	1.021		0.536		
35	2450373.0	3922.3	0.002118	2418352.0	19081.8	0.001030	0.514	1.021		0.535		
36	2479148.0	3982.3	0.002052	2446752.0	19110.5	0.000987	0.519	0.994		0.514		

STANTON NUMBER RATIO BASED ON ST*PR**0.4=0.0295*REX**(-.2)*(1.-(XI/(X-XVO))**0.9)**(-1./9.)

STANTON NUMBER RATIO FOR TH=1 IS CONVERTED TO COMPARABLE TRANSPIRATION VALUE
USING ALOG(1 + B)/B EXPRESSION IN THE BLOWN SECTION

RUN 092374 *** DISCRETE HOLE RIG *** NAS-3-14336 STANTON NUMBER DATA

TADB= 23.77 DEG C UINF= 13.47 M/S TINF= 23.63 DEG C
RHO= 1.170 KG/M3 VISC= 0.15526E-04 M2/S XVC= 22.4 CM
CP= 1014. J/KGK PR= 0.717

*** 2700STEP130 M=1.3 TH=0 P/D=5 ***

PLATE	X	REX	TO	REENTH	STANTON NO	DST	DREEN	M	F	T2	THETA	DTH
1	127.8	0.11858E 07	34.21	0.10173E 03	0.35604E-02	0.791E-04	2.					
2	132.8	0.12429E 07	34.21	0.29203E 03	0.30997E-02	0.751E-04	36.	1.33	0.0432	23.98	0.033	0.029
3	137.9	0.13001E 07	34.25	0.55365E 03	0.32452E-02	0.760E-04	63.	1.33	0.0431	24.00	0.035	0.029
4	143.0	0.13572E 07	34.23	0.84341E 03	0.38753E-02	0.819E-04	80.	1.32	0.0426	24.06	0.041	0.029
5	148.1	0.14144E 07	34.23	0.11666E 04	0.39644E-02	0.828E-04	95.	1.34	0.0433	24.10	0.044	0.029
6	153.2	0.14715E 07	34.23	0.15007E 04	0.38968E-02	0.821E-04	108.	1.33	0.0429	24.16	0.050	0.029
7	158.2	0.15286E 07	34.21	0.18399E 04	0.36900E-02	0.803E-04	119.	1.32	0.0428	24.37	0.070	0.029
8	163.3	0.15858E 07	34.21	0.22182E 04	0.35915E-02	0.794E-04	129.	1.32	0.0426	24.41	0.073	0.029
9	168.4	0.16429E 07	34.21	0.26014E 04	0.35789E-02	0.793E-04	139.	1.33	0.0430	24.43	0.075	0.029
10	173.5	0.17001E 07	34.23	0.29903E 04	0.35898E-02	0.792E-04	148.	1.32	0.0427	24.37	0.070	0.029
11	178.6	0.17572E 07	34.23	0.33667E 04	0.36047E-02	0.794E-04	156.	1.30	0.0419	24.47	0.079	0.029
12	183.6	0.18144E 07	34.21	0.37598E 04	0.35031E-02	0.786E-04	164.	1.30	0.0421	24.46	0.078	0.029
13	187.5	0.18578E 07	33.20	0.40999E 04	0.35767E-02	0.122E-03	168.					
14	190.1	0.18872E 07	33.08	0.42034E 04	0.34454E-02	0.123E-03	168.					
15	192.7	0.19167E 07	33.50	0.43027E 04	0.32992E-02	0.119E-03	168.					
16	195.4	0.19462E 07	33.56	0.43982E 04	0.31810E-02	0.114E-03	168.					
17	198.0	0.19758E 07	33.62	0.44911E 04	0.31267E-02	0.112E-03	168.					
18	200.6	0.20052E 07	33.65	0.45823E 04	0.30639E-02	0.110E-03	168.					
19	203.2	0.20347E 07	33.69	0.46709E 04	0.29468E-02	0.105E-03	168.					
20	205.8	0.20641E 07	33.81	0.47578E 04	0.29507E-02	0.106E-03	168.					
21	208.5	0.20935E 07	33.75	0.48433E 04	0.28576E-02	0.102E-03	168.					
22	211.1	0.21230E 07	33.85	0.49272E 04	0.28357E-02	0.103E-03	168.					
23	213.7	0.21524E 07	33.79	0.50099E 04	0.27735E-02	0.993E-04	168.					
24	216.3	0.21820E 07	33.96	0.50916E 04	0.27757E-02	0.101E-03	168.					
25	218.9	0.22115E 07	33.90	0.51731E 04	0.27555E-02	0.994E-04	168.					
26	221.6	0.22410E 07	33.85	0.52535E 04	0.27038E-02	0.102E-03	168.					
27	224.2	0.22704E 07	32.72	0.53321E 04	0.26299E-02	0.904E-04	168.					
28	226.8	0.22998E 07	33.88	0.54101E 04	0.26606E-02	0.101E-03	168.					
29	229.4	0.23293E 07	33.85	0.54874E 04	0.25859E-02	0.922E-04	168.					
30	232.0	0.23587E 07	34.23	0.55642E 04	0.26272E-02	0.963E-04	168.					
31	234.6	0.23881E 07	34.25	0.56405E 04	0.25566E-02	0.929E-04	168.					
32	237.3	0.24177E 07	34.13	0.57148E 04	0.24850E-02	0.902E-04	168.					
33	239.9	0.24473E 07	34.13	0.57880E 04	0.24812E-02	0.909E-04	168.					
34	242.5	0.24767E 07	33.88	0.58604E 04	0.24359E-02	0.871E-04	168.					
35	245.1	0.25061E 07	34.11	0.59321E 04	0.24278E-02	0.907E-04	168.					
36	247.8	0.25356E 07	33.94	0.60024E 04	0.23481E-02	0.945E-04	168.					

UNCERTAINTY IN REX=28573. UNCERTAINTY IN F=0.05031 IN RATIO

RUN 092474 *** DISCRETE HOLE RIG *** NAS-3-14336 STANTON NUMBER DATA

TADB= 21.61 DEG C UINF= 17.39 M/S TINF= 21.47 DEG C
RHO= 1.183 KG/M3 VISC= 0.15278E-04 M2/S XVO= 22.4 CM
CP= 1013. J/KGK PR= 0.717

*** 2700STEP130 M=1.3 TH=1 P/D=5 ***

PLATE	X	REX	TO	REENTH	STANTON NO	DST	DREEN	M	F	T2	THETA	DTH
1	127.8	0.12000E 07	37.90	0.10022E 03	0.34660E-02	0.522E-04	2.					
2	132.8	0.12578E 07	37.90	0.27907E 03	0.27194E-02	0.474E-04	58.	1.19	0.0386	37.07	0.949	0.019
3	137.9	0.13156E 07	37.92	0.25665E 04	0.30379E-02	0.493E-04	100.	1.21	0.0391	37.28	0.961	0.019
4	143.0	0.13735E 07	37.92	0.49196E 04	0.32415E-02	0.506E-04	131.	1.22	0.0394	37.78	0.991	0.019
5	148.1	0.14313E 07	37.92	0.73609E 04	0.31025E-02	0.497E-04	158.	1.22	0.0394	38.26	1.021	0.019
6	153.2	0.14891E 07	37.92	0.98561E 04	0.27723E-02	0.477E-04	181.	1.21	0.0391	38.15	1.014	0.019
7	158.2	0.15470E 07	37.92	0.12305E 05	0.27106E-02	0.473E-04	201.	1.19	0.0385	38.33	1.025	0.019
8	163.3	0.16048E 07	37.90	0.14740E 05	0.25496E-02	0.464E-04	219.	1.18	0.0382	38.59	1.042	0.019
9	168.4	0.16626E 07	37.92	0.17186E 05	0.24187E-02	0.457E-04	236.	1.18	0.0384	38.57	1.039	0.019
10	173.5	0.17204E 07	37.92	0.19629E 05	0.23468E-02	0.453E-04	251.	1.20	0.0389	38.31	1.024	0.019
11	178.6	0.17783E 07	37.92	0.22064E 05	0.22360E-02	0.447E-04	266.	1.18	0.0382	38.25	1.020	0.019
12	183.6	0.18361E 07	37.92	0.24443E 05	0.21348E-02	0.442E-04	279.	1.19	0.0385	37.61	0.981	0.019
13	187.5	0.18801E 07	36.44	0.26714E 05	0.17846E-02	0.581E-04	285.					
14	190.1	0.19098E 07	36.17	0.26767E 05	0.17727E-02	0.616E-04	285.					
15	192.7	0.19396E 07	36.55	0.26819E 05	0.17115E-02	0.613E-04	285.					
16	195.4	0.19695E 07	36.61	0.26869E 05	0.16526E-02	0.586E-04	285.					
17	198.0	0.19995E 07	36.67	0.26918E 05	0.16149E-02	0.574E-04	285.					
18	200.6	0.20293E 07	36.74	0.26965E 05	0.15532E-02	0.557E-04	285.					
19	203.2	0.20590E 07	36.80	0.27011E 05	0.14863E-02	0.530E-04	285.					
20	205.8	0.20888E 07	36.93	0.27055E 05	0.14829E-02	0.531E-04	285.					
21	208.5	0.21186E 07	36.97	0.27098E 05	0.14077E-02	0.506E-04	285.					
22	211.1	0.21484E 07	37.05	0.27140E 05	0.13947E-02	0.510E-04	285.					
23	213.7	0.21782E 07	37.03	0.27181E 05	0.13473E-02	0.488E-04	285.					
24	216.3	0.22081E 07	37.24	0.27221E 05	0.13381E-02	0.499E-04	285.					
25	218.9	0.22380E 07	37.18	0.27260E 05	0.13198E-02	0.485E-04	285.					
26	221.6	0.22678E 07	37.12	0.27299E 05	0.12897E-02	0.498E-04	285.					
27	224.2	0.22976E 07	36.27	0.27336E 05	0.11558E-02	0.406E-04	285.					
28	226.8	0.23274E 07	37.20	0.27372E 05	0.12596E-02	0.492E-04	285.					
29	229.4	0.23572E 07	37.16	0.27409E 05	0.12256E-02	0.446E-04	285.					
30	232.0	0.23869E 07	37.49	0.27446E 05	0.12591E-02	0.475E-04	285.					
31	234.6	0.24167E 07	37.52	0.27483E 05	0.12124E-02	0.455E-04	285.					
32	237.3	0.24466E 07	37.39	0.27518E 05	0.11938E-02	0.446E-04	285.					
33	239.9	0.24766E 07	37.39	0.27554E 05	0.11854E-02	0.447E-04	285.					
34	242.5	0.25064E 07	37.20	0.27589E 05	0.11453E-02	0.422E-04	285.					
35	245.1	0.25361E 07	37.35	0.27623E 05	0.11612E-02	0.452E-04	285.					
36	247.8	0.25659E 07	37.16	0.27657E 05	0.11160E-02	0.471E-04	285.					

UNCERTAINTY IN REX=28915. UNCERTAINTY IN F=0.05031 IN RATIO

RUN 092374 *** DISCRETE HOLE RIG *** NAS-3-14336 STANTON NUMBER DATA

*** 2700STEP130 M=1.3 TH=0 P/D=5 ***

RUN 092474 *** DISCRETE HOLE RIG *** NAS-3-14336 STANTON NUMBER DATA

*** 2700STEP130 M=1.3 TH=1 P/D=5 ***

LINEAR SUPERPOSITION IS APPLIED TO STANTON NUMBER DATA FROM
RUN NUMBERS 092374 AND 092474 TO OBTAIN STANTON NUMBER DATA AT TH=0 AND TH=1

PLATE	REXCOL	RE DEL2	ST(TH=0)	REXHOT	RE DEL2	ST(TH=1)	ETA	STCR	F-COL	STHR	F-HOT	LOGB
1	1185771.0	101.7	0.003560	1199974.0	100.2	0.003466	UUUUU	1.016	0.0000	0.989	0.0000	0.989
2	1242917.0	292.4	0.003113	1257804.0	278.5	0.002698	0.133	0.825	0.0432	0.976	0.0386	5.121
3	1300062.0	474.3	0.003253	1315634.0	2678.9	0.003028	0.069	0.965	0.0431	1.164	0.0391	5.707
4	1357208.0	678.7	0.003901	1373464.0	5118.9	0.003226	0.173	1.247	0.0426	1.292	0.0394	6.114
5	1414354.0	904.5	0.004002	1431295.0	7580.7	0.003108	0.224	1.352	0.0433	1.285	0.0394	6.230
6	1471499.0	1131.8	0.003951	1489125.0	10029.8	$\boxed{0.002792}$	0.293	1.395	0.0429	1.185	0.0391	6.126
7	1528645.0	1351.9	0.003751	1546955.0	12449.0	0.002730	0.272	1.374	0.0428	1.185	0.0385	6.156
8	1585791.0	1563.9	0.003669	1604785.0	14829.5	0.002586	0.295	1.387	0.0426	1.144	0.0382	6.132
9	1642936.0	1773.5	0.003668	1662615.0	17186.6	0.002467	0.327	1.425	0.0430	1.111	0.0384	6.153
10	1700082.0	1983.6	0.003684	1720445.0	19544.9	0.002387	0.352	1.466	0.0427	1.092	0.0389	6.240
11	1757227.0	2194.9	0.003713	1778275.0	21928.8	0.002267	0.389	1.510	0.0419	1.052	0.0382	6.147
12	1814373.0	2404.4	0.003620	1836105.0	24264.5	0.002135	0.410	1.502	0.0421	1.003	0.0385	6.140
13	1857804.0	2562.8	0.003729	1880056.0	26578.8	0.001785	0.521	1.569		0.847		
14	1887234.0	2670.6	0.003588	1909839.0	26631.8	0.001773	0.506	1.523		0.846		
15	1916664.0	2774.0	0.003435	1939621.0	26683.8	0.001712	0.502	1.470		0.822		
16	1946236.0	2873.4	0.003311	1969548.0	26734.0	0.001653	0.501	1.430		0.798		
17	1975809.0	2970.2	0.003256	1999475.0	26782.7	0.001615	0.504	1.417		0.784		
18	2005239.0	3065.2	0.003193	2029258.0	26829.9	0.001554	0.513	1.400		0.758		
19	2034669.0	3157.5	0.003071	2059040.0	26875.3	0.001487	0.516	1.357		0.729		
20	2064099.0	3248.0	0.003076	2088822.0	26919.6	0.001483	0.518	1.368		0.731		
21	2093530.0	3337.3	0.002981	2118605.0	26962.7	0.001408	0.528	1.336		0.698		
22	2122960.0	3424.8	0.002959	2148388.0	27004.5	0.001395	0.528	1.334		0.694		
23	2152390.0	3511.0	0.002895	2178170.0	27045.4	0.001348	0.534	1.314		0.674		
24	2181962.0	3596.4	0.002898	2208097.0	27085.4	0.001339	0.538	1.324		0.672		
25	2211535.0	3681.4	0.002878	2238024.0	27125.1	0.001320	0.541	1.323		0.666		
26	2240965.0	3765.5	0.002824	2267807.0	27164.0	0.001290	0.543	1.306		0.654		
27	2270395.0	3847.7	0.002756	2297589.0	27208.4	0.001156	0.580	1.282		0.588		
28	2299825.0	3929.2	0.002780	2327372.0	27236.5	0.001260	0.547	1.300		0.644		
29	2329255.0	4010.0	0.002702	2357155.0	27273.5	0.001226	0.546	1.271		0.629		
30	2358685.0	4090.2	0.002744	2386937.0	27310.6	$\boxed{0.001260}$	0.541	1.297		0.649		
31	2388115.0	4170.0	0.002671	2416719.0	27347.5	0.001213	0.546	1.269		0.627		
32	2417688.0	4247.6	0.002595	2446646.0	27383.3	0.001194	0.540	1.240		0.620		
33	2447261.0	4324.0	0.002592	2476573.0	27418.8	0.001186	0.542	1.244		0.618		
34	2476691.0	4399.7	0.002546	2506356.0	27453.6	0.001146	0.550	1.228		0.599		
35	2506121.0	4474.6	0.002536	2536138.0	27488.0	0.001162	0.542	1.229		0.609		
36	2535551.0	4548.1	0.002453	2565921.0	27521.9	0.001116	0.545	1.195		0.588		

STANTON NUMBER RATIO BASED ON ST*PR**0.4=0.0295*REX**(-.2)*(1.-(XI/(X-XVO))**0.9)**(-1./9.)

STANTON NUMBER RATIO FOR TH=1 IS CONVERTED TO COMPARABLE TRANSPIRATION VALUE
USING ALOG(1 + B)/B EXPRESSION IN THE BLOWN SECTION

RUN 121174 VELOCITY PROFILE

REX =	0.12950E 07	REM =	2871.
XVO =	13.04 CM.	DEL2 =	0.254 CM.
UINF =	16.82 M/S	DEL99=	2.100 CM.
VISC =	0.14902E-04 M2/S	DEL1 =	0.355 CM.
PORT =	19	H =	1.396
XLOC =	127.76 CM.	CF/2 =	0.16496E-02

Y(CM.)	Y/DEL	U(M/S)	U/UINF	Y+	U+
0.025	0.012	7.26	0.432	11.6	10.63
0.028	0.013	7.39	0.440	12.8	10.82
0.030	0.015	7.63	0.454	14.0	11.17
0.033	0.016	7.84	0.466	15.1	11.48
0.038	0.018	8.22	0.489	17.5	12.03
0.046	0.022	8.56	0.509	21.0	12.53
0.056	0.027	8.99	0.534	25.6	13.15
0.069	0.033	9.38	0.558	31.4	13.73
0.084	0.040	9.72	0.578	38.4	14.23
0.102	0.048	10.00	0.594	46.6	14.63
0.122	0.058	10.25	0.609	55.9	15.00
0.147	0.070	10.49	0.624	67.5	15.36
0.178	0.085	10.76	0.640	81.5	15.75
0.213	0.102	11.06	0.658	97.8	16.19
0.254	0.121	11.33	0.673	116.4	16.58
0.300	0.143	11.59	0.689	137.4	16.97
0.351	0.167	11.88	0.706	160.7	17.38
0.414	0.197	12.18	0.724	189.8	17.83
0.490	0.233	12.51	0.743	224.7	18.30
0.592	0.282	12.93	0.768	271.3	18.92
0.719	0.342	13.42	0.798	329.5	19.64
0.871	0.415	13.94	0.828	399.4	20.40
1.024	0.487	14.43	0.858	469.3	21.12
1.214	0.578	14.97	0.890	556.6	21.91
1.405	0.669	15.46	0.919	644.0	22.63
1.595	0.759	15.89	0.945	731.3	23.26
1.786	0.850	16.25	0.966	818.6	23.79
1.976	0.941	16.56	0.984	906.0	24.24
2.167	1.032	16.69	0.992	993.3	24.43
2.357	1.122	16.79	0.998	1080.6	24.56
2.548	1.213	16.82	1.000	1168.0	24.62

RUN 121174 *** DISCRETE HOLE RIG *** NAS-3-14336 STANTON NUMBER DATA

TADB= 19.46 DEG C   UINF= 16.88 M/S   TINF= 19.33 DEG C
RHO= 1.208 KG/M3   VISC= 0.14903E-04 M2/S   XVO= 13.0 CM
CP= 1011. J/KGK   PR= 0.716

*** 2900STEP FP P/D =10 ***

PLATE	X	REX	TO	REENTH	STANTON NO	DST	DREEN	ST(THEO)	RATIO
1	127.8	0.12997E 07	32.26	0.10283E 03	0.35737E-02	0.661E-04	2.	0.31195E-02	1.146
2	132.8	0.13572E 07	32.24	0.28901E 03	0.28970E-02	0.611E-04	3.	0.27498E-02	1.054
3	137.9	0.14148E 07	32.24	0.44890E 03	0.26599E-02	0.594E-04	4.	0.25879E-02	1.028
4	143.0	0.14723E 07	32.26	0.59929E 03	0.25668E-02	0.587E-04	5.	0.24836E-02	1.034
5	148.1	0.15299E 07	32.28	0.74425E 03	0.24711E-02	0.580E-04	5.	0.24065E-02	1.027
6	153.2	0.15874E 07	32.24	0.88572E 03	0.24455E-02	0.580E-04	6.	0.23453E-02	1.043
7	158.2	0.16450E 07	32.28	0.10234E 04	0.23386E-02	0.572E-04	6.	0.22944E-02	1.019
8	163.3	0.17025E 07	32.24	0.11575E 04	0.23211E-02	0.573E-04	7.	0.22510E-02	1.031
9	168.4	0.17601E 07	32.22	0.12894E 04	0.22631E-02	0.570E-04	7.	0.22129E-02	1.023
10	173.5	0.18176E 07	32.22	0.14191E 04	0.22473E-02	0.569E-04	8.	0.21792E-02	1.031
11	178.6	0.18752E 07	32.24	0.15455E 04	0.21458E-02	0.562E-04	8.	0.21488E-02	0.999
12	183.6	0.19327E 07	32.26	0.16686E 04	0.21316E-02	0.561E-04	8.	0.21212E-02	1.005
13	187.5	0.19765E 07	31.86	0.17617E 04	0.21400E-02	0.739E-04	9.	0.21017E-02	1.018
14	190.1	0.20061E 07	31.70	0.18249E 04	0.21224E-02	0.745E-04	9.	0.20892E-02	1.016
15	192.7	0.20357E 07	32.07	0.18877E 04	0.21089E-02	0.755E-04	9.	0.20772E-02	1.015
16	195.4	0.20655E 07	32.09	0.19501E 04	0.20966E-02	0.740E-04	9.	0.20656E-02	1.015
17	198.0	0.20953E 07	32.11	0.20121E 04	0.20855E-02	0.740E-04	9.	0.20544E-02	1.015
18	200.6	0.21249E 07	32.03	0.20739E 04	0.20747E-02	0.735E-04	9.	0.20437E-02	1.015
19	203.2	0.21546E 07	31.95	0.21353E 04	0.20647E-02	0.722E-04	9.	0.20333E-02	1.015
20	205.8	0.21842E 07	32.07	0.21964E 04	0.20539E-02	0.727E-04	10.	0.20233E-02	1.015
21	208.5	0.22138E 07	32.01	0.22572E 04	0.20447E-02	0.720E-04	10.	0.20136E-02	1.015
22	211.1	0.22435E 07	32.03	0.23177E 04	0.20346E-02	0.728E-04	10.	0.20042E-02	1.015
23	213.7	0.22731E 07	31.90	0.23780E 04	0.20261E-02	0.716E-04	10.	0.19951E-02	1.016
24	216.3	0.23029E 07	31.97	0.24373E 04	0.19725E-02	0.707E-04	10.	0.19862E-02	0.993
25	218.9	0.23327E 07	32.07	0.24963E 04	0.20072E-02	0.721E-04	10.	0.19775E-02	1.015
26	221.6	0.23623E 07	31.97	0.25558E 04	0.19993E-02	0.751E-04	10.	0.19692E-02	1.015
27	224.2	0.23919E 07	30.79	0.26151E 04	0.19966E-02	0.662E-04	10.	0.19610E-02	1.018
28	226.8	0.24216E 07	31.99	0.26741E 04	0.19833E-02	0.751E-04	10.	0.19531E-02	1.015
29	229.4	0.24512E 07	31.91	0.27328E 04	0.19755E-02	0.688E-04	11.	0.19454E-02	1.015
30	232.0	0.24809E 07	32.39	0.27913E 04	0.19660E-02	0.718E-04	11.	0.19378E-02	1.015
31	234.6	0.25105E 07	32.35	0.28495E 04	0.19581E-02	0.701E-04	11.	0.19305E-02	1.014
32	237.3	0.25403E 07	32.20	0.29075E 04	0.19518E-02	0.696E-04	11.	0.19233E-02	1.015
33	239.9	0.25701E 07	32.18	0.29653E 04	0.19449E-02	0.702E-04	11.	0.19163E-02	1.015
34	242.5	0.25997E 07	31.88	0.30230E 04	0.19389E-02	0.675E-04	11.	0.19094E-02	1.015
35	245.1	0.26293E 07	32.14	0.30804E 04	0.19311E-02	0.715E-04	11.	0.19027E-02	1.015
36	247.8	0.26590E 07	31.86	0.31376E 04	0.19258E-02	0.770E-04	11.	0.18962E-02	1.016

RUN 121474 *** DISCRETE HOLE RIG *** NAS-3-14336 STANTON NUMBER DATA

TADB= 19.34 DEG C UINF= 16.71 M/S TINF= 19.22 DEG C
RHO= 1.215 KG/M3 VISC= 0.14814E-04 M2/S XVO= 13.0 CM
CP= 1011. J/KGK PR= 0.716

*** 2900STEP40 M=0.4 TH=0 P/D=10 ***

PLATE	X	REX	TO	REENTH	STANTON NO	DST	DREEN	M	F	T2	THETA	DTH
1	127.8	0.12945E 07	30.50	0.10312E 03	0.35982E-02	0.754E-04	2.					
2	132.8	0.13518E 07	30.52	0.28954E 03	0.29068E-02	0.695E-04	5.	0.39	0.0032	21.08	0.165	0.027
3	137.9	0.14091E 07	30.48	0.48118E 03	0.27312E-02	0.684E-04	6.	0.00	0.0032	30.48	0.165	0.028
4	143.0	0.14664E 07	30.50	0.66196E 03	0.25277E-02	0.668E-04	8.	0.39	0.0031	21.36	0.190	0.027
5	148.1	0.15237E 07	30.52	0.84019E 03	0.25057E-02	0.666E-04	9.	0.00	0.0031	30.52	0.190	0.027
6	153.2	0.15811E 07	30.50	0.10138E 04	0.23663E-02	0.657E-04	10.	0.39	0.0032	21.34	0.188	0.027
7	158.2	0.16384E 07	30.54	0.11840E 04	0.23745E-02	0.656E-04	11.	0.00	0.0032	30.54	0.188	0.027
8	163.3	0.16957E 07	30.48	0.13520E 04	0.22879E-02	0.653E-04	12.	0.39	0.0031	21.41	0.194	0.027
9	168.4	0.17530E 07	30.50	0.15174E 04	0.22646E-02	0.650E-04	13.	0.00	0.0031	30.50	0.194	0.028
10	173.5	0.18103E 07	30.44	0.16804E 04	0.22033E-02	0.650E-04	14.	0.39	0.0032	21.40	0.194	0.027
11	178.6	0.18676E 07	30.50	0.18416E 04	0.21898E-02	0.646E-04	14.	0.00	0.0032	30.50	0.194	0.028
12	183.6	0.19249E 07	30.48	0.20003E 04	0.21117E-02	0.642E-04	15.	0.41	0.0033	21.42	0.196	0.027
13	187.5	0.19685E 07	30.56	0.21299E 04	0.21801E-02	0.782E-04	16.					
14	190.1	0.19980E 07	30.48	0.22310E 04	0.21610E-02	0.777E-04	16.					
15	192.7	0.20275E 07	30.80	0.22947E 04	0.21497E-02	0.782E-04	16.					
16	195.4	0.20572E 07	30.80	0.23579E 04	0.21272E-02	0.763E-04	16.					
17	198.0	0.20869E 07	30.82	0.24207E 04	0.21200E-02	0.763E-04	16.					
18	200.6	0.21164E 07	30.79	0.24829E 04	0.20937E-02	0.754E-04	16.					
19	203.2	0.21459E 07	30.77	0.25443E 04	0.20631E-02	0.737E-04	16.					
20	205.8	0.21754E 07	30.84	0.26057E 04	0.20870E-02	0.750E-04	16.					
21	208.5	0.22049E 07	30.77	0.26669E 04	0.20546E-02	0.734E-04	16.					
22	211.1	0.22345E 07	30.84	0.27273E 04	0.20377E-02	0.744E-04	16.					
23	213.7	0.22640E 07	30.75	0.27869E 04	0.19918E-02	0.727E-04	16.					
24	216.3	0.22936E 07	30.61	0.28458E 04	0.19993E-02	0.724E-04	16.					
25	218.9	0.23233E 07	30.73	0.29054E 04	0.20324E-02	0.744E-04	17.					
26	221.6	0.23528E 07	30.69	0.29654E 04	0.20281E-02	0.776E-04	17.					
27	224.2	0.23823E 07	29.62	0.30252E 04	0.20191E-02	0.690E-04	17.					
28	226.8	0.24118E 07	30.71	0.30850E 04	0.20239E-02	0.778E-04	17.					
29	229.4	0.24414E 07	30.63	0.31448E 04	0.20237E-02	0.719E-04	17.					
30	232.0	0.24709E 07	31.02	0.32047E 04	0.20300E-02	0.750E-04	17.					
31	234.6	0.25004E 07	31.02	0.32642E 04	0.19949E-02	0.728E-04	17.					
32	237.3	0.25301E 07	30.88	0.33227E 04	0.19655E-02	0.718E-04	17.					
33	239.9	0.25597E 07	30.80	0.33811E 04	0.19898E-02	0.728E-04	17.					
34	242.5	0.25892E 07	30.57	0.34396E 04	0.19691E-02	0.703E-04	17.					
35	245.1	0.26188E 07	30.79	0.34976E 04	0.19543E-02	0.737E-04	17.					
36	247.8	0.26483E 07	30.54	0.35548E 04	0.19203E-02	0.785E-04	17.					

UNCERTAINTY IN REX=28658. UNCERTAINTY IN F=0.05034 IN RATIO

RUN 121274-2 *** DISCRETE HOLE RIG *** NAS-3-14336 STANTON NUMBER DATA

TADB= 19.92 DEG C UINF= 16.77 M/S TINF= 19.80 DEG C
RHO= 1.206 KG/M3 VISC= 0.14946E-04 M2/S XVO= 13.0 CM
CP= 1011. J/KGK PR= 0.715

*** 2900STEP40 M=0.4 TH=1 P/D=10 ***

PLATE	X	REX	TO	REENTH	STANTON NO	DST	DREEN	M	F	T2	THETA	DTH
1	127.8	0.12876E 07	32.47	0.98512E 02	0.34558E-02	0.668E-04	2.					
2	132.8	0.13446E 07	32.45	0.27435E 03	0.27126E-02	0.613E-04	5.	0.35	0.0028	31.86	0.953	0.024
3	137.9	0.14017E 07	32.47	0.57405E 03	0.24306E-02	0.594E-04	9.	0.00	0.0028	32.47	0.953	0.025
4	143.0	0.14587E 07	32.45	0.86107E 03	0.22676E-02	0.584E-04	11.	0.35	0.0029	31.31	0.910	0.024
5	148.1	0.15157E 07	32.45	0.11340E 04	0.21162E-02	0.576E-04	13.	0.00	0.0029	32.45	0.910	0.025
6	153.2	0.15727E 07	32.43	0.14005E 04	0.20436E-02	0.572E-04	14.	0.39	0.0031	31.54	0.929	0.024
7	158.2	0.16297E 07	32.45	0.16819E 04	0.19950E-02	0.569E-04	16.	0.00	0.0031	32.45	0.929	0.025
8	163.3	0.16867E 07	32.43	0.19605E 04	0.19446E-02	0.567E-04	17.	0.33	0.0027	31.67	0.939	0.024
9	168.4	0.17437E 07	32.45	0.22115E 04	0.18419E-02	0.561E-04	18.	0.00	0.0027	32.45	0.939	0.025
10	173.5	0.18007E 07	32.45	0.24592E 04	0.18267E-02	0.560E-04	20.	0.39	0.0031	31.39	0.916	0.024
11	178.6	0.18577E 07	32.43	0.27256E 04	0.17890E-02	0.559E-04	21.	0.00	0.0031	32.43	0.916	0.025
12	183.6	0.19148E 07	32.43	0.29897E 04	0.17434E-02	0.557E-04	22.	0.36	0.0029	31.16	0.899	0.024
13	187.5	0.19581E 07	32.34	0.32164E 04	0.17712E-02	0.639E-04	22.					
14	190.1	0.19875E 07	32.16	0.34200E 04	0.18056E-02	0.653E-04	22.					
15	192.7	0.20168E 07	32.43	0.34735E 04	0.18307E-02	0.669E-04	22.					
16	195.4	0.20463E 07	32.43	0.35272E 04	0.18286E-02	0.660E-04	22.					
17	198.0	0.20758E 07	32.45	0.35811E 04	0.18336E-02	0.664E-04	22.					
18	200.6	0.21052E 07	32.39	0.36350E 04	0.18335E-02	0.664E-04	23.					
19	203.2	0.21345E 07	32.32	0.36887E 04	0.18248E-02	0.652E-04	23.					
20	205.8	0.21639E 07	32.39	0.37427E 04	0.18476E-02	0.665E-04	23.					
21	208.5	0.21933E 07	32.34	0.37967E 04	0.18225E-02	0.654E-04	23.					
22	211.1	0.22226E 07	32.37	0.38502E 04	0.18227E-02	0.666E-04	23.					
23	213.7	0.22520E 07	32.26	0.39036E 04	0.18065E-02	0.655E-04	23.					
24	216.3	0.22815E 07	32.24	0.39563E 04	0.17813E-02	0.652E-04	23.					
25	218.9	0.23110E 07	32.28	0.40097E 04	0.18484E-02	0.672E-04	23.					
26	221.6	0.23404E 07	32.28	0.40637E 04	0.18284E-02	0.698E-04	23.					
27	224.2	0.23697E 07	31.28	0.41168E 04	0.17867E-02	0.612E-04	23.					
28	226.8	0.23991E 07	32.26	0.41700E 04	0.18306E-02	0.701E-04	23.					
29	229.4	0.24284E 07	32.18	0.42237E 04	0.18243E-02	0.649E-04	23.					
30	232.0	0.24578E 07	32.53	0.42777E 04	0.18463E-02	0.681E-04	23.					
31	234.6	0.24872E 07	32.53	0.43314E 04	0.18098E-02	0.664E-04	23.					
32	237.3	0.25167E 07	32.30	0.43850E 04	0.18325E-02	0.662E-04	23.					
33	239.9	0.25462E 07	32.32	0.44384E 04	0.18064E-02	0.664E-04	23.					
34	242.5	0.25755E 07	32.07	0.44916E 04	0.18076E-02	0.643E-04	23.					
35	245.1	0.26049E 07	32.28	0.45446E 04	0.18039E-02	0.679E-04	23.					
36	247.8	0.26343E 07	32.05	0.45972E 04	0.17720E-02	0.720E-04	23.					

UNCERTAINTY IN REX=28506. UNCERTAINTY IN F=0.05034 IN RATIO

RUN 121474 *** DISCRETE HOLE RIG *** NAS-3-14336 STANTON NUMBER DATA

*** 2900STEP40 M=0.4 TH=0 P/D=10 ***

RUN 121274-2 *** DISCRETE HOLE RIG *** NAS-3-14336 STANTON NUMBER DATA

*** 2900STEP40 M=0.4 TH=1 P/D=10 ***

LINEAR SUPERPOSITION IS APPLIED TO STANTON NUMBER DATA FROM
RUN NUMBERS 121474 AND 121274-2 TO OBTAIN STANTON NUMBER DATA AT TH=0 AND TH=1

PLATE	REXCOL	RE DEL2	ST(TH=0)	REXHOT	RE DEL2	ST(TH=1)	ETA	STCR	F-COL	STHR	F-HOT	LOG3
1	1294474.0	103.1	0.003598	1287625.0	98.5	0.003456	UUUUU	1.007	0.0000	0.967	0.0000	0.967
2	1351789.0	290.7	0.002947	1344638.0	274.0	0.002701	0.084	0.780	0.0032	0.930	0.0028	1.431
3	1409105.0	455.2	0.002794	1401650.0	580.4	0.002413	0.136	0.827	0.0032	0.931	0.0028	1.404
4	1466421.0	609.5	0.002589	1458662.0	873.7	0.002244	0.133	0.826	0.0031	0.902	0.0029	1.397
5	1523736.0	758.4	0.002609	1515675.0	1159.2	0.002067	0.208	0.880	0.0031	0.857	0.0029	1.364
6	1581052.0	903.4	0.002450	1572687.0	1438.0	0.002008	0.180	0.863	0.0032	0.855	0.0031	1.419
7	1638367.0	1044.4	0.002471	1629700.0	1730.1	0.001959	0.207	0.903	0.0032	0.852	0.0031	1.428
8	1695683.0	1183.3	0.002376	1686712.0	2019.4	0.001914	0.194	0.896	0.0031	0.849	0.0027	1.356
9	1752999.0	1319.5	0.002375	1743725.0	2277.8	0.001808	0.239	0.921	0.0031	0.815	0.0027	1.328
10	1810314.0	1453.5	0.002303	1800737.0	2532.6	0.001790	0.223	0.915	0.0032	0.820	0.0031	1.417
11	1867630.0	1585.3	0.002297	1857749.0	2811.6	0.001743	0.242	0.933	0.0032	0.809	0.0031	1.413
12	1924946.0	1714.6	0.002212	1914762.0	3087.9	0.001696	0.233	0.916	0.0033	0.798	0.0029	1.376
13	1968506.0	1811.9	0.002292	1958091.0	3329.4	0.001718	0.250	0.963		0.816		
14	1998023.0	1879.1	0.002258	1987453.0	3548.4	0.001760	0.221	0.957		0.841		
15	2027541.0	1945.5	0.002237	2016814.0	3600.6	0.001790	0.200	0.956		0.860		
16	2057201.0	2011.2	0.002209	2046318.0	3653.2	0.001790	0.190	0.952		0.865		
17	2086862.0	2076.3	0.002198	2075822.0	3705.9	0.001797	0.183	0.955		0.873		
18	2116380.0	2140.8	0.002165	2105183.0	3758.8	0.001800	0.169	0.948		0.879		
19	2145897.0	2204.3	0.002128	2134545.0	3811.6	0.001794	0.157	0.939		0.881		
20	2175415.0	2267.5	0.002152	2163906.0	3864.7	0.001817	0.156	0.956		0.896		
21	2204933.0	2330.6	0.002118	2193268.0	3917.7	0.001792	0.154	0.947		0.888		
22	2234450.0	2392.9	0.002097	2222629.0	3970.4	0.001795	0.144	0.944		0.894		
23	2263968.0	2454.0	0.002042	2251990.0	4023.0	0.001783	0.127	0.926		0.892		
24	2293628.0	2514.6	0.002059	2281494.0	4075.0	0.001753	0.149	0.939		0.881		
25	2323289.0	2575.8	0.002083	2310998.0	4127.6	0.001825	0.124	0.956		0.921		
26	2352807.0	2637.4	0.002083	2340359.0	4180.9	0.001803	0.134	0.962		0.914		
27	2382324.0	2698.9	0.002083	2369721.0	4233.2	0.001757	0.157	0.967		0.894		
28	2411842.0	2760.4	0.002077	2399082.0	4285.6	0.001806	0.131	0.970		0.923		
29	2441360.0	2821.8	0.002078	2428444.0	4338.5	0.001799	0.135	0.976		0.923		
30	2470877.0	2883.3	0.002080	2457805.0	4391.8	0.001823	0.124	0.982		0.939		
31	2500395.0	2944.2	0.002046	2487167.0	4444.8	0.001786	0.127	0.971		0.923		
32	2530056.0	3004.0	0.002002	2516670.0	4497.7	0.001815	0.093	0.955		0.942		
33	2559716.0	3063.8	0.002040	2546174.0	4550.6	0.001783	0.126	0.978		0.928		
34	2589234.0	3123.6	0.002018	2575536.0	4603.1	0.001787	0.112	0.970		0.934		
35	2618752.0	3182.9	0.001995	2604897.0	4655.6	0.001784	0.106	0.966		0.936		
36	2648269.0	3241.3	0.001961	2634258.0	4707.6	0.001753	0.106	0.953		0.923		

STANTON NUMBER RATIO BASED ON ST*PR**0.4=0.0295*REX**(-.2)*(1.-(XI/(X-XVO))**0.9)**(-1./9.)

STANTON NUMBER RATIO FOR TH=1 IS CONVERTED TO COMPARABLE TRANSPIRATION VALUE
USING ALOG(1 + B)/B EXPRESSION IN THE BLOWN SECTION

RUN 121674-1 *** DISCRETE HOLE RIG *** NAS-3-14336 STANTON NUMBER DATA

TADB= 20.15 DEG C UINF= 16.65 M/S TINF= 20.03 DEG C
RHO= 1.206 KG/M3 VISC= 0.14957E-04 M2/S XVO= 13.0 CM
CP= 1011. J/KGK PR= 0.716

*** 2900STEP75 M=0.75 TH=0 P/D=10 ***

PLATE	X	REX	TO	REENTH	STANTON NO	DST	DREEN	M	F	T2	THETA	DTH
1	127.8	0.12775E 07	30.79	0.10311E 03	0.36459E-02	0.799E-04	2.					
2	132.8	0.13340E 07	30.79	0.29060E 03	0.29837E-02	0.741E-04	6.	0.78	0.0063	20.92	0.083	0.028
3	137.9	0.13906E 07	30.82	0.48861E 03	0.29717E-02	0.738E-04	10.	0.00	0.0063	30.82	0.083	0.029
4	143.0	0.14471E 07	30.80	0.68057E 03	0.27694E-02	0.723E-04	13.	0.78	0.0063	21.10	0.099	0.028
5	148.1	0.15037E 07	30.82	0.87280E 03	0.27734E-02	0.722E-04	15.	0.00	0.0063	30.82	0.099	0.029
6	153.2	0.15603E 07	30.80	0.10591E 04	0.25591E-02	0.707E-04	17.	0.78	0.0063	21.09	0.098	0.028
7	158.2	0.16168E 07	30.80	0.12415E 04	0.26453E-02	0.713E-04	19.	0.00	0.0063	30.80	0.098	0.029
8	163.3	0.16734E 07	30.79	0.14223E 04	0.25023E-02	0.704E-04	20.	0.78	0.0063	21.24	0.112	0.028
9	168.4	0.17299E 07	30.79	0.16041E 04	0.25107E-02	0.705E-04	22.	0.00	0.0063	30.79	0.112	0.029
10	173.5	0.17865E 07	30.80	0.17831E 04	0.23978E-02	0.695E-04	23.	0.78	0.0063	21.22	0.110	0.028
11	178.6	0.18431E 07	30.80	0.19595E 04	0.24447E-02	0.699E-04	25.	0.00	0.0063	30.80	0.110	0.029
12	183.6	0.18996E 07	30.80	0.21348E 04	0.23545E-02	0.692E-04	26.	0.78	0.0063	21.26	0.114	0.028
13	187.5	0.19426E 07	30.52	0.22777E 04	0.24395E-02	0.867E-04	26.					
14	190.1	0.19717E 07	30.38	0.23892E 04	0.24120E-02	0.871E-04	26.					
15	192.7	0.20009E 07	30.73	0.24592E 04	0.23861E-02	0.873E-04	27.					
16	195.4	0.20301E 07	30.75	0.25282E 04	0.23486E-02	0.849E-04	27.					
17	198.0	0.20594E 07	30.77	0.25965E 04	0.23377E-02	0.848E-04	27.					
18	200.6	0.20885E 07	30.73	0.26645E 04	0.23234E-02	0.843E-04	27.					
19	203.2	0.21177E 07	30.71	0.27316E 04	0.22763E-02	0.820E-04	27.					
20	205.8	0.21468E 07	30.79	0.27983E 04	0.23014E-02	0.833E-04	27.					
21	208.5	0.21759E 07	30.71	0.28650E 04	0.22713E-02	0.817E-04	27.					
22	211.1	0.22051E 07	30.80	0.29306E 04	0.22420E-02	0.824E-04	27.					
23	213.7	0.22342E 07	30.73	0.29954E 04	0.21849E-02	0.806E-04	27.					
24	216.3	0.22635E 07	30.56	0.30594E 04	0.22039E-02	0.801E-04	27.					
25	218.9	0.22927E 07	30.73	0.31240E 04	0.22280E-02	0.823E-04	27.					
26	221.6	0.23219E 07	30.69	0.31889E 04	0.22198E-02	0.853E-04	27.					
27	224.2	0.23510E 07	29.64	0.32535E 04	0.22158E-02	0.768E-04	27.					
28	226.8	0.23801E 07	30.71	0.33183E 04	0.22253E-02	0.859E-04	27.					
29	229.4	0.24093E 07	30.65	0.33829E 04	0.22031E-02	0.792E-04	27.					
30	232.0	0.24384E 07	31.00	0.34477E 04	0.22393E-02	0.829E-04	27.					
31	234.6	0.24675E 07	31.02	0.35120E 04	0.21750E-02	0.800E-04	27.					
32	237.3	0.24968E 07	30.86	0.35752E 04	0.21588E-02	0.791E-04	28.					
33	239.9	0.25261E 07	30.82	0.36386E 04	0.21851E-02	0.806E-04	28.					
34	242.5	0.25552E 07	30.57	0.37021E 04	0.21700E-02	0.780E-04	28.					
35	245.1	0.25843E 07	30.77	0.37652E 04	0.21585E-02	0.816E-04	28.					
36	247.8	0.26134E 07	30.56	0.38272E 04	0.20969E-02	0.860E-04	28.					

UNCERTAINTY IN REX=28281. UNCERTAINTY IN F=0.05035 IN RATIO

RUN 121674-2 *** DISCRETE HOLE RIG *** NAS-3-14336 STANTON NUMBER DATA

TADB= 19.63 DEG C UINF= 16.64 M/S TINF= 19.51 DEG C
RHO= 1.208 KG/M3 VISC= 0.14911E-04 M2/S XVO= 13.0 CM
CP= 1011. J/KGK PR= 0.716

*** 2900STEP75 M=0.75 TH=1 P/D=10 ***

PLATE	X	REX	TO	REENTH	STANTON NO	DST	DREEN	M	F	T2	THETA	DTH
1	127.8	0.12802E 07	31.55	0.97654E 02	0.34456E-02	0.702E-04	2.					
2	132.8	0.13369E 07	31.57	0.27431E 03	0.27876E-02	0.650E-04	10.	0.74	0.0060	31.81	1.020	0.026
3	137.9	0.13936E 07	31.55	0.77672E 03	0.27609E-02	0.649E-04	17.	0.00	0.0060	31.55	1.020	0.026
4	143.0	0.14502E 07	31.59	0.12712E 04	0.25065E-02	0.630E-04	22.	0.75	0.0060	31.59	1.000	0.026
5	148.1	0.15069E 07	31.57	0.17526E 04	0.24254E-02	0.625E-04	26.	0.00	0.0060	31.57	1.000	0.026
6	153.2	0.15636E 07	31.57	0.22264E 04	0.22406E-02	0.614E-04	30.	0.76	0.0061	31.55	0.998	0.026
7	158.2	0.16203E 07	31.55	0.26994E 04	0.22047E-02	0.612E-04	33.	0.00	0.0061	31.55	0.998	0.026
8	163.3	0.16770E 07	31.57	0.31690E 04	0.21202E-02	0.606E-04	36.	0.75	0.0061	31.48	0.992	0.026
9	168.4	0.17336E 07	31.59	0.36327E 04	0.21389E-02	0.607E-04	39.	0.00	0.0061	31.59	0.992	0.026
10	173.5	0.17903E 07	31.59	0.40946E 04	0.20576E-02	0.602E-04	41.	0.75	0.0061	31.14	0.963	0.026
11	178.6	0.18470E 07	31.63	0.45434E 04	0.20545E-02	0.600E-04	43.	0.00	0.0061	31.63	0.963	0.026
12	183.6	0.19037E 07	31.61	0.49901E 04	0.19879E-02	0.597E-04	45.	0.77	0.0062	30.92	0.943	0.025
13	187.5	0.19468E 07	31.30	0.54080E 04	0.20977E-02	0.742E-04	46.					
14	190.1	0.19760E 07	31.09	0.58006E 04	0.21306E-02	0.759E-04	46.					
15	192.7	0.20052E 07	31.44	0.58625E 04	0.21065E-02	0.766E-04	46.					
16	195.4	0.20345E 07	31.44	0.59240E 04	0.21043E-02	0.753E-04	46.					
17	198.0	0.20638E 07	31.46	0.59855E 04	0.20993E-02	0.754E-04	46.					
18	200.6	0.20930E 07	31.44	0.60464E 04	0.20728E-02	0.746E-04	46.					
19	203.2	0.21222E 07	31.42	0.61066E 04	0.20414E-02	0.729E-04	46.					
20	205.8	0.21514E 07	31.44	0.61670E 04	0.20935E-02	0.747E-04	47.					
21	208.5	0.21806E 07	31.42	0.62272E 04	0.20274E-02	0.725E-04	47.					
22	211.1	0.22098E 07	31.47	0.62865E 04	0.20275E-02	0.738E-04	47.					
23	213.7	0.22390E 07	31.36	0.63452E 04	0.19936E-02	0.723E-04	47.					
24	216.3	0.22683E 07	31.28	0.64031E 04	0.19642E-02	0.713E-04	47.					
25	218.9	0.22976E 07	31.38	0.64615E 04	0.20366E-02	0.741E-04	47.					
26	221.6	0.23268E 07	31.34	0.65207E 04	0.20105E-02	0.764E-04	47.					
27	224.2	0.23560E 07	30.33	0.65788E 04	0.19648E-02	0.672E-04	47.					
28	226.8	0.23852E 07	31.36	0.66370E 04	0.20212E-02	0.771E-04	47.					
29	229.4	0.24144E 07	31.30	0.66956E 04	0.19891E-02	0.708E-04	47.					
30	232.0	0.24436E 07	31.63	0.67544E 04	0.20371E-02	0.747E-04	47.					
31	234.6	0.24728E 07	31.65	0.68132E 04	0.19833E-02	0.724E-04	47.					
32	237.3	0.25021E 07	31.44	0.68709E 04	0.19645E-02	0.715E-04	47.					
33	239.9	0.25315E 07	31.30	0.69292E 04	0.20265E-02	0.732E-04	47.					
34	242.5	0.25607E 07	31.19	0.69874E 04	0.19535E-02	0.699E-04	47.					
35	245.1	0.25898E 07	31.40	0.70446E 04	0.19614E-02	0.734E-04	47.					
36	247.8	0.26190E 07	31.21	0.71012E 04	0.19144E-02	0.774E-04	47.					

UNCERTAINTY IN REX=28341. UNCERTAINTY IN F=0.05035 IN RATIO

RUN 121674-1 *** DISCRETE HOLE RIG *** NAS-3-14336 STANTON NUMBER DATA

*** 2900STEP75 M=0.75 TH=0 P/D=10 ***

RUN 121674-2 *** DISCRETE HOLE RIG *** NAS-3-14336 STANTON NUMBER DATA

*** 2900STEP75 M=0.75 TH=1 P/D=10 ***

LINEAR SUPERPOSITION IS APPLIED TO STANTON NUMBER DATA FROM
RUN NUMBERS 121674-1 AND 121674-2 TO OBTAIN STANTON NUMBER DATA AT TH=0 AND TH=1

PLATE	REXCOL	RE DEL2	ST(TH=0)	REXHOT	RE DEL2	ST(TH=1)	ETA	STCR	F-COL	STHR	F-HOT	LOGB
1	1277451.0	103.1	0.003646	1280184.0	97.7	0.003446	UUUUU	1.020	0.0000	0.964	0.0000	0.964
2	1334013.0	291.1	0.003001	1336867.0	274.4	0.002792	0.070	0.792	0.0063	1.012	0.0060	1.892
3	1390575.0	460.5	0.002990	1393550.0	770.3	0.002765	0.075	0.883	0.0063	1.065	0.0060	2.000
4	1447137.0	624.2	0.002795	1450233.0	1258.2	0.002509	0.102	0.890	0.0063	1.007	0.0060	1.976
5	1503699.0	782.7	0.002812	1506916.0	1739.7	0.002425	0.137	0.946	0.0063	1.005	0.0060	2.000
6	1560261.0	935.6	0.002594	1563599.0	2213.6	0.002240	0.136	0.912	0.0063	0.952	0.0061	1.977
7	1616823.0	1085.2	0.002693	1620282.0	2687.2	0.002204	0.182	0.982	0.0063	0.958	0.0061	2.003
8	1673385.0	1233.4	0.002547	1676965.0	3157.3	0.002118	0.168	0.959	0.0063	0.938	0.0061	1.993
9	1729947.0	1377.8	0.002558	1733648.0	3623.5	0.002136	0.165	0.989	0.0063	0.962	0.0061	2.036
10	1786508.0	1519.1	0.002441	1790331.0	4087.8	0.002049	0.161	0.967	0.0063	0.937	0.0061	2.019
11	1843070.0	1658.8	0.002495	1847014.0	4548.6	0.002038	0.183	1.011	0.0063	0.945	0.0061	2.042
12	1899632.0	1797.3	0.002403	1903697.0	5007.1	0.001967	0.181	0.993	0.0063	0.925	0.0062	2.046
13	1942620.0	1901.5	0.002485	1946776.0	5444.2	0.002079	0.164	1.041		0.986		
14	1971749.0	1973.5	0.002449	1975968.0	5856.3	0.002115	0.137	1.035		1.009		
15	2000878.0	2044.5	0.002423	2005160.0	5917.8	0.002091	0.137	1.033		1.004		
16	2030149.0	2114.6	0.002381	2034493.0	5978.9	0.002091	0.122	1.024		1.009		
17	2059420.0	2183.8	0.002370	2063826.0	6039.9	0.002086	0.120	1.027		1.012		
18	2088549.0	2252.8	0.002357	2093018.0	6100.5	0.002059	0.126	1.029		1.004		
19	2117678.0	2320.8	0.002308	2122210.0	6160.2	0.002028	0.121	1.015		0.995		
20	2146808.0	2388.4	0.002329	2151401.0	6220.3	0.002082	0.106	1.032		1.026		
21	2175938.0	2456.0	0.002304	2180593.0	6280.1	0.002014	0.126	1.028		0.997		
22	2205067.0	2522.7	0.002271	2209785.0	6339.0	0.002015	0.112	1.020		1.003		
23	2234196.0	2588.0	0.002210	2238977.0	6397.4	0.001983	0.103	0.999		0.991		
24	2263467.0	2652.8	0.002236	2268310.0	6454.9	0.001951	0.128	1.017		0.979		
25	2292738.0	2718.3	0.002254	2297643.0	6513.0	0.002026	0.101	1.032		1.021		
26	2321867.0	2783.9	0.002248	2326835.0	6571.8	0.001999	0.111	1.035		1.012		
27	2350996.0	2849.5	0.002249	2356027.0	6629.6	0.001951	0.133	1.042		0.992		
28	2380126.0	2915.2	0.002253	2385218.0	6687.4	0.002010	0.108	1.049		1.026		
29	2409256.0	2980.5	0.002232	2414411.0	6745.7	0.001977	0.114	1.045		1.013		
30	2438385.0	3046.1	0.002266	2443602.0	6804.2	0.002026	0.106	1.067		1.042		
31	2467514.0	3111.3	0.002201	2472794.0	6862.6	0.001973	0.104	1.042		1.019		
32	2496785.0	3175.2	0.002185	2502127.0	6920.0	0.001954	0.106	1.039		1.013		
33	2526056.0	3239.2	0.002206	2531461.0	6978.0	0.002018	0.085	1.055		1.050		
34	2555185.0	3303.5	0.002199	2560652.0	7035.9	0.001941	0.117	1.056		1.014		
35	2584314.0	3367.4	0.002185	2589844.0	7092.8	0.001950	0.107	1.055		1.022		
36	2613444.0	3430.2	0.002121	2619036.0	7149.1	0.001904	0.102	1.029		1.001		

STANTON NUMBER RATIO BASED ON ST*PR**0.4=0.0295*REX**(-.2)*(1.-(XI/(X-XVO))**0.9)**(-1./9.)

STANTON NUMBER RATIO FOR TH=1 IS CONVERTED TO COMPARABLE TRANSPIRATION VALUE
USING ALOG(1 + B)/B EXPRESSION IN THE BLOWN SECTION

RUN 092074 VELOCITY PROFILE

REX = 0.74658E 06 REM = 1848.

XVO = 10.07 CM. DEL2 = 0.291 CM.
UINF = 9.78 M/S DEL99= 2.408 CM.
VISC = 0.15419E-04 M2/S DEL1 = 0.410 CM.
PORT = 9 H = 1.407
XLOC = 127.76 CM. CF/2 = 0.18480E-02

Y(CM.)	Y/DEL	U(M/S)	U/UINF	Y+	U+
0.025	0.011	3.31	0.338	6.9	7.87
0.028	0.012	3.42	0.350	7.6	8.14
0.030	0.013	3.57	0.365	8.3	8.50
0.033	0.014	3.63	0.371	9.0	8.63
0.038	0.016	4.01	0.410	10.4	9.54
0.046	0.019	4.35	0.444	12.5	10.34
0.056	0.023	4.79	0.489	15.2	11.38
0.069	0.028	5.09	0.520	18.7	12.10
0.084	0.035	5.38	0.550	22.9	12.80
0.102	0.042	5.58	0.570	27.7	13.26
0.122	0.051	5.79	0.592	33.2	13.78
0.145	0.060	5.91	0.604	39.5	14.05
0.170	0.071	6.15	0.629	46.4	14.64
0.201	0.083	6.27	0.641	54.7	14.91
0.236	0.098	6.38	0.652	64.4	15.18
0.277	0.115	6.53	0.667	75.5	15.52
0.323	0.134	6.71	0.686	88.0	15.95
0.373	0.155	6.86	0.701	101.8	16.31
0.437	0.181	6.98	0.714	119.1	16.61
0.513	0.213	7.16	0.732	139.9	17.03
0.615	0.255	7.40	0.756	167.6	17.59
0.742	0.308	7.64	0.781	202.3	18.16
0.894	0.371	7.95	0.813	243.8	18.91
1.046	0.435	8.17	0.835	285.4	19.44
1.199	0.498	8.40	0.859	326.9	19.98
1.351	0.561	8.63	0.882	368.5	20.52
1.504	0.624	8.86	0.906	410.1	21.06
1.656	0.688	9.03	0.923	451.6	21.48
1.808	0.751	9.21	0.942	493.2	21.91
1.961	0.814	9.38	0.959	534.7	22.31
2.113	0.878	9.50	0.971	576.3	22.60
2.266	0.941	9.62	0.983	617.8	22.87
2.418	1.004	9.71	0.992	659.4	23.08
2.570	1.067	9.75	0.997	701.0	23.20
2.723	1.131	9.78	1.000	742.5	23.26

RUN 092074 *** DISCRETE HOLE RIG *** NAS-3-14336 STANTON NUMBER DATA

TADB= 23.61 DEG C UINF= 9.77 M/S TINF= 23.57 DEG C
RHO= 1.177 KG/M3 VISC= 0.15419E-04 M2/S XVO= 3.6 CM
CP= 1015. J/KGK PR= 0.717

*** 1900STEPFP P/D =5 ***

PLATE	X	REX	TO	REENTH	STANTON NO	DST	DREEN	ST(THEO)	RATIO
1	127.8	0.78737E 06	37.16	0.65659E 02	0.40778E-02	0.118E-03	2.	0.34758E-02	1.173
2	132.8	0.81958E 06	37.20	0.18724E 03	0.34731E-02	0.109E-03	3.	0.30647E-02	1.133
3	137.9	0.85178E 06	37.20	0.29626E 03	0.32976E-02	0.107E-03	4.	0.28851E-02	1.143
4	143.0	0.88398E 06	37.16	0.40081E 03	0.31954E-02	0.106E-03	5.	0.27696E-02	1.154
5	148.1	0.91619E 06	37.18	0.50159E 03	0.30636E-02	0.104E-03	5.	0.26842E-02	1.141
6	153.2	0.94839E 06	37.20	0.59833E 03	0.29447E-02	0.102E-03	6.	0.26165E-02	1.125
7	158.2	0.98059E 06	37.18	0.69291E 03	0.29288E-02	0.102E-03	6.	0.25604E-02	1.144
8	163.3	0.10128E 07	37.16	0.78585E 03	0.28434E-02	0.101E-03	7.	0.25123E-02	1.132
9	168.4	0.10450E 07	37.16	0.87605E 03	0.27586E-02	0.100E-03	7.	0.24704E-02	1.117
10	173.5	0.10772E 07	37.16	0.96433E 03	0.27241E-02	0.999E-04	7.	0.24331E-02	1.120
11	178.6	0.11094E 07	37.16	0.10507E 04	0.26396E-02	0.989E-04	8.	0.23995E-02	1.100
12	183.6	0.11416E 07	37.20	0.11354E 04	0.26182E-02	0.985E-04	8.	0.23690E-02	1.105
13	187.5	0.11661E 07	37.11	0.11987E 04	0.25477E-02	0.102E-03	8.	0.23476E-02	1.085
14	190.1	0.11827E 07	37.07	0.12406E 04	0.25045E-02	0.103E-03	8.	0.23338E-02	1.073
15	192.7	0.11993E 07	37.37	0.12814E 04	0.24022E-02	0.100E-03	9.	0.23205E-02	1.035
16	195.4	0.12159E 07	37.35	0.13211E 04	0.23899E-02	0.983E-04	9.	0.23077E-02	1.036
17	198.0	0.12326E 07	37.33	0.13609E 04	0.23935E-02	0.985E-04	9.	0.22954E-02	1.043
18	200.6	0.12492E 07	37.33	0.14004E 04	0.23647E-02	0.978E-04	9.	0.22835E-02	1.036
19	203.2	0.12658E 07	37.31	0.14393E 04	0.23299E-02	0.951E-04	9.	0.22721E-02	1.025
20	205.8	0.12823E 07	37.43	0.14781E 04	0.23410E-02	0.964E-04	9.	0.22610E-02	1.035
21	208.5	0.12989E 07	37.37	0.15167E 04	0.23024E-02	0.943E-04	9.	0.22503E-02	1.023
22	211.1	0.13155E 07	37.45	0.15547E 04	0.22817E-02	0.956E-04	9.	0.22399E-02	1.019
23	213.7	0.13321E 07	37.39	0.15924E 04	0.22546E-02	0.935E-04	9.	0.22298E-02	1.011
24	216.3	0.13488E 07	37.49	0.16301E 04	0.22834E-02	0.962E-04	9.	0.22200E-02	1.029
25	218.9	0.13654E 07	37.43	0.16678E 04	0.22599E-02	0.946E-04	9.	0.22104E-02	1.022
26	221.6	0.13820E 07	37.31	0.17051E 04	0.22380E-02	0.983E-04	9.	0.22012E-02	1.017
27	224.2	0.13986E 07	36.31	0.17432E 04	0.23425E-02	0.913E-04	9.	0.21922E-02	1.069
28	226.8	0.14152E 07	37.37	0.17809E 04	0.22071E-02	0.982E-04	9.	0.21835E-02	1.011
29	229.4	0.14318E 07	37.30	0.18179E 04	0.22524E-02	0.919E-04	10.	0.21749E-02	1.036
30	232.0	0.14483E 07	37.68	0.18551E 04	0.22182E-02	0.949E-04	10.	0.21666E-02	1.024
31	234.6	0.14649E 07	37.68	0.18917E 04	0.21888E-02	0.922E-04	10.	0.21585E-02	1.014
32	237.3	0.14816E 07	37.56	0.19278E 04	0.21700E-02	0.915E-04	10.	0.21506E-02	1.009
33	239.9	0.14982E 07	37.51	0.19640E 04	0.21873E-02	0.922E-04	10.	0.21428E-02	1.021
34	242.5	0.15148E 07	37.30	0.20002E 04	0.21705E-02	0.891E-04	10.	0.21352E-02	1.017
35	245.1	0.15314E 07	37.49	0.20359E 04	0.21338E-02	0.937E-04	10.	0.21278E-02	1.003
36	247.8	0.15480E 07	37.14	0.20712E 04	0.21110E-02	0.102E-03	10.	0.21206E-02	0.995

RUN 092274-1 *** DISCRETE HOLE RIG *** NAS-3-14336 STANTON NUMBER DATA

TADB= 21.22 DEG C UINF= 9.79 M/S TINF= 21.18 DEG C
RHO= 1.183 KG/M3 VISC= 0.15274E-04 M2/S XVO= 3.6 CM
CP= 1012. J/KGK PR= 0.716

*** 1900STEP40 M=0.4 TH=0 P/D=5 ***

PLATE	X	REX	TO	REENTH	STANTON NO	DST	DREEN	M	F	T2	THETA	DTH
1	127.8	0.79629E 06	35.41	0.69342E 02	0.42583E-02	0.116E-03	2.					
2	132.8	0.82886E 06	35.41	0.19786E 03	0.36340E-02	0.107E-03	6.	0.40	0.0128	22.06	0.062	0.022
3	137.9	0.86143E 06	35.39	0.33907E 03	0.34489E-02	0.105E-03	9.	0.39	0.0127	22.49	0.092	0.021
4	143.0	0.89400E 06	35.35	0.48597E 03	0.32402E-02	0.102E-03	11.	0.39	0.0127	22.40	0.086	0.022
5	148.1	0.92657E 06	35.39	0.62539E 03	0.31305E-02	0.101E-03	13.	0.39	0.0127	22.39	0.085	0.022
6	153.2	0.95913E 06	35.37	0.76094E 03	0.30295E-02	0.997E-04	15.	0.38	0.0123	22.42	0.088	0.022
7	158.2	0.99170E 06	35.37	0.89393E 03	0.29796E-02	0.991E-04	16.	0.39	0.0125	22.56	0.098	0.021
8	163.3	0.10243E 07	35.39	0.10295E 04	0.29006E-02	0.981E-04	18.	0.39	0.0126	22.54	0.096	0.021
9	168.4	0.10568E 07	35.37	0.11620E 04	0.28074E-02	0.971E-04	19.	0.39	0.0125	22.55	0.097	0.021
10	173.5	0.10894E 07	35.35	0.12930E 04	0.28207E-02	0.973E-04	20.	0.37	0.0121	22.57	0.098	0.022
11	178.6	0.11220E 07	35.35	0.14228E 04	0.27642E-02	0.967E-04	21.	0.39	0.0126	22.58	0.099	0.022
12	183.6	0.11545E 07	35.35	0.15507E 04	0.25825E-02	0.946E-04	22.	0.39	0.0125	22.58	0.099	0.022
13	187.5	0.11793E 07	24.93	0.16550E 04	0.26181E-02	0.102E-03	23.					
14	190.1	0.11961E 07	34.95	0.16974E 04	0.24302E-02	0.995E-04	23.					
15	192.7	0.12128E 07	35.30	0.17371E 04	0.23014E-02	0.957E-04	23.					
16	195.4	0.12297E 07	35.30	0.17755E 04	0.22682E-02	0.930E-04	23.					
17	198.0	0.12465E 07	35.31	0.18134E 04	0.22405E-02	0.922E-04	23.					
18	200.6	0.12633E 07	35.33	0.18505E 04	0.21774E-02	0.903E-04	23.					
19	203.2	0.12801E 07	35.35	0.18864E 04	0.21093E-02	0.867E-04	23.					
20	205.8	0.12969E 07	35.47	0.19219E 04	0.21075E-02	0.872E-04	23.					
21	208.5	0.13136E 07	35.45	0.19568E 04	0.20528E-02	0.849E-04	23.					
22	211.1	0.13304E 07	35.52	0.19910E 04	0.20251E-02	0.857E-04	23.					
23	213.7	0.13472E 07	35.49	0.20247E 04	0.19832E-02	0.833E-04	23.					
24	216.3	0.13640E 07	35.58	0.20581E 04	0.19965E-02	0.853E-04	23.					
25	218.9	0.13809E 07	35.52	0.20912E 04	0.19485E-02	0.831E-04	23.					
26	221.6	0.13977E 07	35.39	0.21242E 04	0.19786E-02	0.878E-04	23.					
27	224.2	0.14144E 07	34.46	0.21581E 04	0.20544E-02	0.813E-04	23.					
28	226.8	0.14312E 07	35.47	0.21916E 04	0.19373E-02	0.874E-04	23.					
29	229.4	0.14480E 07	35.39	0.22246E 04	0.19939E-02	0.822E-04	23.					
30	232.0	0.14648E 07	35.75	0.22578E 04	0.19572E-02	0.849E-04	23.					
31	234.6	0.14815E 07	35.75	0.22904E 04	0.19362E-02	0.825E-04	23.					
32	237.3	0.14984E 07	35.66	0.23229E 04	0.19287E-02	0.824E-04	23.					
33	239.9	0.15152E 07	35.60	0.23554E 04	0.19457E-02	0.829E-04	23.					
34	242.5	0.15320E 07	35.39	0.23879E 04	0.19184E-02	0.799E-04	23.					
35	245.1	0.15488E 07	35.52	0.24200E 04	0.19044E-02	0.848E-04	23.					
36	247.8	0.15656E 07	25.16	0.24518E 04	0.18828E-02	0.935E-04	23.					

UNCERTAINTY IN REX=16284. UNCERTAINTY IN F=0.05299 IN RATIO

RUN 092274-2 *** DISCRETE HOLE RIG *** NAS-3-14336 STANTON NUMBER DATA

TADB= 21.74 DEG C UINF= 9.82 M/S TINF= 21.70 DEG C
RHO= 1.181 KG/M3 VISC= 0.15321E-04 M2/S XVO= 3.6 CM
CP= 1013. J/KGK PR= 0.716

*** 1900STEP40 M=0.4 TH=1 P/D=5 ***

PLATE	X	REX	TO	REENTH	STANTON NO	DST	DREEN	M	F	T2	THETA	DTH
1	127.8	0.79638E 06	38.10	0.63026E 02	0.38700E-02	0.102E-03	2.					
2	132.8	0.82895E 06	38.10	0.17452E 03	0.29760E-02	0.894E-04	10.	0.35	0.0115	36.65	0.912	0.019
3	137.9	0.86152E 06	38.11	0.60502E 03	0.25316E-02	0.840E-04	18.	0.37	0.0121	37.21	0.945	0.019
4	143.0	0.89409E 06	38.11	0.10531E 04	0.21143E-02	0.796E-04	23.	0.36	0.0117	37.30	0.950	0.019
5	148.1	0.92666E 06	38.11	0.14825E 04	0.19749E-02	0.782E-04	27.	0.36	0.0115	37.13	0.940	0.019
6	153.2	0.95924E 06	38.11	0.18963E 04	0.17885E-02	0.765E-04	31.	0.36	0.0118	37.00	0.932	0.019
7	158.2	0.99181E 06	38.11	0.23123E 04	0.17732E-02	0.764E-04	34.	0.32	0.0103	36.94	0.928	0.019
8	163.3	0.10244E 07	38.11	0.26804E 04	0.16985E-02	0.757E-04	36.	0.32	0.0105	37.85	0.984	0.019
9	168.4	0.10570E 07	38.13	0.30698E 04	0.16089E-02	0.749E-04	39.	0.33	0.0106	37.15	0.940	0.019
10	173.5	0.10895E 07	38.13	0.34445E 04	0.15580E-02	0.745E-04	41.	0.37	0.0120	36.67	0.911	0.019
11	178.6	0.11221E 07	38.15	0.38513E 04	0.15116E-02	0.741E-04	43.	0.32	0.0105	36.53	0.901	0.019
12	183.6	0.11547E 07	38.19	0.42068E 04	0.14042E-02	0.731E-04	45.	0.37	0.0120	36.56	0.901	0.018
13	187.5	0.11794E 07	37.83	0.45936E 04	0.15212E-02	0.637E-04	46.					
14	190.1	0.11962E 07	37.73	0.46191E 04	0.15103E-02	0.665E-04	46.					
15	192.7	0.12130E 07	38.06	0.46437E 04	0.14265E-02	0.643E-04	46.					
16	195.4	0.12298E 07	38.06	0.46678E 04	0.14351E-02	0.633E-04	46.					
17	198.0	0.12467E 07	38.06	0.46919E 04	0.14441E-02	0.637E-04	46.					
18	200.6	0.12635E 07	28.06	0.47160E 04	0.14194E-02	0.632E-04	46.					
19	203.2	0.12802E 07	38.04	0.47397E 04	0.14077E-02	0.614E-04	46.					
20	205.8	0.12970E 07	38.13	0.47635E 04	0.14197E-02	0.622E-04	46.					
21	208.5	0.13138E 07	38.13	0.47869E 04	0.13703E-02	0.609E-04	46.					
22	211.1	0.13306E 07	28.10	0.48102E 04	0.14045E-02	0.628E-04	46.					
23	213.7	0.13473E 07	38.08	0.48336E 04	0.13758E-02	0.615E-04	46.					
24	216.3	0.13642E 07	38.19	0.48567E 04	0.13813E-02	0.632E-04	46.					
25	218.9	0.13810E 07	38.13	0.48797E 04	0.13576E-02	0.619E-04	46.					
26	221.6	0.13978E 07	37.94	0.49031E 04	0.14298E-02	0.658E-04	46.					
27	224.2	0.14146E 07	37.28	0.49270E 04	0.14132E-02	0.602E-04	46.					
28	226.8	0.14314E 07	38.06	0.49504E 04	0.13786E-02	0.654E-04	46.					
29	229.4	0.14481E 07	37.98	0.49739E 04	0.14213E-02	0.620E-04	46.					
30	232.0	0.14649E 07	38.21	0.49980E 04	0.14478E-02	0.654E-04	46.					
31	234.6	0.14817E 07	38.23	0.50220E 04	0.14067E-02	0.636E-04	46.					
32	237.3	0.14985E 07	38.04	0.50460E 04	0.14535E-02	0.645E-04	46.					
33	239.9	0.15154E 07	38.02	0.50703E 04	0.14369E-02	0.644E-04	46.					
34	242.5	0.15322E 07	37.81	0.50945E 04	0.14464E-02	0.627E-04	46.					
35	245.1	0.15489E 07	37.92	0.51187E 04	0.14350E-02	0.669E-04	46.					
36	247.8	0.15657E 07	37.60	0.51428E 04	0.14357E-02	0.734E-04	46.					

UNCERTAINTY IN REX=16286. UNCERTAINTY IN F=0.05296 IN RATIO

RUN 092274-1 *** DISCRETE HOLE RIG *** NAS-3-14336 STANTON NUMBER DATA

*** 1900STEP40 M=0.4 TH=0 P/D=5 ***

RUN 092274-2 *** DISCRETE HOLE RIG *** NAS-3-14336 STANTON NUMBER DATA

*** 1900STEP40 M=0.4 TH=1 P/D=5 ***

LINEAR SUPERPOSITION IS APPLIED TO STANTON NUMBER DATA FROM
RUN NUMBERS 092274-1 AND 092274-2 TO OBTAIN STANTON NUMBER DATA AT TH=0 AND TH=1

PLATE	REXCOL	RE DEL2	ST(TH=0)	REXHOT	RE DEL2	ST(TH=1)	ETA	STCR	F-COL	STHR	F-HOT	LOGB
1	796292.8	69.3	0.004258	796377.3	63.0	0.003870	UUUUU	1.044	0.0000	0.949	0.0000	0.949
2	828861.1	198.6	0.003682	828948.9	173.4	0.002908	0.210	0.869	0.0128	0.950	0.0115	2.346
3	861429.3	316.1	0.003532	861520.6	634.4	0.002455	0.305	0.933	0.0127	0.852	0.0121	2.360
4	893997.5	428.3	0.003357	894092.3	1101.7	0.002046	0.391	0.955	0.0127	0.740	0.0117	2.223
5	926565.7	535.8	0.003246	926663.9	1547.7	0.001900	0.415	0.976	0.0127	0.709	0.0115	2.199
6	959133.9	640.1	0.003156	959235.6	1981.4	0.001695	0.463	0.992	0.0123	0.649	0.0118	2.175
7	991702.1	742.2	0.003113	991807.3	2420.2	0.001673	0.463	1.015	0.0125	0.654	0.0103	2.048
8	1024270.0	842.3	0.003036	1024378.0	2809.7	0.001637	0.461	1.022	0.0126	0.653	0.0105	2.086
9	1056838.0	939.6	0.002941	1056950.0	3202.7	0.001556	0.471	1.017	0.0125	0.631	0.0106	2.086
10	1089406.0	1035.9	0.002969	1089522.0	3595.4	0.001444	0.514	1.052	0.0121	0.595	0.0120	2.218
11	1121975.0	1131.7	0.002918	1122093.0	4032.9	0.001366	0.532	1.057	0.0126	0.570	0.0105	2.027
12	1154543.0	1223.7	0.002728	1154665.0	4417.5	0.001259	0.539	1.008	0.0125	0.532	0.0120	2.151
13	1179295.0	1291.2	0.002754	1179420.0	4839.3	0.001386	0.497	1.032		0.591		
14	1196067.0	1335.7	0.002544	1196194.0	4862.7	0.001397	0.451	0.962		0.600		
15	1212840.0	1377.3	0.002410	1212968.0	4885.5	0.001319	0.453	0.919		0.569		
16	1229694.0	1417.5	0.002371	1229824.0	4907.7	0.001332	0.438	0.912		0.579		
17	1246548.0	1457.0	0.002339	1246680.0	4930.2	0.001346	0.425	0.907		0.587		
18	1263320.0	1495.7	0.002271	1263454.0	4952.7	0.001326	0.416	0.887		0.582		
19	1280093.0	1533.2	0.002196	1280229.0	4974.9	0.001321	0.398	0.864		0.583		
20	1296866.0	1570.1	0.002193	1297003.0	4997.2	0.001335	0.391	0.869		0.591		
21	1313639.0	1606.4	0.002137	1313778.0	5019.2	0.001286	0.398	0.853		0.573		
22	1330411.0	1642.0	0.002102	1330552.0	5041.2	0.001328	0.368	0.845		0.594		
23	1347184.0	1677.0	0.002058	1347327.0	5063.2	0.001301	0.368	0.832		0.584		
24	1364038.0	1711.6	0.002073	1364182.0	5085.1	0.001305	0.370	0.844		0.589		
25	1380892.0	1746.0	0.002022	1381038.0	5106.9	0.001285	0.364	0.828		0.582		
26	1397664.0	1780.2	0.002047	1397813.0	5129.1	0.001362	0.334	0.843		0.620		
27	1414437.0	1815.3	0.002134	1414587.0	5151.8	0.001334	0.375	0.884		0.610		
28	1431210.0	1850.0	0.002006	1431361.0	5174.0	0.001310	0.347	0.836		0.601		
29	1447982.0	1884.2	0.002065	1448136.0	5196.3	0.001351	0.346	0.865		0.622		
30	1464755.0	1918.5	0.002020	1464910.0	5219.3	0.001385	0.314	0.851		0.640		
31	1481528.0	1952.3	0.002002	1481685.0	5242.2	0.001341	0.330	0.849		0.623		
32	1498382.0	1985.8	0.001988	1498540.0	5265.2	0.001395	0.298	0.846		0.650		
33	1515236.0	2019.4	0.002009	1515396.0	5288.4	0.001374	0.316	0.859		0.642		
34	1532008.0	2052.8	0.001977	1532171.0	5311.6	0.001388	0.298	0.850		0.651		
35	1548781.0	2085.9	0.001963	1548945.0	5334.8	0.001377	0.298	0.848		0.648		
36	1565554.0	2118.6	0.001938	1565720.0	5358.0	0.001381	0.288	0.841		0.652		

STANTON NUMBER RATIO BASED ON ST*PR**0.4=0.0295*REX**(-.2)*(1.-(XI/(X-XVO))**0.9)**(-1./9.)

STANTON NUMBER RATIO FOR TH=1 IS CONVERTED TO COMPARABLE TRANSPIRATION VALUE
USING ALOG(1 + B)/B EXPRESSION IN THE BLOWN SECTION

RUN 090874 VELOCITY PROFILE

```
REX  = 0.24107E 07       REM  =       4720.

XVO  =       17.81 CM.   DEL2 =       0.215 CM.
UINF =       34.19 M/S   DEL99=       1.914 CM.
VISC = 0.15594E-04 M2/S  DEL1 =       0.295 CM.
PORT =           9       H    =       1.369
XLOC =      127.76 CM.   CF/2 = 0.15421E-02
```

Y(CM.)	Y/DEL	U(M/S)	U/UINF	Y+	U+
0.025	0.013	17.30	0.506	21.9	12.88
0.028	0.015	17.69	0.517	24.1	13.18
0.030	0.016	18.12	0.530	26.2	13.49
0.033	0.017	18.37	0.537	28.4	13.66
0.038	0.020	18.77	0.549	32.8	13.98
0.043	0.023	19.18	0.561	37.2	14.28
0.051	0.027	19.63	0.574	43.7	14.62
0.061	0.032	20.03	0.586	52.5	14.92
0.074	0.038	20.43	0.598	63.4	15.22
0.089	0.046	21.02	0.615	76.5	15.66
0.107	0.056	21.52	0.629	91.8	16.03
0.127	0.066	21.97	0.643	109.3	16.37
0.150	0.078	22.39	0.655	129.0	16.68
0.175	0.092	23.01	0.673	150.9	17.14
0.206	0.107	23.28	0.681	177.1	17.34
0.241	0.126	23.96	0.701	207.8	17.85
0.282	0.147	24.55	0.718	242.7	18.29
0.356	0.186	25.33	0.741	306.2	18.87
0.411	0.215	25.87	0.757	354.3	19.27
0.475	0.248	26.51	0.775	408.9	19.75
0.546	0.285	27.09	0.793	470.2	20.18
0.622	0.325	27.72	0.811	535.8	20.64
0.711	0.372	28.32	0.828	612.3	21.09
0.813	0.425	29.08	0.851	699.8	21.66
0.927	0.484	29.80	0.872	798.2	22.20
1.054	0.551	30.56	0.894	907.5	22.76
1.181	0.617	30.94	0.905	1016.9	23.05
1.308	0.683	31.96	0.935	1126.2	23.80
1.435	0.750	32.53	0.951	1235.6	24.25
1.562	0.816	33.05	0.967	1344.9	24.62
1.689	0.883	33.37	0.976	1454.3	24.86
1.816	0.949	33.73	0.986	1563.6	25.12
1.943	1.015	34.03	0.995	1672.9	25.34
2.070	1.082	34.14	0.999	1782.3	25.43
2.197	1.148	34.19	1.000	1891.6	25.47

RUN 090874 *** DISCRETE HOLE RIG *** NAS-3-14336 STANTON NUMBER DATA

TADB= 26.38 DEG C UINF= 34.25 M/S TINF= 25.86 DEG C
RHO= 1.169 KG/M3 VISC= 0.15620E-04 M2/S XVO= 17.8 CM
CP= 1014. J/KGK PR= 0.717

*** 4700STEPFP P/D=5 ***

PLATE	X	REX	TO	REENTH	STANTON NO	DST	DREEN	ST(THEO)	RATIO
1	127.8	0.24108E 07	35.64	0.16943E 03	0.30424E-02	0.557E-04	3.	0.27424E-02	1.109
2	132.8	0.25222E 07	35.64	0.48866E 03	0.26901E-02	0.519E-04	5.	0.24169E-02	1.113
3	137.9	0.26335E 07	35.64	0.78162E 03	0.25706E-02	0.506E-04	7.	0.22743E-02	1.130
4	143.0	0.27449E 07	35.66	0.10608E 04	0.24422E-02	0.492E-04	8.	0.21823E-02	1.119
5	148.1	0.28563E 07	35.66	0.13298E 04	0.23880E-02	0.487E-04	9.	0.21143E-02	1.129
6	153.2	0.29677E 07	35.64	0.15931E 04	0.23413E-02	0.483E-04	10.	0.20602E-02	1.136
7	158.2	0.30791E 07	35.64	0.18510E 04	0.22891E-02	0.478E-04	10.	0.20153E-02	1.136
8	163.3	0.31904E 07	35.66	0.21024E 04	0.22253E-02	0.471E-04	11.	0.19769E-02	1.126
9	168.4	0.33018E 07	35.64	0.23482E 04	0.21875E-02	0.468E-04	12.	0.19434E-02	1.126
10	173.5	0.34132E 07	35.64	0.25892E 04	0.21413E-02	0.464E-04	12.	0.19135E-02	1.119
11	178.6	0.35246E 07	35.64	0.28259E 04	0.21091E-02	0.461E-04	13.	0.18867E-02	1.118
12	183.6	0.36359E 07	35.62	0.30581E 04	0.20607E-02	0.457E-04	13.	0.18623E-02	1.107
13	187.5	0.37206E 07	35.26	0.32279E 04	0.19170E-02	0.673E-04	14.	0.18451E-02	1.039
14	190.1	0.37780E 07	35.10	0.33385E 04	0.19321E-02	0.684E-04	14.	0.18341E-02	1.053
15	192.7	0.38353E 07	35.45	0.34490E 04	0.19178E-02	0.687E-04	14.	0.18234E-02	1.052
16	195.4	0.38929E 07	35.43	0.35587E 04	0.19006E-02	0.674E-04	15.	0.18132E-02	1.048
17	198.0	0.39506E 07	35.43	0.36678E 04	0.19004E-02	0.675E-04	15.	0.18033E-02	1.054
18	200.6	0.40079E 07	35.41	0.37768E 04	0.18966E-02	0.674E-04	15.	0.17938E-02	1.057
19	203.2	0.40653E 07	35.39	0.38846E 04	0.18562E-02	0.656E-04	16.	0.17847E-02	1.040
20	205.8	0.41227E 07	35.47	0.39918E 04	0.18785E-02	0.667E-04	16.	0.17758E-02	1.058
21	208.5	0.41800E 07	35.41	0.40987E 04	0.18424E-02	0.651E-04	16.	0.17672E-02	1.043
22	211.1	0.42374E 07	35.49	0.42044E 04	0.18398E-02	0.658E-04	16.	0.17589E-02	1.046
23	213.7	0.42947E 07	35.41	0.43091E 04	0.18075E-02	0.641E-04	16.	0.17509E-02	1.032
24	216.3	0.43524E 07	35.52	0.44139E 04	0.18404E-02	0.660E-04	17.	0.17430E-02	1.056
25	218.9	0.44100E 07	35.45	0.45196E 04	0.18424E-02	0.655E-04	17.	0.17354E-02	1.062
26	221.6	0.44674E 07	35.41	0.46248E 04	0.18212E-02	0.678E-04	17.	0.17280E-02	1.054
27	224.2	0.45247E 07	34.19	0.47268E 04	0.17317E-02	0.594E-04	17.	0.17208E-02	1.006
28	226.8	0.45821E 07	35.35	0.48294E 04	0.18412E-02	0.686E-04	18.	0.17138E-02	1.074
29	229.4	0.46395E 07	35.30	0.49329E 04	0.17616E-02	0.621E-04	18.	0.17070E-02	1.032
30	232.0	0.46968E 07	35.70	0.50360E 04	0.18312E-02	0.660E-04	18.	0.17003E-02	1.077
31	234.6	0.47542E 07	35.68	0.51401E 04	0.17919E-02	0.640E-04	18.	0.16939E-02	1.058
32	237.3	0.48118E 07	35.51	0.52422E 04	0.17647E-02	0.628E-04	18.	0.16875E-02	1.046
33	239.9	0.48695E 07	35.51	0.53438E 04	0.17729E-02	0.638E-04	19.	0.16813E-02	1.054
34	242.5	0.49268E 07	35.20	0.54451E 04	0.17569E-02	0.617E-04	19.	0.16753E-02	1.049
35	245.1	0.49842E 07	35.49	0.55465E 04	0.17735E-02	0.647E-04	19.	0.16694E-02	1.062
36	247.8	0.50415E 07	35.31	0.56479E 04	0.17592E-02	0.674E-04	19.	0.16636E-02	1.057

RUN 091474 *** DISCRETE HOLE RIG *** NAS-3-14336 STANTON NUMBER DATA

TADB= 26.19 DEG C UINF= 34.16 M/S TINF= 25.67 DEG C
RHO= 1.171 KG/M3 VISC= 0.15579E-04 M2/S XVO= 17.8 CM
CP= 1015. J/KGK PR= 0.717

*** 4700STEP40 M=0.4 TH=0 P/D=5 ***

PLATE	X	REX	TO	REENTH	STANTON NO	DST	DREEN	M	F	T2	THETA	DTH
1	127.8	0.24111E 07	35.01	0.17080E 03	0.30665E-02	0.587E-04	3.					
2	132.8	0.25225E 07	34.99	0.48837E 03	0.26353E-02	0.539E-04	24.	0.40	0.0128	25.89	0.023	0.033
3	137.9	0.26339E 07	35.03	0.80813E 03	0.25062E-02	0.523E-04	41.	0.39	0.0127	26.03	0.038	0.033
4	143.0	0.27453E 07	35.01	0.11367E 04	0.24244E-02	0.515E-04	53.	0.39	0.0128	26.04	0.039	0.033
5	148.1	0.28567E 07	34.99	0.14597E 04	0.23821E-02	0.512E-04	63.	0.39	0.0127	26.04	0.039	0.033
6	153.2	0.29681E 07	35.01	0.17773E 04	0.23207E-02	0.504E-04	71.	0.39	0.0128	26.04	0.039	0.033
7	158.2	0.30795E 07	35.03	0.20919E 04	0.23222E-02	0.504E-04	79.	0.39	0.0128	26.19	0.055	0.033
8	163.3	0.31908E 07	35.01	0.24287E 04	0.23121E-02	0.504E-04	86.	0.40	0.0128	26.17	0.054	0.033
9	168.4	0.33022E 07	35.01	0.27604E 04	0.22736E-02	0.500E-04	92.	0.40	0.0129	26.17	0.053	0.033
10	173.5	0.34136E 07	35.01	0.30912E 04	0.22862E-02	0.501E-04	98.	0.39	0.0127	26.14	0.050	0.033
11	178.6	0.35250E 07	35.03	0.34147E 04	0.22454E-02	0.496E-04	103.	0.39	0.0128	26.18	0.055	0.033
12	183.6	0.36364E 07	35.01	0.37400E 04	0.22015E-02	0.492E-04	109.	0.40	0.0128	26.17	0.053	0.033
13	187.5	0.37211E 07	34.40	0.40008E 04	0.21706E-02	0.759E-04	111.					
14	190.1	0.37784E 07	34.30	0.41239E 04	0.21156E-02	0.757E-04	111.					
15	192.7	0.38358E 07	34.67	0.42442E 04	0.20734E-02	0.748E-04	111.					
16	195.4	0.38935E 07	34.70	0.43617E 04	0.20190E-02	0.722E-04	111.					
17	198.0	0.39511E 07	34.76	0.44768E 04	0.19888E-02	0.712E-04	111.					
18	200.6	0.40085E 07	34.78	0.45899E 04	0.19496E-02	0.698E-04	111.					
19	203.2	0.40658E 07	34.80	0.46999E 04	0.18807E-02	0.670E-04	112.					
20	205.8	0.41232E 07	34.91	0.48081E 04	0.18860E-02	0.674E-04	112.					
21	208.5	0.41806E 07	34.89	0.49146E 04	0.18230E-02	0.650E-04	112.					
22	211.1	0.42379E 07	34.97	0.50189E 04	0.18105E-02	0.652E-04	112.					
23	213.7	0.42953E 07	34.93	0.51217E 04	0.17673E-02	0.632E-04	112.					
24	216.3	0.43530E 07	35.09	0.52236E 04	0.17826E-02	0.646E-04	112.					
25	218.9	0.44106E 07	35.01	0.53260E 04	0.17826E-02	0.640E-04	112.					
26	221.6	0.44680E 07	34.93	0.54279E 04	0.17641E-02	0.662E-04	112.					
27	224.2	0.45253E 07	33.77	0.55274E 04	0.17019E-02	0.589E-04	112.					
28	226.8	0.45827E 07	34.93	0.56271E 04	0.17701E-02	0.667E-04	112.					
29	229.4	0.46401E 07	34.88	0.57270E 04	0.17083E-02	0.607E-04	112.					
30	232.0	0.46974E 07	35.26	0.58266E 04	0.17592E-02	0.639E-04	112.					
31	234.6	0.47548E 07	35.24	0.59267E 04	0.17270E-02	0.621E-04	112.					
32	237.3	0.48124E 07	35.09	0.60251E 04	0.16989E-02	0.611E-04	112.					
33	239.9	0.48701E 07	35.03	0.61235E 04	0.17273E-02	0.626E-04	112.					
34	242.5	0.49275E 07	34.74	0.62222E 04	0.17111E-02	0.607E-04	112.					
35	245.1	0.49848E 07	34.99	0.63209E 04	0.17242E-02	0.635E-04	112.					
36	247.8	0.50422E 07	34.80	0.64192E 04	0.16998E-02	0.662E-04	112.					

UNCERTAINTY IN REX=55696. UNCERTAINTY IN F=0.05002 IN RATIO

RUN 091674 *** DISCRETE HOLE RIG *** NAS-3-14336 STANTON NUMBER DATA

TADB= 24.41 DEG C UINF= 33.83 M/S TINF= 23.91 DEG C
RHO= 1.178 KG/M3 VISC= 0.15411E-04 M2/S XVO= 17.8 CM
CP= 1015. J/KGK PR= 0.717

*** 4700STEP40 M=0.4 TH=1 P/D=5 ***

PLATE	X	REX	TO	REENTH	STANTON NO	DST	DREEN	M	F	T2	THETA	DTH
1	127.8	0.24137E 07	36.71	0.16627E 03	0.29820E-02	0.420E-04	2.					
2	132.8	0.25252E 07	36.71	0.46104E 03	0.23048E-02	0.365E-04	38.	0.37	0.0120	36.74	1.003	0.024
3	137.9	0.26367E 07	36.71	0.20262E 04	0.17966E-02	0.329E-04	65.	0.37	0.0119	36.67	0.997	0.024
4	143.0	0.27482E 07	36.71	0.35331E 04	0.14853E-02	0.310E-04	83.	0.37	0.0120	36.80	1.007	0.024
5	148.1	0.28598E 07	36.69	0.50378E 04	0.13982E-02	0.305E-04	99.	0.38	0.0123	36.74	1.004	0.024
6	153.2	0.29713E 07	36.69	0.65665E 04	0.13360E-02	0.302E-04	113.	0.38	0.0123	36.39	0.977	0.024
7	158.2	0.30828E 07	36.71	0.80535E 04	0.13005E-02	0.300E-04	124.	0.37	0.0120	36.43	0.978	0.024
8	163.3	0.31943E 07	36.67	0.95104E 04	0.12894E-02	0.300E-04	135.	0.38	0.0121	36.65	0.998	0.024
9	168.4	0.33058E 07	36.69	0.11002E 05	0.12055E-02	0.295E-04	145.	0.38	0.0122	36.43	0.980	0.024
10	173.5	0.34173E 07	36.67	0.12465E 05	0.11937E-02	0.295E-04	154.	0.38	0.0122	36.12	0.957	0.024
11	178.6	0.35288E 07	36.67	0.13903E 05	0.11557E-02	0.293E-04	163.	0.38	0.0122	35.77	0.930	0.024
12	183.6	0.36404E 07	36.71	0.15294E 05	0.11103E-02	0.290E-04	170.	0.38	0.0124	35.13	0.877	0.024
13	187.5	0.37251E 07	36.52	0.16599E 05	0.11080E-02	0.387E-04	174.					
14	190.1	0.37825E 07	36.31	0.16664E 05	0.11581E-02	0.404E-04	174.					
15	192.7	0.38400E 07	36.59	0.16731E 05	0.11750E-02	0.416E-04	174.					
16	195.4	0.38977E 07	36.61	0.16798E 05	0.11589E-02	0.406E-04	174.					
17	198.0	0.39554E 07	36.61	0.16865E 05	0.11606E-02	0.407E-04	174.					
18	200.6	0.40128E 07	36.57	0.16931E 05	0.11598E-02	0.407E-04	174.					
19	203.2	0.40702E 07	36.53	0.16997E 05	0.11348E-02	0.395E-04	174.					
20	205.8	0.41277E 07	36.61	0.17063E 05	0.11549E-02	0.404E-04	174.					
21	208.5	0.41851E 07	36.59	0.17128E 05	0.11183E-02	0.392E-04	174.					
22	211.1	0.42425E 07	36.61	0.17193E 05	0.11348E-02	0.401E-04	174.					
23	213.7	0.43000E 07	36.57	0.17258E 05	0.11107E-02	0.389E-04	174.					
24	216.3	0.43577E 07	36.71	0.17322E 05	0.11348E-02	0.404E-04	174.					
25	218.9	0.44154E 07	36.63	0.17388E 05	0.11444E-02	0.403E-04	174.					
26	221.6	0.44728E 07	36.52	0.17453E 05	0.11379E-02	0.419E-04	174.					
27	224.2	0.45302E 07	35.45	0.17516E 05	0.10411E-02	0.347E-04	174.					
28	226.8	0.45877E 07	36.50	0.17579E 05	0.11477E-02	0.425E-04	174.					
29	229.4	0.46451E 07	36.40	0.17644E 05	0.11255E-02	0.390E-04	174.					
30	232.0	0.47025E 07	36.74	0.17711E 05	0.11812E-02	0.421E-04	174.					
31	234.6	0.47599E 07	36.72	0.17778E 05	0.11607E-02	0.410E-04	174.					
32	237.3	0.48177E 07	36.52	0.17845E 05	0.11570E-02	0.406E-04	174.					
33	239.9	0.48754E 07	36.46	0.17912E 05	0.11767E-02	0.417E-04	174.					
34	242.5	0.49328E 07	36.17	0.17979E 05	0.11624E-02	0.401E-04	174.					
35	245.1	0.49902E 07	36.38	0.18047E 05	0.11893E-02	0.428E-04	174.					
36	247.8	0.50477E 07	36.17	0.18115E 05	0.11733E-02	0.449E-04	174.					

UNCERTAINTY IN REX=55757. UNCERTAINTY IN F=0.05002 IN RATIO

RUN 091474 *** DISCRETE HOLE RIG *** NAS-3-14336 STANTON NUMBER DATA

*** 4700STEP40 M=0.4 TH=0 P/D=5 ***

RUN 091674 *** DISCRETE HOLE RIG *** NAS-3-14336 STANTON NUMBER DATA

*** 4700STEP40 M=0.4 TH=1 P/D=5 ***

LINEAR SUPERPOSITION IS APPLIED TO STANTON NUMBER DATA FROM
RUN NUMBERS 091474 AND 091674 TO OBTAIN STANTON NUMBER DATA AT TH=0 AND TH=1

PLATE	REXCOL	RE DEL2	ST(TH=0)	REXHOT	RE DEL2	ST(TH=1)	ETA	STCR	F-COL	STHR	F-HOT	LOGB
1	2411097.0	170.8	0.003067	2413706.0	166.3	0.002982	UUUUU	1.008	0.0000	0.980	0.0000	0.980
2	2522490.0	438.8	0.002643	2525219.0	461.1	0.002306	0.128	0.800	0.0128	0.955	0.0120	2.716
3	2633883.0	776.9	0.002529	2636732.0	2022.5	0.001797	0.290	0.857	0.0127	0.791	0.0119	2.579
4	2745276.0	1054.8	0.002462	2748246.0	3533.3	0.001487	0.396	0.899	0.0128	0.682	0.0120	2.492
5	2856669.0	1326.9	0.002422	2859759.0	5028.9	0.001404	0.420	0.935	0.0127	0.665	0.0123	2.554
6	2968062.0	1593.3	0.002361	2971272.0	6551.4	0.001326	0.438	0.952	0.0128	0.644	0.0123	2.564
7	3079455.0	1857.0	0.002374	3082786.0	8068.0	0.001276	0.463	0.993	0.0128	0.634	0.0120	2.548
8	3190847.0	2121.4	0.002372	3194299.0	9551.6	$\boxed{0.001277}$	0.462	1.024	0.0128	0.646	0.0121	2.613
9	3302240.0	2383.5	0.002335	3305812.0	11043.6	0.001193	0.489	1.036	0.0129	0.614	0.0122	2.594
10	3413633.0	2644.3	0.002348	3417326.0	12532.1	0.001156	0.508	1.067	0.0127	0.604	0.0122	2.613
11	3525026.0	2903.7	0.002310	3528839.0	14022.7	0.001086	0.530	1.073	0.0128	0.576	0.0122	2.585
12	3636419.0	3158.8	0.002271	3640352.0	15499.2	0.000986	0.566	1.076	0.0128	0.530	0.0124	2.552
13	3721078.0	3349.5	0.002238	3725103.0	16963.2	0.000987	0.559	1.076		0.535		
14	3778445.0	3476.3	0.002176	3782532.0	17021.7	0.001049	0.518	1.055		0.572		
15	3835812.0	3600.0	0.002130	3839961.0	17082.7	0.001073	0.497	1.042		0.589		
16	3893457.0	3720.7	0.002074	3897669.0	17144.0	0.001061	0.488	1.023		0.586		
17	3951103.0	3838.9	0.002041	3955377.0	17205.2	0.001066	0.478	1.015		0.592		
18	4008470.0	3954.9	0.002000	4012807.0	17266.6	0.001070	0.465	1.002		0.597		
19	4065838.0	4067.7	0.001928	4070236.0	17327.5	0.001050	0.455	0.973		0.589		
20	4123205.0	4178.6	0.001932	4127665.0	17388.5	0.001071	0.445	0.982		0.604		
21	4180573.0	4287.7	0.001868	4185095.0	17449.1	0.001038	0.444	0.956		0.588		
22	4237940.0	4394.5	0.001853	4242525.0	17509.4	0.001058	0.429	0.955		0.602		
23	4295308.0	4499.7	0.001809	4299954.0	17569.6	0.001036	0.427	0.938		0.592		
24	4352953.0	4604.1	0.001824	4357662.0	17629.9	0.001061	0.418	0.952		0.609		
25	4410599.0	4708.8	0.001823	4415370.0	17691.2	0.001072	0.412	0.957		0.618		
26	4467966.0	4812.9	0.001804	4472799.0	17752.6	0.001066	0.409	0.953		0.618		
27	4525333.0	4914.8	0.001744	4530229.0	17811.1	0.000966	0.446	0.927		0.562		
28	4582700.0	5016.9	0.001810	4587658.0	17869.8	0.001077	0.405	0.967		0.629		
29	4640069.0	5118.9	0.001745	4645088.0	17931.2	0.001059	0.393	0.938		0.621		
30	4697436.0	5220.6	0.001796	4702517.0	17993.7	0.001115	0.379	0.970		0.656		
31	4754803.0	5322.3	0.001763	4759947.0	18057.3	0.001096	0.378	0.957		0.648		
32	4812448.0	5423.2	0.001733	4817654.0	18120.3	0.001095	0.368	0.946		0.649		
33	4870094.0	5523.6	0.001762	4875363.0	18183.8	0.001114	0.368	0.967		0.663		
34	4927462.0	5624.4	0.001746	4932792.0	18247.4	0.001100	0.370	0.962		0.657		
35	4984829.0	5725.0	0.001758	4990221.0	18311.5	0.001128	0.358	0.974		0.676		
36	5042196.0	5825.3	0.001733	5047650.0	18375.9	0.001113	0.358	0.964		0.670		

STANTON NUMBER RATIO BASED ON ST*PR**0.4=0.0295*REX**(-.2)*(1.-(XI/(X-XVO))**0.9)**(-1./9.)

STANTON NUMBER RATIO FOR TH=1 IS CONVERTED TO COMPARABLE TRANSPIRATION VALUE
USING ALOG(1 + B)/B EXPRESSION IN THE BLOWN SECTION

RUN 102274 VELOCITY AND TEMPERATURE PROFILES

REX = 0.15100E 06		REM = 515.		REH = 448.	
XVC =	108.36 CM.	DEL2 =	0.066 CM.	DEH2 =	0.058 CM.
UINF =	11.83 M/S	DEL99=	0.476 CM.	DELT99 =	0.456 CM.
VISC =	0.15200E-04 M2/S	DEL1 =	0.130 CM.	UINF =	11.84 M/S
PORT =	19	H =	1.959	VISC =	0.15238E-04 M2/S
XLCC =	127.76 CM.	CF/2 =	0.17374E-02	TINF =	21.54 DEG C
				TPLATE =	38.29 DEG C

Y(CM.)	Y/DEL	U(M/S)	U/UINF	Y+	U+	Y(CM.)	T(DEG C)	TBAR	TBAR
0.025	0.053	4.14	0.350	8.2	8.41	0.0165	35.44	0.171	0.829
0.028	0.059	4.36	0.369	9.1	8.85	0.0190	34.66	0.217	0.783
0.030	0.064	4.40	0.372	9.9	8.93	0.0216	33.76	0.271	0.729
0.033	0.069	4.51	0.382	10.7	9.15	0.0241	33.35	0.295	0.705
0.038	0.080	4.71	0.398	12.4	9.56	0.0292	32.68	0.336	0.664
0.043	0.091	4.86	0.411	14.0	9.86	0.0343	32.09	0.371	0.629
0.051	0.107	5.09	0.430	16.5	10.32	0.0394	31.61	0.400	0.600
0.058	0.123	5.38	0.455	19.0	10.91	0.0444	31.26	0.421	0.579
0.069	0.144	5.55	0.469	22.2	11.25	0.0521	30.81	0.448	0.552
0.081	0.171	5.91	0.500	26.4	11.98	0.0597	30.49	0.467	0.533
0.094	0.197	6.25	0.528	30.5	12.67	0.0698	29.97	0.498	0.502
0.109	0.229	6.66	0.563	35.4	13.51	0.0825	29.54	0.524	0.476
0.127	0.267	6.98	0.590	41.2	14.16	0.0952	28.93	0.560	0.440
0.147	0.309	7.38	0.624	47.8	14.97	0.1105	28.48	0.588	0.412
0.168	0.352	7.91	0.669	54.4	16.05	0.1283	27.78	0.629	0.371
0.191	0.400	8.51	0.720	61.8	17.27	0.1486	26.95	0.679	0.321
0.213	0.448	8.99	0.760	69.2	18.22	0.1714	26.31	0.717	0.283
0.236	0.496	9.40	0.795	76.6	19.06	0.1994	25.38	0.774	0.226
0.262	0.550	9.88	0.835	84.9	20.03	0.2248	24.58	0.821	0.179
0.287	0.603	10.26	0.867	93.1	20.81	0.2502	23.97	0.858	0.142
0.312	0.656	10.60	0.896	101.3	21.49	0.2756	23.39	0.893	0.107
0.338	0.710	10.92	0.923	109.6	22.15	0.3010	22.96	0.919	0.081
0.376	0.790	11.26	0.952	121.9	22.84	0.3264	22.61	0.940	0.060
0.414	0.870	11.47	0.970	134.3	23.26	0.3645	22.22	0.962	0.038
0.452	0.950	11.63	0.984	146.7	23.60	0.4026	21.96	0.978	0.022
0.490	1.030	11.75	0.993	159.0	23.83	0.4407	21.80	0.988	0.012
0.528	1.110	11.80	0.997	171.4	23.93	0.4788	21.71	0.993	0.007
0.566	1.190	11.83	1.000	183.7	23.99	0.5169	21.64	0.998	0.002
						0.555	21.61	0.999	0.001
						0.593	21.60	1.000	0.000

RUN 102274 *** DISCRETE HOLE RIG *** NAS-3-14336 STANTON NUMBER DATA

TADB= 21.40 DEG C UINF= 11.74 M/S TINF= 21.33 DEG C
RHO= 1.188 KG/M3 VISC= 0.15218E-04 M2/S XVO= 108.4 CM
CP= 1013. J/KGK PR= 0.717

*** 520HSLFP P/D=5 ***

PLATE	X	REX	TO	REENTH	STANTON NO	DST	DREEN	ST(THEO)	RATIO
1	127.8	0.14973E 06	38.10	0.43899E 03	0.27628E-02	0.689E-04	20.	0.31093E-02	0.889
2	132.8	0.18892E 06	38.08	0.55327E 03	0.30687E-02	0.717E-04	20.	0.29681E-02	1.034
3	137.9	0.22812E 06	38.08	0.67220E 03	0.30001E-02	0.711E-04	20.	0.28582E-02	1.050
4	143.0	0.26731E 06	38.08	0.78825E 03	0.29214E-02	0.703E-04	20.	0.27690E-02	1.055
5	148.1	0.30651E 06	38.10	0.90145E 03	0.28546E-02	0.697E-04	20.	0.26943E-02	1.060
6	153.2	0.34570E 06	38.11	0.10108E 04	0.27267E-02	0.685E-04	20.	0.26302E-02	1.037
7	158.2	0.38490E 06	38.08	0.11178E 04	0.27297E-02	0.687E-04	20.	0.25743E-02	1.060
8	163.3	0.42409E 06	38.08	0.12228E 04	0.26337E-02	0.678E-04	20.	0.25249E-02	1.043
9	168.4	0.46329E 06	38.10	0.13250E 04	0.25812E-02	0.673E-04	20.	0.24806E-02	1.041
10	173.5	0.50248E 06	38.11	0.14245E 04	0.24944E-02	0.666E-04	20.	0.24406E-02	1.022
11	178.6	0.54168E 06	38.11	0.15219E 04	0.24739E-02	0.664E-04	21.	0.24043E-02	1.029
12	183.6	0.58087E 06	38.08	0.16181E 04	0.24375E-02	0.662E-04	21.	0.23709E-02	1.028
13	187.5	0.61066E 06	36.40	0.16872E 04	0.21056E-02	0.726E-04	21.	0.23473E-02	0.897
14	190.1	0.63085E 06	36.08	0.17300E 04	0.21353E-02	0.801E-04	21.	0.23321E-02	0.916
15	192.7	0.65103E 06	36.31	0.17730E 04	0.21177E-02	0.810E-04	21.	0.23174E-02	0.914
16	195.4	0.67132E 06	36.31	0.18156E 04	0.21026E-02	0.796E-04	21.	0.23033E-02	0.913
17	198.0	0.69160E 06	36.33	0.18581E 04	0.21004E-02	0.799E-04	21.	0.22896E-02	0.917
18	200.6	0.71178E 06	36.27	0.19005E 04	0.21000E-02	0.798E-04	21.	0.22765E-02	0.922
19	203.2	0.73197E 06	36.21	0.19428E 04	0.20775E-02	0.779E-04	21.	0.22638E-02	0.918
20	205.8	0.75216E 06	36.31	0.19849E 04	0.20934E-02	0.793E-04	21.	0.22515E-02	0.930
21	208.5	0.77234E 06	36.23	0.20270E 04	0.20711E-02	0.780E-04	21.	0.22396E-02	0.925
22	211.1	0.79253E 06	36.27	0.20690E 04	0.20838E-02	0.797E-04	21.	0.22281E-02	0.935
23	213.7	0.81271E 06	36.23	0.21106E 04	0.20390E-02	0.776E-04	21.	0.22169E-02	0.920
24	216.3	0.83300E 06	36.33	0.21520E 04	0.20504E-02	0.797E-04	21.	0.22060E-02	0.929
25	218.9	0.85328E 06	36.15	0.21933E 04	0.20422E-02	0.780E-04	21.	0.21954E-02	0.930
26	221.6	0.87346E 06	36.06	0.22346E 04	0.20441E-02	0.823E-04	21.	0.21851E-02	0.935
27	224.2	0.89365E 06	35.01	0.22761E 04	0.20606E-02	0.733E-04	21.	0.21752E-02	0.947
28	226.8	0.91384E 06	36.12	0.23174E 04	0.20280E-02	0.826E-04	21.	0.21655E-02	0.937
29	229.4	0.93402E 06	36.04	0.23590E 04	0.20861E-02	0.776E-04	21.	0.21560E-02	0.968
30	232.0	0.95421E 06	36.48	0.24006E 04	0.20315E-02	0.799E-04	21.	0.21468E-02	0.946
31	234.6	0.97439E 06	36.42	0.24417E 04	0.20396E-02	0.780E-04	21.	0.21379E-02	0.954
32	237.3	0.99468E 06	36.34	0.24825E 04	0.19949E-02	0.770E-04	21.	0.21291E-02	0.937
33	239.9	0.10150E 07	36.27	0.25232E 04	0.20320E-02	0.782E-04	21.	0.21205E-02	0.958
34	242.5	0.10351E 07	36.04	0.25638E 04	0.19841E-02	0.746E-04	21.	0.21122E-02	0.939
35	245.1	0.10553E 07	36.21	0.26039E 04	0.19910E-02	0.794E-04	21.	0.21040E-02	0.946
36	247.8	0.10755E 07	35.89	0.26436E 04	0.19315E-02	0.850E-04	21.	0.20961E-02	0.921

RUN 103074-1 *** DISCRETE HOLE RIG *** NAS-3-14336 STANTON NUMBER DATA

TADB= 20.29 DEG C U INF= 11.70 M/S T INF= 20.23 DEG C
RHO= 1.200 KG/M3 VISC= 0.15041E-04 M2/S XVO= 108.4 CM
CP= 1011. J/KGK PR= 0.716

*** 520HSL40 M=0.4 TH=0 P/D=5 ***

PLATE	X	REX	TO	REENTH	STANTON NO	DST	DREEN	M	F	T2	THETA	DTH
1	127.8	0.15085E 06	36.06	0.48211E 03	0.29776E-02	0.736E-04	20.					
2	132.8	0.19047E 06	36.08	0.60465E 03	0.32246E-02	0.759E-04	21.	0.42	0.0137	21.58	0.085	0.019
3	137.9	0.22999E 06	36.08	0.77660E 03	0.31458E-02	0.751E-04	22.	0.41	0.0134	21.96	0.109	0.019
4	143.0	0.26951E 06	36.13	0.95585E 03	0.29995E-02	0.736E-04	23.	0.41	0.0132	21.89	0.104	0.019
5	148.1	0.30902E 06	36.08	0.11284E 04	0.29808E-02	0.736E-04	25.	0.40	0.0131	21.86	0.103	0.019
6	153.2	0.34854E 06	36.10	0.12974E 04	0.28816E-02	0.726E-04	26.	0.40	0.0130	21.94	0.108	0.019
7	158.2	0.38806E 06	36.06	0.14667E 04	0.28799E-02	0.728E-04	27.	0.42	0.0137	22.06	0.115	0.019
8	163.3	0.42757E 06	36.02	0.16428E 04	0.28699E-02	0.728E-04	28.	0.41	0.0133	21.96	0.109	0.019
9	168.4	0.46709E 06	36.08	0.18127E 04	0.28183E-02	0.721E-04	29.	0.41	0.0131	22.01	0.112	0.019
10	173.5	0.50661E 06	36.08	0.19828E 04	0.28561E-02	0.725E-04	30.	0.40	0.0131	22.02	0.113	0.019
11	178.6	0.54612E 06	36.10	0.21528E 04	0.28013E-02	0.719E-04	31.	0.40	0.0129	22.07	0.116	0.019
12	183.6	0.58564E 06	36.08	0.23208E 04	0.27017E-02	0.711E-04	32.	0.40	0.0130	22.06	0.115	0.019
13	187.5	0.61567E 06	34.17	0.24579E 04	0.23870E-02	0.809E-04	32.					
14	190.1	0.63603E 06	33.85	0.25064E 04	0.23756E-02	0.884E-04	32.					
15	192.7	0.65638E 06	34.13	0.25540E 04	0.22927E-02	0.875E-04	32.					
16	195.4	0.67683E 06	34.17	0.26002E 04	0.22427E-02	0.849E-04	32.					
17	198.0	0.69728E 06	34.21	0.26456E 04	0.22141E-02	0.841E-04	32.					
18	200.6	0.71763E 06	34.21	0.26901E 04	0.21576E-02	0.824E-04	32.					
19	203.2	0.73798E 06	34.19	0.27335E 04	0.21002E-02	0.794E-04	32.					
20	205.8	0.75833E 06	34.27	0.27765E 04	0.21203E-02	0.805E-04	32.					
21	208.5	0.77868E 06	34.27	0.28187E 04	0.20207E-02	0.769E-04	33.					
22	211.1	0.79903E 06	34.40	0.28595E 04	0.19867E-02	0.777E-04	33.					
23	213.7	0.81938E 06	34.32	0.28998E 04	0.19671E-02	0.757E-04	33.					
24	216.3	0.83983E 06	34.44	0.29399E 04	0.19722E-02	0.776E-04	33.					
25	218.9	0.86028E 06	34.34	0.29796E 04	0.19188E-02	0.750E-04	33.					
26	221.6	0.88064E 06	34.23	0.30186E 04	0.19132E-02	0.785E-04	33.					
27	224.2	0.90099E 06	33.25	0.30581E 04	0.19645E-02	0.714E-04	33.					
28	226.8	0.92134E 06	34.30	0.30975E 04	0.19068E-02	0.790E-04	33.					
29	229.4	0.94169E 06	34.28	0.31367E 04	0.19346E-02	0.738E-04	33.					
30	232.0	0.96204E 06	34.63	0.31759E 04	0.19121E-02	0.761E-04	33.					
31	234.6	0.98239E 06	34.63	0.32145E 04	0.18771E-02	0.737E-04	33.					
32	237.3	0.10028E 07	34.53	0.32526E 04	0.18631E-02	0.731E-04	33.					
33	239.9	0.10233E 07	34.51	0.32904E 04	0.18491E-02	0.732E-04	33.					
34	242.5	0.10436E 07	34.25	0.33282E 04	0.18636E-02	0.712E-04	33.					
35	245.1	0.10640E 07	34.40	0.33657E 04	0.18128E-02	0.744E-04	33.					
36	247.8	0.10843E 07	34.07	0.34021E 04	0.17657E-02	0.805E-04	33.					

UNCERTAINTY IN REX=1975. UNCERTAINTY IN F=0.05145 IN RATIO

RUN 103074-2 *** DISCRETE HOLE RIG *** NAS-3-14336 STANTON NUMBER DATA

TADB= 20.31 DEG C UINF= 11.68 M/S TINF= 20.25 DEG C
RHO= 1.200 KG/M3 VISC= 0.15043E-04 M2/S XVO= 108.4 CM
CP= 1011. J/KGK PR= 0.716

*** 520HSL40 M=0.4 TH=1 P/D=5 ***

PLATE	X	REX	TO	REENTH	STANTON NO	DST	DREEN	M	F	T2	THETA	DTH
1	127.8	0.15071E 06	37.41	0.48134E 03	0.28623E-02	0.684E-04	20.					
2	132.8	0.19017E 06	37.41	0.59124E 03	0.27090E-02	0.670E-04	23.	0.39	0.0126	35.40	0.883	0.018
3	137.9	0.22962E 06	37.41	0.11283E 04	0.22744E-02	0.635E-04	29.	0.40	0.0129	36.15	0.926	0.018
4	143.0	0.26908E 06	37.45	0.16832E 04	0.18708E-02	0.605E-04	35.	0.39	0.0125	36.16	0.925	0.018
5	148.1	0.30853E 06	37.43	0.22129E 04	0.17922E-02	0.601E-04	39.	0.40	0.0130	35.93	0.913	0.018
6	153.2	0.34798E 06	37.45	0.27492E 04	0.17142E-02	0.595E-04	43.	0.41	0.0132	35.79	0.903	0.018
7	158.2	0.38744E 06	37.47	0.32877E 04	0.16797E-02	0.593E-04	47.	0.40	0.0131	35.59	0.891	0.018
8	163.3	0.42689E 06	37.45	0.38132E 04	0.16504E-02	0.591E-04	50.	0.38	0.0122	36.29	0.932	0.018
9	168.4	0.46635E 06	37.43	0.43272E 04	0.16210E-02	0.590E-04	53.	0.38	0.0121	35.63	0.895	0.018
10	173.5	0.50580E 06	37.45	0.48195E 04	0.15877E-02	0.588E-04	56.	0.43	0.0138	35.11	0.864	0.018
11	178.6	0.54525E 06	37.47	0.53530E 04	0.15653E-02	0.586E-04	59.	0.41	0.0132	34.88	0.850	0.018
12	183.6	0.58471E 06	37.45	0.58556E 04	0.15301E-02	0.584E-04	61.	0.41	0.0134	34.72	0.841	0.018
13	187.5	0.61469E 06	36.34	0.63457E 04	0.14113E-02	0.526E-04	63.					
14	190.1	0.63501E 06	36.06	0.63750E 04	0.14703E-02	0.588E-04	63.					
15	192.7	0.65533E 06	36.31	0.64046E 04	0.14428E-02	0.588E-04	63.					
16	195.4	0.67565E 06	36.31	0.64341E 04	0.14528E-02	0.583E-04	63.					
17	198.0	0.69616E 06	36.31	0.64637E 04	0.14577E-02	0.585E-04	63.					
18	200.6	0.71648E 06	36.31	0.64930E 04	0.14273E-02	0.578E-04	63.					
19	203.2	0.73680E 06	36.29	0.65216E 04	0.13838E-02	0.558E-04	63.					
20	205.8	0.75712E 06	36.21	0.65506E 04	0.14633E-02	0.574E-04	63.					
21	208.5	0.77744E 06	36.34	0.65792E 04	0.13512E-02	0.552E-04	63.					
22	211.1	0.79776E 06	36.33	0.66071E 04	0.13937E-02	0.568E-04	63.					
23	213.7	0.81808E 06	36.33	0.66352E 04	0.13629E-02	0.555E-04	63.					
24	216.3	0.83849E 06	36.48	0.66629E 04	0.13584E-02	0.570E-04	63.					
25	218.9	0.85891E 06	36.34	0.66904E 04	0.13534E-02	0.558E-04	63.					
26	221.6	0.87923E 06	36.19	0.67182E 04	0.13787E-02	0.586E-04	63.					
27	224.2	0.89955E 06	35.51	0.67458E 04	0.13287E-02	0.521E-04	63.					
28	226.8	0.91987E 06	36.31	0.67730E 04	0.13505E-02	0.587E-04	63.					
29	229.4	0.94019E 06	36.23	0.68008E 04	0.13791E-02	0.551E-04	63.					
30	232.0	0.96051E 06	36.50	0.68290E 04	0.13928E-02	0.580E-04	63.					
31	234.6	0.98082E 06	36.52	0.68569E 04	0.13532E-02	0.563E-04	63.					
32	237.3	0.10012E 07	36.33	0.68848E 04	0.13914E-02	0.568E-04	63.					
33	239.9	0.10217E 07	36.33	0.69130E 04	0.13757E-02	0.569E-04	63.					
34	242.5	0.10420E 07	36.12	0.69409E 04	0.13668E-02	0.548E-04	63.					
35	245.1	0.10623E 07	36.21	0.69686E 04	0.13633E-02	0.584E-04	63.					
36	247.8	0.10826E 07	35.94	0.69960E 04	0.13265E-02	0.628E-04	63.					

UNCERTAINTY IN REX=19727. UNCERTAINTY IN F=0.05146 IN RATIO

RUN 103074-1 *** DISCRETE HOLE RIG *** NAS-3-14336 STANTON NUMBER DATA

*** 520HSL40 M=0.4 TH=0 P/D=5 ***

RUN 103074-2 *** DISCRETE HOLE RIG *** NAS-3-14336 STANTON NUMBER DATA

*** 520HSL40 M=0.4 TH=1 P/D=5 ***

LINEAR SUPERPOSITION IS APPLIED TO STANTON NUMBER DATA FROM
RUN NUMBERS 103074-1 AND 103074-2 TO OBTAIN STANTON NUMBER DATA AT TH=0 AND TH=1

PLATE	REXCOL	RE DEL2	ST(TH=0)	REXHOT	RE DEL2	ST(TH=1)	ETA	STCR	F-COL	STHR	F-HOT	LOG3
1	150954.8	482.1	0.002978	150713.9	481.3	0.002862	UUUJJ	1.078	0.0000	1.036	0.0000	1.036
2	190471.8	605.7	0.003280	190167.8	585.7	0.002633	0.197	1.106	0.0137	0.888	0.0126	2.420
3	229988.8	734.8	0.003251	229621.7	1181.6	0.002171	0.332	1.139	0.0134	0.760	0.0129	2.336
4	269505.8	861.2	0.003147	269075.6	1770.1	0.001768	0.438	1.138	0.0132	0.639	0.0125	2.157
5	309022.7	985.2	0.003132	308529.5	2332.5	0.001674	0.466	1.164	0.0131	0.622	0.0130	2.222
6	348539.7	1107.1	0.003035	347983.4	2908.5	0.001590	0.479	1.155	0.0130	0.601	0.0132	2.250
7	388056.7	1227.3	0.003050	387437.3	3491.8	0.001523	0.501	1.186	0.0137	0.592	0.0131	2.249
8	427573.6	1347.6	0.003041	426891.3	4067.9	0.001516	0.502	1.206	0.0133	0.601	0.0122	2.197
9	467090.6	1466.7	0.002983	466345.1	4609.2	0.001493	0.500	1.204	0.0131	0.602	0.0121	2.215
10	506607.6	1585.7	0.003042	505799.1	5145.2	0.001388	0.544	1.248	0.0131	0.569	0.0138	2.369
11	546124.6	1704.9	0.002991	545252.9	5744.4	0.001327	0.556	1.246	0.0129	0.552	0.0132	2.293
12	585641.6	1821.1	$\boxed{0.002887}$	584706.9	6315.4	0.001282	0.556	1.219	0.0130	0.541	0.0134	2.323
13	615674.6	1904.0	0.002541	614691.9	6882.6	0.001205	0.526	1.084		0.514		
14	636025.8	1955.6	0.002519	635010.6	6907.9	0.001279	0.492	1.081		0.549		
15	656377.0	2006.0	0.002427	655329.4	6933.8	0.001263	0.480	1.049		0.545		
16	676826.8	2054.8	0.002368	675746.6	6959.7	0.001286	0.457	1.029		0.559		
17	697276.9	2102.7	0.002334	696164.0	6986.0	0.001298	0.444	1.020		0.567		
18	717628.1	2149.6	0.002273	716482.8	7012.1	0.001273	0.440	1.000		0.560		
19	737979.3	2195.3	0.002214	736801.5	7037.6	0.001232	0.443	0.979		0.545		
20	758330.6	2240.6	0.002224	757120.3	7063.6	0.001324	0.405	0.989		0.589		
21	778682.1	2284.9	0.002127	777439.3	7089.4	0.001210	0.431	0.951		0.541		
22	799033.3	2327.7	0.002080	797758.0	7114.6	0.001268	0.390	0.935		0.570		
23	819384.5	2369.9	0.002063	818076.8	7140.0	0.001235	0.401	0.932		0.558		
24	839834.3	2412.0	0.002069	838493.9	7165.1	0.001228	0.406	0.939		0.557		
25	860284.4	2453.6	0.002008	858911.4	7190.1	0.001234	0.386	0.916		0.562		
26	880635.6	2494.4	0.001998	879230.1	7215.6	0.001266	0.366	0.915		0.580		
27	900986.9	2535.8	0.002065	899548.9	7240.6	0.001194	0.422	0.950		0.549		
28	921338.1	2577.2	0.001995	919867.6	7265.3	0.001233	0.382	0.922		0.570		
29	941689.6	2618.1	0.002023	940186.6	7290.6	0.001262	0.376	0.939		0.586		
30	962040.8	2659.0	0.001994	960505.4	7316.5	0.001283	0.357	0.930		0.598		
31	982392.0	2699.3	0.001960	980824.1	7342.2	0.001242	0.366	0.918		0.582		
32	1002841.0	2739.0	0.001938	1001241.0	7368.0	0.001292	0.333	0.911		0.607		
33	1023291.0	2778.3	0.001924	1021658.0	7394.1	0.001276	0.337	0.908		0.602		
34	1043643.0	2817.7	0.001942	1041977.0	7419.9	0.001262	0.350	0.921		0.598		
35	1063994.0	2856.7	0.001884	1062296.0	7445.6	0.001268	0.327	0.896		0.603		
36	1084345.0	2894.6	0.001835	1082614.0	7471.1	0.001234	0.328	0.877		0.589		

STANTON NUMBER RATIO BASED ON ST*PR**0.4=0.0295*REX**(-.2)

STANTON NUMBER RATIO FOR TH=1 IS CONVERTED TO COMPARABLE TRANSPIRATION VALUE
USING ALOG(1 + B)/B EXPRESSION IN THE BLOWN SECTION

RUN 102874 *** DISCRETE HOLE RIG *** NAS-3-14336 STANTON NUMBER DATA

TADB= 21.55 DEG C UINF= 11.76 M/S TINF= 21.49 DEG C
RHO= 1.185 KG/M3 VISC= 0.15252E-04 M2/S XVO= 108.4 CM
CP= 1014. J/KGK PR= 0.717

*** 520HSL75 M=0.75 TH=0 P/D=5 ***

PLATE	X	REX	TO	REENTH	STANTON NO	DST	DREEN	M	F	T2	THETA	DTH
1	127.8	0.14957E 06	37.12	0.52663E 03	0.30046E-02	0.749E-04	20.					
2	132.8	0.18873E 06	37.09	0.65069E 03	0.33323E-02	0.781E-04	22.	0.78	0.0254	21.89	0.026	0.020
3	137.9	0.22788E 06	37.09	0.81210E 03	0.35951E-02	0.807E-04	26.	0.79	0.0256	22.14	0.042	0.020
4	143.0	0.26703E 06	37.11	0.99426E 03	0.35709E-02	0.804E-04	30.	0.79	0.0257	22.10	0.039	0.020
5	148.1	0.30619E 06	37.11	0.11720E 04	0.35069E-02	0.797E-04	33.	0.79	0.0256	22.09	0.038	0.020
6	153.2	0.34534E 06	37.09	0.13457E 04	0.34026E-02	0.788E-04	36.	0.79	0.0254	22.15	0.042	0.020
7	158.2	0.38450E 06	37.09	0.15215E 04	0.34224E-02	0.790E-04	39.	0.78	0.0253	22.25	0.049	0.020
8	163.3	0.42365E 06	37.09	0.17034E 04	0.34109E-02	0.789E-04	41.	0.78	0.0254	22.21	0.046	0.020
9	168.4	0.46281E 06	37.07	0.18832E 04	0.34233E-02	0.791E-04	44.	0.79	0.0255	22.19	0.045	0.020
10	173.5	0.50196E 06	37.11	0.20630E 04	0.34535E-02	0.792E-04	46.	0.79	0.0255	22.19	0.045	0.020
11	178.6	0.54112E 06	37.11	0.22425E 04	0.34421E-02	0.791E-04	48.	0.79	0.0256	22.27	0.050	0.020
12	183.6	0.58027E 06	37.12	0.24255E 04	0.33651E-02	0.783E-04	50.	0.79	0.0255	22.28	0.050	0.020
13	187.5	0.61003E 06	34.78	0.25717E 04	0.29853E-02	0.990E-04	51.					
14	190.1	0.63019E 06	34.42	0.26312E 04	0.29097E-02	0.106E-03	51.					
15	192.7	0.65036E 06	34.76	0.26888E 04	0.27964E-02	0.105E-03	51.					
16	195.4	0.67062E 06	34.82	0.27445E 04	0.27242E-02	0.102E-03	51.					
17	198.0	0.69088E 06	34.86	0.27990E 04	0.26714E-02	0.100E-03	51.					
18	200.6	0.71105E 06	34.80	0.28525E 04	0.26266E-02	0.985E-04	51.					
19	203.2	0.73121E 06	34.74	0.29051E 04	0.25871E-02	0.954E-04	51.					
20	205.8	0.75138E 06	35.01	0.29562E 04	0.24778E-02	0.940E-04	51.					
21	208.5	0.77164E 06	34.89	0.30063E 04	0.24791E-02	0.921E-04	51.					
22	211.1	0.79171E 06	35.05	0.30556E 04	0.24107E-02	0.922E-04	51.					
23	213.7	0.81187E 06	35.01	0.31038E 04	0.23607E-02	0.891E-04	51.					
24	216.3	0.83213E 06	35.14	0.31512E 04	0.23358E-02	0.904E-04	51.					
25	218.9	0.85240E 06	34.99	0.31978E 04	0.22854E-02	0.871E-04	51.					
26	221.6	0.87256E 06	34.95	0.32437E 04	0.22621E-02	0.912E-04	51.					
27	224.2	0.89273E 06	33.92	0.32896E 04	0.22818E-02	0.815E-04	51.					
28	226.8	0.91289E 06	35.05	0.33351E 04	0.22270E-02	0.906E-04	51.					
29	229.4	0.93306E 06	35.03	0.33800E 04	0.22224E-02	0.832E-04	51.					
30	232.0	0.95322E 06	35.49	0.34243E 04	0.21672E-02	0.856E-04	51.					
31	234.6	0.97338E 06	35.45	0.34679E 04	0.21442E-02	0.826E-04	51.					
32	237.3	0.99365E 06	35.37	0.35106E 04	0.20922E-02	0.811E-04	51.					
33	239.9	0.10139E 07	35.35	0.35527E 04	0.20782E-02	0.812E-04	51.					
34	242.5	0.10341E 07	35.09	0.35946E 04	0.20716E-02	0.782E-04	51.					
35	245.1	0.10542E 07	35.30	0.36357E 04	0.20019E-02	0.813E-04	51.					
36	247.8	0.10744E 07	34.97	0.36757E 04	0.19567E-02	0.873E-04	51.					

UNCERTAINTY IN REX=19577. UNCERTAINTY IN F=0.05146 IN RATIO

RUN 102974 *** DISCRETE HOLE RIG *** NAS-3-14336 STANTON NUMBER DATA

TADB= 21.24 DEG C UINF= 11.75 M/S TINF= 21.18 DEG C
RHO= 1.186 KG/M3 VISC= 0.15254E-04 M2/S XVO= 108.4 CM
CP= 1011. J/KGK PR= 0.715

*** 520HSL75 M=0.75 TH=1 P/D=5 ***

PLATE	X	REX	TO	REENTH	STANTON NO	DST	DREEN	M	F	T2	THETA	DTH
1	127.8	0.14948E 06	38.15	0.52632E 03	0.29512E-02	0.700E-04	20.					
2	132.8	0.18861E 06	38.13	0.63889E 03	0.28023E-02	0.687E-04	31.	0.74	0.0241	36.86	0.925	0.018
3	137.9	0.22774E 06	38.13	0.16217E 04	0.28625E-02	0.693E-04	46.	0.73	0.0238	37.03	0.935	0.018
4	143.0	0.26688E 06	38.11	0.25959E 04	0.25182E-02	0.664E-04	57.	0.74	0.0238	37.30	0.952	0.018
5	148.1	0.30601E 06	38.13	0.35770E 04	0.23260E-02	0.648E-04	67.	0.70	0.0227	37.14	0.941	0.018
6	153.2	0.34514E 06	38.13	0.45012E 04	0.22077E-02	0.639E-04	74.	0.73	0.0238	36.83	0.923	0.018
7	158.2	0.38427E 06	38.13	0.54459E 04	0.22073E-02	0.639E-04	82.	0.73	0.0236	36.85	0.924	0.018
8	163.3	0.42340E 06	38.13	0.63830E 04	0.21405E-02	0.634E-04	88.	0.72	0.0233	37.14	0.941	0.018
9	168.4	0.46253E 06	38.15	0.73257E 04	0.21097E-02	0.631E-04	94.	0.73	0.0237	36.74	0.917	0.018
10	173.5	0.50166E 06	38.13	0.82585E 04	0.20745E-02	0.629E-04	100.	0.72	0.0234	36.39	0.897	0.018
11	178.6	0.54080E 06	38.15	0.91618E 04	0.20348E-02	0.626E-04	105.	0.72	0.0233	36.11	0.879	0.018
12	183.6	0.57993E 06	38.15	0.10041E 05	0.19961E-02	0.623E-04	109.	0.71	0.0231	35.44	0.840	0.018
13	187.5	0.60967E 06	36.67	0.10857E 05	0.18335E-02	0.644E-04	111.					
14	190.1	0.62982E 06	36.40	0.10893E 05	0.17976E-02	0.691E-04	111.					
15	192.7	0.64997E 06	36.72	0.10929E 05	0.17283E-02	0.683E-04	111.					
16	195.4	0.67022E 06	36.78	0.10964E 05	0.16892E-02	0.661E-04	111.					
17	198.0	0.69047E 06	36.84	0.10997E 05	0.16454E-02	0.650E-04	111.					
18	200.6	0.71063E 06	36.84	0.11030E 05	0.15977E-02	0.634E-04	111.					
19	203.2	0.73078E 06	36.86	0.11062E 05	0.15378E-02	0.603E-04	111.					
20	205.8	0.75093E 06	37.03	0.11092E 05	0.15012E-02	0.599E-04	111.					
21	208.5	0.77108E 06	37.05	0.11122E 05	0.14372E-02	0.578E-04	111.					
22	211.1	0.79124E 06	37.05	0.11151E 05	0.14366E-02	0.585E-04	111.					
23	213.7	0.81139E 06	37.05	0.11179E 05	0.13848E-02	0.564E-04	111.					
24	216.3	0.83164E 06	37.22	0.11207E 05	0.13515E-02	0.572E-04	111.					
25	218.9	0.85189E 06	37.12	0.11234E 05	0.13032E-02	0.547E-04	111.					
26	221.6	0.87204E 06	36.99	0.11260E 05	0.13242E-02	0.571E-04	111.					
27	224.2	0.89219E 06	36.36	0.11286E 05	0.12336E-02	0.499E-04	111.					
28	226.8	0.91235E 06	37.16	0.11311E 05	0.12535E-02	0.559E-04	111.					
29	229.4	0.93250E 06	37.12	0.11336E 05	0.12614E-02	0.518E-04	111.					
30	232.0	0.95265E 06	37.45	0.11362E 05	0.12432E-02	0.540E-04	111.					
31	234.6	0.97281E 06	37.47	0.11386E 05	0.12052E-02	0.519E-04	111.					
32	237.3	0.99306E 06	37.35	0.11411E 05	0.12063E-02	0.517E-04	111.					
33	239.9	0.10133E 07	37.35	0.11435E 05	0.11869E-02	0.514E-04	111.					
34	242.5	0.10335E 07	37.16	0.11459E 05	0.11673E-02	0.492E-04	111.					
35	245.1	0.10536E 07	37.24	0.11482E 05	0.11575E-02	0.526E-04	111.					
36	247.8	0.10738E 07	36.93	0.11505E 05	0.11298E-02	0.559E-04	111.					

UNCERTAINTY IN REX=19566. UNCERTAINTY IN F=0.05146 IN RATIO

RUN 102874 *** DISCRETE HOLE RIG *** NAS-3-14336 STANTON NUMBER DATA

*** 520HSL75 M=0.75 TH=0 P/D=5 ***

RUN 102974 *** DISCRETE HOLE RIG *** NAS-3-14336 STANTON NUMBER DATA

*** 520HSL75 M=0.75 TH=1 P/D=5 ***

LINEAR SUPERPOSITION IS APPLIED TO STANTON NUMBER DATA FROM
RUN NUMBERS 102874 AND 102974 TO OBTAIN STANTON NUMBER DATA AT TH=0 AND TH=1

PLATE	REXCOL	RE DEL2	ST(TH=0)	REXHOT	RE DEL2	ST(TH=1)	ETA	STCR	F-COL	STHR	F-HOT	LOGB
1	149570.7	526.6	0.003005	149481.8	526.3	0.002951	UUUUU	1.088	0.0000	1.068	0.0000	1.068
2	188725.4	651.0	0.003348	188613.1	638.0	0.002758	0.176	1.127	0.0254	0.928	0.0241	3.563
3	227880.0	787.4	0.003623	227744.4	1689.6	0.002805	0.226	1.266	0.0256	0.981	0.0238	3.693
4	267034.7	929.2	0.003618	266875.8	2721.9	0.002452	0.322	1.306	0.0257	0.885	0.0238	3.622
5	306189.3	1069.7	0.003557	306007.2	3745.2	0.002256	0.366	1.319	0.0256	0.837	0.0227	3.501
6	345343.9	1207.0	0.003457	345138.6	4718.5	0.002117	0.388	1.313	0.0254	0.804	0.0238	3.605
7	384498.6	1342.9	0.003485	384269.9	5731.0	0.002102	0.397	1.353	0.0253	0.816	0.0236	3.654
8	423653.3	1479.2	0.003479	423401.3	6734.1	0.002044	0.413	1.377	0.0254	0.809	0.0233	3.666
9	462807.9	1615.7	0.003491	462532.6	7726.5	0.002004	0.426	1.406	0.0255	0.807	0.0237	3.743
10	501962.6	1753.1	0.003525	501664.0	8731.6	0.001926	0.454	1.443	0.0255	0.788	0.0234	3.721
11	541117.2	1891.0	0.003521	540795.3	9722.4	0.001848	0.475	1.463	0.0256	0.768	0.0233	3.704
12	580271.9	2027.5	0.003450	579926.7	10702.8	0.001759	0.490	1.454	0.0255	0.741	0.0231	3.673
13	610029.4	2125.9	0.003056	609666.6	11656.7	0.001634	0.465	1.301		0.695		
14	630194.1	2186.8	0.002978	629819.3	11689.3	0.001605	0.461	1.276		0.688		
15	650358.7	2245.7	0.002862	649971.9	11721.1	0.001543	0.461	1.234		0.665		
16	670621.0	2302.8	0.002788	670222.1	11751.9	0.001510	0.458	1.209		0.655		
17	690883.6	2358.5	0.002735	690472.7	11781.9	0.001468	0.463	1.193		0.640		
18	711048.3	2413.3	0.002690	710625.3	11811.1	0.001420	0.472	1.181		0.623		
19	731212.9	2467.2	0.002652	730777.9	11839.1	0.001356	0.489	1.170		0.598		
20	751377.5	2519.6	0.002538	750930.6	11866.2	0.001332	0.475	1.126		0.591		
21	771542.4	2570.9	0.002543	771083.5	11892.3	0.001257	0.506	1.135		0.561		
22	791707.0	2621.5	0.002471	791236.1	11917.8	0.001268	0.487	1.108		0.568		
23	811871.6	2670.9	0.002421	811388.8	11942.8	0.001216	0.498	1.091		0.548		
24	832133.9	2719.5	0.002397	831639.0	11967.0	0.001181	0.507	1.085		0.535		
25	852396.6	2767.4	0.002346	851889.5	11990.3	0.001133	0.517	1.068		0.516		
26	872561.1	2814.5	0.002320	872042.2	12013.5	0.001162	0.499	1.061		0.531		
27	892725.8	2861.6	0.002346	892194.8	12035.8	0.001052	0.552	1.078		0.483		
28	912890.4	2908.4	0.002287	912347.4	12057.4	0.001085	0.526	1.055		0.501		
29	933055.3	2954.5	0.002282	932500.3	12079.4	0.001095	0.520	1.057		0.507		
30	953219.9	3000.0	0.002224	952652.9	12101.4	0.001083	0.513	1.035		0.504		
31	973384.6	3044.7	0.002202	972805.6	12122.8	0.001043	0.527	1.029		0.487		
32	993646.9	3088.6	0.002147	993055.8	12143.9	0.001053	0.510	1.008		0.494		
33	1013909.0	3131.8	0.002133	1013306.0	12165.0	0.001033	0.516	1.005		0.486		
34	1034074.0	3174.8	0.002127	1033459.0	12185.6	0.001011	0.525	1.006		0.478		
35	1054238.0	3217.0	0.002054	1053611.0	12206.0	0.001011	0.508	0.975		0.480		
36	1074403.0	3258.0	0.002008	1073764.0	12226.1	0.000987	0.509	0.957		0.470		

STANTON NUMBER RATIO BASED ON ST*PR**0.4=0.0295*REX**(-.2)

STANTON NUMBER RATIO FOR TH=1 IS CONVERTED TO COMPARABLE TRANSPIRATION VALUE
USING ALOG(1 + B)/B EXPRESSION IN THE BLOWN SECTION

RUN 120274 VELOCITY AND TEMPERATURE PROFILES

REX	= 0.14592E 06		REM =	501.		REH =	430.	
XVO =	109.04	CM.	DEL2 =	0.064	CM.	DEH2 =	0.055	CM.
UINF =	11.62	M/S	DEL99=	0.468	CM.	DELT99 =	0.479	CM.
VISC =	0.14911E-04	M2/S	DEL1 =	0.137	CM.	UINF =	11.62	M/S
PORT =	19		H =	2.130		VISC =	0.14931E-04	M2/S
XLOC =	127.76	CM.	CF/2 =	0.15863E-02		TINF =	17.86	DEG C
						TPLATE =	34.06	DEG C

Y(CM.)	Y/DEL	U(M/S)	U/UINF	Y+	U+	Y(CM.)	T(DEG C)	TBAR	TBAR
0.025	0.054	3.21	0.276	7.9	6.93	0.0165	31.77	0.141	0.859
0.028	0.060	3.30	0.284	8.7	7.14	0.0191	30.65	0.211	0.789
0.030	0.065	3.36	0.289	9.5	7.27	0.0216	30.12	0.244	0.756
0.033	0.071	3.45	0.297	10.2	7.47	0.0241	29.81	0.263	0.737
0.038	0.081	3.59	0.309	11.8	7.76	0.0292	29.22	0.299	0.701
0.043	0.092	3.88	0.334	13.4	8.39	0.0343	28.65	0.335	0.665
0.051	0.108	4.19	0.361	15.8	9.05	0.0419	28.12	0.368	0.632
0.061	0.130	4.48	0.386	18.9	9.68	0.0495	27.55	0.403	0.597
0.074	0.157	4.83	0.415	22.9	10.43	0.0597	26.99	0.438	0.562
0.089	0.190	5.33	0.459	27.6	11.52	0.0724	26.42	0.473	0.527
0.107	0.228	5.69	0.490	33.1	12.29	0.0851	25.80	0.512	0.488
0.127	0.271	6.36	0.547	39.4	13.74	0.1003	25.21	0.548	0.452
0.150	0.320	7.02	0.604	46.5	15.17	0.1156	24.66	0.582	0.418
0.175	0.374	7.86	0.676	54.4	16.98	0.1334	23.87	0.631	0.369
0.201	0.428	8.53	0.734	62.3	18.43	0.1537	23.07	0.681	0.319
0.226	0.483	9.13	0.786	70.2	19.73	0.1791	22.17	0.737	0.263
0.251	0.537	9.61	0.827	78.0	20.76	0.2045	21.39	0.784	0.216
0.277	0.591	9.98	0.859	85.9	21.56	0.2299	20.72	0.826	0.174
0.302	0.645	10.41	0.896	93.8	22.50	0.2553	20.10	0.864	0.136
0.328	0.700	10.76	0.926	101.7	23.24	0.2807	19.56	0.898	0.102
0.353	0.754	10.90	0.938	109.6	23.56	0.3061	19.23	0.919	0.081
0.378	0.808	11.10	0.955	117.5	23.99	0.3315	18.89	0.940	0.060
0.404	0.862	11.25	0.968	125.3	24.31	0.3569	18.61	0.957	0.043
0.429	0.917	11.35	0.977	133.2	24.52	0.3823	18.42	0.969	0.031
0.455	0.971	11.47	0.987	141.1	24.78	0.4077	18.30	0.976	0.024
0.480	1.025	11.51	0.990	149.0	24.87	0.4331	18.17	0.984	0.016
0.505	1.079	11.55	0.994	156.9	24.97	0.4585	18.12	0.987	0.013
0.531	1.134	11.62	1.000	164.8	25.11	0.4839	18.05	0.992	0.008
						0.509	18.00	0.995	0.005
						0.535	17.98	0.996	0.004
						0.560	17.95	0.998	0.002
						0.585	17.92	1.000	0.000

RUN 120274 *** DISCRETE HOLE RIG *** NAS-3-14336 STANTON NUMBER DATA

TADB= 17.70 DEG C UINF= 11.55 M/S TINF= 17.64 DEG C
RHO= 1.202 KG/M3 VISC= 0.14911E-04 M2/S XVO= 109.1 CM
CP= 1012. J/KGK PR= 0.717

*** 520HSLFP P/D=10 ***

PLATE	X	REX	TO	REENTH	STANTON NO	DST	DREEN	ST(THEO)	RATIO
1	127.8	0.14482E 06	33.63	0.42884E 03	0.24237E-02	0.692E-04	39.	0.31299E-02	0.774
2	132.8	0.18417E 06	33.62	0.53195E 03	0.28176E-02	0.726E-04	39.	0.29831E-02	0.945
3	137.9	0.22351E 06	33.65	0.64285E 03	0.28203E-02	0.725E-04	39.	0.28698E-02	0.983
4	143.0	0.26285E 06	33.65	0.75171E 03	0.27133E-02	0.715E-04	40.	0.27782E-02	0.977
5	148.1	0.30220E 06	33.63	0.85825E 03	0.27025E-02	0.715E-04	40.	0.27018E-02	1.000
6	153.2	0.34154E 06	33.65	0.96241E 03	0.25923E-02	0.705E-04	40.	0.26364E-02	0.983
7	158.2	0.38088E 06	33.69	0.10630E 04	0.25213E-02	0.698E-04	40.	0.25796E-02	0.977
8	163.3	0.42023E 06	33.69	0.11602E 04	0.24206E-02	0.690E-04	40.	0.25293E-02	0.957
9	168.4	0.45957E 06	33.65	0.12550E 04	0.23988E-02	0.689E-04	40.	0.24845E-02	0.965
10	173.5	0.49891E 06	33.63	0.13489E 04	0.23739E-02	0.688E-04	40.	0.24440E-02	0.971
11	178.6	0.53826E 06	33.65	0.14409E 04	0.23021E-02	0.682E-04	40.	0.24072E-02	0.956
12	183.6	0.57760E 06	33.67	0.15312E 04	0.22901E-02	0.680E-04	40.	0.23734E-02	0.965
13	187.5	0.60750E 06	32.24	0.15967E 04	0.20178E-02	0.712E-04	40.	0.23496E-02	0.859
14	190.1	0.62776E 06	31.66	0.16390E 04	0.21461E-02	0.805E-04	40.	0.23342E-02	0.919
15	192.7	0.64802E 06	32.09	0.16822E 04	0.21198E-02	0.813E-04	40.	0.23195E-02	0.914
16	195.4	0.66838E 06	32.09	0.17251E 04	0.21015E-02	0.799E-04	40.	0.23051E-02	0.912
17	198.0	0.68874E 06	32.07	0.17678E 04	0.21148E-02	0.805E-04	40.	0.22914E-02	0.923
18	200.6	0.70901E 06	31.99	0.18107E 04	0.21121E-02	0.804E-04	40.	0.22781E-02	0.927
19	203.2	0.72927E 06	31.93	0.18533E 04	0.20924E-02	0.785E-04	40.	0.22653E-02	0.924
20	205.8	0.74953E 06	32.05	0.18957E 04	0.20866E-02	0.799E-04	40.	0.22529E-02	0.926
21	208.5	0.76979E 06	31.82	0.19380E 04	0.20791E-02	0.783E-04	40.	0.22409E-02	0.928
22	211.1	0.79005E 06	31.82	0.19808E 04	0.21458E-02	0.813E-04	40.	0.22293E-02	0.963
23	213.7	0.81032E 06	31.97	0.20229E 04	0.19965E-02	0.772E-04	40.	0.22181E-02	0.900
24	216.3	0.83068E 06	32.07	0.20640E 04	0.20617E-02	0.802E-04	40.	0.22071E-02	0.934
25	218.9	0.85104E 06	31.93	0.21055E 04	0.20266E-02	0.779E-04	40.	0.21964E-02	0.923
26	221.6	0.87130E 06	31.84	0.21468E 04	0.20480E-02	0.827E-04	40.	0.21861E-02	0.937
27	224.2	0.89156E 06	30.80	0.21886E 04	0.20741E-02	0.743E-04	40.	0.21761E-02	0.953
28	226.8	0.91182E 06	31.88	0.22303E 04	0.20389E-02	0.831E-04	40.	0.21663E-02	0.941
29	229.4	0.93208E 06	31.82	0.22722E 04	0.20866E-02	0.781E-04	40.	0.21568E-02	0.967
30	232.0	0.95234E 06	32.20	0.23142E 04	0.20533E-02	0.804E-04	40.	0.21476E-02	0.956
31	234.6	0.97261E 06	32.20	0.23554E 04	0.20084E-02	0.778E-04	40.	0.21385E-02	0.939
32	237.3	0.99297E 06	32.05	0.23960E 04	0.19943E-02	0.769E-04	40.	0.21297E-02	0.936
33	239.9	0.10133E 07	32.03	0.24363E 04	0.19780E-02	0.770E-04	40.	0.21211E-02	0.933
34	242.5	0.10336E 07	31.78	0.24764E 04	0.19818E-02	0.747E-04	40.	0.21127E-02	0.938
35	245.1	0.10539E 07	31.95	0.25163E 04	0.19455E-02	0.783E-04	40.	0.21045E-02	0.924
36	247.8	0.10741E 07	31.65	0.25548E 04	0.18581E-02	0.829E-04	40.	0.20965E-02	0.886

RUN 121074-1 *** DISCRETE HOLE RIG *** NAS-3-14336 STANTON NUMBER DATA

TADB= 18.88 DEG C UINF= 11.49 M/S TINF= 18.82 DEG C
RHO= 1.202 KG/M3 VISC= 0.14960E-04 M2/S XVO= 109.1 CM
CP= 1011. J/KGK PR= 0.716

*** 520HSL40 M=0.4 TH=0 P/D=10 ***

PLATE	X	REX	TO	REENTH	STANTON NO	DST	DREEN	M	F	T2	THETA	DTH
1	127.8	0.14364E 06	21.95	0.52290E 03	0.25906E-02	0.835E-04	39.					
2	132.8	0.18266E 06	21.95	0.63028E 03	0.29126E-02	0.863E-04	39.	0.42	0.0034	20.76	0.147	0.023
3	137.9	0.22169E 06	21.95	0.76327E 03	0.29108E-02	0.863E-04	39.	0.00	0.0034	31.95	0.147	0.024
4	143.0	0.26071E 06	21.95	0.89115E 03	0.26511E-02	0.840E-04	39.	0.42	0.0034	21.09	0.173	0.023
5	148.1	0.29973E 06	31.95	0.10194E 04	0.27423E-02	0.848E-04	40.	0.00	0.0034	31.95	0.173	0.024
6	153.2	0.33875E 06	21.97	0.11442E 04	0.24729E-02	0.824E-04	40.	0.42	0.0034	21.10	0.173	0.023
7	158.2	0.37778E 06	31.95	0.12666E 04	0.26305E-02	0.838E-04	40.	0.00	0.0034	31.95	0.173	0.024
8	163.3	0.41680E 06	21.97	0.13891E 04	0.24807E-02	0.825E-04	40.	0.42	0.0034	21.19	0.180	0.023
9	168.4	0.45582E 06	31.99	0.15099E 04	0.24966E-02	0.825E-04	40.	0.00	0.0034	31.99	0.180	0.024
10	173.5	0.49484E 06	21.97	0.16286E 04	0.23724E-02	0.816E-04	40.	0.42	0.0034	21.23	0.183	0.023
11	178.6	0.53387E 06	31.95	0.17457E 04	0.24021E-02	0.819E-04	40.	0.00	0.0034	31.95	0.183	0.024
12	183.6	0.57289E 06	21.97	0.18613E 04	0.22931E-02	0.810E-04	40.	0.42	0.0034	21.27	0.186	0.023
13	187.5	0.60255E 06	30.59	0.19523E 04	0.21369E-02	0.777E-04	41.					
14	190.1	0.62264E 06	30.31	0.20206E 04	0.21949E-02	0.873E-04	41.					
15	192.7	0.64274E 06	30.50	0.20644E 04	0.21670E-02	0.871E-04	41.					
16	195.4	0.66293E 06	30.50	0.21080E 04	0.21618E-02	0.860E-04	41.					
17	198.0	0.68313E 06	30.50	0.21516E 04	0.21707E-02	0.866E-04	41.					
18	200.6	0.70322E 06	30.44	0.21954E 04	0.21862E-02	0.872E-04	41.					
19	203.2	0.72332E 06	30.38	0.22390E 04	0.21450E-02	0.844E-04	41.					
20	205.8	0.74342E 06	30.46	0.22825E 04	0.21768E-02	0.861E-04	41.					
21	208.5	0.76351E 06	30.42	0.23253E 04	0.20816E-02	0.827E-04	41.					
22	211.1	0.78361E 06	30.48	0.23676E 04	0.21244E-02	0.858E-04	41.					
23	213.7	0.80371E 06	30.44	0.24097E 04	0.20623E-02	0.832E-04	41.					
24	216.3	0.82390E 06	30.48	0.24520E 04	0.21416E-02	0.869E-04	41.					
25	218.9	0.84410E 06	30.42	0.24945E 04	0.20792E-02	0.845E-04	41.					
26	221.6	0.86419E 06	30.31	0.25367E 04	0.21110E-02	0.889E-04	41.					
27	224.2	0.88429E 06	29.50	0.25791E 04	0.21105E-02	0.815E-04	41.					
28	226.8	0.90439E 06	30.35	0.26215E 04	0.20973E-02	0.890E-04	41.					
29	229.4	0.92448E 06	30.33	0.26642E 04	0.21500E-02	0.846E-04	41.					
30	232.0	0.94458E 06	30.65	0.27070E 04	0.21022E-02	0.865E-04	41.					
31	234.6	0.96468E 06	30.65	0.27487E 04	0.20485E-02	0.833E-04	41.					
32	237.3	0.98487E 06	30.56	0.27897E 04	0.20273E-02	0.828E-04	41.					
33	239.9	0.10051E 07	30.50	0.28305E 04	0.20261E-02	0.826E-04	41.					
34	242.5	0.10252E 07	30.33	0.28710E 04	0.20017E-02	0.799E-04	41.					
35	245.1	0.10453E 07	30.46	0.29110E 04	0.19746E-02	0.842E-04	41.					
36	247.8	0.10654E 07	30.17	0.29500E 04	0.18951E-02	0.888E-04	41.					

UNCERTAINTY IN REX=1951.1. UNCERTAINTY IN F=0.05155 IN RATIO

RUN 121074-2 *** DISCRETE HOLE RIG *** NAS-3-14336 STANTON NUMBER DATA

TADB= 18.94 DEG C UINF= 11.49 M/S TINF= 18.88 DEG C
RHO= 1.202 KG/M3 VISC= 0.14965E-04 M2/S XVO= 109.1 CM
CP= 1011. J/KGK PR= 0.716

*** 520HSL40 M=0.4 TH=1 P/D=10 ***

PLATE	X	REX	TD	REENTH	STANTON NO	DST	DREEN	M	F	T2	THETA	DTH
1	127.8	0.14361E 06	32.57	0.52278E 03	0.24872E-02	0.798E-04	39.					
2	132.8	0.18262E 06	32.58	0.62237E 03	0.26185E-02	0.807E-04	39.	0.42	0.0034	32.27	0.977	0.023
3	137.9	0.22163E 06	32.60	0.85153E 03	0.25181E-02	0.798E-04	40.	0.00	0.0034	32.60	0.977	0.023
4	143.0	0.26065E 06	32.60	0.10750E 04	0.23261E-02	0.783E-04	40.	0.37	0.0030	31.34	0.908	0.022
5	148.1	0.29966E 06	32.58	0.12698E 04	0.22601E-02	0.779E-04	40.	0.00	0.0030	32.58	0.908	0.023
6	153.2	0.33867E 06	32.60	0.14607E 04	0.21201E-02	0.768E-04	41.	0.39	0.0032	31.26	0.902	0.022
7	158.2	0.37769E 06	32.60	0.16558E 04	0.21561E-02	0.770E-04	41.	0.00	0.0032	32.60	0.902	0.023
8	163.3	0.41670E 06	32.60	0.18504E 04	0.20969E-02	0.766E-04	41.	0.32	0.0026	31.61	0.928	0.022
9	168.4	0.45571E 06	32.58	0.20238E 04	0.20237E-02	0.762E-04	41.	0.00	0.0026	32.58	0.928	0.023
10	173.5	0.49473E 06	32.58	0.21945E 04	0.19612E-02	0.757E-04	42.	0.39	0.0031	31.03	0.887	0.022
11	178.6	0.53374E 06	32.62	0.23781E 04	0.19052E-02	0.752E-04	42.	0.00	0.0031	32.62	0.887	0.023
12	183.6	0.57275E 06	32.58	0.25597E 04	0.18647E-02	0.751E-04	42.	0.34	0.0027	30.88	0.875	0.022
13	187.5	0.60240E 06	31.46	0.27116E 04	0.21799E-02	0.725E-04	42.					
14	190.1	0.62250E 06	32.97	0.28416E 04	0.14356E-02	0.689E-04	42.					
15	192.7	0.64259E 06	33.21	0.28735E 04	0.17405E-02	0.699E-04	42.					
16	195.4	0.66278E 06	33.21	0.29086E 04	0.17520E-02	0.694E-04	42.					
17	198.0	0.68297E 06	33.20	0.29442E 04	0.17827E-02	0.705E-04	42.					
18	200.6	0.70306E 06	33.14	0.29801E 04	0.17873E-02	0.707E-04	42.					
19	203.2	0.72315E 06	33.10	0.30159E 04	0.17722E-02	0.691E-04	42.					
20	205.8	0.74324E 06	33.18	0.30520E 04	0.18160E-02	0.709E-04	42.					
21	208.5	0.76333E 06	33.16	0.30875E 04	0.17200E-02	0.681E-04	42.					
22	211.1	0.78342E 06	33.12	0.31229E 04	0.17964E-02	0.714E-04	42.					
23	213.7	0.80352E 06	33.04	0.31588E 04	0.17755E-02	0.697E-04	42.					
24	216.3	0.82371E 06	33.23	0.31944E 04	0.17629E-02	0.717E-04	42.					
25	218.9	0.84390E 06	33.12	0.32300E 04	0.17737E-02	0.708E-04	42.					
26	221.6	0.86399E 06	32.95	0.32661E 04	0.18175E-02	0.744E-04	42.					
27	224.2	0.88408E 06	32.24	0.33019E 04	0.17406E-02	0.661E-04	42.					
28	226.8	0.90417E 06	33.08	0.33371E 04	0.17576E-02	0.737E-04	42.					
29	229.4	0.92426E 06	33.00	0.33729E 04	0.18053E-02	0.700E-04	42.					
30	232.0	0.94435E 06	33.27	0.34093E 04	0.18108E-02	0.729E-04	43.					
31	234.6	0.96445E 06	33.29	0.34451E 04	0.17505E-02	0.706E-04	43.					
32	237.3	0.98464E 06	33.08	0.34806E 04	0.17774E-02	0.704E-04	43.					
33	239.9	0.10048E 07	33.10	0.35159E 04	0.17362E-02	0.701E-04	43.					
34	242.5	0.10249E 07	32.87	0.35509E 04	0.17377E-02	0.678E-04	43.					
35	245.1	0.10450E 07	33.02	0.35855E 04	0.17046E-02	0.717E-04	43.					
36	247.8	0.10651E 07	32.66	0.36196E 04	0.16870E-02	0.758E-04	43.					

UNCERTAINTY IN REX=19507. UNCERTAINTY IN F=0.05155 IN RATIO

RUN 121074-1 *** DISCRETE HOLE RIG *** NAS-3-14336 STANTON NUMBER DATA

*** 520HSL40 M=0.4 TH=0 P/D=10 ***

RUN 121074-2 *** DISCRETE HOLE RIG *** NAS-3-14336 STANTON NUMBER DATA

*** 520HSL40 M=0.4 TH=1 P/D=10 ***

LINEAR SUPERPOSITION IS APPLIED TO STANTON NUMBER DATA FROM
RUN NUMBERS 121074-1 AND 121074-2 TO OBTAIN STANTON NUMBER DATA AT TH=0 AND TH=1

PLATE	REXCOL	RE DEL2	ST(TH=0)	REXHOT	RE DEL2	ST(TH=1)	ETA	STCR	F-COL	STHR	F-HOT	LOGB
1	143641.8	522.9	0.002591	143607.7	522.8	0.002487	UUUUJ	1.069	0.0000	1.026	0.0000	1.026
2	182664.3	631.3	0.002965	182620.9	622.2	0.002610	0.120	0.992	0.0034	0.873	0.0034	1.361
3	221686.8	747.3	0.002980	221634.1	854.0	0.002507	0.159	1.036	0.0034	0.872	0.0034	1.377
4	260709.3	858.5	0.002718	260647.4	1079.8	0.002302	0.153	0.976	0.0034	0.827	0.0030	1.288
5	299731.8	967.2	0.002856	299660.6	1283.7	0.002200	0.230	1.055	0.0034	0.812	0.0030	1.284
6	338754.4	1072.8	0.002556	338673.9	1483.2	0.002074	0.189	0.967	0.0034	0.785	0.0032	1.294
7	377776.9	1176.2	0.002743	377687.1	1688.2	0.002093	0.237	1.061	0.0034	0.809	0.0032	1.330
8	416799.4	1279.9	0.002572	416700.3	1892.9	0.002053	0.202	1.015	0.0034	0.810	0.0026	1.249
9	455821.9	1381.0	0.002610	455713.6	2071.7	0.001978	0.242	1.048	0.0034	0.794	0.0026	1.240
10	494844.4	1480.3	0.002475	494726.8	2247.8	0.001909	0.229	1.011	0.0034	0.779	0.0031	1.316
11	533866.9	1577.9	0.002531	533740.0	2442.6	0.001825	0.279	1.049	0.0034	0.757	0.0031	1.298
12	572889.4	1674.3	0.002407	572753.3	2635.0	0.001792	0.256	1.012	0.0034	0.753	0.0027	1.241
13	602546.6	1742.6	0.002125	602403.4	2798.9	0.002187	*****	0.903		0.929		
14	622643.1	1788.1	0.002396	622495.2	2940.9	0.001306	0.455	1.024		0.558		
15	642739.8	1835.2	0.002280	642587.0	2970.8	0.001668	0.269	0.981		0.717		
16	662933.6	1880.9	0.002270	662776.1	3004.5	0.001682	0.259	0.983		0.728		
17	683127.9	1926.6	0.002273	682965.5	3038.7	0.001717	0.245	0.990		0.747		
18	703224.4	1972.6	0.002292	703057.3	3073.2	0.001719	0.250	1.004		0.753		
19	723321.0	2018.2	0.002244	723149.1	3107.7	0.001709	0.238	0.988		0.753		
20	743417.6	2063.6	0.002272	743240.9	3142.6	0.001755	0.228	1.006		0.777		
21	763514.4	2108.4	0.002177	763333.0	3176.9	0.001658	0.238	0.970		0.738		
22	783611.0	2152.6	0.002211	783424.8	3211.1	0.001740	0.213	0.990		0.779		
23	803707.6	2196.3	0.002138	803516.6	3245.9	0.001727	0.193	0.962		0.777		
24	823901.5	2240.4	0.002242	823705.7	3280.4	0.001698	0.242	1.014		0.768		
25	844095.7	2284.7	0.002160	843895.1	3314.8	0.001722	0.203	0.981		0.782		
26	864192.3	2328.4	0.002189	863986.9	3349.9	0.001767	0.192	0.999		0.807		
27	884288.8	2372.7	0.002208	884078.7	3384.5	0.001678	0.240	1.013		0.769		
28	904385.4	2416.9	0.002187	904170.5	3418.5	0.001700	0.223	1.008		0.783		
29	924482.3	2461.4	0.002241	924262.6	3453.1	0.001747	0.221	1.037		0.808		
30	944578.8	2505.9	0.002179	944354.4	3488.4	0.001761	0.192	1.013		0.818		
31	964675.4	2549.2	0.002127	964446.2	3523.2	0.001700	0.201	0.993		0.793		
32	984869.3	2591.7	0.002094	984635.3	3557.8	0.001735	0.171	0.981		0.813		
33	1005063.0	2633.9	0.002103	1004824.0	3592.2	0.001687	0.198	0.989		0.794		
34	1025160.0	2675.9	0.002072	1024916.0	3626.2	0.001693	0.183	0.978		0.799		
35	1045256.0	2717.3	0.002046	1045008.0	3659.9	0.001658	0.189	0.970		0.786		
36	1065353.0	2757.5	0.001950	1065100.0	3693.2	0.001651	0.153	0.928		0.786		

STANTON NUMBER RATIO BASED ON ST*PR**0.4=0.0295*REX**(-.2)

STANTON NUMBER RATIO FOR TH=1 IS CONVERTED TO COMPARABLE TRANSPIRATION VALUE
USING ALOG(1 + B)/B EXPRESSION IN THE BLOWN SECTION

RUN 120574-1 *** DISCRETE HOLE RIG *** NAS-3-14336 STANTON NUMBER DATA

TADB= 19.95 DEG C UINF= 11.52 M/S TINF= 19.89 DEG C
RHO= 1.201 KG/M3 VISC= 0.15027E-04 M2/S XVO= 109.1 CM
CP= 1010. J/KGK PR= 0.715

*** 520HSL80 M=0.8 TH=0 P/D=10 ***

PLATE	X	REX	TO	REENTH	STANTON NO	DST	DREEN	M	F	T2	THETA	DTH
1	127.8	0.14331E 06	32.55	0.52170E 03	0.28012E-02	0.879E-04	39.					
2	132.8	0.18225E 06	32.55	0.63470E 03	0.30034E-02	0.897E-04	39.	0.81	0.0065	21.82	0.153	0.024
3	137.9	0.22118E 06	32.57	0.79163E 03	0.30626E-02	0.901E-04	39.	0.00	0.0065	32.57	0.153	0.024
4	143.0	0.26011E 06	32.53	0.94583E 03	0.28626E-02	0.885E-04	40.	0.82	0.0066	22.09	0.174	0.024
5	148.1	0.29904E 06	32.55	0.11030E 04	0.29117E-02	0.889E-04	40.	0.00	0.0066	32.55	0.174	0.025
6	153.2	0.33798E 06	32.55	0.12572E 04	0.27089E-02	0.871E-04	41.	0.81	0.0066	22.04	0.170	0.024
7	158.2	0.37691E 06	32.57	0.14074E 04	0.27737E-02	0.875E-04	41.	0.00	0.0066	32.57	0.170	0.024
8	163.3	0.41584E 06	32.53	0.15566E 04	0.26571E-02	0.867E-04	41.	0.81	0.0066	22.10	0.175	0.024
9	168.4	0.45478E 06	32.53	0.17044E 04	0.26383E-02	0.866E-04	42.	0.00	0.0066	32.53	0.175	0.025
10	173.5	0.49371E 06	32.51	0.18516E 04	0.26265E-02	0.866E-04	42.	0.81	0.0066	22.10	0.175	0.024
11	178.6	0.53264E 06	32.55	0.19992E 04	0.26551E-02	0.866E-04	42.	0.00	0.0066	32.55	0.175	0.025
12	183.6	0.57158E 06	32.55	0.21454E 04	0.25573E-02	0.858E-04	43.	0.82	0.0066	22.12	0.176	0.024
13	187.5	0.60117E 06	31.13	0.22636E 04	0.23024E-02	0.837E-04	43.					
14	190.1	0.62122E 06	30.82	0.23560E 04	0.23921E-02	0.947E-04	43.					
15	192.7	0.64127E 06	31.00	0.24038E 04	0.23724E-02	0.948E-04	43.					
16	195.4	0.66141E 06	31.00	0.24514E 04	0.23677E-02	0.938E-04	43.					
17	198.0	0.68156E 06	31.00	0.24990E 04	0.23727E-02	0.942E-04	43.					
18	200.6	0.70161E 06	30.96	0.25465E 04	0.23657E-02	0.941E-04	43.					
19	203.2	0.72166E 06	30.92	0.25937E 04	0.23370E-02	0.919E-04	43.					
20	205.8	0.74171E 06	30.96	0.26412E 04	0.23948E-02	0.942E-04	43.					
21	208.5	0.76176E 06	30.90	0.26884E 04	0.23003E-02	0.908E-04	43.					
22	211.1	0.78181E 06	30.98	0.27347E 04	0.23209E-02	0.935E-04	43.					
23	213.7	0.80186E 06	30.92	0.27810E 04	0.22854E-02	0.913E-04	43.					
24	216.3	0.82201E 06	31.00	0.28273E 04	0.23276E-02	0.944E-04	43.					
25	218.9	0.84216E 06	30.90	0.28739E 04	0.23221E-02	0.931E-04	43.					
26	221.6	0.86221E 06	30.82	0.29204E 04	0.23104E-02	0.969E-04	43.					
27	224.2	0.88226E 06	30.00	0.29667E 04	0.23006E-02	0.886E-04	43.					
28	226.8	0.90231E 06	30.86	0.30129E 04	0.22979E-02	0.971E-04	43.					
29	229.4	0.92236E 06	30.80	0.30596E 04	0.23571E-02	0.922E-04	43.					
30	232.0	0.94241E 06	31.15	0.31063E 04	0.22998E-02	0.942E-04	43.					
31	234.6	0.96246E 06	31.13	0.31520E 04	0.22515E-02	0.909E-04	43.					
32	237.3	0.98261E 06	31.02	0.31971E 04	0.22398E-02	0.905E-04	43.					
33	239.9	0.10028E 07	31.02	0.32418E 04	0.22125E-02	0.902E-04	43.					
34	242.5	0.10228E 07	30.80	0.32861E 04	0.22035E-02	0.874E-04	43.					
35	245.1	0.10429E 07	30.94	0.33302E 04	0.21828E-02	0.920E-04	43.					
36	247.8	0.10629E 07	30.69	0.33728E 04	0.20681E-02	0.958E-04	43.					

UNCERTAINTY IN REX=19467. UNCERTAINTY IN F=0.05154 IN RATIO

RUN 120574-2 *** DISCRETE HOLE RIG *** NAS-3-14336 STANTON NUMBER DATA

TADB= 19.71 DEG C UINF= 11.57 M/S TINF= 19.65 DEG C
RHO= 1.202 KG/M3 VISC= 0.15006E-04 M2/S XVO= 109.1 CM
CP= 1010. J/KGK PR= 0.715

*** 520HSL80 M=0.8 TH=1 P/D=10 ***

PLATE	X	REX	TO	REENTH	STANTON NO	DST	DREEN	M	F	T2	THETA	DTH
1	127.8	0.14412E 06	32.87	0.52465E 03	0.26996E-02	0.834E-04	39.					
2	132.8	0.18327E 06	32.87	0.63126E 03	0.27465E-02	0.838E-04	40.	0.76	0.0062	32.28	0.955	0.023
3	137.9	0.22243E 06	32.87	0.97105E 03	0.27865E-02	0.842E-04	41.	0.00	0.0062	32.87	0.955	0.023
4	143.0	0.26158E 06	32.85	0.13074E 04	0.25702E-02	0.825E-04	42.	0.80	0.0065	31.88	0.927	0.023
5	148.1	0.30073E 06	32.83	0.16429E 04	0.25304E-02	0.822E-04	43.	0.00	0.0065	32.83	0.927	0.024
6	153.2	0.33988E 06	32.87	0.19733E 04	0.23100E-02	0.803E-04	44.	0.81	0.0066	31.92	0.928	0.023
7	158.2	0.37904E 06	32.83	0.23046E 04	0.24034E-02	0.812E-04	45.	0.00	0.0066	32.83	0.928	0.024
8	163.3	0.41819E 06	32.85	0.26353E 04	0.22795E-02	0.802E-04	46.	0.76	0.0061	31.85	0.924	0.023
9	168.4	0.45734E 06	32.87	0.29461E 04	0.22885E-02	0.801E-04	47.	0.00	0.0061	32.87	0.924	0.023
10	173.5	0.49650E 06	32.89	0.32554E 04	0.22009E-02	0.794E-04	48.	0.82	0.0067	31.54	0.898	0.023
11	178.6	0.53565E 06	32.87	0.35771E 04	0.22627E-02	0.799E-04	49.	0.00	0.0067	32.87	0.898	0.023
12	183.6	0.57480E 06	32.87	0.38988E 04	0.21998E-02	0.795E-04	50.	0.86	0.0069	31.42	0.891	0.023
13	187.5	0.60456E 06	31.55	0.42043E 04	0.20756E-02	0.761E-04	51.					
14	190.1	0.62472E 06	31.23	0.44886E 04	0.21724E-02	0.860E-04	51.					
15	192.7	0.64488E 06	31.44	0.45321E 04	0.21326E-02	0.858E-04	51.					
16	195.4	0.66515E 06	31.44	0.45753E 04	0.21500E-02	0.853E-04	51.					
17	198.0	0.68541E 06	31.44	0.46189E 04	0.21681E-02	0.862E-04	51.					
18	200.6	0.70557E 06	31.40	0.46627E 04	0.21691E-02	0.863E-04	51.					
19	203.2	0.72573E 06	31.36	0.47062E 04	0.21471E-02	0.843E-04	51.					
20	205.8	0.74590E 06	31.40	0.47502E 04	0.22098E-02	0.867E-04	51.					
21	208.5	0.76606E 06	31.36	0.47934E 04	0.20719E-02	0.830E-04	51.					
22	211.1	0.78623E 06	31.23	0.48370E 04	0.22492E-02	0.883E-04	51.					
23	213.7	0.80639E 06	31.34	0.48809E 04	0.20950E-02	0.843E-04	51.					
24	216.3	0.82665E 06	31.46	0.49237E 04	0.21451E-02	0.870E-04	51.					
25	218.9	0.84691E 06	31.38	0.49670E 04	0.21461E-02	0.861E-04	51.					
26	221.6	0.86708E 06	31.26	0.50105E 04	0.21629E-02	0.899E-04	51.					
27	224.2	0.88724E 06	30.50	0.50536E 04	0.21083E-02	0.811E-04	51.					
28	226.8	0.90740E 06	31.32	0.50963E 04	0.21224E-02	0.894E-04	51.					
29	229.4	0.92757E 06	31.26	0.51396E 04	0.21688E-02	0.849E-04	51.					
30	232.0	0.94773E 06	31.55	0.51833E 04	0.21602E-02	0.878E-04	51.					
31	234.6	0.96789E 06	31.57	0.52260E 04	0.20685E-02	0.841E-04	51.					
32	237.3	0.98816E 06	31.38	0.52680E 04	0.20894E-02	0.842E-04	51.					
33	239.9	0.10084E 07	31.32	0.53102E 04	0.20903E-02	0.843E-04	51.					
34	242.5	0.10286E 07	31.21	0.53517E 04	0.20230E-02	0.807E-04	51.					
35	245.1	0.10487E 07	31.32	0.53926E 04	0.20275E-02	0.851E-04	51.					
36	247.8	0.10689E 07	31.11	0.54325E 04	0.19295E-02	0.887E-04	51.					

UNCERTAINTY IN REX=19576. UNCERTAINTY IN F=0.05151 IN RATIO

RUN 120574-1 *** DISCRETE HOLE RIG *** NAS-3-14336 STANTON NUMBER DATA

*** 520HSL80 M=0.8 TH=0 P/D=10 ***

RUN 120574-2 *** DISCRETE HOLE RIG *** NAS-3-14336 STANTON NUMBER DATA

*** 520HSL80 M=0.8 TH=1 P/D=10 ***

LINEAR SUPERPOSITION IS APPLIED TO STANTON NUMBER DATA FROM
RUN NUMBERS 120574-1 AND 120574-2 TO OBTAIN STANTON NUMBER DATA AT TH=0 AND TH=1

PLATE	REXCOL	RE DEL2	ST(TH=0)	REXHOT	RE DEL2	ST(TH=1)	ETA	STCR	F-COL	STHR	F-HOT	LOGB
1	143312.5	521.7	0.002801	144121.1	524.6	0.002700	UUUUU	1.156	0.0000	1.114	0.0000	1.114
2	182245.5	635.7	0.003052	183273.8	631.0	0.002732	0.105	1.020	0.0065	0.914	0.0062	1.750
3	221178.6	755.7	0.003115	222426.5	981.0	0.002771	0.110	1.082	0.0065	0.964	0.0062	1.834
4	260111.6	873.3	0.002924	261579.3	1327.5	0.002548	0.129	1.049	0.0066	0.915	0.0065	1.842
5	299044.6	988.6	0.003000	300731.9	1680.5	0.002493	0.169	1.107	0.0066	0.921	0.0065	1.871
6	337977.7	1101.5	0.002800	339884.6	2028.2	0.002272	0.189	1.059	0.0066	0.860	0.0066	1.831
7	376910.7	1211.6	0.002857	379037.4	2376.5	0.002368	0.171	1.104	0.0066	0.916	0.0066	1.915
8	415843.8	1320.6	0.002744	418190.1	2724.4	0.002242	0.183	1.081	0.0066	0.885	0.0061	1.835
9	454776.8	1427.0	0.002720	457342.8	3052.0	0.002253	0.172	1.091	0.0066	0.905	0.0061	1.873
10	493709.8	1533.0	0.002728	496495.5	3377.7	0.002149	0.212	1.113	0.0066	0.878	0.0067	1.929
11	532642.9	1639.7	0.002750	535648.2	3724.0	0.002207	0.197	1.139	0.0066	0.915	0.0067	1.987
12	571575.9	1744.7	0.002645	574800.9	4070.3	0.002147	0.188	1.111	0.0066	0.903	0.0069	2.021
13	601165.1	1819.8	0.002358	604557.1	4404.1	0.002042	0.134	1.001		0.868		
14	621215.6	1868.1	0.002446	624720.7	4717.4	0.002140	0.125	1.045		0.915		
15	641266.1	1917.0	0.002431	644884.3	4760.2	0.002097	0.137	1.045		0.903		
16	661413.7	1965.7	0.002421	665145.6	4802.7	0.002118	0.125	1.047		0.917		
17	681561.6	2014.3	0.002423	685407.2	4845.7	0.002138	0.118	1.054		0.931		
18	701612.1	2062.9	0.002414	705570.8	4888.9	0.002140	0.113	1.056		0.938		
19	721662.6	2111.0	0.002383	725734.4	4931.9	0.002119	0.111	1.049		0.934		
20	741713.1	2159.4	0.002440	745898.1	4975.3	0.002183	0.106	1.080		0.967		
21	761763.9	2207.6	0.002356	766062.0	5017.9	0.002038	0.135	1.048		0.908		
22	781814.4	2254.7	0.002338	786225.6	5061.1	0.002239	0.043	1.046		1.002		
23	801864.9	2301.6	0.002332	806389.3	5104.5	0.002067	0.114	1.048		0.930		
24	822012.5	2348.8	0.002372	826650.5	5146.8	0.002118	0.107	1.072		0.958		
25	842160.4	2396.4	0.002365	846912.1	5189.6	0.002120	0.104	1.074		0.963		
26	862210.9	2443.6	0.002346	867075.8	5232.6	0.002141	0.087	1.070		0.978		
27	882261.4	2490.8	0.002348	887239.4	5275.2	0.002080	0.114	1.076		0.954		
28	902311.9	2537.8	0.002341	907403.0	5317.3	0.002097	0.104	1.077		0.966		
29	922362.7	2585.4	0.002403	927566.9	5360.1	0.002141	0.109	1.111		0.991		
30	942413.2	2633.0	0.002334	947730.6	5403.3	0.002140	0.033	1.084		0.994		
31	962463.6	2679.5	0.002296	967894.2	5445.5	0.002042	0.111	1.071		0.953		
32	982611.3	2725.4	0.002277	988155.4	5487.0	0.002067	0.092	1.066		0.969		
33	1002759.0	2770.7	0.002242	1008417.0	5528.8	0.002072	0.076	1.054		0.975		
34	1022809.0	2815.8	0.002248	1028580.0	5569.8	0.001996	0.112	1.061		0.943		
35	1042860.0	2860.6	0.002221	1048744.0	5610.2	0.002005	0.097	1.052		0.951		
36	1062910.0	2904.0	0.002102	1068907.0	5649.7	0.001909	0.092	1.000		0.909		

STANTON NUMBER RATIO BASED ON ST*PR**0.4=0.0295*REX**(-.2)

STANTON NUMBER RATIO FOR TH=1 IS CONVERTED TO COMPARABLE TRANSPIRATION VALUE
USING ALOG(1 + B)/B EXPRESSION IN THE BLOWN SECTION

Appendix II

SPANWISE PROFILE DATA

Contained in this appendix is a numerical tabulation of the spanwise profiles that are discussed in Section 3.4, and plotted in Figures 3.23 and 3.24 for velocity, and Figures 3.27 through 3.30 for temperature. Note that the same velocity profile points accompany the $\theta = 1$ and $\theta = 0$ temperature profiles. See Appendix I for the computer listing nomenclature.

RUN 092974/100374 SPANWISE PROFILE TH=1 (1)

REX =	0.10000E 01	REM =	6833.	REH =	10259.
XVO =	0.00 CM	DEL2 =	0.626 CM	DEH2 =	0.934 CM
UINF =	16.71 M/S	DEL99=	3.629 CM	DELT99 =	4.066 CM
VISC =	0.15323E-04 M2/S	DEL1 =	1.048 CM	UINF =	16.67 M/S
PORT =	1	H =	1.672	VISC =	0.15175E-04 M2/S
XLOC =	176.40 CM	CF/2 =	0.10000E 01	TINF =	21.25 DEG C
				TPLATE =	36.82 DEG C

Y(CM)	Y/DEL	U(M/S)	U/UINF	Y+	U+	Y(CM)	T(DEG C)	TBAR	TBAR
0.025	0.007	4.86	0.291	277.0	0.29	0.0546	34.98	0.118	0.882
0.028	0.008	5.00	0.299	304.7	0.30	0.0571	34.66	0.139	0.861
0.030	0.008	5.22	0.312	332.4	0.31	0.0597	34.54	0.146	0.854
0.033	0.009	5.42	0.324	360.2	0.32	0.0648	34.28	0.163	0.837
0.038	0.010	5.73	0.343	415.6	0.34	0.0724	34.06	0.178	0.822
0.046	0.013	6.14	0.367	498.7	0.37	0.0825	33.76	0.196	0.804
0.056	0.015	6.49	0.388	609.5	0.39	0.0952	33.49	0.214	0.786
0.069	0.019	6.80	0.407	748.0	0.41	0.1105	33.28	0.228	0.772
0.084	0.023	7.13	0.427	914.2	0.43	0.1308	33.02	0.244	0.756
0.102	0.028	7.40	0.442	1108.2	0.44	0.1562	32.80	0.258	0.742
0.122	0.034	7.63	0.456	1329.8	0.46	0.1867	32.61	0.270	0.730
0.147	0.041	7.86	0.470	1606.8	0.47	0.2222	32.46	0.280	0.720
0.178	0.049	8.08	0.484	1939.3	0.48	0.2629	32.38	0.285	0.715
0.213	0.059	8.24	0.493	2327.1	0.49	0.3086	32.32	0.289	0.711
0.254	0.070	8.37	0.501	2770.4	0.50	0.3619	32.35	0.287	0.713
0.300	0.083	8.45	0.505	3269.1	0.51	0.4254	32.27	0.292	0.708
0.351	0.097	8.47	0.507	3823.1	0.51	0.4889	32.30	0.290	0.710
0.406	0.112	8.47	0.507	4432.6	0.51	0.5524	32.28	0.291	0.709
0.467	0.129	8.44	0.505	5097.5	0.51	0.6159	32.19	0.298	0.702
0.538	0.148	8.41	0.503	5873.2	0.50	0.6794	32.15	0.300	0.700
0.620	0.171	8.36	0.500	6759.8	0.50	0.7429	31.96	0.312	0.688
0.696	0.192	8.41	0.503	7590.9	0.50	0.8064	31.91	0.315	0.685
0.772	0.213	8.48	0.508	8422.0	0.51	0.8699	31.70	0.329	0.671
0.848	0.234	8.68	0.519	9253.1	0.52	0.9334	31.57	0.337	0.663
0.925	0.255	8.87	0.531	10084.2	0.53	1.0604	31.47	0.344	0.656
1.026	0.283	9.26	0.554	11192.4	0.55	1.1874	30.90	0.381	0.619
1.128	0.311	9.65	0.578	12300.5	0.58	1.3144	30.26	0.421	0.579
1.229	0.339	10.08	0.603	13408.7	0.60	1.4414	29.67	0.459	0.541
1.356	0.374	10.52	0.630	14793.9	0.63	1.5684	28.89	0.510	0.490
1.483	0.409	10.92	0.653	16179.1	0.65	1.8224	28.18	0.555	0.445
1.610	0.444	11.26	0.674	17564.3	0.67	2.0764	26.99	0.632	0.368
1.737	0.479	11.65	0.697	18949.5	0.70	2.3304	25.90	0.701	0.299
1.864	0.514	12.07	0.722	20334.7	0.72	2.5844	24.91	0.765	0.235
2.118	0.584	12.90	0.772	23105.1	0.77	2.8385	23.94	0.827	0.173
2.372	0.654	13.72	0.821	25875.5	0.82	3.0924	23.12	0.880	0.120
2.626	0.724	14.46	0.865	28645.9	0.87	3.3464	22.49	0.921	0.079
2.880	0.794	15.15	0.906	31416.2	0.91	3.6004	21.93	0.957	0.043
3.134	0.864	15.73	0.941	34186.6	0.94	3.8544	21.60	0.978	0.022
3.388	0.934	16.21	0.970	36957.1	0.97	4.1084	21.38	0.992	0.008
3.642	1.004	16.50	0.987	39727.4	0.99	4.3624	21.28	0.998	0.002
3.896	1.074	16.65	0.996	42497.8	1.00	4.6164	21.25	1.000	-0.000
4.150	1.144	16.71	1.000	45268.2	1.00				

RUN C92974/100374 SPANWISE PROFILE TH=1 (2)

REX = 0.10000E 01 REM = 6759. REH = 8861.

XVO = 0.00 CM DEL2 = 0.619 CM DEH2 = 0.806 CM
UINF = 16.73 M/S DEL99= 3.627 CM DELT99 = 3.815 CM
VISC = 0.15316E-04 M2/S DEL1 = 0.977 CM UINF = 16.68 M/S
PORT = 2 H = 1.579 VISC = 0.15179E-04 M2/S
XLOC = 176.40 CM CF/2 = 0.10000E 01 TINF = 21.30 DEG C
TPLATE = 36.76 DEG C

Y(CM)	Y/DEL	U(M/S)	U/UINF	Y+	U+	Y(CM)	T(DEG C)	TBAR	TBAR
0.025	0.007	5.56	0.333	277.4	0.33	0.0546	33.81	0.191	0.809
0.028	0.008	5.70	0.341	305.1	0.34	0.0571	33.57	0.207	0.793
0.030	0.008	5.95	0.356	332.8	0.36	0.0597	33.36	0.220	0.780
0.033	0.009	6.18	0.370	360.6	0.37	0.0648	33.10	0.237	0.763
0.038	0.011	6.55	0.392	416.0	0.39	0.0724	32.77	0.258	0.742
0.046	0.013	6.98	0.417	499.2	0.42	0.0825	32.45	0.279	0.721
0.056	0.015	7.35	0.440	610.2	0.44	0.0952	32.11	0.301	0.699
0.069	0.019	7.72	0.462	748.9	0.46	0.1105	31.80	0.321	0.679
0.084	0.023	8.14	0.487	915.3	0.49	0.1308	31.52	0.339	0.661
0.102	0.028	8.38	0.501	1109.4	0.50	0.1562	31.26	0.356	0.644
0.122	0.034	8.64	0.516	1331.3	0.52	0.1867	31.08	0.368	0.632
0.147	0.041	8.86	0.530	1608.7	0.53	0.2222	30.98	0.374	0.626
0.178	0.049	9.10	0.544	1941.5	0.54	0.2629	30.82	0.385	0.615
0.213	0.059	9.29	0.555	2329.8	0.56	0.3086	30.80	0.386	0.614
0.254	0.070	9.43	0.564	2773.6	0.56	0.3619	30.80	0.386	0.614
0.300	0.083	9.52	0.569	3272.8	0.57	0.4254	30.80	0.386	0.614
0.351	0.097	9.59	0.573	3827.6	0.57	0.4889	30.83	0.384	0.616
0.406	0.112	9.63	0.576	4437.8	0.58	0.5524	30.85	0.382	0.618
0.467	0.129	9.62	0.575	5103.4	0.57	0.6159	30.88	0.380	0.620
0.538	0.148	9.49	0.567	5880.0	0.57	0.6794	30.85	0.382	0.618
0.620	0.171	9.44	0.565	6767.6	0.56	0.7429	30.80	0.386	0.614
0.696	0.192	9.39	0.562	7599.7	0.56	0.8064	30.70	0.392	0.608
0.772	0.213	9.41	0.563	8431.7	0.56	0.8699	30.59	0.399	0.601
0.848	0.234	9.49	0.567	9263.8	0.57	0.9334	30.51	0.405	0.595
0.925	0.255	9.63	0.576	10095.9	0.58	1.0604	30.12	0.430	0.570
1.026	0.283	9.86	0.590	11205.3	0.59	1.1874	29.63	0.462	0.538
1.128	0.311	10.13	0.606	12314.8	0.61	1.3144	29.04	0.500	0.500
1.229	0.339	10.40	0.622	13424.2	0.62	1.4414	28.47	0.537	0.463
1.356	0.374	10.68	0.638	14811.0	0.64	1.5684	27.93	0.571	0.429
1.483	0.409	10.98	0.656	16197.8	0.66	1.8224	26.81	0.644	0.356
1.610	0.444	11.23	0.672	17584.6	0.67	2.0764	25.83	0.707	0.293
1.737	0.479	11.67	0.697	18971.4	0.70	2.3304	24.87	0.769	0.231
1.864	0.514	12.06	0.721	20358.2	0.72	2.5844	23.96	0.828	0.172
2.118	0.584	12.92	0.773	23131.8	0.77	2.8385	23.14	0.881	0.119
2.372	0.654	13.75	0.822	25905.4	0.82	3.0924	22.51	0.922	0.078
2.626	0.724	14.53	0.869	28679.0	0.87	3.3464	21.98	0.956	0.044
2.880	0.794	15.21	0.910	31452.6	0.91	3.6004	21.65	0.978	0.022
3.134	0.864	15.83	0.946	34226.2	0.95	3.8544	21.43	0.991	0.009
3.388	0.934	16.23	0.970	36999.8	0.97	4.1084	21.33	0.998	0.002
3.642	1.004	16.53	0.988	39773.4	0.99	4.3624	21.32	0.999	0.001
3.896	1.074	16.66	0.996	42547.0	1.00	4.6164	21.30	1.000	-0.000
4.150	1.144	16.72	1.000	45320.6	1.00				
4.404	1.214	16.73	1.000	48094.2	1.00				

RUN 092974/100374 SPANWISE PROFILE TH=1 (3)

REX = 0.10000E 01 REM = 6181. REH = 8137.

XVO =	0.00 CM	DEL2 =	0.565 CM	DEH2 =	0.740 CM
UINF =	16.72 M/S	DEL99=	3.681 CM	DELT99 =	3.802 CM
VISC =	0.15300E-04 M2/S	DEL1 =	0.814 CM	UINF =	16.69 M/S
PORT =	3	H =	1.440	VISC =	0.15179E-04 M2/S
XLCC =	176.40 CM	CF/2 =	0.10000E 01	TINF =	21.30 DEG C
				TPLATE =	36.71 DEG C

Y(CM)	Y/DEL	U(M/S)	U/UINF	Y+	U+	Y(CM)	T(DEG C)	TBAR'	TBAR
0.025	0.007	6.43	0.384	277.6	0.38	0.0546	32.98	0.242	0.758
0.028	0.008	6.46	0.386	305.4	0.39	0.0571	32.66	0.263	0.737
0.030	0.008	6.76	0.404	333.2	0.40	0.0597	32.43	0.278	0.722
0.033	0.009	6.97	0.417	360.9	0.42	0.0622	32.28	0.287	0.713
0.038	0.010	7.47	0.447	416.5	0.45	0.0648	32.07	0.301	0.699
0.046	0.012	7.87	0.471	499.7	0.47	0.0724	31.63	0.329	0.671
0.056	0.015	8.28	0.495	610.8	0.50	0.0825	31.23	0.356	0.644
0.069	0.019	8.70	0.520	749.6	0.52	0.0952	30.87	0.379	0.621
0.084	0.023	9.02	0.539	916.2	0.54	0.1308	30.56	0.399	0.601
0.102	0.028	9.34	0.558	1110.5	0.56	0.1562	30.23	0.420	0.580
0.122	0.033	9.53	0.570	1332.6	0.57	0.1867	29.99	0.436	0.564
0.147	0.040	9.75	0.583	1610.3	0.58	0.2222	29.74	0.452	0.548
0.178	0.048	9.99	0.597	1943.4	0.60	0.2629	29.58	0.463	0.537
0.213	0.058	10.23	0.612	2332.1	0.61	0.3086	29.23	0.485	0.515
0.254	0.069	10.41	0.622	2776.4	0.62	0.3619	29.15	0.490	0.510
0.300	0.081	10.57	0.632	3276.1	0.63	0.4254	29.05	0.497	0.503
0.351	0.095	10.70	0.640	3831.4	0.64	0.4889	28.95	0.503	0.497
0.406	0.110	10.85	0.649	4442.2	0.65	0.5524	28.87	0.508	0.492
0.467	0.127	10.94	0.654	5108.5	0.65	0.6159	28.82	0.512	0.488
0.538	0.146	10.99	0.657	5885.9	0.66	0.6794	28.74	0.517	0.483
0.620	0.168	11.08	0.662	6774.3	0.66	0.8064	28.58	0.528	0.472
0.721	0.196	11.11	0.664	7884.8	0.66	0.9334	28.40	0.539	0.461
0.848	0.230	11.17	0.668	9273.0	0.67	1.0604	28.17	0.554	0.446
0.963	0.262	11.25	0.673	10522.4	0.67	1.1874	27.86	0.574	0.426
1.102	0.300	11.41	0.682	12049.4	0.68	1.3144	27.55	0.594	0.406
1.229	0.334	11.57	0.692	13437.5	0.69	1.4414	27.17	0.619	0.381
1.356	0.369	11.80	0.706	14825.7	0.71	1.5684	26.75	0.647	0.353
1.483	0.403	11.99	0.717	16213.9	0.72	1.8224	25.97	0.697	0.303
1.610	0.438	12.27	0.734	17602.1	0.73	2.0764	25.18	0.748	0.252
1.737	0.472	12.54	0.750	18990.3	0.75	2.3304	24.36	0.801	0.199
1.864	0.507	12.84	0.768	20378.4	0.77	2.5844	23.62	0.850	0.150
2.118	0.576	13.47	0.805	23154.8	0.81	2.8385	22.94	0.894	0.106
2.372	0.645	14.16	0.847	25931.1	0.85	3.0924	22.36	0.931	0.069
2.626	0.714	14.80	0.885	28707.5	0.88	3.3464	21.91	0.960	0.040
2.880	0.783	15.38	0.920	31483.8	0.92	3.6004	21.62	0.980	0.020
3.134	0.852	15.87	0.949	34260.2	0.95	3.8544	21.43	0.991	0.009
3.388	0.921	16.27	0.973	37036.5	0.97	4.1084	21.33	0.998	0.002
3.642	0.990	16.50	0.987	39812.9	0.99	4.3624	21.30	1.000	-0.000
3.896	1.059	16.67	0.997	42589.2	1.00				
4.150	1.128	16.69	0.998	45365.6	1.00				
4.404	1.197	16.73	1.000	48141.9	1.00				

RUN 092974/100374 SPANWISE PROFILE TH=1 (4)

REX = 0.10000E 01		REM =	5769.	REH =	8341.
XVO =	0.00 CM	DEL2 =	0.527 CM	DEH2 =	0.758 CM
UINF =	16.74 M/S	DEL99=	3.656 CM	DELT99 =	3.894 CM
VISC =	0.15306E-04 M2/S	DEL1 =	0.736 CM	UINF =	16.71 M/S
PORT =	4	H =	1.396	VISC =	0.15178E-04 M2/S
XLOC =	176.40 CM	CF/2 =	0.10000E 01	TINF =	21.28 DEG C
				TPLATE =	36.65 DEG C

Y(CM)	Y/DEL	U(M/S)	U/UINF	Y+	U+	Y(CM)	T(DEG C)	TBAR	TBAR
0.025	0.007	6.54	0.391	277.9	0.39	0.0546	33.04	0.235	0.765
0.028	0.008	6.85	0.409	305.6	0.41	0.0571	32.75	0.254	0.746
0.030	0.008	7.13	0.426	333.4	0.43	0.0597	32.54	0.267	0.733
0.036	0.010	7.55	0.451	389.0	0.45	0.0622	32.38	0.278	0.722
0.043	0.012	8.01	0.478	472.4	0.48	0.0648	32.10	0.296	0.704
0.053	0.015	8.40	0.502	583.5	0.50	0.0724	31.79	0.316	0.684
0.066	0.018	8.81	0.526	722.4	0.53	0.0825	31.39	0.342	0.658
0.081	0.022	9.18	0.548	889.2	0.55	0.0952	31.01	0.367	0.633
0.099	0.027	9.47	0.566	1083.7	0.57	0.1105	30.65	0.390	0.610
0.119	0.033	9.66	0.577	1305.9	0.58	0.1308	30.38	0.408	0.592
0.145	0.040	9.94	0.593	1583.8	0.59	0.1562	30.13	0.424	0.576
0.175	0.048	10.13	0.605	1917.2	0.60	0.1867	29.87	0.441	0.559
0.211	0.058	10.38	0.620	2306.3	0.62	0.2222	29.62	0.457	0.543
0.251	0.069	10.61	0.634	2750.8	0.63	0.2629	29.40	0.472	0.528
0.297	0.081	10.83	0.647	3251.0	0.65	0.3086	29.30	0.479	0.521
0.348	0.095	11.01	0.658	3806.7	0.66	0.3619	29.05	0.494	0.506
0.404	0.110	11.17	0.667	4418.0	0.67	0.4254	28.90	0.504	0.496
0.465	0.127	11.27	0.673	5084.9	0.67	0.4889	28.81	0.511	0.489
0.536	0.147	11.42	0.682	5862.9	0.68	0.5524	28.67	0.519	0.481
0.617	0.169	11.55	0.690	6752.0	0.69	0.6159	28.54	0.528	0.472
0.719	0.197	11.65	0.696	7863.5	0.70	0.6794	28.43	0.535	0.465
0.846	0.231	11.78	0.704	9252.8	0.70	0.8064	28.25	0.547	0.453
0.960	0.263	11.89	0.710	10503.2	0.71	0.9334	27.97	0.565	0.435
1.138	0.311	12.11	0.723	12448.2	0.72	1.0604	27.71	0.582	0.418
1.354	0.370	12.48	0.745	14810.0	0.75	1.1874	27.43	0.600	0.400
1.608	0.440	12.91	0.771	17588.6	0.77	1.3144	27.15	0.618	0.382
1.862	0.509	13.41	0.801	20367.2	0.80	1.4414	26.82	0.640	0.360
2.116	0.579	13.97	0.834	23145.9	0.83	1.5684	26.49	0.661	0.339
2.370	0.648	14.45	0.863	25924.5	0.86	1.8224	25.79	0.707	0.293
2.624	0.718	14.99	0.895	28703.1	0.89	2.0764	25.06	0.754	0.246
2.878	0.787	15.50	0.926	31481.7	0.93	2.3304	24.34	0.801	0.199
3.132	0.857	15.95	0.952	34260.3	0.95	2.5844	23.65	0.846	0.154
3.386	0.926	16.30	0.973	37038.9	0.97	2.8385	23.02	0.887	0.113
3.640	0.996	16.53	0.987	39817.5	0.99	3.0924	22.49	0.921	0.079
3.894	1.065	16.68	0.996	42596.2	1.00	3.3464	22.03	0.952	0.048
4.148	1.135	16.75	1.000	45374.8	1.00	3.6004	21.70	0.973	0.027
						3.854	21.47	0.988	0.012
						4.108	21.35	0.996	0.004
						4.362	21.32	0.998	0.002
						4.616	21.28	1.000	-0.000

RUN 092974/100374 SPANWISE PROFILE TH=1 (5)

REX = 0.10000E 01		REM = 6654.		REH = 9920.	
XVO =	0.00 CM	DEL2 =	0.609 CM	DEH2 =	0.902 CM
UINF =	16.73 M/S	DEL99=	3.805 CM	DELT99 =	4.072 CM
VISC =	0.15309E-04 M2/S	DEL1 =	0.907 CM	UINF =	16.69 M/S
PORT =	5	H =	1.490	VISC =	0.15175E-04 M2/S
XLCC =	176.40 CM	CF/2 =	0.10000E 01	TINF =	21.25 DEG C
				TPLATE =	36.59 DEG C

Y(CM)	Y/DEL	U(M/S)	U/UINF	Y+	U+	Y(CM)	T(DEG C)	TBAR	TBAR
0.025	0.007	6.95	0.418	277.5	0.42	0.0546	34.10	0.163	0.837
0.028	0.007	7.22	0.431	305.3	0.43	0.0571	33.97	0.171	0.829
0.030	0.008	7.49	0.448	333.0	0.45	0.0597	33.87	0.177	0.823
0.036	0.009	7.83	0.468	388.5	0.47	0.0622	33.84	0.179	0.821
0.043	0.011	8.13	0.486	471.8	0.49	0.0673	33.76	0.185	0.815
0.053	0.014	8.30	0.496	582.8	0.50	0.0749	33.82	0.181	0.819
0.066	0.017	8.44	0.504	721.5	0.50	0.0851	33.93	0.173	0.827
0.081	0.021	8.49	0.508	888.1	0.51	0.0978	34.08	0.164	0.836
0.102	0.027	8.44	0.505	1110.1	0.50	0.1130	34.32	0.148	0.852
0.122	0.032	8.47	0.506	1332.1	0.51	0.1333	34.58	0.131	0.869
0.147	0.039	8.60	0.514	1609.6	0.51	0.1587	34.77	0.118	0.882
0.178	0.047	8.68	0.519	1942.6	0.52	0.1968	34.92	0.109	0.891
0.213	0.056	8.93	0.534	2331.1	0.53	0.2476	34.89	0.111	0.889
0.249	0.065	8.99	0.537	2719.7	0.54	0.2984	34.54	0.133	0.867
0.290	0.076	9.24	0.552	3163.7	0.55	0.3492	34.01	0.168	0.832
0.335	0.088	9.43	0.564	3663.2	0.56	0.4000	33.44	0.205	0.795
0.386	0.101	9.61	0.575	4218.3	0.57	0.4509	32.79	0.248	0.752
0.442	0.116	9.81	0.586	4828.8	0.59	0.5016	32.11	0.292	0.708
0.503	0.132	10.00	0.598	5494.8	0.60	0.5524	31.61	0.325	0.675
0.579	0.152	10.27	0.614	6327.4	0.61	0.6032	31.27	0.347	0.653
0.681	0.179	10.47	0.626	7437.5	0.63	0.6540	30.68	0.385	0.615
0.808	0.212	10.69	0.639	8825.0	0.64	0.7048	30.32	0.409	0.591
0.960	0.252	10.92	0.653	10490.2	0.65	0.7556	30.08	0.425	0.575
1.138	0.299	11.18	0.668	12432.8	0.67	0.8064	29.77	0.445	0.555
1.354	0.356	11.54	0.690	14791.7	0.69	0.8572	29.57	0.457	0.543
1.608	0.423	12.08	0.722	17556.8	0.72	0.9080	29.36	0.471	0.529
1.862	0.489	12.64	0.756	20342.0	0.76	0.9588	29.23	0.480	0.520
2.116	0.556	13.25	0.792	23117.2	0.79	1.0096	29.04	0.493	0.507
2.370	0.623	13.81	0.826	25892.4	0.83	1.0604	28.92	0.500	0.500
2.624	0.690	14.40	0.861	28667.5	0.86	1.1239	28.77	0.510	0.490
2.878	0.756	14.95	0.896	31442.7	0.90	1.1874	28.58	0.522	0.478
3.132	0.823	15.53	0.928	34217.9	0.93	1.3144	28.27	0.543	0.457
3.386	0.890	15.97	0.955	36993.1	0.95	1.4414	27.87	0.568	0.432
3.640	0.957	16.36	0.978	39768.2	0.98	1.5584	27.46	0.595	0.405
3.894	1.023	16.58	0.991	42543.4	0.99	1.8224	26.60	0.652	0.348
4.148	1.090	16.64	0.995	45318.6	0.99	2.0764	25.76	0.706	0.294
4.402	1.157	16.71	0.999	48093.8	1.00	2.3304	24.98	0.757	0.243
4.656	1.224	16.73	1.000	50868.9	1.00	2.5844	24.24	0.805	0.195
						2.838	23.53	0.851	0.149
						3.092	22.87	0.894	0.106
						3.346	22.29	0.932	0.068
						3.600	21.86	0.960	0.040
						3.854	21.57	0.980	0.020
						4.108	21.38	0.991	0.009
						4.362	21.30	0.997	0.003
						4.616	21.25	1.000	-0.000

RUN 052974/100374 SPANWISE PROFILE TH=1 (6)

REX	= 0.10000E 01	REM =	6814.	REH =	9642.
XVO =	0.00 CM	DEL2 =	0.625 CM	DEH2 =	0.878 CM
UINF =	16.70 M/S	DEL99=	3.866 CM	DELT99 =	4.034 CM
VISC =	0.15314E-04 M2/S	DEL1 =	1.216 CM	UINF =	16.67 M/S
PORT =	6	H =	1.947	VISC =	0.15184E-04 M2/S
XLOC =	176.40 CM	CF/2 =	0.10000E 01	TINF =	21.35 DEG C
				TPLATE =	36.55 DEG C

Y(CM)	Y/DEL	U(M/S)	U/UINF	Y+	U+	Y(CM)	T(DEG C)	TBAR	TBAR
0.025	0.007	0.00	0.000	277.0	0.00	0.0546	35.80	0.049	0.951
0.084	0.022	0.00	0.000	914.3	0.00	0.0673	35.67	0.058	0.942
0.147	0.038	0.00	0.000	1606.9	0.00	0.0800	35.67	0.058	0.942
0.173	0.045	0.00	0.000	1883.9	0.00	0.0927	35.72	0.055	0.945
0.198	0.051	0.00	0.000	2161.0	0.00	0.1054	35.77	0.052	0.948
0.211	0.055	0.00	0.000	2299.5	0.00	0.1181	35.78	0.051	0.949
0.224	0.058	1.70	0.101	2438.0	0.10	0.1308	35.83	0.047	0.953
0.236	0.061	2.82	0.169	2576.6	0.17	0.1435	35.87	0.045	0.955
0.249	0.064	3.69	0.221	2715.1	0.22	0.1562	35.93	0.041	0.959
0.262	0.068	4.55	0.273	2853.6	0.27	0.1689	35.99	0.037	0.963
0.274	0.071	5.20	0.311	2992.1	0.31	0.1943	36.12	0.028	0.972
0.287	0.074	5.91	0.354	3130.7	0.35	0.2197	36.30	0.017	0.983
0.300	0.078	6.48	0.388	3269.2	0.39	0.2451	36.46	0.006	0.994
0.312	0.081	6.98	0.418	3407.7	0.42	0.2705	36.58	-0.002	1.002
0.325	0.084	7.45	0.446	3546.2	0.45	0.2959	36.67	-0.008	1.008
0.338	0.087	7.85	0.470	3684.7	0.47	0.3467	36.76	-0.014	1.014
0.358	0.093	8.30	0.497	3905.4	0.50	0.3975	36.68	-0.008	1.008
0.389	0.101	8.70	0.521	4238.8	0.52	0.4483	36.47	0.006	0.994
0.429	0.111	9.02	0.540	4662.1	0.54	0.4991	36.08	0.031	0.969
0.480	0.124	9.21	0.551	5236.2	0.55	0.5499	35.58	0.064	0.936
0.541	0.140	9.31	0.557	5901.1	0.56	0.6007	34.87	0.111	0.889
0.617	0.160	9.33	0.558	6732.3	0.56	0.6515	34.12	0.160	0.840
0.693	0.179	9.33	0.558	7563.4	0.56	0.7023	33.36	0.210	0.790
0.770	0.199	9.33	0.559	8394.6	0.56	0.7531	32.68	0.255	0.745
0.846	0.219	9.40	0.563	9225.7	0.56	0.8039	32.12	0.292	0.708
0.922	0.238	9.48	0.568	10056.9	0.57	0.8547	31.58	0.327	0.673
1.024	0.265	9.62	0.576	11165.1	0.58	0.9055	31.08	0.360	0.640
1.100	0.284	9.71	0.581	11996.2	0.58	0.9563	30.77	0.381	0.619
1.176	0.304	9.87	0.591	12827.4	0.59	1.0071	30.46	0.401	0.599
1.278	0.330	10.02	0.600	13935.6	0.60	1.0579	30.20	0.418	0.582
1.405	0.363	10.29	0.616	15320.6	0.62	1.1087	30.02	0.430	0.570
1.557	0.403	10.66	0.638	16983.1	0.64	1.1595	29.81	0.444	0.556
1.709	0.442	11.08	0.663	18645.4	0.66	1.2357	29.60	0.458	0.542
1.913	0.495	11.61	0.695	20861.8	0.70	1.3119	29.37	0.473	0.527
2.141	0.554	12.30	0.737	23355.2	0.74	1.4389	29.02	0.495	0.505
2.395	0.620	13.06	0.782	26125.7	0.78	1.5659	28.58	0.524	0.476
2.649	0.685	13.80	0.826	28896.2	0.83	1.6929	28.14	0.553	0.447
2.903	0.751	14.51	0.869	31666.7	0.87	1.8199	27.63	0.587	0.413
3.157	0.817	15.18	0.909	34437.2	0.91	2.0739	26.66	0.650	0.350
3.411	0.882	15.76	0.944	37207.6	0.94	2.3279	25.71	0.713	0.287
3.665	0.948	16.21	0.971	39978.1	0.97	2.5819	24.85	0.770	0.230
3.919	1.014	16.51	0.988	42748.6	0.99	2.8359	24.05	0.823	0.177
4.173	1.079	16.67	0.998	45519.1	1.00	3.0899	23.29	0.873	0.127
4.427	1.145	16.71	1.000	48289.6	1.00	3.3439	22.63	0.916	0.084
						3.596	22.08	0.952	0.048
						3.852	21.70	0.977	0.023
						4.106	21.45	0.993	0.007
						4.360	21.35	1.000	-0.000

RUN 092974/100374 SPANWISE PROFILE TH=1 (7)

REX = 0.10000E 01 REM = 7734. REH = 10138.

XVO = 0.00 CM DEL2 = 0.699 CM DEH2 = 0.917 CM
UINF = 16.77 M/S DEL99= 3.954 CM DELT99 = 4.089 CM
VISC = 0.15158E-04 M2/S DEL1 = 1.136 CM UINF = 16.78 M/S
PORT = 7 H = 1.625 VISC = 0.15171E-04 M2/S
XLOC = 176.40 CM CF/2 = 0.10000E 01 TINF = 21.20 DEG C
TPLATE = 36.74 DEG C

Y(CM)	Y/DEL	U(M/S)	U/UINF	Y+	U+	Y(CM)	T(DEG C)	TBAR	TBAR
0.025	0.006	6.32	0.377	281.0	0.38	0.0546	34.13	0.168	0.832
0.028	0.007	6.32	0.377	309.1	0.38	0.0571	34.07	0.172	0.828
0.030	0.008	6.35	0.379	337.1	0.38	0.0597	34.00	0.176	0.824
0.036	0.009	6.78	0.405	393.3	0.40	0.0622	33.83	0.188	0.812
0.043	0.011	7.26	0.433	477.6	0.43	0.0673	33.63	0.200	0.800
0.053	0.013	7.53	0.449	590.0	0.45	0.0698	33.57	0.204	0.796
0.066	0.017	7.64	0.455	730.5	0.46	0.0775	33.50	0.209	0.791
0.081	0.021	7.55	0.450	899.1	0.45	0.0876	33.49	0.210	0.790
0.102	0.026	7.43	0.443	1123.8	0.44	0.1003	33.63	0.200	0.800
0.122	0.031	7.36	0.439	1348.6	0.44	0.1156	33.81	0.189	0.811
0.147	0.037	7.38	0.440	1629.6	0.44	0.1359	34.04	0.174	0.826
0.178	0.045	7.56	0.451	1966.7	0.45	0.1613	34.26	0.160	0.840
0.213	0.054	7.91	0.472	2360.0	0.47	0.1994	34.62	0.137	0.863
0.249	0.063	8.30	0.495	2753.4	0.50	0.2502	34.78	0.127	0.873
0.290	0.073	8.63	0.515	3202.9	0.51	0.3010	34.86	0.122	0.878
0.335	0.085	8.91	0.531	3708.6	0.53	0.3518	34.61	0.137	0.863
0.386	0.098	9.04	0.539	4270.6	0.54	0.4026	34.30	0.157	0.843
0.442	0.112	9.12	0.544	4886.7	0.54	0.4534	33.85	0.186	0.814
0.503	0.127	9.16	0.546	5563.0	0.55	0.5042	33.41	0.214	0.786
0.579	0.146	9.15	0.546	6405.8	0.55	0.5550	32.94	0.245	0.755
0.681	0.172	9.22	0.550	7529.7	0.55	0.6058	32.39	0.280	0.720
0.808	0.204	9.36	0.559	8934.5	0.56	0.6566	31.94	0.309	0.691
0.960	0.243	9.53	0.568	10620.2	0.57	0.7074	31.60	0.331	0.669
1.138	0.288	9.71	0.579	12586.9	0.58	0.7582	31.22	0.355	0.645
1.354	0.342	10.00	0.596	14975.1	0.60	0.8090	30.90	0.376	0.624
1.608	0.407	10.59	0.631	17784.6	0.63	0.8598	30.62	0.394	0.606
1.862	0.471	11.26	0.672	20594.2	0.67	0.9106	30.41	0.407	0.593
2.116	0.535	12.01	0.716	23403.8	0.72	0.9614	30.25	0.418	0.582
2.370	0.599	12.83	0.765	26213.4	0.77	1.0122	30.09	0.428	0.572
2.624	0.664	13.56	0.809	29023.0	0.81	1.0630	29.96	0.437	0.563
2.878	0.728	14.28	0.852	31832.5	0.85	1.1265	29.79	0.447	0.553
3.132	0.792	14.99	0.894	34642.1	0.89	1.1900	29.66	0.456	0.544
3.386	0.856	15.61	0.931	37451.7	0.93	1.3170	29.30	0.479	0.521
3.640	0.920	16.17	0.964	40261.3	0.96	1.4440	28.98	0.500	0.500
3.894	0.985	16.50	0.984	43070.9	0.98	1.5710	28.60	0.524	0.476
4.148	1.049	16.67	0.994	45880.4	0.99	1.8250	27.65	0.585	0.415
4.402	1.113	16.75	0.995	48690.0	1.00	2.0790	26.70	0.646	0.354
4.656	1.177	16.77	1.000	51499.6	1.00	2.3330	25.73	0.709	0.291
						2.587	24.82	0.767	0.233
						2.841	24.02	0.819	0.181
						3.095	23.21	0.871	0.129
						3.349	22.53	0.915	0.085
						3.603	22.01	0.948	0.052
						3.857	21.62	0.973	0.027
						4.111	21.33	0.991	0.009
						4.365	21.23	0.998	0.002
						4.619	21.20	1.000	0.000

RUN 092974/100374 SPANWISE PROFILE TH=1 (8)

REX	= 0.10000E 01	REM =	7051.	REH =	9077.
XVO =	0.00 CM	DEL2 =	0.640 CM	DEH2 =	0.823 CM
UINF =	16.74 M/S	DEL99=	3.898 CM	DELT99 =	4.022 CM
VISC =	0.15195E-04 M2/S	DEL1 =	0.953 CM	UINF =	16.73 M/S
PORT =	8	H =	1.488	VISC =	0.15175E-04 M2/S
XLOC =	176.40 CM	CF/2 =	0.10000E 01	TINF =	21.25 DEG C
				TPLATE =	36.76 DEG C

Y(CM)	Y/DEL	U(M/S)	U/UINF	Y+	U+	Y(CM)	T(DEG C)	TBAR	TBAR
0.025	0.007	5.90	0.353	279.8	0.35	0.0546	33.71	0.197	0.803
0.028	0.007	5.94	0.355	307.7	0.35	0.0571	33.66	0.200	0.800
0.033	0.008	6.32	0.378	363.7	0.38	0.0597	33.36	0.220	0.780
0.041	0.010	6.94	0.415	447.6	0.41	0.0622	33.08	0.237	0.763
0.051	0.013	7.56	0.451	559.5	0.45	0.0648	32.92	0.248	0.752
0.063	0.016	7.94	0.474	699.4	0.47	0.0673	32.76	0.258	0.742
0.079	0.020	8.34	0.498	867.3	0.50	0.0749	32.37	0.283	0.717
0.097	0.025	8.60	0.514	1063.1	0.51	0.0851	31.96	0.310	0.690
0.117	0.030	8.84	0.528	1287.0	0.53	0.0978	31.60	0.333	0.667
0.142	0.036	9.06	0.541	1566.7	0.54	0.1130	31.24	0.356	0.644
0.173	0.044	9.31	0.556	1902.5	0.56	0.1333	31.02	0.371	0.629
0.208	0.053	9.56	0.571	2294.1	0.57	0.1587	30.66	0.394	0.606
0.249	0.064	9.77	0.584	2741.8	0.58	0.1892	30.57	0.399	0.601
0.295	0.076	9.98	0.596	3245.4	0.60	0.2248	30.25	0.420	0.580
0.345	0.089	10.13	0.605	3804.9	0.61	0.2603	30.07	0.432	0.568
0.401	0.103	10.28	0.614	4420.4	0.61	0.3111	29.86	0.445	0.555
0.462	0.119	10.36	0.619	5091.9	0.62	0.3645	29.72	0.454	0.546
0.533	0.137	10.45	0.624	5875.2	0.62	0.4280	29.56	0.464	0.536
0.615	0.158	10.50	0.627	6770.5	0.63	0.4915	29.46	0.471	0.529
0.716	0.184	10.58	0.632	7889.6	0.63	0.5550	29.41	0.474	0.526
0.843	0.216	10.63	0.635	9288.4	0.63	0.6185	29.33	0.479	0.521
0.958	0.246	10.74	0.642	10547.4	0.64	0.6820	29.23	0.485	0.515
1.135	0.291	10.88	0.650	12505.6	0.65	0.8090	29.09	0.495	0.505
1.351	0.347	11.20	0.669	14863.9	0.67	0.9360	28.91	0.506	0.494
1.605	0.412	11.66	0.697	17681.6	0.70	1.0630	28.71	0.519	0.481
1.859	0.477	12.18	0.728	20479.3	0.73	1.1900	28.47	0.535	0.465
2.113	0.542	12.75	0.762	23277.1	0.76	1.3170	28.19	0.553	0.447
2.367	0.607	13.36	0.798	26074.8	0.80	1.4440	27.88	0.573	0.427
2.621	0.672	13.99	0.836	28872.5	0.84	1.5710	27.53	0.595	0.405
2.875	0.738	14.66	0.876	31670.2	0.88	1.8250	26.79	0.643	0.357
3.129	0.803	15.23	0.910	34467.9	0.91	2.0790	26.02	0.692	0.308
3.383	0.868	15.79	0.943	37265.7	0.94	2.3330	25.18	0.746	0.254
3.637	0.933	16.24	0.970	40063.4	0.97	2.5870	24.43	0.795	0.205
3.891	0.998	16.53	0.988	42861.1	0.99	2.8410	23.65	0.845	0.155
4.145	1.063	16.71	0.998	45658.8	1.00	3.0950	23.04	0.885	0.115
4.399	1.129	16.74	1.000	48456.6	1.00	3.3490	22.43	0.924	0.076
						3.603	21.93	0.956	0.044
						3.857	21.57	0.980	0.020
						4.111	21.37	0.993	0.007
						4.365	21.28	0.998	0.002
						4.619	21.25	1.000	0.000

RUN 092974/100374 SPANWISE PROFILE TH=1 (9)

REX	= 0.10000E 01	REM	= 6381.	REH	= 8617.
XVO	= 0.00 CM	DEL2	= 0.584 CM	DEH2	= 0.782 CM
UINF	= 16.78 M/S	DEL99	= 3.859 CM	DELT99	= 3.969 CM
VISC	= 0.15365E-04 M2/S	DEL1	= 0.829 CM	UINF	= 16.72 M/S
PORT	= 9	H	= 1.419	VISC	= 0.15181E-04 M2/S
XLOC	= 176.40 CM	CF/2	= 0.10000E 01	TINF	= 21.32 DEG C
				TPLATE	= 36.78 DEG C

Y(CM)	Y/DEL	U(M/S)	U/UINF	Y+	U+	Y(CM)	T(DEG C)	TBAR	TBAR
0.025	0.007	6.51	0.388	277.5	0.39	0.0546	33.47	0.214	0.786
0.028	0.007	6.53	0.389	305.2	0.39	0.0571	33.40	0.219	0.781
0.033	0.009	7.01	0.417	360.7	0.42	0.0597	33.34	0.223	0.777
0.041	0.011	7.56	0.450	443.9	0.45	0.0622	33.04	0.242	0.758
0.051	0.013	8.11	0.483	554.9	0.48	0.0673	32.56	0.273	0.727
0.063	0.016	8.60	0.513	693.7	0.51	0.0749	32.09	0.304	0.696
0.079	0.020	8.95	0.534	860.1	0.53	0.0851	31.60	0.335	0.665
0.097	0.025	9.29	0.553	1054.4	0.55	0.0978	31.13	0.366	0.634
0.117	0.030	9.58	0.571	1276.3	0.57	0.1130	30.74	0.391	0.609
0.142	0.037	9.79	0.583	1553.8	0.58	0.1333	30.41	0.412	0.588
0.173	0.045	10.01	0.597	1886.8	0.60	0.1587	30.18	0.427	0.573
0.208	0.054	10.25	0.611	2275.2	0.61	0.1892	29.89	0.446	0.554
0.249	0.064	10.43	0.622	2719.2	0.62	0.2248	29.79	0.452	0.548
0.295	0.076	10.62	0.633	3218.6	0.63	0.2654	29.58	0.466	0.534
0.345	0.090	10.78	0.642	3773.5	0.64	0.3111	29.48	0.472	0.528
0.401	0.104	10.95	0.652	4384.0	0.65	0.3645	29.30	0.484	0.516
0.462	0.120	11.03	0.657	5049.9	0.66	0.4280	29.23	0.488	0.512
0.533	0.138	11.10	0.661	5826.8	0.66	0.4915	29.12	0.496	0.504
0.615	0.159	11.21	0.668	6714.7	0.67	0.5550	29.02	0.502	0.498
0.716	0.186	11.25	0.670	7824.5	0.67	0.6185	28.94	0.507	0.493
0.843	0.219	11.37	0.678	9211.9	0.68	0.6820	28.87	0.512	0.488
0.958	0.248	11.52	0.686	10460.4	0.69	0.7455	28.76	0.519	0.481
1.097	0.284	11.67	0.695	11986.5	0.70	0.8090	28.66	0.525	0.475
1.224	0.317	11.82	0.704	13373.8	0.70	0.8725	28.56	0.532	0.468
1.351	0.350	11.98	0.714	14761.2	0.71	0.9360	28.49	0.536	0.464
1.478	0.383	12.22	0.728	16148.5	0.73	1.0630	28.22	0.554	0.446
1.605	0.416	12.44	0.741	17535.8	0.74	1.1900	27.89	0.575	0.425
1.732	0.449	12.67	0.755	18923.1	0.76	1.3170	27.56	0.596	0.404
1.859	0.482	12.96	0.772	20310.5	0.77	1.4440	27.25	0.616	0.384
2.113	0.548	13.43	0.800	23085.1	0.80	1.5710	26.89	0.640	0.360
2.367	0.613	13.98	0.833	25859.8	0.83	1.8250	26.15	0.687	0.313
2.621	0.679	14.51	0.865	28634.4	0.86	2.0790	25.41	0.735	0.265
2.875	0.745	15.08	0.898	31409.1	0.90	2.3330	24.67	0.783	0.217
3.129	0.811	15.57	0.928	34183.7	0.93	2.5870	24.00	0.827	0.173
3.383	0.877	16.03	0.955	36958.4	0.95	2.8410	23.32	0.871	0.129
3.637	0.942	16.38	0.976	39733.0	0.98	3.0950	22.71	0.910	0.090
3.891	1.008	16.62	0.990	42507.7	0.99	3.3490	22.23	0.941	0.059
4.145	1.074	16.74	0.997	45282.3	1.00	3.6030	21.85	0.966	0.034
4.399	1.140	16.78	1.000	48057.0	1.00	3.8570	21.55	0.985	0.015
4.653	1.206	16.79	1.000	50831.7	1.00	4.1110	21.42	0.994	0.006
						4.365	21.33	0.999	0.001
						4.619	21.32	1.000	-0.000

RUN 092974/100374 SPANWISE PROFILE TH=1 (10)

REX = 0.10000E 01 REM = 6720. REH = 9158.

XVO = 0.00 CM DEL2 = 0.612 CM DEH2 = 0.832 CM
UINF = 16.72 M/S DEL99= 3.831 CM DELT99 = 3.944 CM
VISC = 0.15224E-04 M2/S DEL1 = 0.908 CM UINF = 16.71 M/S
PORT = 10 H = 1.483 VISC = 0.15175E-04 M2/S
XLCC = 176.40 CM CF/2 = 0.10000E 01 TINF = 21.25 DEG C
TPLATE = 36.80 DEG C

Y(CM)	Y/DEL	U(M/S)	U/UINF	Y+	U+	Y(CM)	T(DEG C)	TBAR	TBAR
0.025	0.007	6.16	0.368	279.0	0.37	0.0546	34.05	0.177	0.823
0.028	0.007	6.31	0.377	306.9	0.38	0.0571	33.97	0.182	0.818
0.033	0.009	6.78	0.405	362.6	0.41	0.0597	33.74	0.197	0.803
0.041	0.011	7.32	0.438	446.3	0.44	0.0622	33.50	0.212	0.788
0.051	0.013	7.82	0.468	557.9	0.47	0.0673	33.13	0.236	0.764
0.063	0.017	8.23	0.492	697.4	0.49	0.0749	32.74	0.261	0.739
0.079	0.021	8.63	0.516	864.8	0.52	0.0851	32.33	0.288	0.712
0.097	0.025	9.01	0.539	1060.1	0.54	0.0978	31.97	0.311	0.689
0.117	0.030	9.20	0.550	1283.2	0.55	0.1130	31.60	0.335	0.665
0.142	0.037	9.49	0.567	1562.2	0.57	0.1333	31.30	0.353	0.647
0.173	0.045	9.69	0.580	1896.9	0.58	0.1587	31.03	0.371	0.629
0.208	0.054	9.90	0.592	2237.5	0.59	0.1892	30.88	0.381	0.619
0.249	0.065	10.02	0.599	2733.8	0.60	0.2248	30.77	0.388	0.612
0.295	0.077	10.13	0.606	3236.0	0.61	0.2654	30.65	0.396	0.604
0.345	0.090	10.20	0.610	3793.9	0.61	0.3111	30.59	0.400	0.600
0.401	0.105	10.23	0.612	4407.6	0.61	0.3645	30.59	0.400	0.600
0.462	0.121	10.23	0.612	5077.1	0.61	0.4280	30.57	0.401	0.599
0.533	0.139	10.25	0.613	5858.2	0.61	0.4915	30.55	0.402	0.598
0.615	0.160	10.25	0.613	6750.9	0.61	0.5550	30.55	0.402	0.598
0.691	0.180	10.28	0.615	7587.8	0.61	0.6185	30.54	0.403	0.597
0.767	0.200	10.36	0.620	8424.6	0.62	0.6820	30.39	0.412	0.588
0.843	0.220	10.41	0.623	9261.5	0.62	0.7455	30.39	0.412	0.588
0.919	0.240	10.49	0.627	10098.4	0.63	0.8090	30.06	0.433	0.567
1.021	0.267	10.70	0.640	11214.3	0.64	0.8725	30.10	0.431	0.569
1.097	0.286	10.81	0.646	12051.1	0.65	0.9360	29.92	0.443	0.557
1.224	0.320	11.10	0.664	13445.9	0.66	1.0630	29.49	0.470	0.530
1.351	0.353	11.38	0.681	14840.8	0.68	1.1900	29.02	0.500	0.500
1.478	0.386	11.62	0.695	16235.6	0.70	1.3170	28.56	0.530	0.470
1.605	0.419	11.88	0.710	17630.4	0.71	1.4440	27.99	0.567	0.433
1.732	0.452	12.18	0.728	19025.2	0.73	1.5710	27.55	0.595	0.405
1.859	0.485	12.52	0.749	20420.0	0.75	1.8250	26.56	0.658	0.342
2.113	0.552	13.19	0.789	23209.6	0.79	2.0790	25.64	0.718	0.282
2.367	0.618	13.83	0.827	25999.2	0.83	2.3330	24.79	0.773	0.227
2.621	0.684	14.45	0.864	28788.8	0.86	2.5870	24.00	0.823	0.177
2.875	0.750	15.01	0.898	31578.4	0.90	2.8410	23.24	0.872	0.128
3.129	0.817	15.35	0.918	34368.0	0.92	3.0950	22.61	0.913	0.087
3.383	0.883	16.00	0.957	37157.7	0.96	3.3490	22.11	0.945	0.055
3.637	0.949	16.33	0.977	39947.3	0.98	3.6030	21.73	0.969	0.031
3.891	1.016	16.56	0.990	42736.9	0.99	3.8570	21.47	0.986	0.014
3.891	1.016	16.56	0.990	42736.9	0.99	4.1110	21.32	0.996	0.004
4.145	1.082	16.70	0.999	45526.5	1.00	4.3650	21.25	1.000	-0.000
4.399	1.148	16.72	1.000	48316.1	1.00				

RUN 092974/100374 SPANWISE PROFILE TH=1 (11)

REX = 0.10000E 01	REM =	7255.	REH	=	9490.
XVO = 0.00 CM	DEL2 =	0.659 CM	DEH2	=	0.862 CM
UINF = 16.72 M/S	DEL99=	3.907 CM	DELT99	=	3.987 CM
VISC = 0.15196E-04 M2/S	DEL1 =	1.099 CM	UINF	=	16.72 M/S
PORT = 11	H =	1.667	VISC	=	0.15178E-04 M2/S
XLOC = 176.40 CM	CF/2 =	0.10000E 01	TINF	=	21.28 DEG C
			TPLATE	=	36.80 DEG C

Y(CM)	Y/DEL	U(M/S)	U/UINF	Y+	U+	Y(CM)	T(DEG C)	TBAR	TBAR
0.025	0.007	4.94	0.296	279.4	0.30	0.0546	35.21	0.103	0.897
0.030	0.008	4.97	0.297	335.3	0.30	0.0571	35.17	0.105	0.895
0.033	0.008	5.14	0.308	363.3	0.31	0.0597	35.16	0.106	0.894
0.036	0.009	5.51	0.329	391.2	0.33	0.0622	35.12	0.108	0.892
0.043	0.011	5.95	0.356	475.1	0.36	0.0648	34.98	0.117	0.883
0.053	0.014	6.34	0.379	586.8	0.38	0.0673	34.82	0.128	0.872
0.066	0.017	6.75	0.404	726.6	0.40	0.0724	34.56	0.145	0.855
0.081	0.021	7.11	0.425	894.2	0.43	0.0800	34.28	0.162	0.838
0.099	0.025	7.34	0.439	1089.8	0.44	0.0902	33.99	0.181	0.819
0.119	0.031	7.59	0.454	1313.4	0.45	0.1029	33.73	0.198	0.802
0.145	0.037	7.85	0.470	1592.9	0.47	0.1181	33.47	0.215	0.785
0.175	0.045	8.07	0.483	1928.2	0.48	0.1384	33.19	0.232	0.768
0.211	0.054	8.22	0.492	2319.4	0.49	0.1638	32.98	0.246	0.754
0.251	0.064	8.34	0.499	2766.5	0.50	0.1943	32.77	0.260	0.740
0.297	0.076	8.45	0.506	3269.5	0.51	0.2299	32.67	0.266	0.734
0.348	0.089	8.44	0.505	3828.4	0.51	0.2705	32.54	0.274	0.726
0.404	0.103	8.46	0.506	4443.2	0.51	0.3162	32.53	0.275	0.725
0.465	0.119	8.40	0.503	5113.9	0.50	0.3696	32.49	0.278	0.722
0.536	0.137	8.36	0.500	5896.3	0.50	0.4331	32.48	0.279	0.721
0.617	0.158	8.33	0.498	6790.6	0.50	0.4966	32.48	0.279	0.721
0.693	0.177	8.32	0.498	7628.9	0.50	0.5601	32.51	0.276	0.724
0.770	0.197	8.42	0.504	8467.3	0.50	0.6236	32.41	0.283	0.717
0.846	0.216	8.56	0.512	9305.6	0.51	0.6871	32.33	0.288	0.712
0.922	0.236	8.77	0.525	10144.0	0.52	0.7506	32.30	0.290	0.710
1.024	0.262	9.11	0.545	11261.7	0.55	0.8141	32.17	0.298	0.702
1.125	0.288	9.56	0.572	12379.5	0.57	0.8776	32.04	0.307	0.693
1.227	0.314	9.92	0.593	13497.3	0.59	0.9411	31.76	0.325	0.675
1.354	0.346	10.31	0.617	14894.6	0.62	1.0681	31.26	0.357	0.643
1.481	0.379	10.69	0.639	16291.8	0.64	1.1951	30.64	0.397	0.603
1.608	0.411	11.03	0.659	17689.0	0.66	1.3221	29.92	0.444	0.556
1.735	0.444	11.39	0.681	19086.3	0.68	1.4491	29.20	0.490	0.510
1.862	0.477	12.04	0.720	20483.5	0.72	1.5761	28.55	0.532	0.468
2.116	0.542	12.56	0.751	23278.0	0.75	1.8301	27.27	0.614	0.386
2.370	0.607	13.34	0.798	26072.5	0.80	2.0841	26.19	0.684	0.316
2.624	0.672	14.11	0.844	28867.0	0.84	2.3381	25.19	0.749	0.251
2.878	0.737	14.78	0.884	31661.4	0.88	2.5921	24.26	0.808	0.192
3.132	0.802	15.40	0.921	34455.9	0.92	2.8461	23.47	0.859	0.141
3.386	0.867	15.87	0.949	37250.4	0.95	3.1001	22.74	0.906	0.094
3.640	0.932	16.26	0.973	40044.9	0.97	3.3541	22.25	0.938	0.062
3.894	0.997	16.51	0.987	42839.4	0.99	3.6081	21.78	0.968	0.032
4.148	1.062	16.65	0.996	45633.8	1.00	3.8621	21.53	0.984	0.016
4.402	1.127	16.72	1.000	48428.3	1.00	4.1161	21.38	0.994	0.006
						4.370	21.30	0.999	0.001
						4.624	21.28	1.000	0.000

SPANWISE AVERAGE OF 11 Z STATIONS

Y(CM)	U(M/S)	U/UINF	T(C)	TBAR	TBAR
0.055	6.77	0.404	34.04	0.174	0.826
0.057	6.83	0.408	33.90	0.183	0.817
0.060	6.89	0.412	33.73	0.194	0.806
0.065	7.01	0.419	33.42	0.214	0.786
0.072	7.16	0.428	33.12	0.234	0.766
0.083	7.33	0.438	32.82	0.253	0.747
0.095	7.48	0.447	32.57	0.269	0.731
0.110	7.61	0.455	32.36	0.283	0.717
0.131	7.77	0.464	32.19	0.293	0.707
0.156	7.94	0.474	32.03	0.304	0.696
0.187	8.12	0.485	31.93	0.310	0.690
0.222	8.50	0.508	31.84	0.316	0.684
0.263	9.07	0.542	31.74	0.322	0.678
0.309	9.51	0.568	31.66	0.328	0.672
0.362	9.82	0.587	31.54	0.336	0.664
0.425	9.99	0.597	31.38	0.346	0.654
0.489	10.07	0.602	31.19	0.358	0.642
0.552	10.12	0.605	31.00	0.371	0.629
0.616	10.15	0.607	30.76	0.386	0.614
0.679	10.18	0.608	30.49	0.404	0.596
0.743	10.22	0.611	30.27	0.418	0.582
0.806	10.28	0.614	30.03	0.434	0.566
0.870	10.33	0.618	29.83	0.446	0.554
0.933	10.43	0.623	29.64	0.459	0.541
1.060	10.63	0.635	29.27	0.482	0.518
1.187	10.86	0.649	28.89	0.507	0.493
1.314	11.10	0.663	28.50	0.533	0.467
1.441	11.35	0.679	28.07	0.560	0.440
1.568	11.62	0.694	27.64	0.588	0.412
1.822	12.24	0.731	26.76	0.646	0.354
2.076	12.90	0.771	25.88	0.703	0.297
2.330	13.57	0.811	25.01	0.759	0.241
2.584	14.23	0.850	24.21	0.811	0.189
2.838	14.86	0.888	23.45	0.860	0.140
3.092	15.41	0.921	22.80	0.902	0.098
3.346	15.92	0.952	22.25	0.937	0.063
3.600	16.30	0.974	21.83	0.965	0.035
3.854	16.55	0.989	21.53	0.984	0.016
4.108	16.66	0.997	21.37	0.994	0.006
4.362	16.73	1.000	21.30	0.999	0.001
4.616	16.73	1.000	21.28	1.000	0.000

AVG UINF = 16.73 M/S   AVG VISC = 0.15273E-04 M/S
AVG REM = 6792.   AVG REH = 9200.   AVG H= 1.548
AVG TC = 36.72 DEG C

RUN 092974/100274   SPANWISE PROFILE TH=0 (1)

REX = 0.10000E 01		REM =	6833.	REH =	3898.
XVO =	0.00 CM	DEL2 =	0.626 CM	DEH2 =	0.356 CM
UINF =	16.71 M/S	DEL99=	3.629 CM	DELT99 =	3.768 CM
VISC = 0.15323E-04 M2/S		DEL1 =	1.048 CM	UINF =	16.70 M/S
PORT =	1	H =	1.672	VISC =	0.15253E-04 M2/S
XLOC =	176.40 CM	CF/2 = 0.10000E 01		TINF =	22.14 DEG C
				TPLATE =	36.17 DEG C

Y(CM)	Y/DEL	U(M/S)	U/UINF	Y+	U+	Y(CM)	T(DEG C)	TBAR	TBAR
0.025	0.007	4.86	0.291	277.0	0.29	0.0546	31.79	0.312	0.688
0.028	0.008	5.00	0.299	304.7	0.30	0.0571	31.60	0.326	0.674
0.030	0.008	5.22	0.312	332.4	0.31	0.0597	31.21	0.354	0.646
0.033	0.009	5.42	0.324	360.2	0.32	0.0648	30.65	0.393	0.607
0.038	0.010	5.73	0.343	415.6	0.34	0.0724	30.04	0.437	0.563
0.046	0.013	6.14	0.367	498.7	0.37	0.0825	29.35	0.486	0.514
0.056	0.015	6.49	0.388	609.5	0.39	0.0952	28.81	0.524	0.476
0.069	0.019	6.80	0.407	748.0	0.41	0.1105	28.28	0.563	0.437
0.084	0.023	7.13	0.427	914.2	0.43	0.1308	27.87	0.592	0.408
0.102	0.028	7.40	0.442	1108.2	0.44	0.1562	27.46	0.621	0.379
0.122	0.034	7.63	0.456	1329.8	0.46	0.1867	27.08	0.648	0.352
0.147	0.041	7.86	0.470	1606.8	0.47	0.2222	26.82	0.666	0.334
0.178	0.049	8.08	0.484	1939.3	0.48	0.2629	26.56	0.685	0.315
0.213	0.059	8.24	0.493	2327.1	0.49	0.3086	26.35	0.700	0.300
0.254	0.070	8.37	0.501	2770.4	0.50	0.3619	26.20	0.711	0.289
0.300	0.083	8.45	0.505	3269.1	0.51	0.4254	26.02	0.723	0.277
0.351	0.097	8.47	0.507	3823.1	0.51	0.4889	25.91	0.732	0.268
0.406	0.112	8.47	0.507	4432.6	0.51	0.5524	25.82	0.737	0.263
0.467	0.129	8.44	0.505	5097.5	0.51	0.6159	25.71	0.745	0.255
0.538	0.148	8.41	0.503	5873.2	0.50	0.6794	25.61	0.752	0.248
0.620	0.171	8.36	0.500	6759.8	0.50	0.8064	25.45	0.764	0.236
0.696	0.192	8.41	0.503	7590.9	0.50	1.0604	25.13	0.787	0.213
0.772	0.213	8.48	0.508	8422.0	0.51	1.1874	24.98	0.797	0.203
0.848	0.234	8.68	0.519	9255.1	0.52	1.3144	24.85	0.807	0.193
0.925	0.255	8.87	0.531	10084.2	0.53	1.4414	24.73	0.815	0.185
1.026	0.283	9.26	0.554	11192.4	0.55	1.5684	24.61	0.824	0.176
1.128	0.311	9.65	0.578	12300.5	0.58	1.8224	24.35	0.843	0.157
1.229	0.339	10.08	0.603	13408.7	0.60	2.0764	24.06	0.863	0.137
1.356	0.374	10.52	0.630	14793.9	0.63	2.3304	23.73	0.887	0.113
1.483	0.409	10.92	0.653	16179.1	0.65	2.5844	23.44	0.907	0.093
1.610	0.444	11.26	0.674	17564.3	0.67	2.8385	23.11	0.931	0.069
1.737	0.479	11.65	0.697	18949.5	0.70	3.0924	22.82	0.951	0.049
1.864	0.514	12.07	0.722	20334.7	0.72	3.3464	22.59	0.968	0.032
2.118	0.584	12.90	0.772	23105.1	0.77	3.6004	22.37	0.983	0.017
2.372	0.654	13.72	0.821	25875.5	0.82	3.8544	22.24	0.993	0.007
2.626	0.724	14.46	0.865	28645.9	0.87	4.1084	22.17	0.998	0.002
2.880	0.794	15.15	0.906	31416.2	0.91	4.3624	22.14	1.000	-0.000
3.134	0.864	15.73	0.941	34186.6	0.94				
3.388	0.934	16.21	0.970	36957.1	0.97				
3.642	1.004	16.50	0.987	39727.4	0.99				
3.896	1.074	16.65	0.996	42497.8	1.00				
4.150	1.144	16.71	1.000	45268.2	1.00				

RUN 092974/100274 SPANWISE PROFILE TH=0 (2)

REX =	0.10000E 01	REM =	6759.	REH =	3924.
XVO =	0.00 CM	DEL2 =	0.619 CM	DEH2 =	0.358 CM
UINF =	16.73 M/S	DEL99=	3.627 CM	DELT99 =	3.763 CM
VISC =	0.15316E-04 M2/S	DEL1 =	0.977 CM	UINF =	16.72 M/S
PORT =	2	H =	1.579	VISC =	0.15262E-04 M2/S
XLOC =	176.40 CM	CF/2 =	0.10000E 01	TINF =	22.24 DEG C
				TPLATE =	36.23 DEG C

Y(CM)	Y/DEL	U(M/S)	U/UINF	Y+	U+	Y(CM)	T(DEG C)	TBAR	TBAR
0.025	0.007	5.58	0.333	277.4	0.33	0.0546	31.66	0.327	0.673
0.028	0.008	5.70	0.341	305.1	0.34	0.0571	31.40	0.345	0.655
0.030	0.008	5.95	0.356	332.8	0.36	0.0597	31.07	0.369	0.631
0.033	0.009	6.18	0.370	360.6	0.37	0.0648	30.45	0.413	0.587
0.038	0.011	6.55	0.392	416.0	0.39	0.0724	29.84	0.457	0.543
0.046	0.013	6.98	0.417	499.2	0.42	0.0825	29.18	0.503	0.497
0.056	0.015	7.35	0.440	610.2	0.44	0.0952	28.60	0.545	0.455
0.069	0.019	7.72	0.462	748.9	0.46	0.1105	28.04	0.585	0.415
0.084	0.023	8.14	0.487	915.3	0.49	0.1308	27.58	0.618	0.382
0.102	0.028	8.38	0.501	1109.4	0.50	0.1562	27.16	0.648	0.352
0.122	0.034	8.64	0.516	1331.3	0.52	0.1867	26.80	0.674	0.326
0.147	0.041	8.86	0.530	1608.7	0.53	0.2222	26.55	0.691	0.309
0.178	0.049	9.10	0.544	1941.5	0.54	0.2629	26.32	0.708	0.292
0.213	0.059	9.29	0.555	2329.8	0.56	0.3086	26.10	0.724	0.276
0.254	0.070	9.43	0.564	2773.6	0.56	0.3619	25.95	0.735	0.265
0.300	0.083	9.52	0.569	3272.8	0.57	0.4254	25.78	0.746	0.254
0.351	0.097	9.59	0.573	3827.6	0.57	0.4889	25.67	0.755	0.245
0.406	0.112	9.63	0.576	4437.8	0.58	0.5524	25.57	0.762	0.238
0.467	0.129	9.62	0.575	5103.4	0.57	0.6159	25.49	0.767	0.233
0.538	0.148	9.49	0.567	5880.0	0.57	0.6794	25.41	0.773	0.227
0.620	0.171	9.44	0.565	6767.6	0.56	0.8064	25.26	0.784	0.216
0.696	0.192	9.39	0.562	7599.7	0.56	0.9334	25.18	0.790	0.210
0.772	0.213	9.41	0.563	8431.7	0.56	1.0604	25.06	0.798	0.202
0.848	0.234	9.49	0.567	9263.8	0.57	1.1874	24.95	0.806	0.194
0.925	0.255	9.63	0.576	10095.9	0.58	1.3144	24.86	0.812	0.188
1.026	0.283	9.86	0.590	11205.3	0.59	1.4414	24.76	0.819	0.181
1.128	0.311	10.13	0.606	12314.8	0.61	1.5684	24.65	0.828	0.172
1.229	0.339	10.40	0.622	13424.2	0.62	1.8224	24.41	0.845	0.155
1.356	0.374	10.68	0.638	14811.0	0.64	2.0764	24.09	0.867	0.133
1.483	0.409	10.98	0.656	16197.8	0.66	2.3304	23.79	0.889	0.111
1.610	0.444	11.23	0.672	17584.6	0.67	2.5844	23.49	0.910	0.090
1.737	0.479	11.67	0.697	18971.4	0.70	2.8385	23.19	0.932	0.068
1.864	0.514	12.06	0.721	20358.2	0.72	3.0924	22.92	0.951	0.049
2.118	0.584	12.92	0.773	23131.8	0.77	3.3464	22.67	0.969	0.031
2.372	0.654	13.75	0.822	25905.4	0.82	3.6004	22.47	0.983	0.017
2.626	0.724	14.53	0.869	28679.0	0.87	3.8544	22.34	0.993	0.007
2.880	0.794	15.21	0.910	31452.6	0.91	4.1084	22.27	0.998	0.002
3.134	0.864	15.83	0.946	34226.2	0.95	4.3524	22.24	1.000	0.000
3.388	0.934	16.23	0.970	36999.8	0.97				
3.642	1.004	16.53	0.988	39773.4	0.99				
3.896	1.074	16.66	0.996	42547.0	1.00				
4.150	1.144	16.72	1.000	45320.6	1.00				
4.404	1.214	16.73	1.000	48094.2	1.00				

RUN 092974/100274 SPANWISE PROFILE TH=0 (3)

REX	= 0.10000E 01	REM	=	6181.	REH	=	3920.
XVO	= 0.00 CM	DEL2	=	0.565 CM	DEH2	=	0.358 CM
UINF	= 16.72 M/S	DEL99	=	3.681 CM	DELT99	=	3.783 CM
VISC	= 0.15300E-04 M2/S	DEL1	=	0.814 CM	UINF	=	16.73 M/S
PORT	= 3	H	=	1.440	VISC	=	0.15268E-04 M2/S
XLCC	= 176.40 CM	CF/2	=	0.10000E 01	TINF	=	22.30 DEG C
					TPLATE	=	36.21 DEG C

Y(CM)	Y/DEL	U(M/S)	U/UINF	Y+	U+	Y(CM)	T(DEG C)	TBAR	TBAR
0.025	0.007	6.43	0.384	277.6	0.38	0.0546	31.28	0.355	0.645
0.028	0.008	6.46	0.386	305.4	0.39	0.0571	31.12	0.366	0.634
0.030	0.008	6.76	0.404	333.2	0.40	0.0597	30.68	0.398	0.602
0.033	0.009	6.97	0.417	360.9	0.42	0.0622	30.38	0.419	0.581
0.038	0.010	7.47	0.447	416.5	0.45	0.0648	30.11	0.439	0.561
0.046	0.012	7.87	0.471	499.7	0.47	0.0724	29.44	0.487	0.513
0.056	0.015	8.28	0.495	610.8	0.50	0.0825	28.71	0.539	0.461
0.069	0.019	8.70	0.520	749.6	0.52	0.0952	28.22	0.575	0.425
0.084	0.023	9.02	0.539	916.2	0.54	0.1105	27.66	0.615	0.385
0.102	0.028	9.34	0.558	1110.5	0.56	0.1308	27.24	0.645	0.355
0.122	0.033	9.53	0.570	1332.6	0.57	0.1562	26.84	0.673	0.327
0.147	0.040	9.75	0.583	1610.3	0.58	0.1867	26.58	0.692	0.308
0.178	0.048	9.99	0.597	1943.4	0.60	0.2222	26.29	0.714	0.286
0.213	0.058	10.23	0.612	2332.1	0.61	0.2629	26.09	0.728	0.272
0.254	0.069	10.41	0.622	2775.4	0.62	0.3086	25.84	0.745	0.255
0.300	0.081	10.57	0.632	3276.1	0.63	0.3619	25.68	0.757	0.243
0.351	0.095	10.70	0.640	3831.4	0.64	0.4254	25.51	0.769	0.231
0.406	0.110	10.85	0.649	4442.2	0.65	0.4889	25.38	0.778	0.222
0.467	0.127	10.94	0.654	5108.5	0.65	0.5524	25.28	0.786	0.214
0.538	0.146	10.99	0.657	5885.9	0.66	0.6159	25.20	0.791	0.209
0.620	0.168	11.08	0.662	6774.3	0.66	0.6794	25.15	0.795	0.205
0.721	0.196	11.11	0.664	7884.8	0.66	0.8064	25.02	0.804	0.196
0.848	0.230	11.17	0.668	9273.0	0.67	0.9334	24.89	0.814	0.186
0.963	0.262	11.25	0.673	10522.4	0.67	1.0604	24.84	0.817	0.183
1.102	0.300	11.41	0.682	12049.4	0.68	1.1874	24.76	0.823	0.177
1.229	0.334	11.57	0.692	13437.5	0.69	1.3144	24.66	0.831	0.169
1.356	0.369	11.80	0.706	14825.7	0.71	1.4414	24.57	0.837	0.163
1.483	0.403	11.99	0.717	16213.9	0.72	1.5684	24.47	0.844	0.156
1.610	0.438	12.27	0.734	17602.1	0.73	1.8224	24.22	0.862	0.138
1.737	0.472	12.54	0.750	18990.3	0.75	2.0764	23.99	0.879	0.121
1.864	0.507	12.84	0.768	20378.4	0.77	2.3304	23.71	0.899	0.101
2.118	0.576	13.47	0.805	23154.8	0.81	2.5844	23.44	0.918	0.082
2.372	0.645	14.16	0.847	25931.1	0.85	2.8385	23.17	0.938	0.062
2.626	0.714	14.80	0.885	28707.5	0.88	3.0924	22.90	0.957	0.043
2.880	0.783	15.38	0.920	31483.8	0.92	3.3464	22.68	0.972	0.028
3.134	0.852	15.87	0.949	34260.2	0.95	3.6004	22.52	0.984	0.016
3.388	0.921	16.27	0.973	37036.5	0.97	3.8544	22.42	0.992	0.008
3.642	0.990	16.50	0.987	39812.9	0.99	4.1084	22.35	0.996	0.004
3.896	1.059	16.67	0.997	42589.2	1.00	4.3624	22.32	0.999	0.001
4.150	1.128	16.69	0.998	45365.6	1.00	4.6164	22.30	1.000	0.000
4.404	1.197	16.73	1.000	48141.9	1.00				

RUN 092974/100274 SPANWISE PROFILE TH=0 (4)

REX = 0.10000E 01 REM = 5769. REH = 3991.

XVO = 0.00 CM DEL2 = 0.527 CM DEH2 = 0.364 CM
UINF = 16.74 M/S DEL99= 3.656 CM DELT99 = 3.760 CM
VISC = 0.15306E-04 M2/S DEL1 = 0.736 CM UINF = 16.75 M/S
PORT = 4 H = 1.396 VISC = 0.15268E-04 M2/S
XLOC = 176.40 CM CF/2 = 0.10000E 01 TINF = 22.30 DEG C
TPLATE = 36.21 DEG C

Y(CM)	Y/DEL	U(M/S)	U/UINF	Y+	U+	Y(CM)	T(DEG C)	TBAR	TBAR
0.025	0.007	6.54	0.391	277.9	0.39	0.0546	31.08	0.369	0.631
0.028	0.008	6.85	0.409	305.6	0.41	0.0571	31.03	0.372	0.628
0.030	0.008	7.13	0.426	333.4	0.43	0.0597	30.76	0.392	0.608
0.036	0.010	7.55	0.451	389.0	0.45	0.0622	30.35	0.421	0.579
0.043	0.012	8.01	0.478	472.4	0.48	0.0673	29.73	0.466	0.534
0.053	0.015	8.40	0.502	583.5	0.50	0.0749	29.11	0.510	0.490
0.066	0.018	8.81	0.526	722.4	0.53	0.0851	28.51	0.554	0.446
0.081	0.022	9.18	0.548	889.2	0.55	0.0978	27.97	0.592	0.408
0.099	0.027	9.47	0.566	1083.7	0.57	0.1130	27.47	0.629	0.371
0.119	0.033	9.66	0.577	1305.9	0.58	0.1333	27.11	0.655	0.345
0.145	0.040	9.94	0.593	1583.8	0.59	0.1587	26.78	0.678	0.322
0.175	0.048	10.13	0.605	1917.2	0.60	0.1892	26.50	0.698	0.302
0.211	0.058	10.38	0.620	2306.3	0.62	0.2248	26.27	0.715	0.285
0.251	0.069	10.61	0.634	2750.8	0.63	0.2654	26.02	0.732	0.268
0.297	0.081	10.83	0.647	3251.0	0.65	0.3111	25.81	0.748	0.252
0.348	0.095	11.01	0.658	3806.7	0.66	0.3645	25.64	0.760	0.240
0.404	0.110	11.17	0.667	4418.0	0.67	0.4280	25.48	0.772	0.228
0.465	0.127	11.27	0.673	5084.9	0.67	0.4915	25.38	0.779	0.221
0.536	0.147	11.42	0.682	5862.9	0.68	0.5550	25.27	0.787	0.213
0.617	0.169	11.55	0.690	6752.0	0.69	0.6185	25.18	0.793	0.207
0.719	0.197	11.65	0.696	7863.5	0.70	0.6820	25.12	0.798	0.202
0.846	0.231	11.78	0.704	9252.8	0.70	0.8090	25.00	0.806	0.194
0.960	0.263	11.89	0.710	10503.2	0.71	0.9360	24.89	0.814	0.186
1.138	0.311	12.11	0.723	12448.2	0.72	1.0630	24.77	0.822	0.178
1.354	0.370	12.48	0.745	14810.0	0.75	1.1900	24.69	0.828	0.172
1.608	0.440	12.91	0.771	17588.6	0.77	1.3170	24.59	0.836	0.164
1.862	0.509	13.41	0.801	20367.2	0.80	1.4440	24.47	0.844	0.156
2.116	0.579	13.97	0.834	23145.9	0.83	1.5710	24.34	0.854	0.146
2.370	0.648	14.45	0.863	25924.5	0.86	1.8250	24.15	0.867	0.133
2.624	0.718	14.99	0.895	28703.1	0.89	2.0790	23.90	0.885	0.115
2.878	0.787	15.50	0.926	31481.7	0.93	2.3330	23.69	0.900	0.100
3.132	0.857	15.95	0.952	34260.3	0.95	2.5870	23.44	0.918	0.082
3.386	0.926	16.30	0.973	37038.9	0.97	2.8410	23.15	0.939	0.061
3.640	0.996	16.53	0.987	39817.5	0.99	3.0950	22.90	0.957	0.043
3.894	1.065	16.68	0.996	42596.2	1.00	3.3490	22.73	0.969	0.031
4.148	1.135	16.75	1.000	45374.8	1.00	3.6030	22.53	0.983	0.017
						3.857	22.42	0.992	0.008
						4.111	22.32	0.999	0.001
						4.365	22.30	1.000	0.000

RUN 092974/100274   SPANWISE PROFILE TH=0 (5)

REX = 0.10000E 01		REM = 6654.		REH = 3910.	
XVO =	0.00 CM	DEL2 =	0.609 CM	DEH2 =	0.357 CM
UINF =	16.73 M/S	DEL99=	3.805 CM	DELT99 =	3.909 CM
VISC =	0.15309E-04 M2/S	DEL1 =	0.907 CM	UINF =	16.73 M/S
PORT =	5	H =	1.490	VISC =	0.15266E-04 M2/S
XLOC =	176.40 CM	CF/2 =	0.10000E 01	TINF =	22.29 DEG C
				TPLATE =	36.19 DEG C

Y(CM)	Y/DEL	U(M/S)	U/UINF	Y+	U+	Y(CM)	T(DEG C)	TBAR	TBAR
0.025	0.007	6.99	0.418	277.5	0.42	0.0546	28.73	0.537	0.463
0.028	0.007	7.22	0.431	305.3	0.43	0.0571	28.21	0.574	0.426
0.030	0.008	7.49	0.448	333.0	0.45	0.0597	27.86	0.599	0.401
0.036	0.009	7.83	0.468	388.5	0.47	0.0648	27.39	0.633	0.367
0.043	0.011	8.13	0.486	471.8	0.49	0.0724	27.03	0.659	0.341
0.053	0.014	8.30	0.496	582.8	0.50	0.0825	26.74	0.680	0.320
0.066	0.017	8.44	0.504	721.5	0.50	0.0952	26.51	0.696	0.304
0.081	0.021	8.49	0.508	888.1	0.51	0.1105	26.35	0.708	0.292
0.102	0.027	8.44	0.505	1110.1	0.50	0.1308	26.18	0.720	0.280
0.122	0.032	8.47	0.506	1332.1	0.51	0.1562	25.99	0.734	0.266
0.147	0.039	8.60	0.514	1609.6	0.51	0.1943	25.64	0.759	0.241
0.178	0.047	8.68	0.519	1942.6	0.52	0.2451	25.09	0.799	0.201
0.213	0.056	8.93	0.534	2331.1	0.53	0.2959	24.77	0.821	0.179
0.249	0.065	8.99	0.537	2719.7	0.54	0.3467	24.77	0.821	0.179
0.290	0.076	9.24	0.552	3163.7	0.55	0.3975	24.87	0.814	0.186
0.335	0.088	9.43	0.564	3663.2	0.56	0.4483	25.00	0.805	0.195
0.386	0.101	9.61	0.575	4218.3	0.57	0.4991	25.11	0.797	0.203
0.442	0.116	9.81	0.586	4828.8	0.59	0.5499	25.21	0.790	0.210
0.503	0.132	10.00	0.598	5494.8	0.60	0.6007	25.29	0.784	0.216
0.579	0.152	10.27	0.614	6327.4	0.61	0.6515	25.34	0.780	0.220
0.681	0.179	10.47	0.626	7437.5	0.63	0.7023	25.37	0.778	0.222
0.808	0.212	10.69	0.639	8825.0	0.64	0.7531	25.37	0.778	0.222
0.960	0.252	10.92	0.653	10490.2	0.65	0.8039	25.37	0.778	0.222
1.138	0.299	11.18	0.668	12432.8	0.67	0.8547	25.37	0.778	0.222
1.354	0.356	11.54	0.690	14791.7	0.69	0.9055	25.32	0.782	0.218
1.608	0.423	12.08	0.722	17566.8	0.72	0.9563	25.25	0.787	0.213
1.862	0.489	12.64	0.756	20342.0	0.76	1.0071	25.22	0.789	0.211
2.116	0.556	13.25	0.792	23117.2	0.79	1.0579	25.17	0.793	0.207
2.370	0.623	13.81	0.826	25892.4	0.83	1.1214	25.07	0.800	0.200
2.624	0.690	14.40	0.861	28667.5	0.86	1.1849	25.01	0.804	0.196
2.878	0.756	14.99	0.896	31442.7	0.90	1.3119	24.89	0.813	0.187
3.132	0.823	15.53	0.928	34217.9	0.93	1.4389	24.74	0.823	0.177
3.386	0.890	15.97	0.955	36993.1	0.95	1.5659	24.61	0.833	0.167
3.640	0.957	16.36	0.978	39768.2	0.98	1.8199	24.37	0.850	0.150
3.894	1.023	16.58	0.991	42543.4	0.99	2.0739	24.11	0.869	0.131
4.148	1.090	16.64	0.995	45318.6	0.99	2.3279	23.86	0.887	0.113
4.402	1.157	16.71	0.999	48093.8	1.00	2.5819	23.60	0.905	0.095
4.656	1.224	16.73	1.000	50868.9	1.00	2.8359	23.34	0.924	0.076
						3.090	23.07	0.944	0.056
						3.344	22.82	0.962	0.038
						3.598	22.62	0.976	0.024
						3.852	22.45	0.988	0.012
						4.106	22.34	0.996	0.004
						4.360	22.29	1.000	0.000

RUN 092974/100274 SPANWISE PROFILE TH=0 (6)

REX = 0.10000E 01		REM =	6814.	REH =	3409.
XVO =	0.00 CM	DEL2 =	0.625 CM	DEH2 =	0.312 CM
UINF =	16.70 M/S	DEL99=	3.866 CM	DELT99 =	3.999 CM
VISC =	0.15314E-04 M2/S	DEL1 =	1.216 CM	UINF =	16.70 M/S
PORT =	6	H =	1.947	VISC =	0.15266E-04 M2/S
XLOC =	176.40 CM	CF/2 =	0.10000E 01	TINF =	22.29 DEG C
				TPLATE =	36.15 DEG C

Y(CM)	Y/DEL	U(M/S)	U/UINF	Y+	U+	Y(CM)	T(DEG C)	TBAR	TBAR
0.025	0.007	0.00	0.000	277.0	0.00	0.0546	32.18	0.287	0.713
0.084	0.022	0.00	0.000	914.3	0.00	0.0673	31.27	0.352	0.648
0.147	0.038	0.00	0.000	1606.9	0.00	0.0800	30.91	0.378	0.622
0.173	0.045	0.00	0.000	1883.9	0.00	0.0927	30.70	0.393	0.607
0.198	0.051	0.00	0.000	2161.0	0.00	0.1054	30.54	0.405	0.595
0.211	0.055	0.00	0.000	2299.5	0.00	0.1181	30.44	0.412	0.588
0.224	0.058	1.70	0.101	2438.0	0.10	0.1308	30.28	0.424	0.576
0.236	0.061	2.82	0.169	2576.6	0.17	0.1435	30.18	0.431	0.569
0.249	0.064	3.69	0.221	2715.1	0.22	0.1562	30.04	0.441	0.559
0.262	0.068	4.55	0.273	2853.6	0.27	0.1689	29.79	0.459	0.541
0.274	0.071	5.20	0.311	2992.1	0.31	0.1943	29.27	0.496	0.504
0.287	0.074	5.91	0.354	3130.7	0.35	0.2197	28.72	0.536	0.464
0.300	0.078	6.48	0.388	3269.2	0.39	0.1943	27.92	0.594	0.406
0.312	0.081	6.98	0.418	3407.7	0.42	0.2705	27.01	0.659	0.341
0.325	0.084	7.45	0.446	3546.2	0.45	0.2959	25.83	0.744	0.256
0.338	0.087	7.85	0.470	3684.7	0.47	0.3213	24.72	0.825	0.175
0.358	0.093	8.30	0.497	3906.4	0.50	0.3467	24.06	0.872	0.128
0.389	0.101	8.70	0.521	4236.8	0.52	0.3975	23.71	0.897	0.103
0.429	0.111	9.02	0.540	4682.1	0.54	0.4483	23.74	0.895	0.105
0.480	0.124	9.21	0.551	5236.2	0.55	0.4991	23.86	0.887	0.113
0.541	0.140	9.31	0.557	5901.1	0.56	0.5499	24.09	0.870	0.130
0.617	0.160	9.33	0.558	6732.3	0.56	0.6007	24.33	0.852	0.148
0.693	0.179	9.33	0.558	7563.4	0.56	0.6515	24.64	0.830	0.170
0.770	0.199	9.33	0.559	8394.6	0.56	0.7023	24.92	0.810	0.190
0.846	0.219	9.40	0.563	9225.7	0.56	0.7531	25.17	0.792	0.208
0.922	0.238	9.48	0.568	10056.9	0.57	0.8039	25.35	0.779	0.221
1.024	0.265	9.62	0.576	11165.1	0.58	0.8547	25.48	0.770	0.230
1.100	0.284	9.71	0.581	11996.2	0.58	0.9055	25.56	0.764	0.236
1.176	0.304	9.87	0.591	12827.4	0.59	0.9563	25.59	0.762	0.238
1.278	0.330	10.02	0.600	13935.6	0.60	1.0071	25.59	0.762	0.238
1.405	0.363	10.29	0.616	15320.8	0.62	1.0579	25.57	0.763	0.237
1.557	0.403	10.66	0.638	16983.1	0.64	1.1087	25.51	0.768	0.232
1.709	0.442	11.08	0.663	18645.4	0.66	1.1595	25.42	0.774	0.226
1.913	0.495	11.61	0.695	20861.8	0.70	1.2357	25.31	0.782	0.218
2.141	0.554	12.30	0.737	23355.2	0.74	1.3119	25.21	0.789	0.211
2.395	0.620	13.06	0.782	26125.7	0.78	1.4389	25.03	0.802	0.198
2.649	0.685	13.80	0.826	28896.2	0.83	1.5659	24.88	0.813	0.187
2.903	0.751	14.51	0.869	31666.7	0.87	1.6929	24.73	0.824	0.176
3.157	0.817	15.18	0.909	34437.2	0.91	1.8199	24.61	0.832	0.168
3.411	0.882	15.76	0.944	37207.6	0.94	2.0739	24.33	0.853	0.147
3.665	0.948	16.21	0.971	39978.1	0.97	2.3279	24.04	0.873	0.127
3.919	1.014	16.51	0.988	42748.6	0.99	2.5819	23.78	0.893	0.107
4.173	1.079	16.67	0.998	45519.1	1.00	2.8359	23.49	0.913	0.087
4.427	1.145	16.71	1.000	48289.6	1.00	3.0899	23.19	0.935	0.065
						3.344	22.94	0.953	0.047
						3.598	22.67	0.972	0.028
						3.852	22.52	0.983	0.017
						4.106	22.37	0.994	0.006
						4.360	22.29	1.000	0.000

RUN 092974/100274 SPANWISE PROFILE TH=0 (7)

REX =	0.10000E 01	REM =	7734.	REH =	4001.
XVO =	0.00 CM	DEL2 =	0.699 CM	DEH2 =	0.363 CM
UINF =	16.77 M/S	DEL99=	3.954 CM	DELT99 =	4.055 CM
VISC =	0.15158E-04 M2/S	DEL1 =	1.136 CM	UINF =	16.82 M/S
PORT =	7	H =	1.625	VISC =	0.15265E-04 M2/S
XLOC =	176.40 CM	CF/2 =	0.10000E 01	TINF =	22.27 DEG C
				TPLATE =	36.21 DEG C

Y(CM)	Y/DEL	U(M/S)	U/UINF	Y+	U+	Y(CM)	T(DEG C)	TBAR	TBAR
0.025	0.006	6.32	0.377	281.0	0.38	0.0546	29.41	0.487	0.513
0.028	0.007	6.32	0.377	309.1	0.38	0.0571	28.94	0.521	0.479
0.030	0.008	6.35	0.379	337.1	0.38	0.0597	28.54	0.550	0.450
0.036	0.009	6.78	0.405	393.3	0.40	0.0648	27.93	0.594	0.406
0.043	0.011	7.26	0.433	477.6	0.43	0.0724	27.46	0.628	0.372
0.053	0.013	7.53	0.449	590.0	0.45	0.0825	27.05	0.657	0.343
0.066	0.017	7.64	0.455	730.5	0.46	0.0952	26.79	0.675	0.325
0.081	0.021	7.55	0.450	899.1	0.45	0.1105	26.58	0.691	0.309
0.102	0.026	7.43	0.443	1123.8	0.44	0.1308	26.39	0.705	0.295
0.122	0.031	7.36	0.439	1348.6	0.44	0.1562	26.24	0.715	0.285
0.147	0.037	7.38	0.440	1629.6	0.44	0.1943	25.93	0.738	0.262
0.178	0.045	7.56	0.451	1966.7	0.45	0.2451	25.43	0.773	0.227
0.213	0.054	7.91	0.472	2360.0	0.47	0.2959	24.96	0.807	0.193
0.249	0.063	8.30	0.495	2753.4	0.50	0.3467	24.84	0.815	0.185
0.290	0.073	8.63	0.515	3202.9	0.51	0.3975	24.91	0.811	0.189
0.335	0.085	8.91	0.531	3708.6	0.53	0.4483	24.99	0.805	0.195
0.386	0.098	9.04	0.539	4270.6	0.54	0.4991	25.12	0.796	0.204
0.442	0.112	9.12	0.544	4888.7	0.54	0.5499	25.26	0.785	0.215
0.503	0.127	9.16	0.546	5563.0	0.55	0.6007	25.35	0.779	0.221
0.579	0.146	9.15	0.546	6405.8	0.55	0.6515	25.48	0.770	0.230
0.681	0.172	9.22	0.550	7529.7	0.55	0.7023	25.57	0.763	0.237
0.806	0.204	9.36	0.559	8934.5	0.56	0.7531	25.64	0.758	0.242
0.960	0.243	9.53	0.568	10620.2	0.57	0.8039	25.67	0.756	0.244
1.138	0.288	9.71	0.579	12586.9	0.58	0.8547	25.69	0.755	0.245
1.354	0.342	10.00	0.596	14975.1	0.60	0.9055	25.65	0.757	0.243
1.608	0.407	10.59	0.631	17784.6	0.63	0.9563	25.62	0.759	0.241
1.862	0.471	11.26	0.672	20594.2	0.67	1.0071	25.57	0.763	0.237
2.116	0.535	12.01	0.716	23403.6	0.72	1.0579	25.52	0.767	0.233
2.370	0.599	12.83	0.765	26213.4	0.77	1.1214	25.44	0.772	0.228
2.624	0.664	13.56	0.809	29023.0	0.81	1.1849	25.36	0.778	0.222
2.878	0.728	14.28	0.852	31832.5	0.85	1.3119	25.19	0.790	0.210
3.132	0.792	14.99	0.894	34642.1	0.89	1.4389	25.05	0.801	0.199
3.386	0.856	15.61	0.931	37451.7	0.93	1.5659	24.90	0.811	0.189
3.640	0.920	16.17	0.964	40261.3	0.96	1.8199	24.63	0.831	0.169
3.894	0.985	16.50	0.984	43070.9	0.98	2.0739	24.36	0.850	0.150
4.148	1.049	16.67	0.994	45880.4	0.99	2.3279	24.09	0.869	0.131
4.402	1.113	16.75	0.999	48690.0	1.00	2.5819	23.83	0.888	0.112
4.656	1.177	16.77	1.000	51499.6	1.00	2.8359	23.52	0.910	0.090
						3.090	23.24	0.930	0.070
						3.344	22.95	0.951	0.049
						3.598	22.67	0.971	0.029
						3.852	22.52	0.982	0.018
						4.106	22.38	0.992	0.008
						4.360	22.30	0.998	0.002
						4.614	22.27	1.000	0.000

RUN 092974/100274 SPANWISE PROFILE TH=0 (8)

REX =	0.10000E 01	REM =	7051.	REH =	4296.
XVO =	0.00 CM	DEL2 =	0.640 CM	DEH2 =	0.391 CM
UINF =	16.74 M/S	DEL99=	3.898 CM	DELT99 =	3.989 CM
VISC =	0.15195E-04 M2/S	DEL1 =	0.953 CM	UINF =	16.77 M/S
PORT =	8	H =	1.488	VISC =	0.15266E-04 M2/S
XLOC =	176.40 CM	CF/2 =	0.10000E 01	TINF =	22.28 DEG C
				TPLATE =	36.21 DEG C

Y(CM)	Y/DEL	U(M/S)	U/UINF	Y+	U+	Y(CM)	T(DEG C)	TBAR	TBAR
0.025	0.007	5.90	0.353	279.8	0.35	0.0546	31.49	0.339	0.661
0.028	0.007	5.94	0.355	307.7	0.35	0.0571	31.23	0.357	0.643
0.033	0.008	6.32	0.378	363.7	0.38	0.0622	30.53	0.408	0.592
0.041	0.010	6.94	0.415	447.6	0.41	0.0698	29.82	0.459	0.541
0.051	0.013	7.56	0.451	559.5	0.45	0.0800	29.20	0.503	0.497
0.063	0.016	7.94	0.474	699.4	0.47	0.0927	28.63	0.544	0.456
0.079	0.020	8.34	0.498	867.3	0.50	0.1079	28.12	0.581	0.419
0.097	0.025	8.60	0.514	1063.1	0.51	0.1283	27.67	0.614	0.386
0.117	0.030	8.84	0.528	1287.0	0.53	0.1537	27.34	0.637	0.363
0.142	0.036	9.06	0.541	1566.7	0.54	0.1841	27.01	0.661	0.339
0.173	0.044	9.31	0.556	1902.5	0.56	0.2197	26.70	0.683	0.317
0.208	0.053	9.56	0.571	2294.1	0.57	0.2604	26.49	0.698	0.302
0.249	0.064	9.77	0.584	2741.8	0.58	0.3061	26.21	0.718	0.282
0.295	0.076	9.98	0.596	3245.4	0.60	0.3594	26.04	0.730	0.270
0.345	0.089	10.13	0.605	3804.9	0.61	0.4229	25.85	0.744	0.256
0.401	0.103	10.28	0.614	4420.4	0.61	0.4864	25.70	0.755	0.245
0.462	0.119	10.36	0.619	5091.9	0.62	0.5499	25.60	0.762	0.238
0.533	0.137	10.45	0.624	5875.2	0.62	0.6134	25.50	0.769	0.231
0.615	0.158	10.50	0.627	6770.5	0.63	0.6769	25.44	0.774	0.226
0.716	0.184	10.58	0.632	7889.6	0.63	0.8039	25.30	0.783	0.217
0.843	0.216	10.63	0.635	9288.4	0.63	0.9309	25.21	0.790	0.210
0.958	0.246	10.74	0.642	10547.4	0.64	1.0579	25.09	0.799	0.201
1.135	0.291	10.88	0.650	12505.8	0.65	1.1849	24.99	0.806	0.194
1.351	0.347	11.20	0.669	14883.9	0.67	1.3119	24.89	0.813	0.187
1.605	0.412	11.66	0.697	17681.6	0.70	1.4389	24.79	0.820	0.180
1.859	0.477	12.18	0.728	20479.3	0.73	1.5659	24.64	0.831	0.169
2.113	0.542	12.75	0.762	23277.1	0.76	1.8199	24.43	0.846	0.154
2.367	0.607	13.36	0.798	26074.8	0.80	2.0739	24.19	0.863	0.137
2.621	0.672	13.99	0.836	28872.5	0.84	2.3279	23.96	0.880	0.120
2.875	0.738	14.66	0.876	31670.2	0.88	2.5819	23.71	0.898	0.102
3.129	0.803	15.23	0.910	34467.9	0.91	2.8359	23.44	0.917	0.083
3.383	0.868	15.79	0.943	37265.7	0.94	3.0899	23.19	0.935	0.065
3.637	0.933	16.24	0.970	40063.4	0.97	3.3439	22.90	0.956	0.044
3.891	0.998	16.53	0.988	42861.1	0.99	3.5979	22.64	0.975	0.025
4.145	1.063	16.71	0.998	45658.8	1.00	3.8519	22.50	0.984	0.016
4.399	1.129	16.74	1.000	48456.6	1.00	4.1059	22.37	0.994	0.006
						4.360	22.30	0.999	0.001
						4.614	22.29	1.000	0.000

RUN 092974/100274 SPANWISE PROFILE TH=0 (9)

REX	= 0.10000E 01	REM	=	6381.	REH	=	4181.
XVO	= 0.00 CM	DEL2	=	0.584 CM	DEH2	=	0.381 CM
UINF	= 16.78 M/S	DEL99	=	3.859 CM	DELT99	=	3.950 CM
VISC	= 0.15365E-04 M2/S	DEL1	=	0.829 CM	UINF	=	16.76 M/S
PORT	= 9	H	=	1.419	VISC	=	0.15263E-04 M2/S
XLOC	= 176.40 CM	CF/2	=	0.10000E 01	TINF	=	22.25 DEG C
					TPLATE	=	36.25 DEG C

Y(CM)	Y/DEL	U(M/S)	U/UINF	Y+	U+	Y(CM)	T(DEG C)	TBAR	TBAR
0.025	0.007	6.51	0.388	277.5	0.39	0.0546	31.26	0.356	0.644
0.028	0.007	6.53	0.389	305.2	0.39	0.0571	31.15	0.364	0.636
0.033	0.009	7.01	0.417	360.7	0.42	0.0597	30.69	0.397	0.603
0.041	0.011	7.56	0.450	443.9	0.45	0.0622	30.30	0.425	0.575
0.051	0.013	8.11	0.483	554.9	0.48	0.0648	30.08	0.441	0.559
0.063	0.016	8.60	0.513	693.7	0.51	0.0724	29.36	0.492	0.508
0.079	0.020	8.95	0.534	860.1	0.53	0.0825	28.67	0.541	0.459
0.097	0.025	9.29	0.553	1054.4	0.55	0.0952	28.09	0.583	0.417
0.117	0.030	9.58	0.571	1276.3	0.57	0.1105	27.58	0.619	0.381
0.142	0.037	9.79	0.583	1553.6	0.58	0.1308	27.11	0.653	0.347
0.173	0.045	10.01	0.597	1886.8	0.60	0.1562	26.76	0.678	0.322
0.208	0.054	10.25	0.611	2275.2	0.61	0.1867	26.47	0.699	0.301
0.249	0.064	10.43	0.622	2719.2	0.62	0.2222	26.24	0.715	0.285
0.295	0.076	10.62	0.633	3218.6	0.63	0.2629	25.97	0.734	0.266
0.345	0.090	10.78	0.642	3773.5	0.64	0.3086	25.83	0.745	0.255
0.401	0.104	10.95	0.652	4384.0	0.65	0.3619	25.63	0.759	0.241
0.462	0.120	11.03	0.657	5049.9	0.66	0.4254	25.48	0.769	0.231
0.533	0.138	11.10	0.661	5626.8	0.66	0.4889	25.38	0.776	0.224
0.615	0.159	11.21	0.668	6714.7	0.67	0.5524	25.30	0.782	0.218
0.716	0.186	11.25	0.670	7824.5	0.67	0.6159	25.20	0.789	0.211
0.843	0.219	11.37	0.678	9211.9	0.68	0.6794	25.17	0.792	0.208
0.958	0.248	11.52	0.686	10460.4	0.69	0.8064	25.04	0.801	0.199
1.097	0.284	11.67	0.695	11986.5	0.70	0.9334	24.95	0.807	0.193
1.224	0.317	11.82	0.704	13373.8	0.70	1.0604	24.87	0.813	0.187
1.351	0.350	11.98	0.714	14761.2	0.71	1.1874	24.79	0.819	0.181
1.478	0.383	12.22	0.728	16148.5	0.73	1.3144	24.71	0.825	0.175
1.605	0.416	12.44	0.741	17535.8	0.74	1.4414	24.59	0.833	0.167
1.732	0.449	12.67	0.755	18923.1	0.76	1.5684	24.49	0.840	0.160
1.859	0.482	12.96	0.772	20310.5	0.77	1.8224	24.27	0.856	0.144
2.113	0.548	13.43	0.800	23085.1	0.80	2.0764	24.04	0.872	0.128
2.367	0.613	13.98	0.833	25859.8	0.83	2.3304	23.79	0.890	0.110
2.621	0.679	14.51	0.865	28634.4	0.86	2.5844	23.55	0.907	0.093
2.875	0.745	15.08	0.898	31409.1	0.90	2.8385	23.30	0.925	0.075
3.129	0.811	15.57	0.928	34183.7	0.93	3.0924	23.05	0.943	0.057
3.383	0.877	16.03	0.955	36958.4	0.95	3.3464	22.79	0.962	0.038
3.637	0.942	16.38	0.976	39733.0	0.98	3.6004	22.58	0.976	0.024
3.891	1.008	16.62	0.990	42507.7	0.99	3.8544	22.43	0.987	0.013
4.145	1.074	16.74	0.997	45282.3	1.00	4.1084	22.33	0.994	0.006
4.399	1.140	16.78	1.000	48057.0	1.00	4.3624	22.27	0.999	0.001
4.653	1.206	16.79	1.000	50831.7	1.00	4.6164	22.25	1.000	-0.000

RUN 092974/100274   SPANWISE PROFILE TH=0 (10)

REX = 0.10000E 01   REM = 6720.   REH = 4158.

XVO = 0.00 CM   DEL2 = 0.612 CM   DEH2 = 0.379 CM
UINF = 16.72 M/S   DEL99= 3.831 CM   DELT99 = 3.934 CM
VISC = 0.15224E-04 M2/S   DEL1 = 0.908 CM   UINF = 16.75 M/S
PORT = 10   H = 1.483   VISC = 0.15265E-04 M2/S
XLOC = 176.40 CM   CF/2 = 0.10000E 01   TINF = 22.27 DEG C
TPLATE = 36.23 DEG C

Y(CM)	Y/DEL	U(M/S)	U/UINF	Y+	U+	Y(CM)	T(DEG C)	TBAR	TBAR
0.025	0.007	6.16	0.368	279.0	0.37	0.0546	31.38	0.347	0.653
0.028	0.007	6.31	0.377	306.9	0.38	0.0571	31.22	0.359	0.641
0.033	0.009	6.78	0.405	362.6	0.41	0.0597	30.78	0.391	0.609
0.041	0.011	7.32	0.438	446.3	0.44	0.0648	30.16	0.435	0.565
0.051	0.013	7.82	0.468	557.9	0.47	0.0724	29.51	0.482	0.518
0.063	0.017	8.23	0.492	697.4	0.49	0.0825	28.79	0.533	0.467
0.079	0.021	8.63	0.516	864.8	0.52	0.0952	28.20	0.575	0.425
0.097	0.025	9.01	0.539	1060.1	0.54	0.1105	27.65	0.615	0.385
0.117	0.030	9.20	0.550	1283.2	0.55	0.1308	27.16	0.650	0.350
0.142	0.037	9.49	0.567	1562.2	0.57	0.1562	26.81	0.674	0.326
0.173	0.045	9.69	0.580	1896.9	0.58	0.1867	26.45	0.700	0.300
0.208	0.054	9.90	0.592	2287.5	0.59	0.2222	26.22	0.717	0.283
0.249	0.065	10.02	0.599	2733.8	0.60	0.2629	26.04	0.730	0.270
0.295	0.077	10.13	0.606	3236.0	0.61	0.3086	25.85	0.744	0.256
0.345	0.090	10.20	0.610	3793.9	0.61	0.3619	25.73	0.752	0.248
0.401	0.105	10.23	0.612	4407.6	0.61	0.4254	25.62	0.760	0.240
0.462	0.121	10.23	0.612	5077.1	0.61	0.4889	25.54	0.766	0.234
0.533	0.139	10.25	0.613	5858.2	0.61	0.5524	25.47	0.771	0.229
0.615	0.160	10.25	0.613	6750.9	0.61	0.6159	25.40	0.775	0.225
0.691	0.180	10.28	0.615	7587.8	0.61	0.6794	25.34	0.780	0.220
0.767	0.200	10.36	0.620	8424.6	0.62	0.8064	25.24	0.787	0.213
0.843	0.220	10.41	0.623	9261.5	0.62	0.9334	25.13	0.795	0.205
0.919	0.240	10.49	0.627	10098.4	0.63	1.0604	25.01	0.804	0.196
1.021	0.267	10.70	0.640	11214.3	0.64	1.1874	24.91	0.811	0.189
1.097	0.286	10.81	0.646	12051.1	0.65	1.3144	24.84	0.816	0.184
1.224	0.320	11.10	0.664	13445.9	0.66	1.4414	24.73	0.824	0.176
1.351	0.353	11.38	0.681	14840.8	0.68	1.5684	24.61	0.832	0.168
1.478	0.386	11.62	0.695	16235.6	0.70	1.8224	24.41	0.847	0.153
1.605	0.419	11.88	0.710	17630.4	0.71	2.0764	24.16	0.865	0.135
1.732	0.452	12.18	0.728	19025.2	0.73	2.3304	23.87	0.885	0.115
1.859	0.485	12.52	0.749	20420.0	0.75	2.5844	23.62	0.903	0.097
2.113	0.552	13.19	0.789	23209.6	0.79	2.8385	23.34	0.923	0.077
2.367	0.618	13.83	0.827	25999.2	0.83	3.0924	23.05	0.944	0.056
2.621	0.684	14.45	0.864	28788.8	0.86	3.3464	22.80	0.962	0.038
2.875	0.750	15.01	0.898	31578.4	0.90	3.6004	22.62	0.975	0.025
3.129	0.817	15.35	0.918	34368.0	0.92	3.8544	22.45	0.987	0.013
3.383	0.883	16.00	0.957	37157.7	0.96	4.1084	22.32	0.996	0.004
3.637	0.949	16.33	0.977	39947.3	0.98	4.3624	22.29	0.999	0.001
3.891	1.016	16.56	0.990	42736.9	0.99	4.6164	22.27	1.000	0.000
3.891	1.016	16.56	0.990	42736.9	0.99				
4.145	1.082	16.70	0.999	45526.5	1.00				
4.399	1.148	16.72	1.000	48316.1	1.00				

RUN 092974/100274 SPANWISE PROFILE TH=0 (11)

REX =	0.10000E 01	REM =	7255.	REH =	4079.
XVO =	0.00 CM	DEL2 =	0.659 CM	DEH2 =	0.372 CM
UINF =	16.72 M/S	DEL99=	3.907 CM	DELT99 =	3.949 CM
VISC =	0.15196E-04 M2/S	DEL1 =	1.099 CM	UINF =	16.76 M/S
PORT =	11	H =	1.667	VISC =	0.15266E-04 M2/S
XLOC =	176.40 CM	CF/2 =	0.10000E 01	TINF =	22.28 DEG C
				TPLATE =	36.19 DEG C

Y(CM)	Y/DEL	U(M/S)	U/UINF	Y+	U+	Y(CM)	T(DEG C)	TBAR	TBAR
0.025	0.007	4.94	0.296	279.4	0.30	0.0546	31.97	0.304	0.696
0.030	0.008	4.97	0.297	335.3	0.30	0.0571	31.81	0.315	0.685
0.033	0.008	5.14	0.308	363.3	0.31	0.0597	31.45	0.341	0.659
0.036	0.009	5.51	0.329	391.2	0.33	0.0648	30.86	0.383	0.617
0.043	0.011	5.95	0.356	475.1	0.36	0.0724	30.18	0.432	0.568
0.053	0.014	6.34	0.379	586.8	0.38	0.0825	29.58	0.475	0.525
0.066	0.017	6.75	0.404	726.6	0.40	0.0952	28.99	0.518	0.482
0.081	0.021	7.11	0.425	894.2	0.43	0.1105	28.49	0.554	0.446
0.099	0.025	7.34	0.439	1089.8	0.44	0.1308	27.98	0.590	0.410
0.119	0.031	7.59	0.454	1313.4	0.45	0.1562	27.61	0.617	0.383
0.145	0.037	7.85	0.470	1592.9	0.47	0.1867	27.23	0.644	0.356
0.175	0.045	8.07	0.483	1928.2	0.48	0.2222	26.95	0.664	0.336
0.211	0.054	8.22	0.492	2319.4	0.49	0.2629	26.67	0.684	0.316
0.251	0.064	8.34	0.499	2766.5	0.50	0.3086	26.48	0.699	0.301
0.297	0.076	8.45	0.506	3263.5	0.51	0.3619	26.31	0.710	0.290
0.348	0.089	8.44	0.505	3828.4	0.51	0.4254	26.17	0.721	0.279
0.404	0.103	8.46	0.506	4443.2	0.51	0.4889	26.04	0.730	0.270
0.465	0.119	8.40	0.503	5113.9	0.50	0.5524	25.94	0.737	0.263
0.536	0.137	8.36	0.500	5896.3	0.50	0.6159	25.81	0.747	0.253
0.617	0.158	8.33	0.498	6790.6	0.50	0.6794	25.73	0.752	0.248
0.693	0.177	8.32	0.498	7628.9	0.50	0.8064	25.56	0.764	0.236
0.770	0.197	8.42	0.504	8467.3	0.50	0.9334	25.41	0.775	0.225
0.846	0.216	8.56	0.512	9305.6	0.51	1.0604	25.26	0.786	0.214
0.922	0.236	8.77	0.525	10144.0	0.52	1.1874	25.15	0.794	0.206
1.024	0.262	9.11	0.545	11261.7	0.55	1.3144	25.00	0.805	0.195
1.125	0.288	9.56	0.572	12379.5	0.57	1.4414	24.90	0.812	0.188
1.227	0.314	9.92	0.593	13497.3	0.59	1.5684	24.81	0.818	0.182
1.354	0.346	10.31	0.617	14894.6	0.62	1.8224	24.58	0.835	0.165
1.481	0.379	10.69	0.639	16291.8	0.64	2.0764	24.31	0.854	0.146
1.608	0.411	11.03	0.659	17689.0	0.66	2.3304	24.02	0.875	0.125
1.735	0.444	11.39	0.681	19086.3	0.68	2.5844	23.71	0.898	0.102
1.862	0.477	12.04	0.720	20483.5	0.72	2.8385	23.40	0.919	0.081
2.116	0.542	12.56	0.751	23278.0	0.75	3.0924	23.12	0.940	0.060
2.370	0.607	13.34	0.798	26072.5	0.80	3.3464	22.85	0.959	0.041
2.624	0.672	14.11	0.844	28867.0	0.84	3.6004	22.64	0.975	0.025
2.878	0.737	14.78	0.884	31661.4	0.88	3.8544	22.47	0.987	0.013
3.132	0.802	15.40	0.921	34455.9	0.92	4.1084	22.37	0.994	0.006
3.386	0.867	15.87	0.949	37250.4	0.95	4.3624	22.30	0.999	0.001
3.640	0.932	16.26	0.973	40044.9	0.97	4.6164	22.29	1.000	0.000
3.894	0.997	16.51	0.987	42839.4	0.99				
4.148	1.062	16.65	0.996	45633.8	1.00				
4.402	1.127	16.72	1.000	48428.3	1.00				

SPANWISE AVERAGE OF 11 Z STATIONS

Y(CM)	U(M/S)	U/UINF	T(C)	TBAR	TBAR
0.055	6.77	0.404	31.21	0.359	0.641
0.057	6.83	0.408	30.99	0.374	0.626
0.060	6.89	0.412	30.65	0.399	0.601
0.065	7.01	0.419	30.07	0.441	0.559
0.072	7.16	0.428	29.49	0.482	0.518
0.083	7.33	0.438	28.92	0.523	0.477
0.095	7.48	0.447	28.45	0.557	0.443
0.110	7.61	0.455	28.01	0.589	0.411
0.131	7.77	0.464	27.63	0.616	0.384
0.156	7.94	0.475	27.31	0.639	0.361
0.187	8.12	0.485	26.95	0.665	0.335
0.222	8.50	0.508	26.47	0.699	0.301
0.263	9.07	0.542	26.19	0.719	0.281
0.309	9.51	0.568	25.75	0.751	0.249
0.362	9.82	0.587	25.46	0.772	0.228
0.425	9.99	0.597	25.33	0.781	0.219
0.489	10.07	0.602	25.28	0.785	0.215
0.552	10.12	0.605	25.26	0.786	0.214
0.616	10.15	0.607	25.26	0.786	0.214
0.679	10.18	0.609	25.27	0.785	0.215
0.806	10.28	0.615	25.26	0.786	0.214
1.060	10.63	0.636	25.11	0.797	0.203
1.187	10.86	0.649	24.99	0.806	0.194
1.314	11.10	0.663	24.88	0.814	0.186
1.441	11.35	0.679	24.75	0.822	0.178
1.568	11.62	0.695	24.63	0.832	0.168
1.822	12.24	0.732	24.40	0.848	0.152
2.076	12.90	0.771	24.13	0.867	0.133
2.330	13.57	0.811	23.87	0.886	0.114
2.584	14.23	0.851	23.60	0.905	0.095
2.838	14.86	0.888	23.32	0.925	0.075
3.092	15.41	0.922	23.05	0.945	0.055
3.346	15.92	0.952	22.80	0.963	0.037
3.600	16.30	0.975	22.58	0.978	0.022
3.854	16.55	0.989	22.44	0.989	0.011
4.108	16.68	0.997	22.33	0.996	0.004
4.362	16.73	1.000	22.28	1.000	0.000

AVG UINF = 16.73 M/S   AVG VISC = 0.15273E-04 M/S
AVG REM = 6781.   AVG REH = 3978.   AVG H= 1.548
AVG TC = 36.21 DEG C

Appendix III

STANTON NUMBER DATA REDUCTION PROGRAM

```
C
C      STANTON NUMBER DATA REDUCTION PROGRAM
C      DISCRETE HOLE RIG  NAS-3-14336
C      THIS PROGRAM USES THE LINEAR SUPERPOSITION  PRINCIPLE TO
C      CALCULATE STANTON NUMBERS AND OTHER INTEGRAL PARAMETERS AT THETA=
C      0. AND 1.
C      REVISED SEPTEMBER 1975
C
       REAL K
       COMMON/ BLK1 /PAMB,PSTAT,TRECOV,RHUM,PDYN
       COMMON/ BLK2 /UINF,TINF,TADIAB,RHOG,VISC,PR,CP,W
       COMMON/ BLK3 /SAFR(12),CI(12),SM(12),F(12),KM,AH,THEAT
       COMMON/ BLK4 /TO(45),T16(12),T2(12),TCAST(12),TCAV(12),TH(12)
       COMMON/ BLK5 /Q(12),HM(45),VAR(12),QDOT(36)
       COMMON/ BLK6 /DXVO,DEND2,DF,DREEN(36),DST(36),DQDOT(36),DTH(12)
       DIMENSION NRN(4),KOMMNT(40),TG(12),TEXIT(12),ST(36),QFLOW(12),
      1  X(36),REX(36),REEN(36),STNEB(36),STO(36),STCOL(36),STHOT(36),
      2  STS(36),STSF(36),STCR(36),STHR(36),STSP(36),SMC(12),FO(12),
      3  BHCOL(12),BHOT(12),REXC(36),RENCOL(36),RENHOT(36),THO(12),
      4  FB(12),D2HOT(36),DTHO(12),DSTO(36),ETA(36),FH(12),SF(12),SFC(12)
       DIMENSION NRNC(4),STHRB(12),KOMNTO(40)
       DATA X/50.3,52.3,54.3,56.3,58.3,60.3,62.3,64.3,66.3,68.3,
      1      70.3,72.3,73.82,74.85,75.88,76.915,77.95,78.98,80.01,81.04,
      2      82.07,83.1,84.13,85.165,86.2,87.23,88.26,89.29,90.32,91.35,
      3      92.38,93.415,94.45,95.48,96.51,97.54/
C
C *1*     READ RUN NUMBER AND CONTROL PARAMETERS
C
C         NRN      8 DIGIT RUN NUMBER
C         IOUT     PARAMETER TO TERMINATE PROGRAM
C                  IOUT=0 TO READ DATA SET
C                  IOUT NE 0 TO TERMINATE PROGRAM
C         KT       DATA TYPE FOR LINEAR SUPERPOSITION
C                  KT=0  FLAT PLATE OR M(TH=0)
C                  KT=1  M(TH=1)
C         KM       PITCH/DIAMETER RATIO OF HOLE ARRAY
C                  KM=0  P/D FIVE
C                  KM=1  P/D TEN
C         L        TYPE OF FLAT PLATE STANTON NUMBER FOR ST NO RATIO
C                  REQUIRED TO SPECIFY L FOR TH=1 RUN ONLY
C                  L=0 STANTON NUMBER BASED ON ST-REX HEATED STARTING
C                    LENGTH CORRELATION
C                  L=1 STANTON NUMBER BASED ON ST-REX UNHEATED STARTING
C                    LENGTH CORRELATION
C                  L=2 FLAT PLATE STANTON NUMBER TEST DATA
C
C         NOTE: DATA SETS MUST BE STACKED FLAT PLATE,M(TH=0),M(TH=1),
C               M(TH=0),M(TH=1),...
C
       WRITE (6,900)
C * * * * * * * * * * * * * * * * * *
C       IPRINT=0 TO PRINT SUMMARY DATA SET ONLY
C       IPRINT=1 TO PRINT ENTIRE DATA REDUCTION
C
        IPRINT=1
C * * * * * * * * * * * * * * * * * *
     5 READ (5,10)   (NRN(I),I=1,4),IOUT,KT,KM,L
    10 FORMAT (4A2,I2,I2,I2,I2)
       IF (IOUT.NE.0) GO TO 2000
```

```
      C
      C *2*     READ DATA RUN DESCRIPTION, A FORMAT  COL 1-80
      C
            READ (5,2) (KOMMNT(I), I=1,40)
          2 FORMAT (40A2)
      C
      C *3*     READ TEST CONDITIONS
      C
      C         TAMB    AMBIENT TEMPERATURE (DEG F)
      C         PAMB    AMBIENT PRESSURE (INCHES HG CORRECTED TO 32 DEG F)
      C         RHUM    RELATIVE HUMIDITY (PERCENT)
      C         THEAT   SECONDARY AIR TEMP, HEATER BOX (I-C TC, MV)
      C         CI(1)   SECONDARY AIR FLOWMETER CURRENT SIGNAL (MV)
      C
            READ (5,20) TAMB,PAMB,RHUM,THEAT,CI(1)
         20 FORMAT (7F10.0)
            DO 22 I=2,12
         22 CI(I)=CI(1)
      C
      C *4*     READ TUNNEL CONDITIONS
      C
      C         TRECOV  TUNNEL AIR RECOVERY TEMPERATURE (I-C TC, MV)
      C         PDYN    TUNNEL AIR VELOCITY DYNAMIC PRESSURE (INCHES H2O)
      C         PSTAT   TUNNEL GAGE STATIC PRESSURE (INCHES H2O)
      C         XVO     VIRTUAL ORIGIN, TBL, FROM PGM PROFILE (INCHES)
      C         END2    ENTHALPY THICKNESS, FROM PGM PROFILE (INCHES)
      C         DXVO    UNCERTAINTY IN XVO, FROM PGM PROFILE (INCHES)
      C         DEND2   UNCERTAINTY IN END2, FROM PGM PROFILE (INCHES)
      C
            READ (5,20) TRECOV,PDYN,PSTAT,XVO,END2,DXVO,DEND2
      C
      C *5*     READ TEST SECTION CONDITIONS
      C
      C         TG(I)   SECONDARY AIR TEMPERATURE IN CAVITY (I-C TC, MV)
      C         TO(I)   PLATE TEMPERATURE (I-C TC, MV)
      C         Q(I)    PLATE POWER (WATTS)
      C         VAR(I)  VARIAC SETTING
      C         SAFR(I) SECONDARY AIR FLOWMETER SIGNAL (MV)
      C
            READ (5,25) (TG(I),TO(I),Q(I),VAR(I),SAFR(I), I=1,12)
         25 FORMAT (5F10.0)
      C * * * * * * * * * * * * * * * * * * * *
      C     IF (SAFR(2).NE.0.) L=2
      C * * * * * * * * * * * * * * * * * * * *
      C
      C *6*     READ RECOVERY SECTION CONDITIONS
      C
      C         TO(I)   PLATE TEMPERATURE (I-C TC, MV)
      C         HM(I)   HEAT FLUX METER SIGNAL (MV)
      C
            READ (5,26) (TO(I),HM(I),I=13,45)
         26 FORMAT(2F10.0)
      C
      C *7*     READ TEMPERATURES
      C
      C         TCAST(I)TEST SECTION CAVITY TEMPERATURE (I-C TC, MV)
      C         T16(I)  SECONDARY AIR TEMPERATURE OUTSIDE CAVITY (I-C TC, MV)
      C         TEXIT(I)SECONDARY AIR TEMPERATURE AT EXIT OF HOLE (I-C TC, MV)
      C
            READ (5,27) (TCAST(I),T16(I),TEXIT(I), I=1,12)
```

```
   27 FORMAT (3F10.0)
C
C        WRITE OUT ALL RAW DATA
C
      IF(IPRINT.NE.0) WRITE (6,900)
      WRITE (6,40) (NRN(I), I=1,4)
   40 FORMAT (10X,'RUN ' '4A2,' *** DISCRETE HOLE RIG *** NAS-3-14336'
     1 ,10X,'STANTON NUMBER DATA'/)
      WRITE (6,610) (KCMMNT(I), I=1,40)
  610 FORMAT (40X,40A2/)
      IF (IPRINT.EQ.0) GO TO 7772
      WRITE (6,45)
   45 FORMAT (10X,'UNITS: PAMB(DEG F),PAMB(IN HG), RHUM(PCT)'/17X,
     1 'PSTAT(IN H2O), TRECOV(MV), PDYN(IN H2O), XVO(IN), TPLATE(MV)'/17
     2X,'TGAS(MV), QDOT(WATTS), SAFR(MV),HM(MV), CI(MV), THEAT(MV)'/)
      WRITE (6,50) TAMB,PAMB,RHUM,THEAT
   50 FORMAT (10X,'TAMB='F6.1,5X,'PAMB='F6.2,5X,'RELHUM='F5.1,6X,
     1  'THEATER='F6.2/)
      WRITE (6,60) PSTAT,TRECOV,PDYN,XVO
   60 FORMAT (10X,'PSTAT='F6.2,5X,'TRECOV='F6.3,5X,'PDYN='F6.3,5X,
     1 'XVO='F6.2//)
      WRITE (6,70)
   70 FORMAT (10X,'PLATE',6X, 'TPLATE',6X,'TGAS',6X,'QDOT',4X,'VARIAC',
     1 5X,'SAFLOW',5X,'CURRENT',6X,'TCAST',5X,'T16',5X,'TEXIT'/)
      NP1=1
      WRITE (6,75) NP1,TO(1),Q(1),VAR(1),TCAST(1)
   75 FORMAT (10X,I3,7X,F7.3,13X,F7.2,3X,F7.1, 27X,F7.3)
      WRITE (6,80) (I,TO(I),TG(I),Q(I),VAR(I),SAFR(I),CI(I),TCAST(I),
     1             T16(I),TEXIT(I), I=2,12)
   80 FORMAT (10X,I3,7X,F7.3,3X,F7.3,3X,F7.2,3X,F7.1,3X,F8.3,3X,F8.3,
     1 5X,F7.3,F9.3,F9.3)
      WRITE(6,71)
   71 FORMAT(/,10X,'PLATE',6X,'TPLATE',6X,'HM')
      WRITE(6,72)(I,TO(I),HM(I),I=13,45)
   72 FORMAT(10X,I3,7X,F7.3,3X,F7.3)
 7772 CONTINUE
C
C        DATA CONVERSION BLOCK
C
C        CONVERT ALL TEMPERATURES FROM MV TO DEG F
      TRECOV=TC(TRECOV)
      THEAT=TC(THEAT)
      DO 90 I=1,12
      TO(I)=TC(TO(I))
      TG(I)=TC(TG(I))
      TCAST(I)=TC( TCAST(I) )
      T16(I)=TC( T16(I) )
      TEXIT(I)=TC( TEXIT(I) )
   90 CONTINUE
      DO 91 I=13,45
   91 TO(I)=TC(TO(I))
C     PLATE AREAS
      A=18.*1.968750/144.
C     HOLE AREA
      AH=(3.141593*0.406*0.406*0.25)/144.
C        COMPUTE WIND TUNNEL FLOW CONDITIONS
      CALL TUNNEL
C        COMPUTE SECONDARY AIR FLOW RATE
      CALL FLOW (KERROR)
      IF (KERROR.GT.0) RETURN
```

```
C          COMPUTE SECONDARY AIR FLOW TEMPERATURES AND QFLOW LOSS
      CALL T2EFF (QFLOW)
C          COMPUTE NET ENERGY TRANSFER FROM TEST SECTION AND RECOVERY
C          REGION
      CALL POWER (TINF,QFLOW,A)
C
C         WRITE ALL CONVERTED DATA
      IF (IPRINT.EQ.0) GO TO 1108
C
      WRITE (6,610) (KOMMNT(I), I=1,40)
      WRITE (6,100)
  100 FORMAT (//,10X,'UNITS: TPLATE(DEGF), TGAS(DEG F), QDCT(WATTS),',
     1 /17X,'SAFLOW(CFM),QFLUX(BTU/HR/SQFT),TEFF2(DEG F)'/)
      WRITE (6,102)
  102 FORMAT (10X,'PLATE',6X, 'TPLATE',5X,'TEFF2',5X,'T16 ',6X,'QDCT',
     1   6X,'QFLUX',6X,'SAFLOW',6X,'TCAST',6X,'TGAS',6X,'TEXIT',
     2   6X,'TCAV'/)
      WRITE (6,105) NP1,TO(1),Q(1),QDCT(1),TCAST(1),TCAV(1)
  105 FORMAT(10X,I3,7X,F7.1,23X,F7.2, 5X,F7.2,14X,F7.1,20X,F10.1)
      WRITE (6,110) (I,TO(I),T2(I),T16(I),Q(I),QDOT(I),SAFR(I),
     1 TCAST(I),TG(I), TEXIT(I),TCAV(I), I=2,12)
  110 FORMAT(10X,I3,7X,F7.1,3X,F7.1,3X,F7.1,3X,F7.2,5X,F7.2,1X,F8.2,
     1   5X,F7.1,3F10.1)
      WRITE (6,106)
  106 FORMAT(/,10X,'PLATE',6X,'TPLATE',6X,'HM',5X,'QFLUX'/)
      WRITE(6,107) (I,TO(I),HM(I),QDOT(I),I=13,36)
  107 FORMAT (10X,I3,7X,F7.3,3X,F7.3,3X,F7.2)
      I=108
      WRITE (6,108) I,TO(45)
  108 FORMAT (10X,I3,7X,F7.3)
C
C          COMPUTE STANTON NUMBER
C
 1108 CONTINUE
      XVI=X(1)-XVO-1.0
      IPD=5
      IF (KM.EQ.1) IPD=10
C     X REYNOLDS NUMBER BASED ON VIRTUAL ORIGIN TBL
  201 FACT=UINF/(VISC*12.)
      DREX=FACT*DXVO
      DO 210 I=1,36
  210 REX(I)=FACT*(X(I)-XVO)
C     COMPUTE STANTON NUMBERS
      DENOM=RHOG*UINF*CP*3600.
      DO 220 I=1,36
      ST(I)=QDCT(I)/(DENOM*(TO(I)-TADIAB))
C    DST(I):  UNCERTAINTY IN ST(I)
C     DP : UNCERTAINTY IN  MANOMETER PRESSURE   , IN H2O
      DP=0.008
C    DT: UNCERTAINTY IN TEMPERATURE, F
      DT=0.25
      DST(I)=ST(I)*SQRT(DQDOT(I)*DQDOT(I)/(QDOT(I)*QDCT(I))+DP*DP/(4.*
     1PDYN*PDYN)+DT*DT/((TO(I)-TINF)*(TO(I)-TINF)))
  220 CONTINUE
C          COMPUTE DEL2 AND REDEL2 BASED ON ACTUAL ST-DATA
      CALL ENTHAL (FACT,ST,REEN,ENC2)
C
      IF (IPRINT.EQ.0) GO TO 3310
       WRITE (6,900)
      WRITE (6,40) (NRN(I), I=1,4)
```

```
      TADBC=5.*(TADIAB-32.)/9.
       TINFC=5.*(TINF-32.)/9.
      UINFMS=UINF*0.3048
      XVOCM=XVO*2.54
      RHOKM3=RHOG*16.02
      VISCI=VISC*0.0929
      CPJKGK=CP*4184.
      WRITE (6,300) TADBC,UINFMS,TINFC,RHOKM3,VISCI,XVOCM,CPJKGK,PR
  300 FORMAT(10X,'TADB='F6.2,' DEG C     UINF='F12.2,' M/S      TINF='F6.2
     1' DEG C'/10X,'RHO='F7.3,' KG/M3     VISC='E12.5,' M2/S     XVO='F7.1
     2 ' CM'/10X,'CP='F8.0,' J/KGK     PR='F14.3/)
      WRITE (6,600) (KOMMNT(I), I=1,40)
  600 FORMAT   (10X,40A2/)
 3310 CONTINUE
C     IF 2ND PLATE HAS NO SECONDARY INJECTION , THIS PROGRAM ASSUMES THAT
C     IT IS A NO-BLOWING CASE.
      IF (SM(2).EQ.0.) GO TO 400
      IF (IPRINT.EQ.0) GO TO 345
      WRITE (6,310)
  310 FORMAT(10X'PLATE',3X'X',5X'REX',9X'TO',6X'REENTH',7X'STANTON NO',
     1 6X'DST',6X'DREEN',4X'M',4X'F',6X'T2',2X'THETA',3X'DTH')
      XCM=X(1)*2.54
      TEMPC=5.*(TO(1)-32.)/9.
      WRITE (6,320) NP1,XCM,REX(1),TEMPC,REEN(1),ST(1),DST(1),DREEN(1)
  320 FORMAT(10XI3,2XF5.1,1XE12.5,1XF6.2,2(2XE12.5),2XE9.3,2XF5.0)
      DO 340 I=2,12
      XCM=X(I)*2.54
      TEMPC=5.*(TO(I)-32.)/9.
      TEMP2=5.*(T2(I)-32.)/9.
      WRITE (6,330)  I,XCM,REX(I),TEMPC,REEN(I),ST(I),DST(I),DREEN(I),
     1SM(I),F(I),TEMP2,TH(I),DTH(I)
  330 FORMAT(10XI3,2XF5.1,1XE12.5,1XF6.2,2(2XE12.5),2XE9.3,2XF5.0,2XF5.2
     1,F7.4,F6.2,F6.3,2XF5.3)
  340 CONTINUE
      DO 341 I=13,36
      XCM=X(I)*2.54
      TEMPC=5.*(TO(I)-32.)/9.
      WRITE (6,331) I,XCM,REX(I),TEMPC,REEN(I),ST(I),DST(I),DREEN(I)
  331 FORMAT(10XI3,2XF5.1,1XE12.5,1XF6.2,2(2XE12.5),2XE9.3,2XF5.0)
  341 CONTINUE
      WRITE (6,334) DREX,DF
  334 FORMAT (/12X,'UNCERTAINTY IN REX=',F6.0,9X'UNCERTAINTY IN F=',F7.5
     1,' IN RATIO')
      GO TO 345
C
C     STORE FLATPLATE EXPERIMENTAL DATA FOR STANTON NUMBER RATIO
C
  400 DO 401 I=1,36
      STNOB(I)=ST(I)
  401 CONTINUE
      WRITE (6,410)
  410 FORMAT(10X'PLATE',3X'X',5X'REX',9X'TO',6X'REENTH',7X'STANTON NO',
     1 6X'DST',6X'DREEN',5X,'ST(THEO)',6X,'RATIO')
      DO 420 I=1,36
      STT=.0295*PR**(-.4)*(REX(I))**(-.2)
      IF (L.EQ.1)STT=STT*(1.-(XVI/(X(I)-XVO))**.9)**(-1./9.)
      RATIO=ST(I)/STT
      XCM=X(I)*2.54
      TEMPC=5.*(TO(I)-32.)/9.
      WRITE (6,430)  I,XCM,REX(I),TEMPC,REEN(I),ST(I),DST(I),DREEN(I),
```

```
     1  STT,RATIC
  430 FORMAT(10XI3,2XF5.1,1XE12.5,1XF6.2,2(2XE12.5),2XE9.3,2XF5.0,
     1 E15.5,F9.3)
  420 CONTINUE
      IF (IPRINT.EQ.0) WRITE (6,900)
      GO TO 5
C
C
C     STORE VALUES FOR TH=0
  345 IF (KT.EQ.1) GO TO 360
C
  350 DO 351 I=1,12
      SMC(I)=SM(I)
      FO(I)=F(I)
      THO(I)=TH(I)
      DTHO(I)=DTH(I)
      STO(I)=ST(I)
      DSTO(I)=DST(I)
      REXO(I)=REX(I)
  351 CONTINUE
      DO 352 I=13,36
      STO(I)=ST(I)
      DSTO(I)=DST(I)
      REXO(I)=REX(I)
  352 CONTINUE
      FACTO=FACT
      DFC=DF
      DO 353 I=1,4
  353 NRNO(I)=NRN(I)
       DO 354 I=1,40
  354 KOMNTO(I)=KOMMNT(I)
      GO TC 5
C
C         COMPUTE STANTON NUMBER AT TH=0 AND TH=1 BY LINEAR SUPERPCSITICN
C
  360 FAVO=0.
      FAV=0.
      THAVO=0.
      THAV=0.
      DO 361 I=2,12
      THAVO=THAVO+THO(I)
      THAV=THAV+TH(I)
      FAVO=FAVO+FC(I)
      FAV=FAV+F(I)
  361 CONTINLE
      THAVO=(THO(11)+THO(12))/2.
      THAV=(TH(11)+TH(12))/2.
      FAVO=FAVO/11.
      FAV=FAV/11.
      FBAV=.5*(FAVO+FAV)
      STCR(1)=STO(1)/STNOB(1)
      STHR(1)=ST(1)/STNOB(1)
      STHRB(1)=STHR(1)
      TH(1)=TH(2)
      THO(1)=THO(2)
      DO 362 I=2,12
      DENOM=(TH(I-1)+TH(I))/2.-(THC(I-1)+THC(I))/2.
      STS(I)=(STO(I)-ST(I))/DENOM
      DNUM=(THO(I-1)+THO(I))/2.
      STCCL(I)=STO(I)+DNUM*STS(I)
```

```
      DNUM=(TH(I-1)+TH(I))/2.-1.
      STHOT(I)=ST(I)+DNUM*STS(I)
      FB(I)=0.5*(FO(I)+F(I))
      ETA(I)=STS(I)/STCOL(I)
C     COMPUTE STANTON NUMBER RATIO FOR TH=1 (IF L=2 USE FLAT PLATE
C     EXPERIMENTAL DATA)
      IF (L.EQ.2) GO TO 374
      STNOB(I)=.0295*PR**(-.4)*(REX(I))**(-.2)
      IF (L.EQ.1)STNOB(I)=STNOB(I)*(1.-(XVI/(X(I)-XVO))**(0.9))**
     1(-1./9.)
  374 STHR(I)=STHOT(I)/STNOB(I)
C     COMPUTE STANTON NUMBER RATIO FOR TH=0 (IF L=0 USE FLAT PLATE
C     EXPERIMENTAL DATA)
      IF (L.EQ.2) GO TO 375
      STNOB(I)=STNOB(I)*(REX(I)/REXO(I))**(0.2)
      IF (L.EQ.1)STNOB(I)=STNOB(I)*(1.-(XVI*FACTO/REXO(I))**(0.9))**
     1(-1./9.)
  375 STCR(I)=STCOL(I)/STNOB(I)
      STSR(I)=STHOT(I)/STCOL(I)
      BHCOL(I)=FO(I)/STCOL(I)
      BHOT(I)=F(I)/STHOT(I)
      STSF(I)=ALOG(1.+BHOT(I))/BHOT(I)
C     CORRECT STANTON NUMBER RATIO FOR TH=1 TO COMPARABLE TRANSPIRATION
C     CASE USING ALOG(1.+B)/B EXPRESSION
      STHRB(I)=STHR(I)/STSF(I)
      STSR(I)=STSR(I)/STSF(I)
      SF(I)=F(I)*STHOT(I)
      SFO(I)=FO(I)*STCOL(I)
  362 CONTINUE
      DO 363 I=13,36
      STS(I)=(STO(I)-ST(I))/(THAV-THAVO)
      STCOL(I)=STO(I)+THAVO*STS(I)
      STHOT(I)=ST(I)+(THAV-1.0)*STS(I)
      ETA(I)=STS(I)/STCOL(I)
C     COMPUTE STANTON NUMBER RATIO FOR RECOVERY REGION, TH=1
      IF (L.EQ.2) GO TO 372
      STNOB(I)=.0295*PR**(-.4)*(REX(I))**(-.2)
      IF (L.EQ.1)STNOB(I)=STNOB(I)*(1.-(XVI/(X(I)-XVO))**(0.9))**
     1(-1./9.)
  372 STHR(I)=STHOT(I)/STNOB(I)
C     COMPUTE STANTON NUMBER RATIO FOR RECOVERY REGION, TH=0
      IF (L.EQ.2) GO TO 373
      STNOB(I)=STNOB(I)*(REX(I)/REXO(I))**(0.2)
      IF (L.EQ.1)STNOB(I)=STNOB(I)*(1.-(XVI*FACTO/REXO(I))**(0.9))**
     1(-1./9.)
  373 STCR(I)=STCOL(I)/STNOB(I)
      STSR(I)=STHOT(I)/STCOL(I)
  363 CONTINUE
C         COMPUTE DEL2 AND REDEL2 BASED ON ST-DATA AT TH=0 AND TH=1
      STCOL(1)=STO(1)
      STHOT(1)=ST(1)
      STS(1)=STO(1)-ST(1)
      DO 370 I=1,12
      FH(I)=F(I)
  370 TH(I)=1.0
      CALL ENTHAL (FACT,STHOT,RENHET,END2)
      DO 450 I=1,12
      F(I)=FO(I)
      TH(I)=0.
  450 DTH(I)=DTHO(I)
```

```
      DF=DFO
      DO 460 I=1,36
  460 DST(I)=DSTC(I)
      CALL ENTHAL (FACTO,STCCL,RENCOL,END2)
C
      IF (IPRINT.NE.1) GO TO 462
      WRITE (6,900)
      WRITE (6,40) (NRNO(I), I=1,4)
      WRITE (6,610) (KCMNTC(I), I=1,40)
      WRITE (6,40) (NRN(I), I=1,4)
      WRITE (6,610) (KOMMNT(I), I=1,40)
  462 WRITE (6,371) (NRNO(I), I=1,4),(NRN(I), I=1,4)
  371 FORMAT (10X,'LINEAR SUPERPOSITION IS APPLIED TO STANTON NUMBER',
     1' DATA FROM'/10X,'RUN NUMBERS ',4A2,' AND ',4A2,' TO OBTAIN'
     2,' STANTON NUMBER DATA AT TH=0 AND TH=1'/)
      WRITE(6,364)
  364 FORMAT   (/,7X,'PLATE',3X,'REXCOL',4X,'RE DEL2',3X,'ST(TH=0)',4X,
     1'REXHOT',4X,'RE DEL2',3X,'ST(TH=1)',4X,'ETA',4X,'STCR',4X'F-COL',
     25X'STHR',4X'F-HOT',4X,'LOGB'/)
      WRITE(6,365)  (I,REXO(I),RENCOL(I),STCOL(I),REX(I),RENHOT(I),
     1STHOT(I),ETA(I),STCR(I),FC(I),STHR(I),FH(I),STHRE(I),I=1,12)
  365 FORMAT((10X,I2,2(2XF9.1),1XF9.6,2(2XF9.1),1XF9.6,2(2XF5.3),2XF7.4,
     12XF7.3,2XF7.4,F8.3))
      WRITE(6,366)  (I,REXO(I),RENCOL(I),STCOL(I),REX(I),RENHOT(I),
     1STHOT(I),ETA(I),STCR(I),STHR(I),I=13,36)
  366 FORMAT((10X,I2,2(2XF9.1),1XF9.6,2(2XF9.1),1XF9.6,2(2XF5.3),11XF7.3
     1))
      IF (L.EQ.0) WRITE (6,505)
  505 FORMAT (//,10X,'STANTON NUMBER RATIO BASED ON ST*PR**0.4=0.0295*RE
     1X**(-.2)')
      IF (L.EQ.1) WRITE (6,510)
  510 FORMAT (//,10X,'STANTON NUMBER RATIO BASED ON ST*PR**0.4=0.0295*RE
     1X**(-.2)*(1.-(XL/(X-XVO))**0.9)**(-1./9.)')
      IF (L.EQ.2) WRITE (6,515)
  515 FORMAT (//,10X,'STANTON NUMBER RATIO BASED ON EXPERIMENTAL FLAT PL
     1ATE VALUE AT SAME X LOCATION')
      WRITE (6,520)
  520 FORMAT (//,10X,'STANTON NUMBER RATIO FOR TH=1 IS CONVERTED TO COMP
     1ARABLE TRANSPIRATION VALUE '/10X,'USING ALOG(1 + B)/B EXPRESSION I
     2N THE BLOWN SECTION')
      IF (IPRINT.EQ.0) WRITE (6,900)
      GO TO 5
 2000 WRITE (6,900)
  900 FORMAT (1H1)
      RETURN
      END


      FUNCTION TC(T)
C     FUNCTION CONVERTS TEMP FROM IRON-CONSTANTAN MV TO DEG F
      TM=-2220.703+781.25*SQRT(7.950782+0.256*T)
      TC=TM+49.97-1.26E-03*TM-.32E-04*TM*TM
      RETURN
      END
```

```
      SUBROUTINE TUNNEL
C
C        THIS ROUTINE COMPUTES THE WIND TUNNEL FLOW CONDITIONS
C
C        UINF       FREE STREAM VELOCITY (FT/SEC)
C        TINF       FREE STREAM STATIC TEMPERATURE (DEG F)
C        RHOG       FREE STREAM DENSITY (LBM/FT3)
C        VISC       FREE STREAM KINEMATIC VISCOSITY (FT2/SEC)
C        CP         FREE STREAM SPECIFIC HEAT (BTU/LBM/DEG R)
C        PR         FREE STREAM PRANDTL NUMBER
C        W          FREE STREAM ABSOLUTE HUMIDITY (LBM H2O/LBM DRY AIR)
C
      COMMON/ BLK1 /PAMB,PSTAT,TRECOV,RHUM,PDYN
      COMMON/ BLK2 /UINF,TINF,TADIAB,RHOG,VISC,PR,CP,W
C
C     SATURATION DATA FROM K AND K 1969 STEAM TABLES
      DIMENSION TEMP(10),PSAT(10),RHOSAT(10)
      DATA TEMP/      40.,      50.0,      60.0,      70.0,      80.0,
     1      90.0,     100.0,     110.0,     120.0,     130.0/
      DATA PSAT/      17.519,    25.636,    36.907,    52.301,    73.051,
     1      100.627,  136.843,   183.787,   244.008,   320.400/
      DATA RHOSAT/   .0004090, .0005868, .0008286, .0011525, .0015803,
     1      .0021381, .0028571, .0037722, .0049261, .0063625/
      REAL NU,MFA,MFV,MWA,MWV,JF
      TAMB=TRECOV
      DO 10 N=1,9
      IF(TEMP(N).GT.TAMB) GO TO 20
   10 CONTINUE
   20 T = TEMP(N)
      EPS = T - TAMB
      VAPH = PSAT(N)
      VAPL = PSAT(N-1)
      VEPS = VAPH - VAPL
      RHOH = RHOSAT(N)
      RHOL = RHOSAT(N-1)
      REPS = RHOH - RHOL
      RHOG = RHOL + (10.0 - EPS)*REPS/10.
      RA=1545.32/28.970
      PG = VAPL + (10.0 - EPS)*VEPS/10.0
      PUNITS=2116.21/33.932/12.
      P=PAMB*2116.21/29.9213 + PSTAT*PUNITS
      RHUM=RHUM/100.
      PVAP = RHUM*PG
      PA = P - PVAP
      RHOA = PA/(RA*(TAMB + 459.67))
      RHOV = RHUM*RHOG
      W=RHOV/RHOA
      RHOM = RHOA + RHOV
      MWA = 28.970
      MWV = 18.016
      MFV = RHOV/RHOM
      MFA = 1.0 - MFV
      RM = 1545.32*(MFA/MWA + MFV/MWV)
      CP = MFA*0.240 + MFV*0.445
      GC=32.1739
      JF=778.26
      RCF=0.7**0.33333
C      RECOVERY FACTOR FOR WIRE NORMAL TO FLOW
      RTC=0.68
      RHOG=(P/RM+PDYN*PUNITS*RCF/(CP*JF))/(TRECOV+459.67)
```

```
      UINF=SQRT(2.*GC*PDYN*PUNITS/RHOG)
      TINF=TRECOV-RTC*UINF*UINF/(2.*GC*JF*CP)
      VISC=(11.+0.0175*TINF)/(1.E06*RHOG)*(1.-.7*W)
      PR=.710*(530./(TINF+459.67))**(.1)*(1.+.9*W)
C     NOTE FOR HIGH VELOCITY THIS ROUTINE SHOULD BE ITERATED
C      CONVERT TO ADIABATIC WALL TEMPERATURE
       RCF=PR**0.33333
       TADIAB=TINF+RCF*UINF*UINF/(2.*GC*JF*CP)
      RETURN
      END


      SUBROUTINE FLOW (KERROR)
C
C        THIS ROUTINE COMPUTES SECONDARY AIR FLOW RATES
C
C        SAFR(I) SECONDARY AIR FLOW RATE CORRECTED FOR TEMPERATURE
C                  AND HUMIDIY (CFM)
C
      COMMON/ BLK1 /PAMB,PSTAT,TRECOV,RHUM,PDYN
      COMMON/ BLK2 /UINF,TINF,TADIAB,RHOG,VISC,PR,CP,W
      COMMON/ BLK3 /SAFR(12),CI(12),SM(12),F(12),KM,AH,THEAT
      COMMON/ BLK4 /TO(45),T16(12),T2(12),TCAST(12),TCAV(12),TH(12)
      DIMENSION X(5),Y(5),B(4),FMC(12),TM(12)
      DATA FMC/  1.0,   1.22,   .92,   .988,   .928,   .906,   .907,   1.01,
     1              .918,   .901,   .920,   .929/
C     CALIBRATION CURVE DATA
      DATA X,Y /0.35, 0.90, 1.12, 1.35, 1.5,
     1            53.0, 4.05, 2.00, 1.00, 0.69/
      KERROR=0
      DO 10 I=1,4
   10 B(I)=ALOG(Y(I)/Y(I+1))/ALOG(X(I)/X(I+1))
      FACT=1.0+0.22*W
      DO 20 I=2,12
      IF (SAFR(I).EQ.0.) GO TO 20
C     TM IS ESTIMATE OF SECONDARY AIR TEMPERATURE AT FLOWMETER STATION
      TM(I)=.5*(T16(I)+THEAT)
      SAFR(I)=SAFR(I)*(((TM(I)+459.67)/530.)**0.7)*FACT*(30.00/CI(I))**2
     1        *FMC(I)
   20 CONTINUE
      FACT=1.0+0.7*W
      DO 40 I=2,12
      IF (SAFR(I).EQ.0.) GO TO 40
      IF (SAFR(I).LT.X(1).OR.SAFR(I).GT.X(5)) GO TO 100
      DO 30 K=1,5
      IF (X(K).GT.SAFR(I)) GO TO 35
   30 CONTINUE
   35 Z=Y(K-1)*(SAFR(I)/X(K-1))**B(K-1)
      SAFR(I)=Z/((530./(TM(I)+459.67))**0.76)/FACT
   40 CONTINUE
C     NOTE UNCERTAINTY CALCULATION FOR FLOWRATE COMPUTED IN
C     SUBROUTINE T2EFF
      RETURN
  100 WRITE (6,200) SAFR(I)
  200 FORMAT (10X,'FLOWMETER READING OUT OF RANGE, EMF='E12.5,//10X,
     1 'DATA SET REDUCTION TERMINATED')
      KERROR=2
      RETURN
      END
```

```
      SUBROUTINE T2EFF (QFLOW)
C
C        THIS ROUTINE COMPUTES
C
C        KFL(I)      EXPERIMENTAL CONDUCTANCE FOR COMPUTING QFLOW
C        KCONV(I)    EXPERIMENTAL CONDUCTANCE FOR COMPUTING T2EFF
C        T2(I)       EFFECTIVE SECONDARY AIR TEMPERATURE
C        QFLOW(I)    ENERGY LOSS FROM PLATE TO SECONDARY AIR
C        TH(I)       THETA=(T2-TINF)/(TO-TINF)
C        SM(I)       VELOCITY*DENSITY RATIO, SECONDARY AIR TO MAINSTREAM
C        F(I)        MASS FLUX RATIO, SECONDARY AIR TO MAINSTREAM, WHERE
C                    F=W/AH/(U*P)
C
      COMMON/ BLK1 /PAMB,PSTAT,TREDV,RHUM,PDYN
      COMMON/ BLK2 /UINF,TINF,TADIAB,RHOG,VISC,PR,CF,W
      COMMON/ BLK3 /SAFR(12),CI(12),SM(12),F(12),K4,AH,THEAT
      COMMON/ BLK4 /TO(45),T6(12),T2(12),TCAST(12),TCAV(12),TH(12)
      COMMON/ BLK6 /DXVO,DEN02,DF,CREEN(36),DST(36),CDULT(36),DTH(12)
      REAL KCONV(12),KFL(12),KL,KR,KBP
      DIMENSION QFLOW(12)
      KL=.333333
      KR=.333333
      KBP=.333333
      TW1=TCAST(1)
      TW12=TCAST(12)
      CALL CAVITY (KL,KR,KBP,TW1,TW12)
      FACT=.074843*.24*60.
      QFLOW(1)=0.0
      HOLE9=9.
      HOLE8=8.
      DO 16 I=2,12,2
      KCONV(I)=0.
      KFL(I)=0.
      IF (SAFR(I).EQ.0.) GO TO 16
      IF (I.NE.1) GO TO 8
      HOLE9=5.
      IF (I.EQ.4.OR.I.EQ.8.OR.I.EQ.12) HOLE9=4.
    8 SAFR(I)=SAFR(I)*9./HOLE9
      IF (SAFR(I).GT.5.) GO TO 12
      KFL(I)=0.015*SAFR(I)**0.3536*HOLE9
      KCONV(I)=0.03*SAFR(I)**0.2739*HOLE9/FACT
      GO TO 16
   12 IF (SAFR(I).GT.10.) GO TO 14
      KFL(I)=0.0030*SAFR(I)**0.7501*HOLE9
      KCONV(I)=0.0170*SAFR(I)**0.0388*HOLE9/FACT
      GO TO 16
   14 KFL(I)=0.012*SAFR(I)**0.5748*HOLE9
      KCONV(I)=0.027*SAFR(I)**0.4386*HOLE9/FACT
   16 CONTINUE
C     KFL COMPUTED FOR 8 HOLE ROW USING FACTOR HOLE9 INSTEAD OF HOLE8
      DO 25 I=3,12,2
      KCONV(I)=0.
      KFL(I)=0.
      IF (SAFR(I).EQ.0.) GO TO 26
      SAFR(I)=SAFR(I)*9./HOLE8
      IF (SAFR(I).GT.5.) GO TO 22
      KFL(I)=0.015*SAFR(I)**0.3536*HOLE9
      KCONV(I)=0.03*SAFR(I)**0.2739*HOLE8/FACT
      GO TO 26
   22 IF (SAFR(I).GT.10.) GO TO 24
```

```
      KFL(I)=0.0080*SAFR(I)**0.7501*HOLE9
      KCONV(I)=0.0170*SAFR(I)**0.6388*HOLE8/FACT
      GO TO 26
   24 KFL(I)=0.012*SAFR(I)**0.5748*HOLE9
      KCONV(I)=0.027*SAFR(I)**0.4386*HOLE8/FACT
   26 CONTINUE
CC       EFFECTIVE  'T2',AND 'QFLOW'.
      DO 30 I=2,12,2
      IF (SAFR(I).EQ.0.) GO TO 31
      IF (KM.NE.1) GO TO 33
      HOLE9=5.
      IF (I.EQ.4.OR.I.EQ.8.OR.I.EQ.12) HOLE9=4.
   33 SAFR(I)=SAFR(I)*HOLE9/9.
      TBAR=(TO(I)+TCAV(I-1))*0.5
      IF (I.EQ.2) TBAR=TO(I)
      IF (I.EQ.2) KCONV(I)=KFL(I)/FACT
      T2(I)=T16(I)+(TBAR-T16(I))*(1.-EXP(-KCONV(I)/SAFR(I)))
      QFLOW(I)=KFL(I)*(TO(I)-T2(I))
      GO TO 30
   31 T2(I)=TO(I)
      QFLOW(I)=0.
   30 CONTINUE
      DO 40 I=3,12,2
      IF (SAFR(I).EQ.0.) GO TO 41
      SAFR(I)=SAFR(I)*HOLE8/9.
      TBAR=(TO(I)+TCAV(I-1))*0.5
      IF (I.EQ.3) TBAR=TO(I)
      T2(I)=T16(I)+(TBAR-T16(I))*(1.-EXP(-KCONV(I)/SAFR(I)))
      QFLOW(I)=KFL(I)*(TO(I)-T2(I))
      GO TO 40
   41 T2(I)=TO(I)
      QFLOW(I)=0.
   40 CONTINUE
C
C     COMPUTE THETA=(T2-TINF)/(TO-TINF)
      TH(1)=0.
      DTH(1)=0.
C    DT: UNCERTAINTY IN TEMPERATURE, F
      DT=0.25
C     DT2, UNCERTAINTY IN T2, DEG F
      DT2=0.5
      DO 200 I=2,12
      TH(I)=(T2(I)-TINF)/(TO(I)-TINF)
C   DTH(I): UNCERTAINTY IN TH(I)
  200 DTH(I)=SQRT(DT2**2+(TH(I)*DT)**2+((1.-TH(I))*DT)**2)/(TO(I)-TINF)
C
      FACT=AH/(2.*2./144.)
      IF (KM.EQ.1) FACT=AH/(4.*4./144.)
      DO 50 I=2,12,2
      IF (KM.NE.1) GO TO 48
      HOLE9=5.
      IF (I.EQ.4.OR.I.EQ.8.OR.I.EQ.12) HOLE9=4.
   48 F9=AH*60.*UINF*HOLE9*RHOG
      RHOS=RHOG*(TINF+459.67)/(T2(I)+459.67)
      SM(I)=SAFR(I)*RHOS/F9
      F(I)=SM(I)*FACT
   50 CONTINUE
      F8=AH*60.*UINF*HOLE8*RHOG
      DO 60 I=3,11,2
      RHOS=RHOG*(TINF+459.67)/(T2(I)+459.67)
```

```
      SM(I)=SAFR(I)*RHOS/F8
      F(I)=SM(I)*FACT
C     ADJUST F,TH FOR P/D=10
      IF (KM.EQ.1) F(I)=F(I-1)
      IF (KM.EQ.1) TH(I)=TH(I-1)
   60 CONTINUE
      SM(1)=0.
      F(1)=0.
C
C     DP : UNCERTAINTY IN  MANOMETER PRESSURE   , IN H2O
      DP=0.008
C     DSAFR:  UNCERTAINTY IN SECONDARY FLOW RATE,RATIO
      DSAFR=0.05
C    DF: UNCERTAINTY IN   F , RATIO
      DF=SQRT(DSAFR*DSAFR+DP*DP/(4.*PDYN*PDYN))
      IF (SM(2).EQ.0.0) DF=0.0
      RETURN
      END

      SUBROUTINE CAVITY (KL,KR,KBP,TW1,TW12)
C
C        THIS ROUTINE COMPUTES TEST SECTION CAVITY TEMPERATURES
C
      REAL KL,KR,KBP
      COMMON/ BLK4 /TO(45),T16(12),T2(12),TCAST(12),TCAV(12),TH(12)
      TCAST2=TCAST(2)
      TCAST5=TCAST(5)
      TCAST8=TCAST(8)
      TCAS11=TCAST(11)
      DBP1=TCAST5-TCAST2
      DBP2=TCAST8-TCAST5
      DSR1=TCAST(6)-TCAST(3)
      DSR2=TCAST(7)-TCAST(4)
      DBP1=TCAST(5)-TCAST(2)
      DBP2=TCAST(8)-TCAST(5)
      TCAV(1)=KL*(TCAST(3)-1./4.*DSR1)+KR*(TCAST(4)-1./4.*DSR2)
     1 +KBP*(TCAST(1)+TW1)
      TCAV(2)=KL*TCAST(3)+KR*TCAST(4)+KBP*TCAST2
      TCAV(3)=KL*(TCAST(3)+1./4.5*DSR1)+KR*(TCAST(4)+1./4.5*DSR2)
     1 +KBP*(TCAST2+1./3.*DBP1)
      TCAV(4)=KL*(TCAST(3)+2./4.5*DSR1)+KR*(TCAST(4)+2./4.5*DSR2)
     1 +KBP*(TCAST2+2./3.*DBP1)
      TCAV(5)=KL*(TCAST(3)+3./4.5*DSR1)+KR*(TCAST(4)+3./4.5*DSR2)
     1 +KBP*TCAST5
      TCAV(6)=KL*(TCAST(3)+4./4.5*DSR1)+KR*(TCAST(4)+4./4.5*DSR2)
     1 +KBP*(TCAST5+1./3.*DBP2)
      DSR1=TCAST(9)-TCAST(6)
      DSR2=TCAST(10)-TCAST(7)
      DBP3=TCAS11-TCAST8
      TCAV(7)=KL*(TCAST(6)+0.5/4.5*DSR1)+KR*(TCAST(7)+0.5/4.5*DSR2)
     1 +KBP*(TCAST5+2./3.*DBP2)
      TCAV(8)=KL*(TCAST(6)+1.5/4.5*DSR1)+KR*(TCAST(7)+1.5/4.5*DSR2)
     1 +KBP*TCAST8
      TCAV(9)=KL*(TCAST(6)+2.5/4.5*DSR1)+KR*(TCAST(7)+2.5/4.5*DSR2)
     1 +KBP*(TCAST8+1./3.*DBP3)
      TCAV(10)=KL*(TCAST(6)+3.5/4.5*DSR1)+KR*(TCAST(7)+3.5/4.5*DSR2)
     1 +KBP*(TCAST8+2./3.*DBP3)
      TCAV(11)=KL*TCAST(9)+KR*TCAST(10)+KBP*TCAS11
      TCAV(12)=KL*(TCAST(6)+5.5/4.5*DSR1)+KR*(TCAST(7)+5.5/4.5*DSR2)
     1 +KBP*(TCAST(12)+TW12)
      RETURN
      END
```

```
      SUBROUTINE POWER (TINF,QFLOW,A)
C
C        THIS ROUTINE :
C
C                  (1) CORRECTS THE INDICATED PLATE POWER READING FOR
C                      WATTMETER CALIBRATION AND CIRCUIT INSERTION LOSSES
C                  (2) COMPUTES NET ENERGY LOST FROM PLATES BY FORCED
C                      CONVECTION HEAT TRANSFER
C                  (3) COMPUTES HEAT FLUX FROM RECOVERY REGION PLATES
C
      COMMON/ BLK4 /TO(45),T16(12),T2(12),TCAST(12),TCAV(12),TH(12)
      COMMON/ BLK5 /Q(12),HM(45),VAR(12),QDOT(36)
      COMMON/ BLK6 /DXVO,CEND2,DF,BREEN(36),DST(36),DQDOT(36),DTH(12)
      REAL KL,KR,KBP,K
      DIMENSION RO(12),RBO(12),RR(12),RLOD(12),RWAT(12),RON(12),RL(12)
      DIMENSION XB(12),QFLOW(1)     ,K(39),S(40)
C        CONDUCTION LOSS CONSTANTS FOR TEST SECTION
      DATA K/    .2700,    .2705,    .1851,    .2800,    .1781,    .2763,
     1           .1760,    .2768,    .1721,    .2832,    .1806,    .2800,
C        HEAT FLUX METER CALIBRATION CONSTANTS NO 13-36
     2           34.00,    35.30,    35.04,    34.04,    33.64,    32.25,
     3           24.83,    34.04,    27.55,    31.55,    29.61,    31.80,
     4           34.01,    34.24,    35.75,    29.30,    24.50,    31.46,
     5           32.06,    39.35,    32.73,    23.60,    36.27,    33.24,
C        HEAT FLUX METER CALIBRATION CONSTANTS NO 106-108
     6           32.53,    32.62,    36.65/
C        AXIAL CONDUCTION LOSS CONSTANTS
      DATA  S/ 1.200 ,  11*2.3,  .850 ,  6.23,   4.962,  5.014,  4.965,
     1           5.118,  5.183,  4.777,  4.494,  5.480,  5.020,  5.597,
     2           5.254,  5.169,  5.254,  5.356,  5.211,  5.370,  5.583,
     3           4.990,  5.435,  4.672,  5.557,  5.545,  5.585,
     4           4.983,  5.056,  6.34 /
C        WATTMETER CIRCUIT RESISTANCES
      DATA RO  /     8.476,  8.595,  8.500,  8.506,  8.478,  8.571,
     1               8.549,  8.641,  8.590,  8.638,  8.481,  8.504/
      DATA RBO /     8.386,  8.502,  8.426,  8.418,  8.386,  8.471,
     1               8.445,  8.574,  8.509,  8.528,  8.391,  8.393/
      DATA RR  /     0.0408, 0.0541, 0.0406, 0.0411, 0.0413, 0.0412,
     1               0.0410, 0.0415, 0.0409, 0.0409, 0.0406, 0.0406/
      DATA RLOD/     8.256,  8.331,  8.237,  8.221,  8.239,  8.269,
     1               8.227,  8.238,  8.250,  8.253,  8.240,  8.248/
      DATA RWAT/     8.400,  8.484,  8.379,  8.367,  8.405,  8.429,
     1               8.422,  8.541,  8.544,  8.413,  8.386,  8.411/
      DATA RON /     8.313,  8.387,  8.281,  8.282,  8.316,  8.335,
     1               8.330,  8.455,  8.451,  8.428,  8.296,  8.291/
      DATA RL  /     8.077,  8.157,  8.057,  8.047,  8.067,  8.087,
     1               8.037,  8.057,  8.067,  8.077,  8.057,  8.057/
      DATA XB  /     12*0./
      DATA RA,XA,RV,RVM/     0.064,  0.063,  7500.0, 5300.0/
C
C        THIS BLOCK CORRECTS INDICATED WATTMETER READING USING
C        WATTMETER CALIBRATION EQUATION
      DO 10 I=1,12
      QP=Q(I)/75.
      QCOR=QP*(0.0728*QP-0.0427*QP*QP-0.0292)
      QCOR=0.99*Q(I)+QCOR*75.
C
C        THIS BLOCK CORRECTS FOR WATTMETER INSERTION LOSSES
      VARR=RR(I)*VAR(I)
      SUMRO=RO(I)*VARR
```

```
          SUMRBO=RBO(I)+VARR
          FP1=RWAT(I)/RVM+1.
          ZROSQ=SUMRO*SUMRO+(XB(I)+XA/FP1)*(XB(I)+XA/FP1)
          ZRBOSQ=SUMRBO*SUMRBO+XB(I)*XB(I)
          RVMONS=(RVM/(RVM+RON(I)))*(RVM/(RVM+RON(I)))
          ZVALSQ=(RV+RA+RLOD(I))*(RV+RA+RLOD(I))+XA*XA
          Q(I)=QCOR*(ZROSQ/ZRBOSQ)*(ZVALSQ/RV/RV)*RVMONS
         1  *FP1*FP1*(RL(I)/(RA+RLOD(I)))
       10 CONTINUE
C
C            THIS BLOCK CORRECTS POWER DELIVERED TO PLATES
C            IN TEST SECTION  FOR CONDUCTION,RADIATION, AND QFLOW LOSSES
          SF=1.
          EMIS=0.15
          TAR=(TINF+460.)/100.
          TW1=TCAST(1)
          TW12=TCAST(12)
          KL=0.5
          KR=0.5
          KBP=0.0
          CALL CAVITY (KL,KR,KBP,TW1,TW12)
          TUP=TO(45)
          TDOWN=TO(13)
          TW1=TO(45)+K(39)*HM(45)/20.5
          TW12=TO(13)+K(13)*HM(13)/20.5
          TO(13)=0.75*TO(13)+0.25*TW12
          TO(45)=0.75*TO(45)+0.25*TW1
          IF (HM(13).EQ.0.) TO(13)=0.5*(TO(12)+TO(13))
          IF (HM(45).EQ.0.) TO(45)=0.5*(TO(1)+TO(45))
          DO 109 I=1,12
          TOR=(TO(I)+460.)/100.
          IF(I.EQ.1)  GO TO  98
          QCOND=K(I)*(TO(I)-TCAV(I))+S(I)*(TO(I)-TO(I-1))+S(I+1)*(TO(I)-
         1   TO(I+1))
          GO TO 100
       98 QCOND=K(I)*(TO(I)-TCAV(I))+S(I)*(TO(I)-TO(45))
         1  +S(I+1)*(TO(I)-TO(I+1))
      100 QRAD=A*SF*EMIS*.1714*(TOR*TOR*TOR*TOR-TAR*TAR*TAR*TAR)
C
C         ENERGY BALANCE IS APPLIED TO PLATE
          QLOSS=QCOND+QRAD+QFLOW(I)
          Q(I)=Q(I)-QLOSS/3.4129
          QDOT(I)=Q(I)*3.4129/A
      109 CONTINUE
          TO(45)=TUP
          TO(13)=TDOWN
C
C            THIS BLOCK COMPUTES HEAT FLUX FROM RECOVERY REGION PLATES
          SF=1.0
          EMIS=0.15
          TO(37)=TO(36)-.333*(TO(36)-TO(37))
          S(13)=7.0*S(13)
          TAR=(TINF+460.)/100.
          DO 200 I=13,36
          TOR=(TO(I)+460.)/100.
      200 QDOT(I)=K(I)*HM(I)*(1.+(80.-TO(I))/700.)
         1-S(I)*(TO(I)-TO(I-1))-S(I+1)*(TO(I)-TO(I+1))
         2  -SF*EMIS*.1714*(TOR*TOR*TOR*TOR-TAR*TAR*TAR*TAR)
          S(13)=S(13)/7.0
C
```

```
C     ASSUME ALL PROPERTIES CORRECT, AFTER TEMPERATURE-HUMIDITY CORRECTION.
C     DQ:  ENERGY BALANCE ERROR, WATT
      DQ=0.3
C   DHM:  UNCERTAINTY IN HM(I),MV
      DHM=0.025
C    DK:  UNCERTAINTY IN HEAT FLUX METER CALIBRATION,RATIO
      DK=0.03
C    DS:  UNCERTAINTY IN CONDUCTION CORRECTION ON HEAT FLUX METER,RATIO
      DS=0.05
C    DT: UNCERTAINTY IN TEMPERATURE, F
      DT=0.25
C   DQDOT: UNCERTAINTY IN HEAT FLUX,BTU/HR.SQFT
      DO 711 I=1,12
  711 DQDOT(I)=DQ*3.4129/A
      DO 712 I=13,36
  712 DQDOT(I)=SQRT(DK*DK*K(I)*K(I)*HM(I)*HM(I)+K(I)*K(I)*DHM*DHM+DT*DT
     1*(S(I)*S(I)+S(I+1)*S(I+1))+DS*DS*(S(I)*S(I)*(TO(I)-TO(I-1))*(TO(I)
     2-TO(I-1))+S(I+1)*S(I+1)*(TO(I)-TO(I+1))*(TO(I)-TO(I+1))))
       RETURN
       END


      SUBROUTINE ENTHAL (FACT,ST,REEN,END2)
C
C     COMPUTE ENTHALPY THICKNESS, ASSUMING THERMAL BL BEGINS AT
C        LEADING EDGE OF PLATE 1. COMPUTATION BASED ON CONTROL
C        VOLUME FOR ENERGY ADDITION WITH BOUNDRIES PLATE CENTER
C        TO PLATE CENTER(EXCEPT PLATE 1)
C
      COMMON/ BLK3 /SAFR(12),CI(12),SM(12),F(12),KF,AH,THEAT
      COMMON/ BLK4 /TO(45),T16(12),T2(12),TCAST(12),TCAV(12),TH(12)
      COMMON/ BLK6 /DXVO,DEND2,DF,DREEN(36),DST(36),DQDOT(36),DTH(12)
      DIMENSION ST(1),REEN(1),D2(36),DD2(36)
      TH(1)=0.0
      DTH(1)=0.
      F(1)=0.0
      DX=1.
      DWX=.515625
C   DDX: UNCERTAINTY IN DX, IN
      DDX=0.005
      D2(1)=END2
      DD2(1)=DEND2
      IF (END2.EQ.0.) D2(1)=ST(1)*DX
      IF(.NOT.END2.EQ.0.)  GO TO 229
C   DD2(I):  UNCERTAINTY IN ENTHALPY THICKNESS, D2, IN
      DD2(1)=SQRT(DX*DX*DST(1)*DST(1)+ST(1)*ST(1)*DDX*DDX)
  229 DO 230 I=2,12
      D2(I)=D2(I-1)+(ST(I-1)+ST(I)+2.*F(I-1)*TH(I-1))*DX
      AL=ST(I)*ST(I)+ST(I-1)*ST(I-1)+F(I)*F(I)*TH(I)*TH(I)+F(I-1)*
     1F(I-1)*TH(I-1)*TH(I-1)
      BE=DST(I)*DST(I)+DST(I-1)*DST(I-1)+F(I)*F(I)*DTH(I)*DTH(I)+
     1F(I-1)*F(I-1)*DTH(I-1)*DTH(I-1)+DF*DF*(F(I)*F(I)*TH(I)*TH(I)+
     2F(I-1)*F(I-1)*TH(I-1)*TH(I-1))
  230 DD2(I)=SQRT(DD2(I-1)*DD2(I-1)+DDX*DDX*AL+DX*DX*BE )
      D2(13)=D2(12)+(ST(12)+2.*F(12)*TH(12))*DX+ST(13)*DWX
      DD2(13)=SQRT(DD2(12)*DD2(12)+DDX*DDX*(ST(12)*ST(12)+ST(13)*ST(13)
     1+F(12)*F(12)*TH(12)*TH(12)) +DWX*DWX*DST(13)*DST(13)+  DX*DX*(
     2DST(12)*DST(12)+F(12)*F(12)*DTH(12)*DTH(12)+DF*DF*F(12)*F(12)*
     3TH(12)*TH(12)))
```

```
      DO 231 I=14,36
      D2(I)=D2(I-1)+(ST(I-1)+ST(I))*DWX
      IF (I.EQ.14.AND.KM.EQ.1)D2(14)=D2(14)+2.*F(12)*TH(12)*DX
  231 DD2(I)= SQRT(DD2(I-1)*DD2(I-1)+DDX*DDX*(ST(I)*ST(I)+ST(I-1)*
     1ST(I-1))+ DWX*DWX*(DST(I)*DST(I)+DST(I-1)*DST(I-1)))
C     COMPUTE ENTHALPY THICKNESS REYNOLDS NUMBER FOR CENTER
C        OF PLATE BASED ON D2(I) FOR ENERGY ADDED TO THAT POINT
      DO 240 I=1,36
      REEN(I)=FACT*D2(I)
  240 DREEN(I)=FACT*DD2(I)
      RETURN
      END
```

Appendix IV

ON THE HEAT TRANSFER BEHAVIOR FOR THE INITIAL FILM-COOLING ROWS

Consider, for example, the data for $\theta = 1$ and $M = 0.4$ in Figure 3.3 or the data for $M = 0.2$ and 0.4 in Figure 3.6. It can be seen that introducing hot fluid onto a hot wall $(\theta = 1)$ causes Stanton number reductions of about 10 and 30 percent for the first two rows of holes, respectively.

The identical Stanton number reduction for $M = 0.2$ and 0.4 with $\theta = 1$ indicates a similar hydrodynamic behavior for the initial blowing rows and low M. (In fact, this type of behavior is seen for low M in all the $P/D = 5$ data.) Presumably, for low blowing ratios the jets are immediately knocked over onto the surface by pressure forces. The Stanton number reduction for low blowing ratios can be explained by considering the following simple analysis, along with the sketch below.

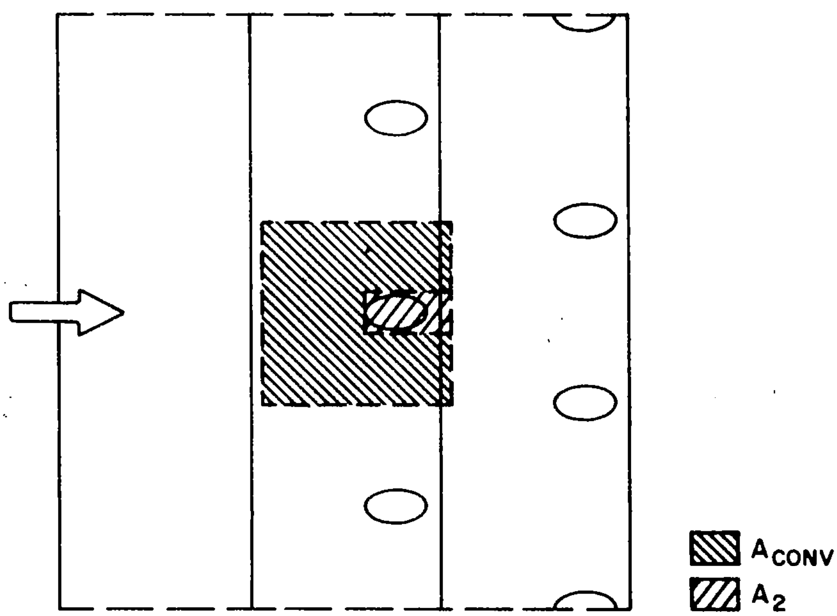

As the jet of coolant emerges from a hole in the first row, it will displace the boundary layer fluid and the new fluid will lie along the surface downstream. The total heat transfer from the surface (for an area associated with one hole) can be decomposed into two parts,

$$\dot{q} = \dot{q}_{conv} + \dot{q}_2 \tag{IV.1}$$

Introducing a convective rate equation, the heat transfer rate becomes

$$\dot{q} = h_{conv}\, A_{conv}(T_o - T_\infty) + h_2\, A_2 (T_o - T_2) \tag{IV.2}$$

where the subscript "2" refers to the injectant conditions.

By forming a Stanton number, equation (IV.2) becomes

$$St = \frac{\dot{q}/A}{\rho_\infty U_\infty c\ (T_o - T_\infty)} = \left(\frac{h_{conv}}{\rho_\infty U_\infty c}\right)\frac{A_{conv}}{A} + \left(\frac{h_2}{\rho_\infty U_\infty c}\right)\frac{A_2}{A}\ (1-\theta) \tag{IV.3}$$

where $A = (A_{conv} + A_2)$ and θ is the temperature parameter. Thus,

$$St(\theta) = St_{conv} \cdot \frac{A_{conv}}{A} + St_2 \frac{A_2}{A}\ (1-\theta) \tag{IV.4}$$

For the first blowing row, in the limit as $M \to 0$, $h_2 \to h_{conv}$; for larger M, $h_2 > h_{conv}$. Consider the limiting case for $P/D = 5$ and $\theta = 1$.

$$St(\theta = 0) = St_o \tag{IV.5a}$$

$$St(\theta = 1) = St_o \left(\frac{A_{conv}}{A}\right) = 0.90\ St_o \tag{IV.5b}$$

where St_o is the Stanton number at $M = 0$. This 10 percent depression is precisely the Stanton number behavior for Figure 3.6 for no upstream thermal boundary layer. Note that the corresponding prediction for $\theta = 0$ is $St(\theta = 0) = St_o$. The fact that $St(\theta = 0) > St_o$ for Figure

3.3 reflects the influence of the existing thermal boundary layer. However, the $St(\theta = 1)$ behavior is identical to that in Figure 3.6.

If the same analysis and assumptions are carried out for the second row of holes, it is found that

$$St(\theta = 1) = 0.70\ St_o \tag{IV.6}$$

which is precisely what the experimental data exhibit in Figures 3.3 and 3.6.

To proceed further would be meaningless because of the fast growth of the thermal boundary layer and increased turbulent mixing. The analysis is intended only to explain the data trend for the first two rows of holes.

Appendix V

ON AN ASYMPTOTIC STANTON NUMBER AND JET COALESCENCE

It is perhaps important to readdress the $\theta = 1$ data and ask whether it will approach a constant, non-zero value or whether it will monotonically continue to decrease. Recall that most of the $\theta = 0$ data approaches an asymptote, independent of the number of rows of holes. The importance of the question is embodied in a relation derived by Choe et al. (1976) to relate the Stanford data to effectiveness data.

$$\eta = 1 - \frac{St(M,\theta=1)}{St(M,\theta=0)} \qquad (V.1)$$

Consideration of this equation is made in light of the η data of Metzger et al. (1973) and Mayle and Camarata (1975). Note that the only ways for η to approach a constant is for $St(\theta = 1)$ and $St(\theta = 0)$ to decrease at the same rate, or for $St(\theta = 1)$ to approach a constant in a manner similar to the $St(\theta = 0)$ data of Figure 3.3.

Metzger's data at $M = 0.2$ (normal-angle injection) showed a near-zero derivative in η at about 40 hole diameters downstream. Mayle and Camarata found that for $M = 0.5$ (compound-angle injection) the derivative $d\eta/dx$ becomes zero (100 hole diameters downstream of the array leading edge) for all P/D. Mayle and Camarata write, in explanation:

> "This result indicates a balance is nearly reached between the jet-mainstream mixing, which reduces the cooling effect, and the periodic coolant injection which, of course, is intended to increase cooling. At higher mass flux ratios the film effectiveness is seen to be still increasing at the last row of holes [writer's note: 25 rows of holes for their $P/D = 8$ surface]; however, the rate of increase is reduced from that of the first half of the pattern. Besides being a consequence of the film approaching the coolant temperature, with the result that each successive injection is less effective when based on the original coolant-mainstream temperature difference, the reduced rate of increase is also a consequence of jet coalescence."

In support of a constant effectiveness, the study by Choe (the normal injection study at Stanford that preceded this study) did obtain data with near-constant effectiveness for $M = 0.2$. However, for these data both $St(\theta = 0)$ and $St(\theta = 1)$ were decreasing at the same rate to produce this constant η condition.

The data reported herein for 30-degree slant-angle injection show no evidence of producing a constant effectiveness, as would be calculated according to equation (3.1). Note that η is calculated for all data sets and is given as a part of the tabulations in Appendix I. However, based on the Mayle work, it is probable that the 55 hole diameter flow length of the $P/D = 5$ Stanford test section is not long enough for establishment of a constant Stanton number with slant-angle injection at low M and $\theta = 1$. It is interesting to note that the film-cooling model, discussed in Chapter 4, predicts that $St(\theta = 1)$ approaches a nearly constant value when the computations are carried out for 24 rows of holes.

The question of jet coalescence with full-coverage film cooling (mentioned in the preceding quote by Mayle and Camarata) was first raised to us in a private communication with Prof. J. H. Whitelaw, Imperial College, London. If the jets begin to coalesce, the cooling will be reduced, as Mayle and Camarata indicate, because the area of coverage will be reduced. This could contribute to an asymptotic Stanton number behavior. Following Whitelaw's suggestion, a check for coalescence downstream of the last blowing row of the slant-angle test section was carried out by S. Yavuzkurt, a research student in the Mechanical Engineering Department at Stanford. He probed the velocity and thermal boundary layers for injectant conditions at high blowing ratios (up to $M = 2.0$) and found no evidence of jet coalescence.

Appendix VI

SHEAR STRESS AND MIXING-LENGTH PROFILES

The shear stress profile is computed following a procedure given in Simpson, Whitten, and Moffat (1970). The shear stress in the boundary layer over a film-cooled surface can be written as

$$\frac{\tau-\tau_o}{\rho_\infty U_\infty^2} = \frac{1}{\delta_2}\frac{d\delta_2}{dx}\left[\int_o^y \frac{\rho U^2}{\rho_\infty U_\infty^2}\,dy - \frac{U}{U_\infty}\int_o^y \frac{\rho U}{\rho_\infty U_\infty}\,dy\right] + \frac{\dot{m}_{jet}/A}{\rho_\infty U_\infty}\left(\frac{U}{U_\infty} - \frac{U_2\cos\alpha}{U_\infty}\right) \tag{VI.1}$$

In the above equation, the mass flux into the boundary layer is presumed to have a velocity component U_x. Integration of equation (VI.1) to $y = \delta$ results in the momentum integral equation of the form given by Choe et al. (1976).

$$\frac{d\delta_2}{dx} = \frac{C_f}{2} - \frac{\dot{m}_{jet}/A}{\rho_\infty U_\infty}\left(1 - \frac{U_2\cos\alpha}{U_\infty}\right) \tag{VI.2}$$

Combining the above two equations, the following equation can be obtained:

$$\tau^+ = 1 + \left[\frac{1 + \frac{F}{C_f/2}(1 - M\cos\alpha)}{\delta_2}\right]\cdot\left[\int_o^y \frac{\rho U^2}{\rho_\infty U_\infty^2}\,dy - \frac{U}{U_\infty}\int_o^y \frac{\rho U}{\rho_\infty U_\infty}\,dy\right] + \frac{F}{C_f/2}\left[\frac{U}{U_\infty} - M\cos\alpha\right] \tag{VI.3}$$

where $\tau^+ = \tau/\tau_o$, $C_f/2 = \tau_o/\rho_\infty U_\infty^2$, and F and M are defined in Chapter 1.

Equation (VI.3) is the computing equation for τ^+. From this the mixing-length can be computed. The shear stress is defined as

$$\frac{\tau}{\rho} = (\nu + \epsilon_M)\frac{\partial U}{\partial y} \tag{VI.4}$$

where ϵ_M is the eddy diffusivity for momentum. It can be defined in terms of the Prandtl mixing-length as

$$\epsilon_M = \ell^2 \left|\frac{\partial U}{\partial y}\right| \tag{VI.5}$$

Combining the above two equations results in the computing equation for the mixing-length profile,

$$\ell = \left[\frac{\tau^+ \rho_\infty U_\infty^2 C_f/2 - \nu \frac{\partial U}{\partial y}}{\left|\frac{\partial U}{\partial y}\right| \frac{\partial U}{\partial y}}\right]^{\frac{1}{2}}$$

The key to computing the shear stress and mixing-length profiles is an assumption for $C_f/2$. This was obtained using the Re_{δ_2} value for the spanwise-averaged profile and an analogy between (C_f/C_{f_o}) and (St/St_o). For the evaluation of the equations, $C_f = 0.001$ was used. The value of the friction coefficient is relatively unimportant; what is important is the qualitative trend of τ^+ and ℓ for the spanwise-averaged profile.

References

Bergeles, G., Gosman, A. D., and Launder, B.E. 1975. The prediction of three-dimensional discrete-hole cooling processes: I - laminar flow. ASME Paper 75-WA/HT-109.

Campbell, J. F., and Schetz, J. A. 1973. Analysis of the injection of a heated turbulent jet into a cross flow. NASA Rep. TR R-413.

Choe, H. 1975. The turbulent boundary layer on a full-coverage film-cooled surface: an experimental heat transfer study with normal injection. Ph.D. Thesis, Stanford University (also published as Choe, Kays, and Moffat 1976).

Choe, H., Kays, W. M., and Moffat, R. J. 1976. Turbulent boundary layer on a full-coverage film-cooled surface - an experimental heat transfer study with normal injection. NASA Rep. CR-2642. (Also Stanford Univ. Dep. Mech. Eng. Rep. HMT-22).

Colladay, R. S. 1972. Importance of combining convection with film cooling. NASA Rep. TM X-67962.

Colladay, R. S., and Russell, L. M. 1975. Flow visualization of discrete hole film cooling for gas turbine applications. NASA Rep. TM X-71766.

Crawford, M. E., and Kays, W. M. 1975. STAN5 - a program for numerical computation of two-dimensional internal/external boundary layer flows. Stanford Univ. Dep. Mech. Eng. Rep. HMT-23.

Eriksen, V. L., Eckert, E. R. G., and Goldstein, R. J. 1971. A model for analysis of the temperature field downstream of a heated jet injected into an isothermal crossflow at an angle of 90°. NASA Rep. CR-72990.

Esgar, J. B. 1971. Turbine cooling - its limitations and its future. High Temperature Turbines, AGARD Conf. Proc. No. 73: 14.1-14.24.

Goldstein, R. J. 1971. Film cooling. Advances in Heat Transfer 7:321-379.

Goldstein, R. J. et al. 1969. Film cooling following injection through inclined circular tubes. NASA Rep. CR-73612.

Herring, H. J. 1975. A method of predicting the behavior of a turbulent boundary layer with discrete transpiration jets. J. Eng. Power 97:214-224.

Kays, W. M. 1966. Convective Heat and Mass Transfer. New York: McGraw-Hill.

Kays, W. M., and Moffat, R. J. 1975. The behavior of transpired turbulent boundary layers. Studies in Convection, Vol. 1. New York: Academic Press, 223-319.

Kline, S. J., and McClintock, F. A. 1953. Describing uncertainties in single-sample experiments. Mech. Eng. 75:3-8.

Launder, B. E., and York, J. 1973. Discrete hole cooling in the presence of free stream turbulence and strong favourable pressure gradient. Imp. Coll. Rep. HTS/73/9.

Le Brocq, P. V., Launder, B. E., and Pridden, C. H. 1971. Discrete hole injection as a means of transpiration cooling - an experimental study. Imp. Coll. Rep. HTS/71/37.

Mayle, R. E., and Camarata, F. J. 1975. Multihole cooling film effectiveness and heat transfer. J. Heat Transfer 97:534-538.

Metzger, D. E., Carper, H. J., and Swank, L. R. 1968. Heat transfer with film cooling near nontangential injection slots. J. Eng. Power 90:157-163.

Metzger, D. E., and Fletcher, D. D. 1971. Evaluation of heat transfer for film-cooled turbine components. J. Aircraft 8:33-38.

Metzger, D. E., Takeuchi, D. I., and Kuenstler, P. A. 1973. Effectiveness and heat transfer with full-coverage film cooling. J. Eng. Power 95:180-184.

Moffat, R. J. 1962. Gas temperature measurement. Temperature - Its Measurement and Control in Science and Industry. New York: Reinhold, 3:553-571.

Moffat, R. J. 1968. Temperature measurement in solids. ISA Paper 68-514.

Pai, B. R., and Whitelaw, J. H. 1971. The prediction of wall temperature in the presence of film cooling. Int. J. Heat Mass Transfer 14:409-426.

Patankar, S. V., Rastogi, A. K., and Whitelaw, J. H. 1973. The effectiveness of three-dimensional film-cooling slots - II. predictions. Int. J. Heat Mass Transfer 16:1673-1681.

Whitten, D. G., Kays, W. M., and Moffat, R. J. 1967. The turbulent boundary layer on a porous plate: experimental heat transfer with variable suction, blowing, and surface temperature. Stanford Univ. Dep. Mech. Eng. Rep. HMT-3.

Simpson, R. L., Whitten, D. G., and Moffat, R. J. 1970. An experimental study of the turbulent Prandtl number of air with injection and suction. Int. J. Heat Mass Transfer 13:125-143.

*U.S. GOVERNMENT PRINTING OFFICE: 1976 - 735-004/20